# Developing a new tool to purify methylated peptides from bacteria in order to study bacterial mechanosensing

Meihua Gong

Par **Meihua GONG**

# *Developing a new tool to purify methylated peptides from bacteria in order to study bacterial mechanosensing*

Thèse présentée
pour l'obtention du grade
de Docteur de l'UTC

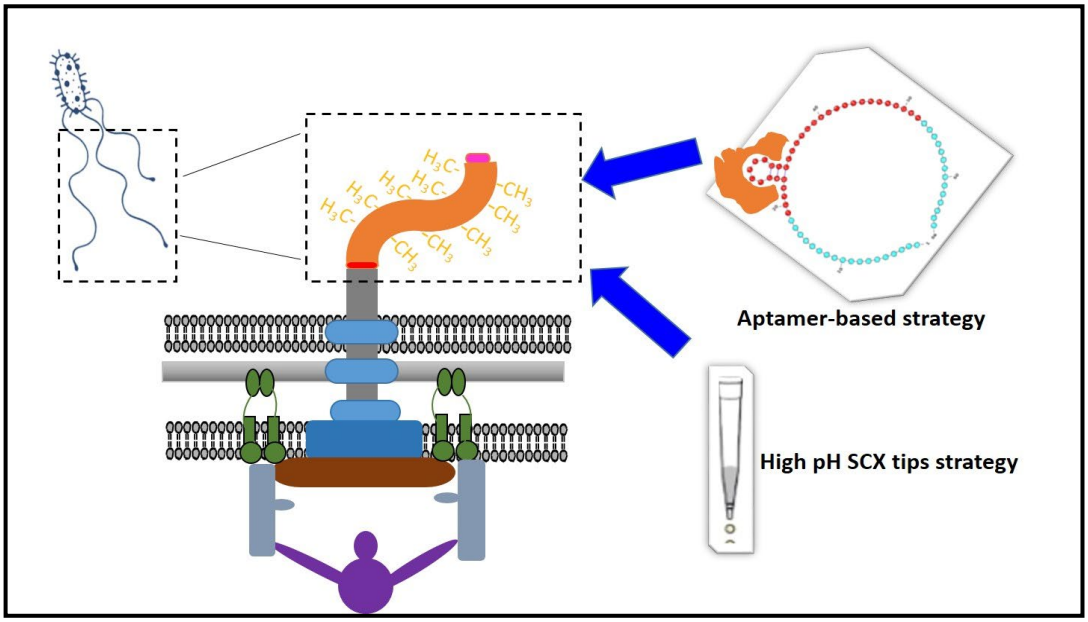


Soutenue le 4 juillet 2023
**Spécialité :** Biotechnologie : Unité de recherche Génie Enzymatique et Cellulaire - GEC (UMR-7025)
D2749

# DOCTORAL THESIS

Submitted for graduation as

**Docteur de l'Université de Technologie de Compiègne**

**Spécialité : Biotechnologie**

By **Meihua GONG**

# Developing a new tool to purify methylated peptides from bacteria in order to study bacterial mechanosensing

Soutenue le 4 juillet 2023

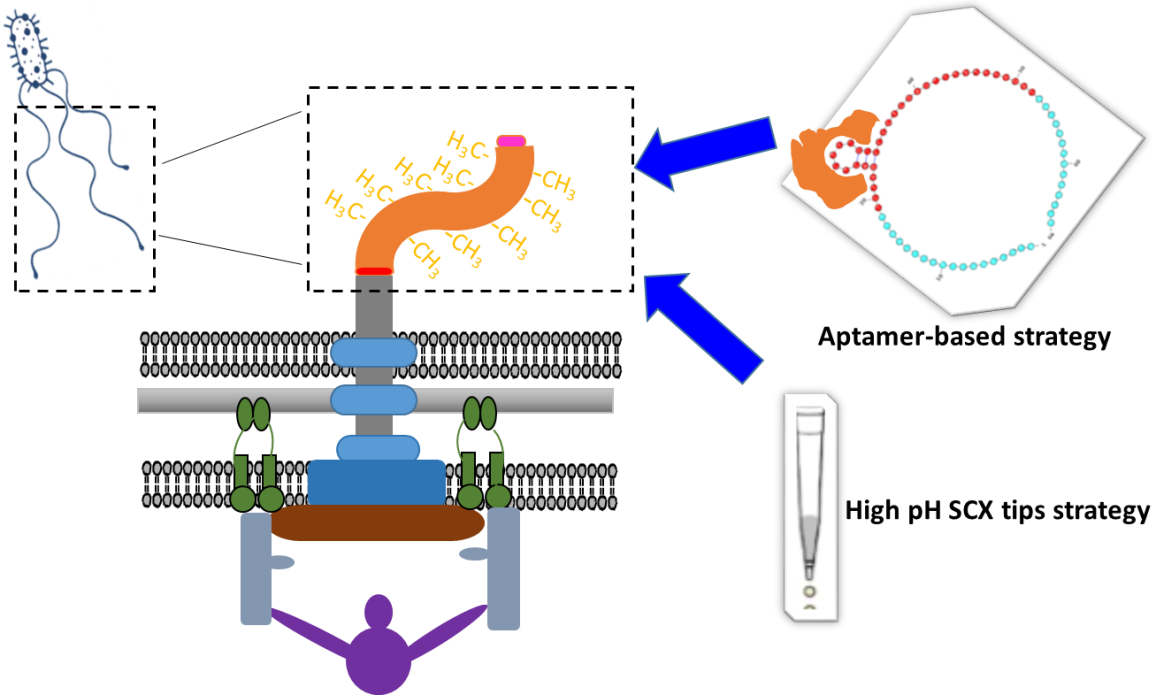


## Composition of jury members

| | | |
|---|---|---|
| Pr. Laure Beven | Univ. de Bordeaux | Rapporteur |
| Dr. Frédéric Ducongé | Univ. de Saclay, Paris | Rapporteur |
| Dr. Julie Hardouin | Univ. de Rouen Normandie | Examinatrice |
| Pr. Bérangère Avalle-Bihan | Univ. de Technologie de Compiègne | Examinatrice |
| Dr. Séverine Padiolleau | Univ. de Technologie de Compiègne | Co-directrice |
| Dr. Yannick Rossez | Univ. de Technologie de Compiègne/ Univ. de Lille | Co-directeur |

# ACKNOWLEDGMENTS

First of all, I would like to thank the members of my thesis committee. I would like to thank Pr. Laure Beven, Dr. Frédéric Ducongé to revise this thesis, and Dr. Julie Hardouin, Pr. Bérabgère Avalle-Bihan to be examiners of this work. Thanks for your valuable feedback and suggestions on my work. I look forward to discussing my work with you all.

Next, I would like to express my sincere gratitude to my supervisors, Dr. Séverine Padiolleau and Dr. Yannick Rossez, whose patient guidance, constant support, and warm-hearted encouragement were invaluable throughout my PhD journey, especially during the worldwide COVID-19 period.

Séverine, thank you very much for your advice and encouragement, which helped me to overcome the tough moment when my experiments reached a bottleneck. I would like to thank you for your suggestions on how to improve my presentation skills and for accompanying me every time I excised. I will cherish your mentorship and patience throughout this time, giving me the chance to become a better me.

Yannick, I am grateful for the time and effort you have invested in my work. I would like to thank you for your patience and advice, which lead me to the creative direction to achieve the goal of the project. Your expertise and insightful comments helped me improve my research and they will shape my academic career. Working with you expanded my knowledge of biochemistry and biotechnology. Your passion for research and life drives me to pursue the truth of research and enjoy our life at the same time. During these three and half years, you were my director and then my friend. I am grateful for the opportunity to learn from you to be a good researcher. And an additional appreciation should be for your kind wife and your lovely children. When I carried out several experiments in Lille, they gave me great help and treated me like a member of your family.

A special thanks should be to my sweet team. I am lucky to be surrounded by you all. The dream team with Séverine, Bérangère, Irene, Stéphane and Adeline, I am grateful for your support, encouragement, and constructive suggestions. Your smiles, your humor, and all our moments of sharing will be unforgettable for me. As well as all my treasured friends in the office, Mellisa, Nicolas, Thomas, Mickaël, and Rémi, who supported me a lot and I enjoy every

moment with you guys. We talked about the different cultures of France, China, and Algeria, made jokes, cared about each other and our families, encouraged each other, and discussed the problems that appeared in our projects. We always had interesting conversations and learned a lot from each other. Mel, Thomas, Nico, and Mick, you have all been there for me whenever I needed it, which has touched me. All members of our team make up a warm family.

I extend my thanks to the staff and faculty members of the GEC lab and those who helped me with my project, for their support and encouragement for my PhD program. I would like to thank Frank, Elise, Luminita, Eric, Rodrigue, Morgane, and Valérie…

It was my greatest pleasure to work with such a great group of people who became my friends, again Mellisa, Ye, Xin, Nico, Thomas, Mickaël, Tiffany, Noel, Ernesto, Christos, Claudia, Camille, Alessia, Salim, Vivi, and Ale. I was lucky to work in the GEC laboratory with a friendly atmosphere. I appreciate the moments, the activities, the trips, the restaurant moments with you guys and I really cherish your company. We celebrated our birthday together and those joys and happiness are so precious to me. We come from different countries and now we are an international family, and forever…

In the end, a warm thankful heart should be for my family and friends in China. My mom, my grandmother, my big brother, my sister-in-law, my nephew, my cousins, my uncles, my aunties, all these lovely families are always by my side. Without their unwavering support and encouragement throughout my academic journey, I would not have been able to complete my research. Their love has kept me motivated and inspired.

# ABSTRACT

Flagella have been described as an important virulence factor for initial attachment to the host or to the surface of hospital equipment. However, how bacteria use their flagella to switch from a floating (planktonic) state to an immediately attached (sessile) state remains an open question. This transition involves flagellar mechanosensing or surface-sensing. It has been illustrated that lysine methylations in *S*. Typhimurium flagella facilitate bacterial adhesion to the surface or receptor *via* hydrophobicity. However, the study of the entire methylome, including non-histone methylation, remains a major challenge because of the lack of efficient methyl protein/peptide enrichment techniques. Here, to investigate protein methylation and its mechanisms in *S*. Typhimurium and its mutants, we applied two complementary strategies for methyl protein enrichment: aptamer-based enrichment technology and high pH SCXtips separation strategy.

The specific DNA aptamers were obtained after performing several rounds of positive selection and one round of negative selection from a random oligonucleotide library through the FluMag-SELEX procedure. The selected ssDNA pools were sequenced and 10%, 11%, and 33% of redundant sequences for MML, DML, and TML, respectively have been observed. The highest redundancy was observed with oligonucleotides directed against TML. The interaction study of this aptamer with its target was then performed by the methods like ITC, PCR, and bead-based binding assays followed by mass spectrometry titration. The specificity was confirmed while the affinity was determined to be $K_D$=2.48±0.14 mM. Then, the selected aptamer has been used as an enrichment tool based on the aptamer-bound beads method, in order to isolate methylated proteins or peptides on various cell lines. After the validation of our approach using a positive control (HEK293 cells), we identified 19 lysine methylation sites on 5 proteins from *Salmonella* Preliminary results from proteomic analysis confirmed that the selected aptamer was indeed able to distinguish and enrich methyllysine-containing proteins from *S*. Typhimurium strains and human cell lines.

In parallel with this, the high pH SCXtips technology was performed as a complementary separation strategy when cultivating the strains in the hM-SILAC medium. Using this method, 23 unique methylation sites in *ΔmetE*, 51 unique methylation sites in *ΔmetEΔmotAB*, and 18 unique sites in *ΔmetEΔfliB* on 19 methylated proteins were identified. By comparing the differences in protein methylation, our results suggest that when bacteria lack motility, lysine methylations in bacterial proteins seem to be upregulated. Besides being methylated by the methylase FliB, a large number of methylation events could be regulated by other methylases.

**Keywords**: Virulence factors, *S*. Typhimurium, bacterial mechanosensing, flagella, methylome, aptamers, post-translational modifications, FluMag-SELEX, high pH SCXtips, enrichment

# RÉSUMÉ

Les flagelles ont été décrits comme un facteur de virulence important pour l'attachement initial à l'hôte ou à la surface des équipements hospitaliers. Cependant, la question de savoir comment les bactéries utilisent leurs flagelles pour passer d'un état flottant (planctonique) à un état d'attachement immédiat (sessile) reste ouverte. Cette transition implique la mécanodétection flagellaire. Il a été démontré que les méthylations des lysines dans les flagelles de *S*. Typhimurium facilitent l'adhésion de la bactérie à la surface ou au récepteur par le biais de l'hydrophobicité. Cependant, l'étude de l'ensemble du méthylome, et plus particulièrement la méthylation des protéines autres que des histones, reste un défi majeur en raison de l'absence de techniques efficaces d'enrichissement des protéines/peptides méthylés. Ici, pour étudier la méthylation des protéines et ses mécanismes chez *S*. Typhimurium et ses mutants, nous avons appliqué deux stratégies complémentaires pour l'enrichissement des protéines méthylées : l'enrichissement sélectif grâce à la sélection d'aptamères spécifiques, et la séparation de protéines/peptides méthylés par la technologie SCXtips à pH élevé.

Des aptamères d'ADN spécifiques ont été obtenus après plusieurs cycles de sélection positive et un cycle de sélection négative à partir d'une bibliothèque d'oligonucléotides aléatoires par le biais de la procédure FluMag-SELEX. Plusieurs oligonucléotides issus du dernier tour de sélection ont été séquencés et des redondances de séquence de 10 %, 11 % et 33 % respectivement contre la MML, DML et TML, ont pu être observées. Une caractérisation plus fine de l'interaction entre l'aptamère sélectionné contre le TML et sa cible a été menée par différentes méthodes (ITC, PCR, liaison sur billes suivie d'une quantification par spectrométrie de masse). La spécificité a été confirmée tandis que l'affinité a été déterminée avec un $K_D$=2,48±0,14 mM. Par la suite, nous avons exploité l'aptamère sélectionné en l'immobilisant à la surface de billes magnétiques afin de disposer d'un outil d'enrichissement des protéines/peptides méthylés sur différents modèles cellulaires. Après avoir validé la démarche sur un contrôle positif (cellules humaines HEK293), nous avons identifié 19 sites de méthylation de la lysine sur 5 protéines de *Salmonella*. Les résultats préliminaires de l'analyse protéomique ont confirmé que l'aptamère sélectionné était effectivement capable de distinguer et d'enrichir les protéines contenant de la méthyllysine provenant de souches de *S*. Typhimurium.

Parallèlement, la technologie SCXtips à pH élevé a été utilisée comme stratégie de séparation à partir culture de souches bactériennes dans le milieu hM-SILAC. Cette méthode a permis d'identifier 23 sites de méthylation uniques chez la souche *ΔmetE*, 51 sites de méthylation uniques chez la souche *ΔmetEΔmotAB*, et enfin 18 sites uniques chez la souche *ΔmetEΔfliB* sur 19 protéines méthylées. En comparant les différences de méthylation des protéines, nos résultats suggèrent que lorsque les bactéries manquent de motilité, les méthylations de lysine

dans les protéines bactériennes semblent être régulées à la hausse. Outre la méthylation par la méthylase FliB, un grand nombre d'événements de méthylation pourraient être régulés par d'autres méthylases.

**Mots clés** : Facteurs de virulence, *S*. Typhimurium, mécanodétection bactérienne, flagella, méthylome, modifications post-traductionelles, aptamères, FluMag-SELEX, SCXtips à pH élevé, enrichissement

# FIGURE lIST

# TABLE LIST

# ABBREVIATIONS

A: Adenine

Ad5: Adenovious type 5

Att: Attractants

Big-1 domain: Bacterial Ig-like domain 1

BSA: Bovine serum albumin

C: Cytosine

cAMP: Cyclic Adenosine Monophosphate

CCW: Counter clockwise

c-di-GMP: Cyclic diguanylate Monophosphate

CD: Circular dichroism spectroscopy

CE-SELEX: Capillary electrophoresis-SELEX

CU pathway: Chaperone-usher pathway

CW: Clockwise

DMEM: Dulbecco's modified eagle medium

DML: Di-methylated lysine

DMS: Dimethyl sulfate

DTT: Dithiothreitol

*E. coli*: *Escherichia coli*

EDTA: Ethylenediaminetetraacetic acid

EF-Tu: Elongation factor Tu

EIC: Extracted-ion chromatogram

ELISA: Enzyme-linked immunosorbent assay

FACS: Fluorescence-activated cell sorting

FGCs: Fimbrial gene clusters

FITC: Fluorescein isothiocynate

fT3SS: Flagellar-associated type III secretion system

G: Guanine

M cells: Microfold cells

MAMPs: Microbe-associated molecular patterns

MBT: Malignant brain tumor

MDA: Malondialdehyde

Met: Methionine

MML: Mono-methylated lysine

MS: Mass spectrometry

M-SELEX: Microfluidic-SELEX

MST: Microscale thermophoresis

NF-κB: Nuclear factor κB

N/P pathway: Nucleation-prepitation pathway

NC: Needle Complex

NGS: Next-generation sequencing

N/nt: nucleotides

OM: Outer membrane

OPA: ortho-phthalaldehyde

PAGE: Polyacrylamide gel cletrophoresis

PCR: Polymerase chain reaction

PDMS: Polydimethylsiloxane

PG: Peptidoglyycan

ProSeAM: Propargylic Se-adenosyl-L-selenomethionine

PRRs: Pattern recognition receptors

PSC: p-sulfonatocalix[4] arene

PSMs: Peptide spectral matches

PTMs: Post-translational modifications

Rep: Repellents

RT-PCR: Reverse transcription-polymerase chain reaction

GO-SELEX: Graphene oxide-SELEX

HEGL: hexaethylene glycol

HEK: Human embryonic kidney

HILIC: Hydrophilic interaction liquid chromatography

HLB: Hydrophilic-Lipophilic Balance

hM-SILAC: heavy Methyl Stable Isotope Labelling by Amino Acids in Cell Culture

hnRNPs: Heterogeneous nuclear ribonucleoproteins

HTS: High-throughput sequencing

IAA: Iodoacetamide

IAP: Immunoaffinity purification

IEX: Ion exchange chromatography

IM: Inner membrane

ITC: Isothermal titration calorimetry

IL-1β: Interleukin 1β

KDMs: Lysine demethylases

KMTs: Lysine methyltransferases

LB: Lysogeny broth

LC: Liquid chromatography

LC-MS/MS: Liquid chromatography-tandem mass spectrometry

LODs: Limits of detection

LPS: Lipopolysaccharide

LSD1: Lysine-specific demethylase 1

SAM: S-adenosyl-L-methionine

SAH: S-adenosylhomocysteine

scFvs: Single-chain variable fragmentc

SCX: Strong cation exchange chromatography

SCV: *Salmonella*-containing vacuoles

SDS-PAGE: Sodium dodecyl sulfate-polyacrylamide gel electrophoresis

*S*. Enteritidis: *Salmonella enterica serovar* Enteritidis

SELEX: Systematic Evolution of Ligands by EXponential

SILAC: Stable isotope labelling by amino acids

SPI: *Salmonella* Pathogenicity Island

SPR: Surface Plasmon Resonance

*S*. Typhi: *Salmonella enterica* subsp. enterica serotype Typhi

*S*. Typhimurium: *Salmonella enterica serovar* Typhimurium

T: Thymine

T3SS: Type III secretion system

TFC: Trifluoroacetic acid

T4P: Type IV pilus

TLRs: Toll-like receptors

TML: Tri-methylated lysine

U: Uracil

vT3SS: Virulence-associated type III secretion system

WT: Wild type

# Table of contents

# General introduction

Flagella are essential organelles and virulence factors through adhesion processes and host colonization. It is well known that flagella are used for initial attachment to the host or to the surface of hospital equipment, but what follows adhesion is less clear. Recently, bacterial flagella have been reported to function as mechanosensors. However, how bacteria use their flagella to switch from a floating (planktonic) to an immediately attached (sessile) state remains an open question. Post-translational modifications (PTMs) are of particular interest in analysing the rapid adaptation of cells to respond to diverse environmental stimuli. It has been illustrated that flagellar methylations, especially lysine methylations, can promote bacterial adhesion to a surface or receptor *via* hydrophobicity. However, the study of the entire methylome (non-histone methylation) remains a challenge for the scientific community. *Salmonella enterica* serovar Typhimurium is a typical pathogenic bacterium with known antibiotic resistance. Different mutants of *S*. Typhimurium have various characterizations, including *ΔmetE*, which lacks the gene encoding methionine biosynthesis, *ΔmetEΔfliB* and *ΔmetEΔmotAB*, which refer to modifications in the genes involved in flagellar methylation and motility. Therefore, these strains were used in my PhD project to study the methylome of *S*. Typhimurium during bacterial mechanosensing. The aim of this thesis is to develop a novel tool to purify methylated peptides from these *S*. Typhimurium strains in order to study the connections between the methylation and bacterial mechanosensing.

We have applied two complementary strategies for targeting methylated lysine to enrich and purify methylated proteins/peptides containing methylated lysine, in particular tri-methyllysine. This PhD thesis consists of four chapters: a bibliographic chapter, two chapters focusing on the selection of DNA aptamers against methylated lysine and the applications of the specific aptamer against tri-methyllysine, and one chapter describing another alternative purification method for methyllysine-containing peptides.

**Chapter I** provided a general overview of the major virulence factors of *Salmonella*, including flagella, adhesins, and injectisomes. Bacterial mechanosensing associated with flagella and lysine methylation were described.

**Chapter II** developed specific DNA aptamers through the *in vitro* selection for mono-, di- and tri-methylated lysine from a random oligonucleotide library using the SELEX strategy. The

characterization of the specific aptamer for tri-methylated lysine was performed using ITC, bead-based assays and HILIC-MS/MS.

**Chapter III** explored the application of the selected aptamer against trimethyllysine to enrich the methylated proteins from the auxotrophic strain *S*. Typhimurium *ΔmetE* and the positive control HEK293 cells, which contain high levels of tri-methylated lysine based on the literature.

**Chapter IV** presented a known strategy, the high pH SCXtips to purify methylated peptides with methylated lysines were labelled in a hM-SILAC medium. A comparison between the high pH SCXtips and the aptamer-based strategy was performed to evaluate the efficiency and limitations of the aptamer-based method.

**Chapter V** provided a general discussion and conclusion of this work, including the background of the project, the selection of the aptamer, the characterization of the selected aptamer, the application of the aptamer-based solid surface to the purification of methylated proteins/peptides from cells, and a comparison with the high pH SCXtip approach.

# Chapter I Bacterial mechanosensing, protein methylation, and associated study tools

## I.1 *Salmonella*

The bacteria belonging to the genus *Salmonella* is one of the most common foodborne bacterial zoonoses (Bell *et al.*, 2016). It's a major public health concern worldwide. Even though there are some rapid developments in technologies such as genomics and metagenomics to monitor and control salmonellosis, millions of salmonellosis cases have been estimated by the World Health Organization (WHO) each year (Besser, 2018). While the symptoms of salmonellosis are relatively mild and self-limiting in healthy individuals, immunocompromised patients, children (< 1 year of age), and the elderly (≥60 years of age) can be affected with diarrhoea and severe dehydration (Cremon *et al.*, 2014). As a result, it may lead to life-threatening bloodstream infections or hypovolemic shock that require appropriate and effective antibiotic therapy (Gut *et al.*, 2018).

However, with the misuse of antimicrobials in both humans and animals, antimicrobial resistance is increasing in pathogenic and commensal bacteria within the treated host (Mcdermott, Zhao and Tate, 2018). Thus, as typical models of global multidrug-resistant bacteria, *Salmonella spp.* are having a great impact on the efficacy of antibiotic treatment (Eng *et al.*, 2015). An increase in mortality rates of infected patients caused by these more virulent pathogens has been attracting the public's attention. In the physiology field, *Salmonella* species are significant not only as a potential threat to public health worldwide, even causing deaths, but also as a fruitful model system for the study of fundamental mechanisms of bacterial pathogenesis during various stages of infection (Ohl and Miller, 2001). Therefore, more investigations of *Salmonella* pathogenesis, its motilities, and the prevalence of *Salmonella* infections, are aiming to find new ways of preventing and treating *Salmonella* infections. Altogether, the studies of this bacterial model will provide further insight into general mechanisms of microbial pathogenesis and bacterial resistance.

### I.1.1 Generalities

*Salmonella* was first discovered and isolated from the intestines of a pig suffering from swine fever in 1855 by Theobald Smith and was named after Dr Daniel Elmer Salmon (Eng *et al.*,

2015). *Salmonella* is a diverse genus of Gram-negative, non-spore-forming, facultative anaerobic, and rod-like shaped bacterial pathogens (Tauxe, 1991). Serotyping is the process of identifying different strains of a single species of bacteria based on the proteins on their surface. In the case of *Salmonella* serotyping, it is performed through the agglutination tests of *Salmonella* cells with the three major antigenic determinants (somatic O, flagellar H, and capsular Vi-antigens) present on the bacteria according to Kauffman-White-scheme (Popoff, Bockemühl and Gheesling, 2004; Kagambèga *et al.*, 2011). The O antigens are components of the bacterial cell wall, especially the lipopolysaccharide (LPS) layer with different chemical constitution (Ibrahim and Morin, 2018). They are used to classify *Salmonella* into different serotypes. The H antigens are parts of the flagellar structures and are used to classify *Salmonella* into different subtypes within a given serotype. The Vi-antigens, the least common antigens, are made of heat-sensitive polysaccharides located at the bacterial capsular surface of some *Salmonella* strains. With the specific combinations of O and H antigens, over 2600 serotypes of *Salmonella* spp. have been isolated and identified (Allerberger *et al.*, 2003).

In general, all *Salmonella* serotypes can be divided into two main groups, typhoidal and nontyphoidal *Salmonellae* (Parry and Threlfall, 2008). In contrast, typhoidal *Salmonellae* are highly restricted to humans and cause systemic infections like typhoid fever, whereas nontyphoidal *Salmonellae* usually cause self-limiting gastrointestinal disease (http://www.who.int/mediacentre/factsheets/fs139/en/) and have a broad range of hosts including humans, poultry, swine, or cattle (Gal-Mor, 2019). There were estimated 153 million gastroenteritis cases due to nontyphoidal *Salmonella* per year, including 56000 deaths (Kirk *et al.*, 2015). *Salmonella* cells are mobile by means of a peritrichous flagellum (**Figure I-1**). Most *Salmonella* serovars (synonymous to serotype) are typically 2- 5 µm in length by 0.5-1.5 µm wide, depending on the serotype, their genome ranges from 4460-4857 kb (Andino and Hanning, 2015; Gut *et al.*, 2018). *Salmonella* belongs to Enterobacteriaceae family and is closely related to the *Escherichia*, *Shigella*, and *Yersinia* genera. Based on differences in 16S rRNA sequence, the genus *Salmonella* is classified into two species, *Salmonella bongori* and *Salmonella enterica* (Finlay and Brumell, 2000). Approximately 60% of all *Salmonella* serotypes belong to the *Salmonella enterica* (Griffith, Carlson and Krull, 2019). *Salmonella enterica* is further subdivided into 2500 serovars belonging to six subspecies, including *S. enterica* subsp. *enterica* (I), *S. enterica* subsp. *salamae* (II), *S. enterica* subsp. *arizonae* (IIIa),

*S. enterica* subsp. *diarizonae* (IIIb), *S. enterica* subsp. *houtenae* (IV), and *S. enterica* subsp. *indica* (VI), based on their genomic relatedness and biochemical properties (Reeves *et al.*, 1989). Among these subspecies, *S. enterica* subsp. *enterica* (I) is found predominantly in mammals and accounts for approximately 99% of *Salmonella* infections in humans and warm-blooded animals (Brenner *et al.*, 2000). In contrast, the other five *Salmonella* subspecies and *Salmonella bongori* are found mainly in the environment and in cold-blooded animals (Aleksic, Heinzerling and Bockemühl, 1996; Eng *et al.*, 2015), including reptiles and amphibians. Additionally, the serotypes of *Salmonella enterica* associated with foodborne illness in humans and animals can also be classified into the serovars Typhimurium (*S*. Typhimurium) and Enteritidis (*S*. Enteritidis) on the basis of their antigenicity and individual's immune system. They have consistently been the 2 most common serovars of nontyphoidal *Salmonellae* reported from sub-Saharan Africa (Gordon *et al.*, 2008).


**Figure I-1 *Salmonella enterica* serovar Typhimurium**
Visualized by scanning electron microscope (left) and colonies of *S*. Typhimurium growing on agar (right). Photo source: downloaded from https://www.reactgroup.org/toolbox/understand/bacteria/.

*Salmonella* species infect a range of hosts and cause several diseases, including gastroenteritis (diarrhoea, abdominal cramps, and fever) and enteric fevers (including typhoid fever) in humans and farm animals especially in poultry, cattle, and pigs (Coburn, Grassl and Finlay, 2007). *Salmonellae* are typically acquired by oral ingestion of contaminated food more specifically uncooked animal products (like eggs and meat), and water. Fruits and vegetables also act as sources of *Salmonella*. Some *Salmonella* serotypes are restricted to a specific host, while others can infect a broad host range and transmission (**Figure I-2**) (Feasey *et al.*, 2012). All *Salmonella* serotypes share the ability to invade the host. For example, *Salmonella* Dublin

and *Salmonella* Choleraesuis are two host-adapted strains in porcine and bovine and are strongly associated with the bacteraemia (Grzymajło *et al.*, 2013). When orally ingested, *Salmonella* can survive in the digestive tract and invade the intestinal epithelia or cross the intestinal barrier to spread throughout the reticuloendothelial system (typhoid fever) to establish systemic infection and replicate in mononuclear phagocytes and eventually lead to disease transmission to other people (Haraga, Ohlson and Miller, 2008). *Salmonella* does not produce exotoxin, but when the cells are lysed, they can release toxic endotoxin, which is the main cause of the disease and can cause the body's cold, fever, and leukopenia (Bischofberger and van der Goot, 2008).

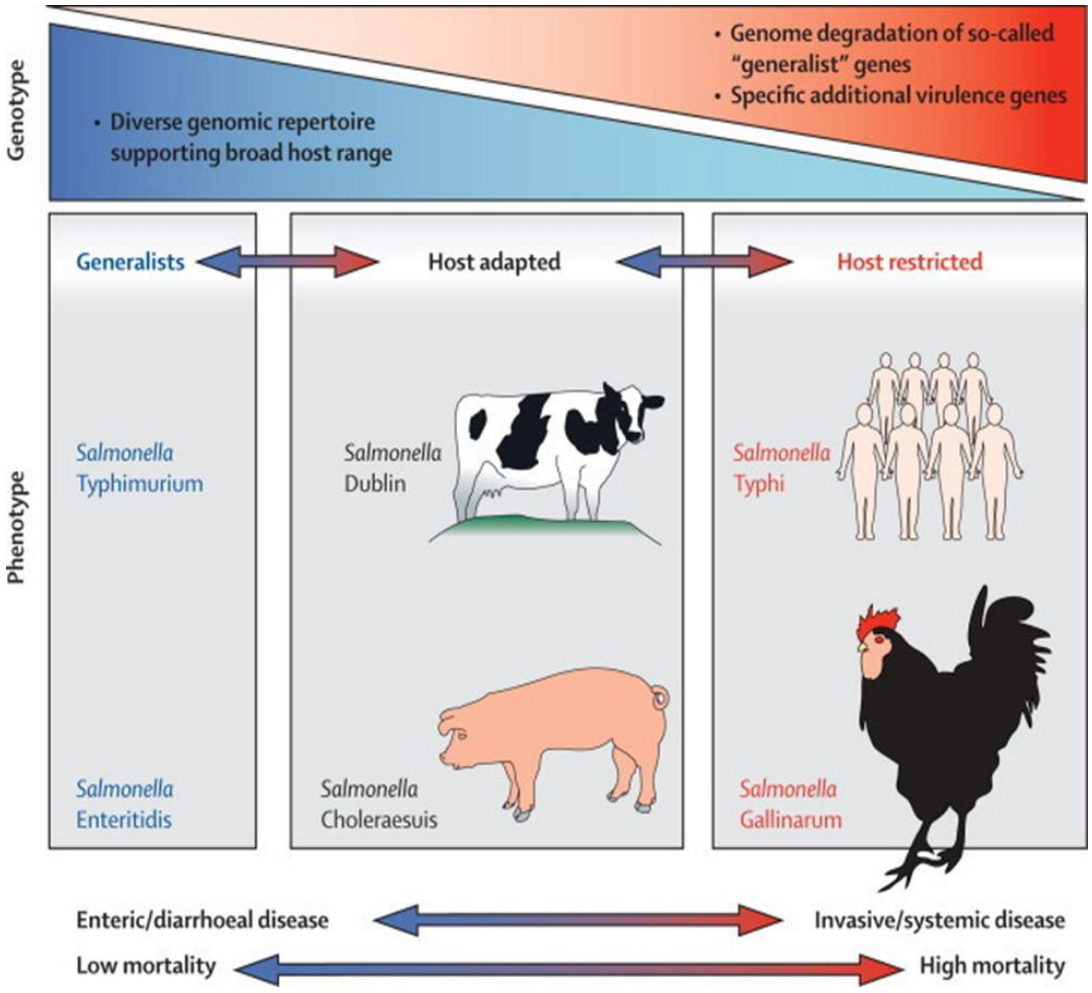


**Figure I-2 Features of host adaptation in salmonellae and effects on the clinical syndrome in the host**
The range of clinical syndromes and their relevance to the host range and transmission of different serotypes. Source: Feasey *et al.*, 2012.

In recent years, the antibiotic resistance rate of *S*. Typhimurium has been increasing throughout the world, resulting in approximately two-thirds of the invasive nontyphoidal

*Salmonella* disease in humans in Africa (Feasey *et al.*, 2012). Therefore, it is important to understand the mechanisms responsible for multidrug resistance in *Salmonella* strains. The molecular mechanisms underlying *Salmonella* colonization, pathogenesis and transmission in reservoir hosts remain ill-defined (Lauteri *et al.*, 2022). Therefore, it's essential to reveal the correlation between *Salmonella* pathogenicity and how the bacteria adapt to its host.

### I.1.2 *Salmonella* pathogenesis

Almost all strains of *Salmonella* are pathogenic due to their ability to invade, replicate and survive in host cells, resulting in potentially fatal disease (Eng *et al.*, 2015). *Salmonella* and other bacteria use their virulence factors in the process of bacterial infections including the route of entry into the host and to fight the host's defence mechanisms. Upon colonization, *Salmonella* begins to secrete several effectors (i.e., AvrA, SopB, SipB, SifA, and SopA) into the intestinal milieu to trigger either inflammation or bacterial entry into the host cells (Srikanth *et al.*, 2010). To get a successful infection, *Salmonella* needs an entry site on the target cell surface. Subsequently, the bacteria move to various tissues to invade host tissues and organs and proliferate to finally cause host infection (**Figure I-3**) (Duan *et al.*, 2013).

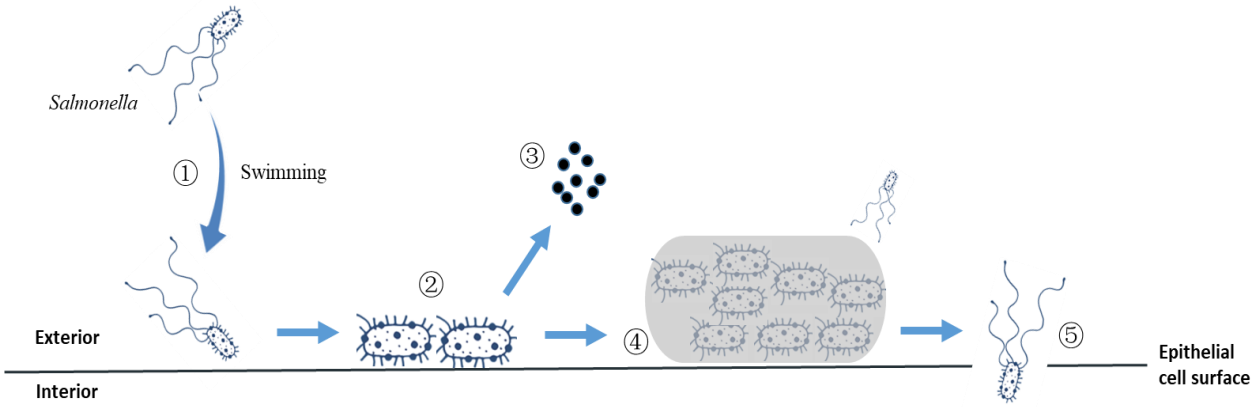


**Figure I-3 The process of *Salmonella* pathogenesis established**

Inspired by Duan *et al.*, 2013. ① Movement of bacteria toward host target sites at the cell surface. ② Adhesion of bacteria to the epithelial cells by reversible attachments firstly mediated by flagella, pili (also known as fimbriae). ③ Upon bacterial colonization, secretion of effectors (black dots). ④ Irreversible cell body attachment and biofilm formation. ⑤ Host invasion.

In the active invasion process of non-phagocytic host cells (Velge *et al.*, 2012), *Salmonella* can induce its phagocytosis, relying on various virulence factors including specialised effectors to gain access to the host cells (Haraga, Ohlson and Miller, 2008; McGhie *et al.*, 2009). These

effectors are a set of bacterial proteins that are delivered into host cells altering host cell physiology for bacterial entry and survival (Srikanth *et al.*, 2011). Active host cell invasion by *Salmonella* requires the function of the evolutionarily conserved type III secretion system (T3SS) encoded on *Salmonella* pathogenicity islands 1 and 2 (SPI-1 and SPI-2). On these SPI, other effectors (translocate virulence proteins) are found to act in concert. These effectors are directly injected across the intestinal epithelial cell membrane into the host cell cytoplasm (Gal-Mor, 2019). Once delivered by the T3SS, these effectors manipulate the host cell to allow bacterial invasion, alter signalling transduction pathways and induce inflammatory responses. For instance, effectors SipA and SipC are involved in rearranging the host cell cytoskeleton to help *Salmonella* to move within the host cell (Myeni and Zhou, 2010). In contrast, other effectors such as SopE/E2 and SopB are translocated by SPI-1, involved in activating the host cell's Rho GTPases (Truong *et al.*, 2018), while SptP mediates the recovery of the membrane ruffling (Agbor and Mccormick, 2011). Effector SpvC contributes to a reduction in intestinal inflammatory response during infection (Haneda *et al.*, 2012). The SPI-2 effectors SseK1 and SseK3 inhibit nuclear factor κB (NF-κB) signalling to control the immune responses and cell survival (Günster *et al.*, 2017). Active invasion of nontyphoidal *Salmonella* is associated with the process of phagocytosis, which effectively limits their dissemination (Larock, Chaudhary and Miller, 2015). Macrophage is another obstacle to innate immunity to fight *Salmonella* once salmonellae are found in the intestinal epithelium (Ohl and Miller, 2001). Macrophages migrate toward infected epithelial cells and recognize *Salmonella* as "non-self" and actively phagocytize the bacteria (Eng *et al.*, 2015). After phagocytosis, *Salmonella* activates virulence mechanisms to enable its survival and replication (Monack, Mueller and Falkow, 2004).

The effective dose for human salmonellosis is from $10^5$ to $10^6$ cells capable of establishing infection in the mucosa of the small intestine (Xu, Lee and Ahn, 2010). During the invasion process to the small intestine, *Salmonella* crosses the intestinal mucus layer and then encounters and adheres to intestinal epithelial cells. Interestingly, *Salmonella* preferably adheres and enters *via* microfold cells (M cells) found in lymphoid structures. These cells help the bacteria to reach the lymphoid cells (T and B cells) and other neutrophils and intestinal macrophages (like dendritic cells) in the underlying Peyer's patches (Jones, Ghori and Falkow, 1994) (shown in **Figure I-4**) (Gart *et al.*, 2016). When in contact with the immune cells, *Salmonella* is engulfed into the cell, and the bacterium is then encased in a membrane

compartment called a vacuole, which is composed of the host cell membrane (Ly and Casanova, 2007).

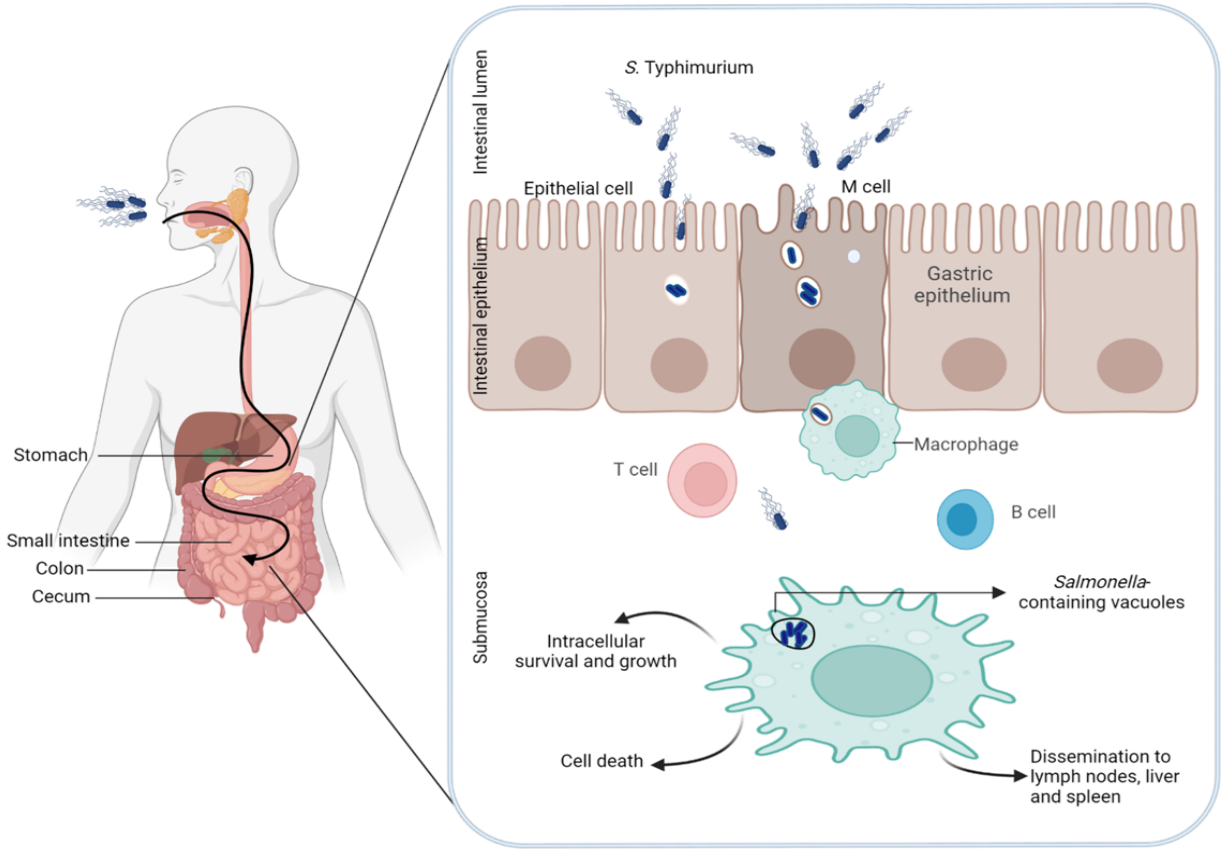


**Figure I-4 Route of infection by *Salmonella* Typhimurium**

The picture resource: created with https://www.biorender.com/, Which inspired from (Haraga, Ohlson and Miller, 2008; Gal-Mor, 2019). *Salmonella* is taken up by consumption of contaminated food or beverage. After gaining access to the intestinal lumen, *Salmonella* can cross the apical pole of the epithelial barrier through M cells in the small intestine, inducing a rearrangement of the host's actin cytoskeleton, leading to active engulfment. Following, the type III secretion system delivers distinct effector proteins directly into host cells, which also triggers gut inflammation. Invasive nontyphoidal *Salmonella* in immunodeficient patients or typhoidal *Salmonella* can evade the immune system, enter subepithelial phagocytic cells such as macrophages, and survive within them. Phagocytic cells can then transport *Salmonella* bacteria *via* the lymphatic system and disseminate the bacteria systemically (mainly to the liver, spleen, and lymph nodes). Within the intracellular environment, *Salmonella*-containing vacuoles support bacterial survival and replication. The presence of *Salmonella* within the cells may lead to cytokine secretion, triggering inflammation and/or programmed cell death (apoptosis).

During this process, *Salmonella* adheres to the apical epithelial surface resulting in actin cytoskeleton rearrangements, and induces the formation of membrane ruffles, which enclose adherent *Salmonella* in large vesicles (Tillotson and Tillotson, 2009). Under normal circumstances, when bacteria invade the host cells, the immune responses are activated, resulting in the fusion of the lysosomes and the secretion of digesting enzymes to degrade

the intracellular bacteria (Ohl and Miller, 2001). However, *Salmonella* uses T3SS to inject effectors into the endocytic vacuole (Agbor and Mccormick, 2011). The remodelled vacuole (*Salmonella*-containing vacuoles, SCV) blocks the fusion of the lysosomes (Steele-mortimer, 2008), to allow the intracellular survival and replication of the bacteria within the host cells. Finally, *Salmonella* can reseed the intestinal lumen through the bile ducts and be shed in the feces to the environment, ready to infect a new host (Gal-Mor, 2019).

### I.1.3 Virulence factors *in Salmonella*

The pathogenicity ability of *Salmonella* and the bacterial model *S*. Typhimurium are closely related to their virulence factors. The virulence factors (**Figure I-5**) are specific molecules or products that contribute to infection and that determine the degree of pathogenicity of the corresponding serotype (Jong *et al.*, 2012).

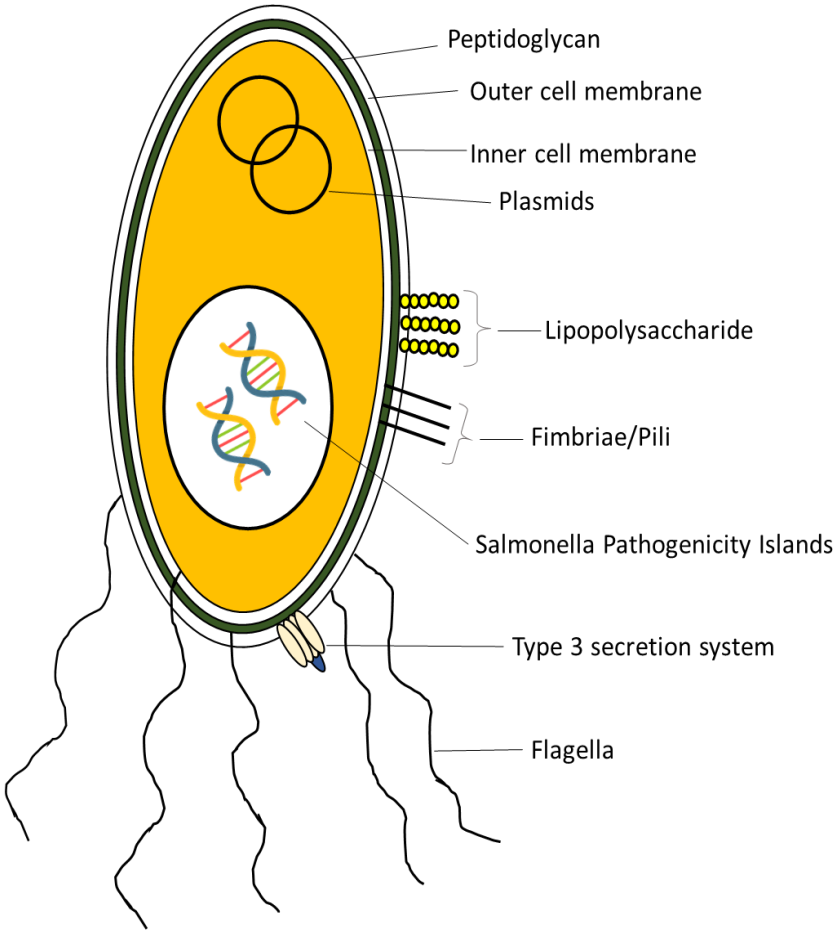


**Figure I-5 Virulence of *S*. Typhimurium**

Based on Jong *et al.*, 2012. *S*. Typhimurium possesses several virulence factors, including the type III secretion system (T3SS), lipopolysaccharide, other surface polysaccharides, fimbriae, flagella, and bacterial DNA.

In addition to unique virulence factors such as typhoid toxin, and Vi antigen in *S*. Typhi, most virulence factors are encoded on T3SS (SPI-1 and SPI-2), or on virulence plasmids (pSLT) containing a highly conserved *spv* operon (Gulig, 1990; Santos, Ferrari and Conte-Junior, 2019). The new and significant insights concerning the most relevant virulence factors including flagella, adhesins (fimbriae/pili), and injectisomes are described as follows.

### I.1.3.1 Bacterial flagella

As one of the most important virulence factors, flagella are involved in the initial phase of the infection process and play a major role in bacterial motility and chemotaxis (Rossez *et al.*, 2015). Flagella are found in both Gram-positive and Gram-negative, long, thin, hair-like structures that protrude from the cell body and act primarily as an organelle of locomotion in the cells of many living microorganisms (Silverman and Simon, 1977). The arrangement and the number of flagella vary among bacterial species. *Salmonella spp.* have peritrichous flagella distributed all over the cells. The flagellum is a complex helical structure, consisting of hundreds of flagellin proteins. Structurally, it consists of three main parts: a basal body, a hook, and a long filament (up to 15-20 µm in length (Wee and Hughes, 2015)) (**Figure I-6**).

The basal body is composed of a motor (MotAB), a rod, and several ring components (LP rings, MS-C rings) that anchor the flagellum in the cytoplasmic membrane, working as a rotary motor powered by proton motive force (PMF) (Kawamoto *et al.*, 2013; Minamino and Imada, 2015). The L ("lipopolysaccharide"), P ("peptidoglycan"), MS ("membrane/supramembrane") and C ("cytoplasmic") ring are in the outer membrane, peptidoglycan layer, cytoplasmic membrane and cytoplasm, respectively (**Figure I-6**).

The MS ring interacts with C ring and forms a MS-C complex which acts as a reversible rotor of the flagella motor (Minamino, Imada and Namba, 2008; Aizawa, 2015). The rod extends the rotor from the inner membrane to the outer membrane and directly connects to the MS-ring and acts as a drive shaft. The flexible hook is made up of about 130 copies of protein FlgE and has an average length of 55 nm under molecular ruler controls (Erhardt *et al.*, 2011). It links the rod and filament, functioning to transmit torque produced by the motor to the filament (Thormann and Paulick, 2010). The filament forms the helical propeller and is composed of thousands of copies of the flagellin (FliC or FljB), which extends from the cell surface and propels the bacterium through its environment (Nedeljković, Sastre and Sundberg,

2021). The stator complex ($MotA_4MotB_2$) working as a proton channel surrounds the basal body rings and is regulated by the active motor complexes that are necessary for flagellar rotation (Minamino, Imada and Namba, 2008; Morimoto and Minamino, 2014).

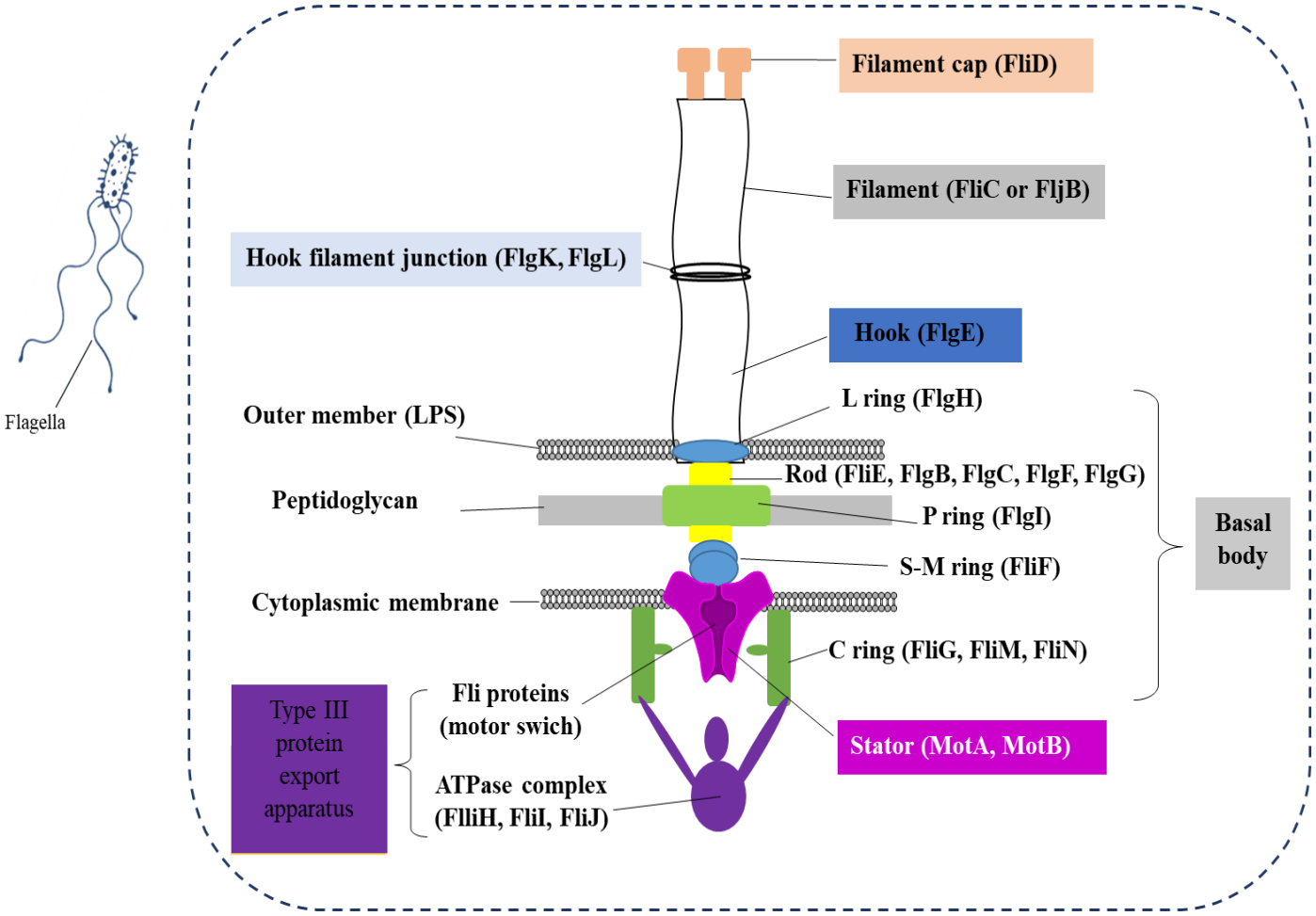


**Figure I-6 Schematic presentation of Salmonella flagellum structure**

Based on Yamaguchi *et al.*, 2020. A flagellum consists of three main parts: the filament, the hook, and the basal body, with includes a flagellar-associated type III secretion system (fT3SS). The basal body contains of the LP rings (brushing), the rod (drive shaft), the MS-C rings (reversible rotor), and the flagellar protein export apparatus. The component proteins are shown in black letters.

*S*. Typhimurium has approximately 6-10 flagella around the cell. The flagellum is typically assembled in a hierarchical process external to the inner membrane. Most proteins that composed the flagellar components are required to be transported through the fT3SS (FlhAB, FliHIJ and FliOPQR) at the base of the basal body. The ATPase complex (FliHIJ) and PMF-driven transmembrane export gate complex (FlhAB and FliOPQR) drive flagellar protein export through the cytoplasmic membrane (Inoue *et al.*, 2019). The T3SS forms the MS- (FliF) and C-ring (FliGMN) independently. The MS-C complex is one important component of the

conserved motor structure (Khan, Reese and Khan, 1992). Next, the rod (FliE, FlhE, and FlgBCFG), P-ring (FlgI)and L-ring (FlgH) self-assemble to form a channel for protein secretion to extracellular components (Minamino, Imada and Namba, 2008). In rod structure, FliE connects with FlgB and forms a junction connecting the MS-ring, whereas FlgG stabilizes the whole rod (Minamino, Yamaguchi and Macnab, 2000; Fujii *et al.*, 2017). The hook is formed by hook-protein FlgE at the tip of the rod. It's a short, curved tubular structure made of 11 protofilaments (Fujii, Kato and Namba, 2009). Four domains D0, Dc, D1, and D2 are found for FlgE. Among them, the interactions of D1-D2 domains probably decide the curvature of the supercoiled structures (Samatey *et al.*, 2004). The domain Dc relates to the polymorphic transformation of the supercoiled form of the hook (Hiraoka *et al.*, 2017). A hook-filament junction (FlgKL) links the hook and the filament and this is essential for the formation of the filament (Herrmann and Aebi, 2000). The filament (FliC or FljB), a rotary and rigid helical structure, drives the cell forward by rotating (Yamaguchi *et al.*, 2020). Flagellin is the structural protein of the flagellum. The expression of FliC or FljB is autonomously regulated by flagellin genes *fliC* and *fljB*. *Salmonella* alternately expresses FljB and FliC at a frequency of $10^{-3}$-$10^{-4}$ per cell per generation for filament formation, in a flagellar phase variation process (Bonifield and Hughes, 2003). The flagellin FliC or FljB consists of 4 domains, including D0, D1, D2 and D3, arranged from the inner core to the outer surface of the filament, respectively, as shown in **Figure I-7**.

To form these domains, flagellin peptides fold back with the termini associated with one another, like an elaborate hairpin. The N-terminal chain begins from ND0, linking ND1 and D2 to reach D3, and then turns back on itself, through CD2, CD1 to end with CD0, the C-terminal extremity (**Figure I-7a**). Among them, domains D0-D1 form the inner core and outer tubes of the concentric double-tubular structure (**Figure I-7b**), which are critical for forming the supercoiled filament as a helical propeller (Beatson, Minamino and Pallen, 2006; Horváth *et al.*, 2019). The conserved hydrophobic residues of domains D0-D1 (α-helixes regions) are responsible for inducing the innate immune defence *in vivo*, whereas the β-hairpin structure in domain D1 helps it switch the conformation of flagellin subunits between the swimming and tumbling states (Samatey *et al.*, 2001; Maki-Yonekura, Yonekura and Namba, 2010). In contrast, the domains D2-D3 (the central hypervariable region) are highly variable, generate antigenic diversity and are directly exposed (**Figure I-7c**). They can increase the stability of

the filament by increasing the diameter (Kim *et al.*, 2018). Compared to the structure of FliC, FljB has an identical conformation except for the position and orientation of the outermost domain D3 (Yamaguchi *et al.*, 2020). Domain D3 plays an important role in determining the antigenicity of flagella and in optimizing the motility function of the filament under different conditions (Yamaguchi *et al.*, 2020). The filament cap (FliD) assembles as a lid with five axially extended leg-like domains, which is crucial for a proper assembly of the flagellin by continuously inserting new flagellin into the tip of the filament (Yonekura *et al.*, 2000; W. S. Song *et al.*, 2017).

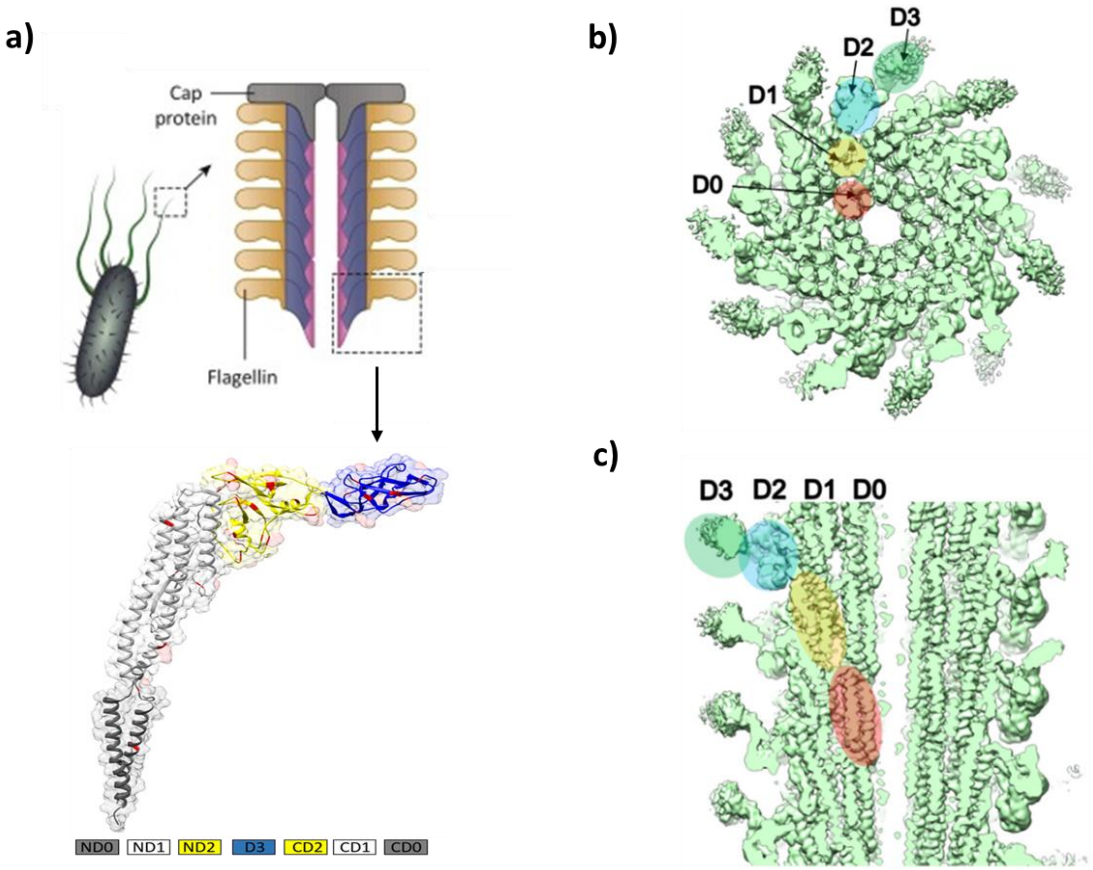


**Figure I-7 Flagellin structures, and domains and methylation sites**

(a) Organization of flagellin and domains in flagellins based on (Rossez *et al.*, 2015; Vijayan *et al.*, 2018). The sites in red correspond to lysine. (b) Cross section and (c) longitudinal section along the filament axis (Yamaguchi *et al.*, 2020). The four domains D0 (the terminal α-helixes), D1 (the central α-helixes), D2 and D3 (the hypervariable β-sheets and turns) are labelled in pink, yellow, blue and green, respectively in (b, c).

The flagellum is able to rotate either clockwise (CW) or counterclockwise (CCW) directions by flagellar motors to change the swimming direction of bacteria. *S*. Typhimurium possesses two types of motility: (i) swimming motility in liquid environment and (ii) swarming motility on

surfaces (Horstmann *et al.*, 2017). When the cell swims straight in a liquid or low agar (0.1-0.3%), the motors rotate to spin CCW and the filaments in the left-handed supercoiled structure form a large bundle behind the cell to generate a thrust force (Yamaguchi *et al.*, 2020). Once one or more motors switch their rotation to the CW direction, the flagellar bundle falls apart by switching the filaments to a right-handed supercoil, resulting in orientation changes by tumbling (**Figure I-8A)**. In the run-tumble swimming pattern, tumbles usually last only a fraction of a second but is sufficient for the direction of the next run (Grognot and Taute, 2021). The transformations between running and tumbling mode occur when bacteria move on towards favourable growing conditions such as attractants while avoiding unfavourable stimulus like repellents (**Figure I-8B**) (Damton *et al.*, 2010). The dynamic C-ring (FliG, FliM, and FliN) and filament structure are responsible for switching the swimming direction.

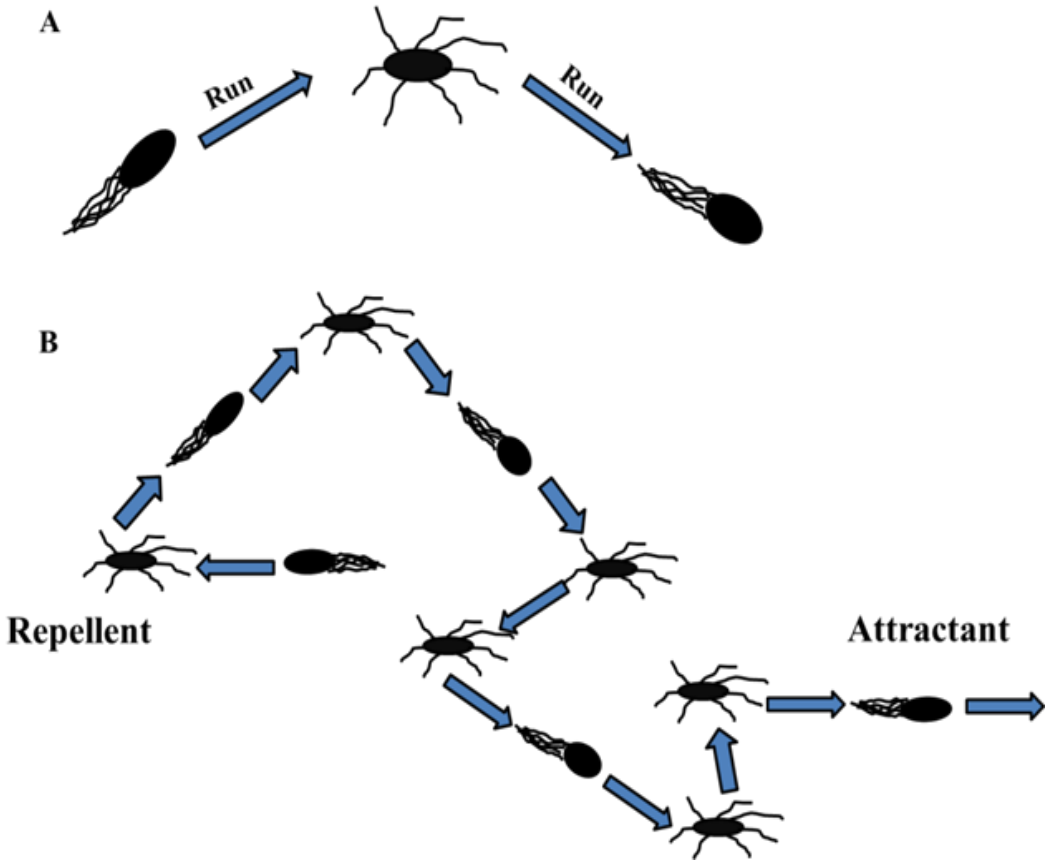


**Figure I-8 *Salmonella* motility model and chemotaxis state**

Based on Wadhams and Armitage, 2004. (A) Bacteria such as *S*. typhimurium exhibit two modes of swimming: runs and tumbles. (B) Cells tend to continue the course when running towards attractants; when swimming away from attractants they tend to tumble and change direction.

To coordinate bacterial walk towards or away from environmental concentration gradients, *Salmonella* achieves chemotaxis that enables the bacteria to find nutrients and navigate towards favourable environments while avoiding harmful ones, using several chemoreceptor systems (Raina *et al.*, 2019). The chemotaxis system is composed of two main components: the chemoreceptors and flagellar motors. The chemoreceptors are located on the surface of the cell and are responsible for detecting chemical gradients in the environment and sending signals *via* phosphorelay to the flagellar motors (Ortega and Zhulin, 2016). The core of signal processing in the bacterial chemotaxis system is a modified two-component system CheA-CheY (Luu *et al.*, 2019), which leads to the autophosphorylation of the sensor kinase CheA and in turn transphosphorylation to the CheY response regulator (**Figure I-9**) (Bi and Sourjik, 2018; Wei *et al.*, 2020).

Repellents and attractants bind to the periplasmic domains of the transmembrane chemoreceptors and control the shifts in the "kinase-on-kinase-off" switch *via* signalling complexes containing the receptors CheA (a histidine autokinase) and CheW (a protein that couples CheA activity to receptor control) (Hazelbauer, Falke and Parkinson, 2008; Briegel *et al.*, 2012). Under an increased repellent or decreased attractant stimulation, CheA is activated ("kinase-on" state) and donates phosphoryl groups to its response regulators, CheY for motor control and CheB for sensory adaptation, using ATP as the phosphodonor. The increased levels of phosphorylated CheY subsequently bind to FliM in the C-ring and trigger the flagellar motors to switch their rotation from CCW to the CW direction. On the contrary, under an increased attractant stimulation, CheA is inhibited ("kinase-off" state) resulting in a decreased level of phosphorylated CheY and the motors revert to default CCW rotation and consequently prolonged running phases towards favourable sites (Krell *et al.*, 2011; Huang *et al.*, 2019). However, phosphorylated CheY is unstable and can be rapidly dephosphorylated by the phosphatase CheZ. This dephosphorylation by CheZ ensures that the CW flagellar rotation is only transient and lasts for a short duration, allowing the cell to switch to CCW rotation and swim toward attractants (Hazelbauer, Falke and Parkinson, 2008).

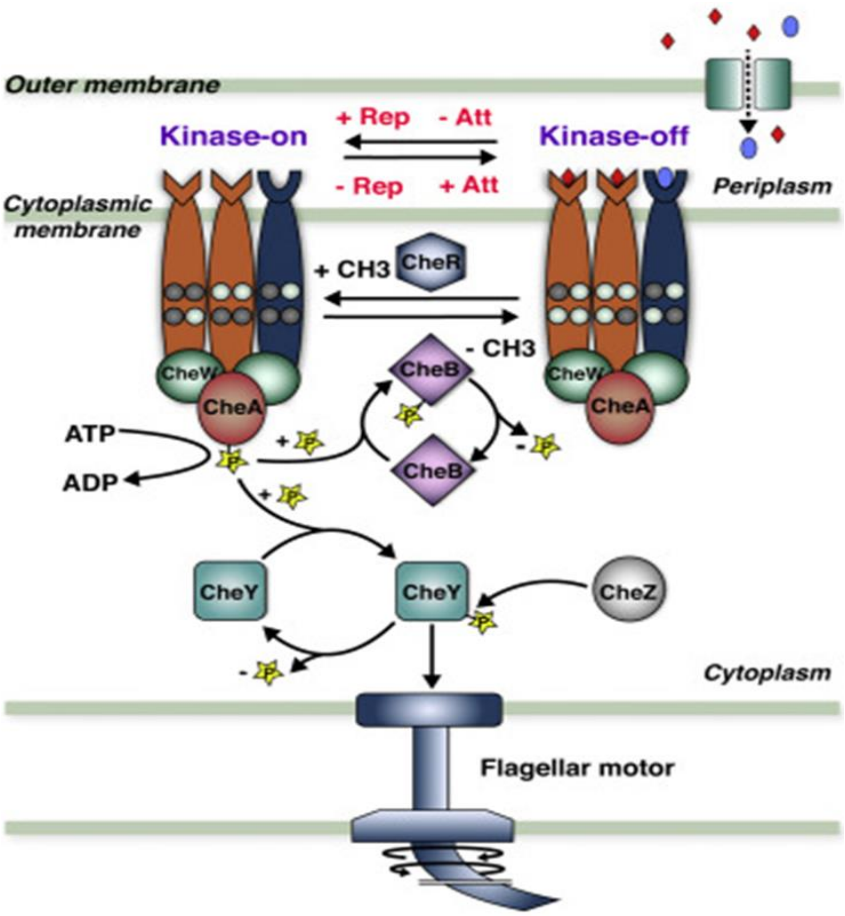


**Figure I-9 Schematic representation of chemotaxis signalling pathways**

Source: Bi and Sourjik, 2018. Attractants (Att, indicated by colored diamonds/ovals) promote an inactive (kinase-off) state of sensory complexes, which leads to counter clockwise rotation of flagellar motors and smooth runs. Repellents (Rep) promote a kinase-on state, leading to clockwise motor rotation and tumbles. CheA (a histidine autokinase) and CheW (a protein coupling CheA actively to receptor control) are chemoreceptors, also termed methyl-accepting chemotaxis proteins. The "kinase-on" conformation activates CheA autophosphorylation, whereas the "kinase-off" conformation deactivates CheA autophosphorylation. An increase in attractant concentration switches receptors to "kinase-off" state, whereas an increase in repellent concentration (or a decrease in attractant concentration) shifts receptors to the "kinase-on" state. CheR and CheB tune receptor methylation and demethylation at specific glutamate residues according to the receptor activity state. CheR methylates inactive receptors, reactivating them, while CheB demethylates active receptors, deactivating them (Pontius, Sneddon and Emonet, 2013).

In addition, reversible chemoreceptor methylations also play a central role in bacterial chemotaxis by methyltransferase CheR and methylesterase CheB (Krembel, Neumann and Sourjik, 2015). Methylation and demethylation of the chemotaxis effectors by CheR and CheB tune receptor sensitivity and kinase activity in a feedback cycle (Toews *et al.*, 1979; Briegel *et al.*, 2012; Dufour *et al.*, 2014). When an attractant is added, CheB is activated and competes with CheY for the phosphoryl group from CheA and eventually carrying out demethylation on

the “kinase-on” receptors CheA, thereby reducing their activity (Stock and Koshland, 1978; Stock, Koshland and Stock, 1985). As a result, the flagella perform smooth swimming by exclusively CCW rotation (Springer, Goy and Adler, 1979). On the contrary, CheR preferentially recognizes the receptors that are in a “kinase-off” state and increases receptor activity through methylation to control its methylation state together with CheB (Clarke *et al.*, 1980; Colin and Sourjik, 2017). Specifically, CheR transforms the methyl groups to glutamate residues in the signaling domains of the chemoreceptors (Antommattei, Munzner and Weis, 2004). The methylation by CheR activates CheA, leading *Salmonella* to follow the gradients by modulating them tumbling (Lupas and Stock, 1989). Recently, overexpression of CheR was found to promote the *S*. Typhimurium invasion of epithelial cells but inhibit intracellular survival (Su *et al.*, 2021).

Therefore, chemotaxis ensures the bacteria to respond appropriately to the environmental changes. This process plays an important role in the survival and pathogenicity of *Salmonella*, allowing them to enhance access to growth substrates and to infect their host (Matilla and Krell, 2018). In addition, the interactions between chemoreceptors and the host are essential for cell adhesion and invasion (Olsen *et al.*, 2013).

Flagella are also associated with the recognition and modulation of the host immune system through pattern recognition receptors (PRRs) (**Figure I-10**), Toll-like receptors (TLRs), more particularly TLR5 (Akira, Uematsu and Takeuchi, 2006) and NOD-like receptors (NLRs), which are expressed by various immune and non-immune host cells. These receptors are located on the surface of endocytic compartments, detecting specific molecular patterns on the surface of the flagella, known as microbe-associated molecular patterns (MAMPs) (Clare, 2021).

Once the PRRs recognize the flagella, they trigger the activation of the immune cells and the production of inflammatory cytokines such as caspase-1 and interleukin 1β and chemokines and result in the immune response aimed at eliminating the bacteria (Bierschenk, Boucher and Schroder, 2017). However, Salmonella developed several mechanisms to modulate the immune response to its advantage (Galán, 2021), including modifying the flagellin structure and downregulating flagella expression. *Salmonella spp*. can therefore prevent immune recognition or induce a weaker immune response.

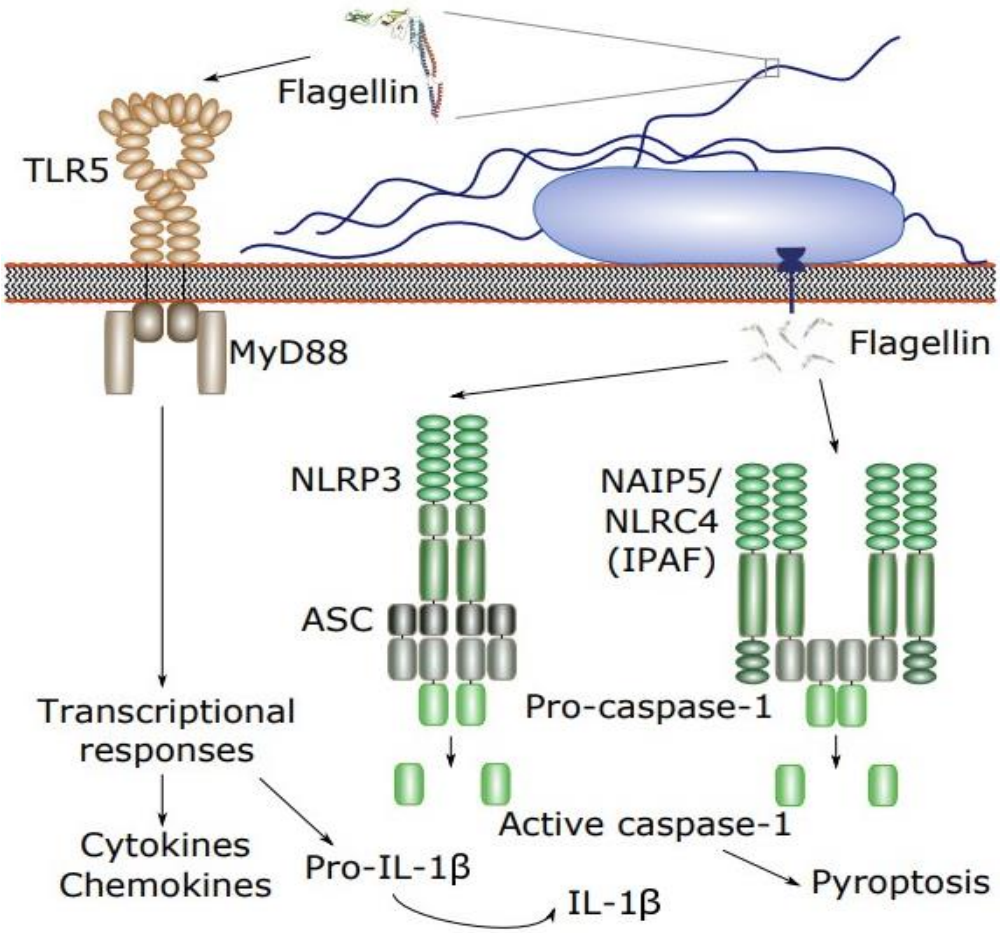


**Figure I-10 Flagellin recognition by the host innate immune system**

Source: Horstmann, 2017. Extracellular flagellin is recognized by the Toll-like receptor TLR5 and NAIP-NLRC4, resulting in the induction of cytokine release and activation of immune cells. Intracellular flagellin is recognized by Nod-like receptors, leading to the activation of caspase-1 and interleukin 1β (IL-1β).

In summary, as an important virulence factor, flagella play multifactorial roles in bacterial pathogenesis including controlling bacterial motility, adhesion to or invasion of epithelial cells, colonization of the host, and exploiting inflammation (**Figure I-11**). The multiple roles of the flagellins ensure the bacterial pathogens' maximal survival in the host microenvironments and efficient infection.

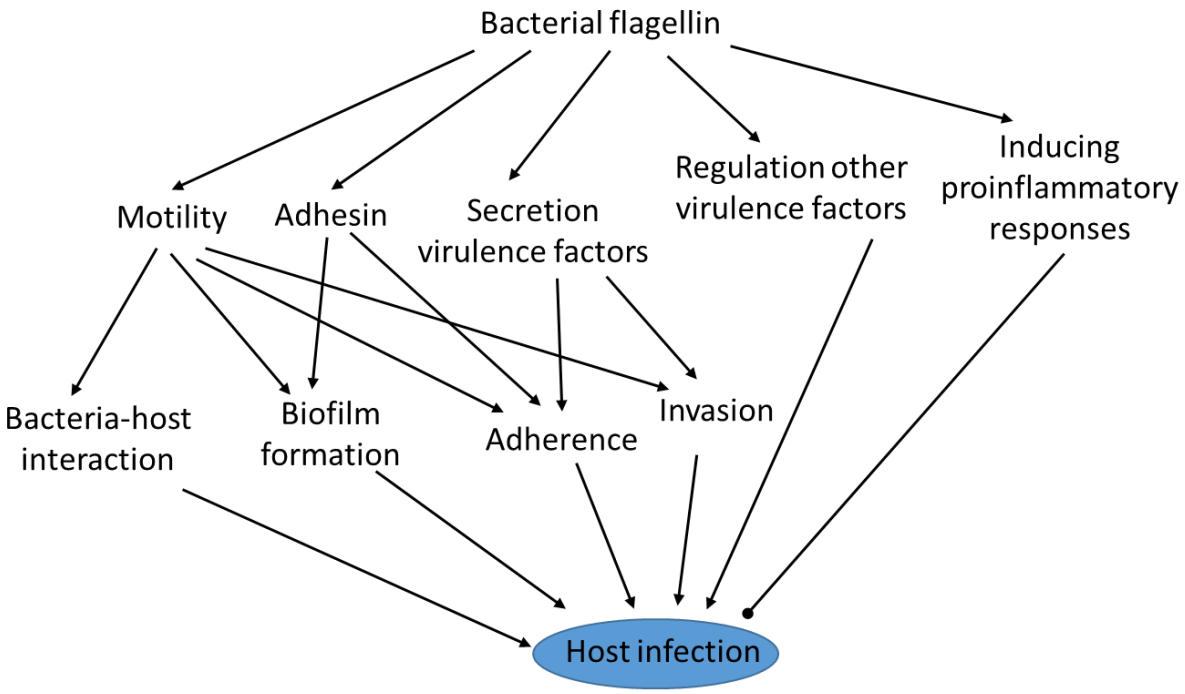


**Figure I-11 The multifactorial role of the flagellar regulation in bacterial pathogenesis**

Source: Duan *et al.*, 2013. Flagella cause host infection by providing motility, by acting as adhesins, secretion of virulence factors, and regulation of other virulence factors. The flagellar motility contributes to bacterial pathogenesis by promoting bacteria-host interactions, biofilm formation, adherence and invasion.

### I.1.3.2 Bacterial adhesins

When bacteria attach to the infection sites, various adhesive structures are produced. The adhesion to the host cell has been considered a key factor for bacterial pathogenesis (Yin *et al.*, 2022). Based on the different assembly pathway, the adhesins are grouped into two major classes, fimbrial and non-fimbrial adhesins (Gerlach and Hensel, 2007). Most of the *Salmonella* adhere to target surfaces by expressing numerous fimbrial adhesins, which are assembled into fimbriae or pili (Soto and Hultgren, 1999; Hansmeier *et al.*, 2017). Fimbriae (for fibers in Latin), or pili are structures that are found on the bacterial surface, which are mainly involved in adhesion, biofilm formation, initial step of colonization, interactions with macrophages, intestinal persistence, and bacterial aggregation with other *Salmonella* serovars (Jong *et al.*, 2012). Fimbriae are hair-like extracellular appendages with 0.5-1 µm in length and 2-8 nm in width (Wagner and Hensel, 2011). Their structural subunits and biogenesis genes are encoded by fimbrial gene clusters (FGCs) (Yue *et al.*, 2012). These FGCs typically consist of 4-15 genes that encode the proteins needed for the assembly, structure,

and regulatory proteins of the fimbriae (Rehman *et al.*, 2019). Various *Salmonella* fimbriae are produced by three types of assembly pathways: (i) chaperone-usher (CU) pathway, (ii) extracellular nucleation-precipitation (N/P) pathway, and (iii) Type IV pilus (T4P) is assembled with a type II secretory system similar mechanism (Nuccio and Ba, 2007; Rehman *et al.*, 2019). The CU assembly, the most common, is characterized by a periplasmic chaperone and an outer-membrane usher assembling the major subunits and forming the final external filamentous structures. This class of fimbriae is subclassified into different clades: α, σ, β, κ, γ and π. The curli fimbriae, in the genome of all types of *Salmonella*, are assembled through the N/P pathway where the major subunits are precipitated to form nucleator in the extracellular environment. Lastly, the T4P subunits for pili formation are assembled or disassembled at the inner-membrane platform and extended to the extracellular environment using ATP.

Each *Salmonella* serovar has a unique combination of fimbrial operons including *agf (csg), fim, lpf, pef, bcf, stb, stc*, *stg,* etc*.* with homology to fimbrial biosynthesis genes (Nuccio and Ba, 2007). The best-studied operon is the *fim* operon that encodes for type I fimbriae through the CU assembly pathway. Type I fimbriae consists of six structural genes *fim*AICDHF (Saini, Pearl and Rao, 2009) and three transcription factors *fim*ZYW (Yeh, Hancox and Clegg, 1995) in *S*. Typhimurium. Its proteinaceous surface structure recognizes specific mannosylated glycoprotein adhesions exposed at the host cell surface *via* the structural tip component FimH (Yin *et al.*, 2022). These genes are expressed in a static liquid medium whereas inhibited in a solid medium (Humphries *et al.*, 2003). Long polar fimbriae (*lpf*) is one of the chromosomal fimbriae, which enhances recognition of and adherence to M cells (Gonzales, Wilde and Roland, 2017).

The curly fimbriae, also termed “thin aggregative fimbriae” (*agf*), is mainly encoded by two operons, including *csg*DEFG and *csg*BA (curli subunit gene) (Evans and Chapman, 2014). Among them, *csg*B and *csg*A encode for the nucleator and subunit, while *csg*C encodes for oxidoreductase. The gene *csg*DEFG encodes for the operon transcriptional regulator (*csg*D) and the periplasmic (CsgE) or outer membrane (CsgG and CsgF) assembly protein (Rehman *et al.*, 2019). Even though their role in pathogenesis is not well studied yet, these two operons have been found to connect to auto-aggregation of *Salmonella spp*., attachment and adhesion to various surfaces, biofilm formation and long-term persistence (Collinson *et al.*, 1993; White *et al.*, 2006; González *et al.*, 2019).

T4P, comprising single-pili repeated subunits, exists in many bacterial pathogens. Their subunits are transported to the periplasm and then are anchored to the inner membrane (Wolfgang *et al.*, 2000). The polymerization of the pilins is mediated by ATPase. The elongation and the retractation of this pilus lead to twitching motility (Craig and Li, 2008). T4P facilitates adhesion to the membrane of intestinal epithelial cells and DNA uptake, which are encoded by *pil* operon located on SPI (Lyczak and Pier, 2002).

The fimbriae play an important function to initiate *Salmonella* infection. After entering the intestine, *Salmonella* fimbriae help traverse the mucous layer and subsequently invade non-phagocytic enterocytes in the epithelium of the intestine and then adhere to the epithelium (Dufresne, Saulnier-Bellemare and Daigle, 2018; Santos, Ferrari and Conte-Junior, 2019). Typically, during the intestinal colonization, *Salmonella* fimbriae preferably adhere to M cells helping them enter intestinal epithelial cells, which shed them in the intestinal lumen where they possibly replicate for their survival (Azriel *et al.*, 2017; Gast *et al.*, 2017).

### I.1.3.3 Injectisomes

In order to get efficient invasion to the host cell, *Salmonella* uses several syringe-like virulence factors functioning as injectisomes (Horstmann, 2017). The virulence-associated T3SS (vT3SS) is responsible for injecting the effector proteins into the host cells and modulating the host cells signalling by secreting corresponding injectisome components (Jong *et al.*, 2012). In Gram-negative bacteria, delivery of various effectors into the host cells across the inner and outer membranes is facilitated by six specialized secretion systems, type I to type VI (T1SS-T6SS), whereas, in Gram-positive bacteria, a specialized type VII secretion system (T7SS) translocates effector proteins across both the membrane and the cell wall (Tseng, Tyler and Setubal, 2009). The structure of vT3SS is similar to fT3SS because they have several homologous proteins. Compared to the flagellar hook and filament, the injectisome poses a needle and a pore-forming translocon complex (Diepold and Wagner, 2014). Of the 21 SPIs identified in *Salmonella*, including 12 SPIs in *S*. Typhimurium, five are involved in virulence during host-pathogen interactions (SPI-1 to SPI-5) (López *et al.*, 2012; Horstmann, 2017). Two distinct vT3SS are encoded by SPI-1 and SPI-2 in *S.* Typhimurium, respectively. Specifically, SPI-1 encodes for a single T3SS (T3SS-1), while SPI-2 encodes for two T3SS systems in different pathogenic bacteria, known as subclass T3SS-2a and T3SS-2b. T3SS-2a is found in *S*.

Typhimurium and contains effector proteins such as SopD2 and SseK3 for invasion and modulation of host cell signalling pathways (Raffatellu *et al.*, 2005), whereas T3SS-2b is found in *Burkholderia pseudomallei* and contains effectors such as BopE and BopA for invasion and host signalling (Stevens *et al.*, 2002). T3SS-1 exists in six to eight copies and locates along the axis of the bacteria, while T3SS-2 exists in one or two copies and locates at the poles of the bacteria (Chakravortty *et al.*, 2005; Bulmer *et al.*, 2012). They play functions at different times during the infection overlaps of the host cells (Diepold and Wagner, 2014). T3SS-1, is primarily associated with the early stage of infection (Kim *et al.*, 2018), facilitating the invasion of non-phagocytic cells, while *Salmonella* relies on T3SS-2 to survive and replicate in the cytosol of phagocytic cells, the so-called spacious phagosomes (Srikanth *et al.*, 2011; Moest and Méresse, 2013). When contacting the host cell membrane, the SPI-1 injectisome is active and translocates effector proteins into the cytoplasm, while the SPI-2 injectisome is active within the phagosome such as microphages and finally translocates effectors into the vacuolar space (Haraga, Ohlson and Miller, 2008).

The structural components of the SPI-1 injectisome are encoded on *spa*, *inv*, *prg*, and *org* operons, whereas the effector proteins comprising a Translocon (SipBCD) are encoded on *sip*/*sic* operons (Kimbrough and Miller, 2002). SipA, SipC, and alongside SipB, translocating the effector molecules into the host cell, play an important role in promoting *Salmonella* invasion into the epithelial cells by inducing actin-cytoskeletal rearrangement and subsequent triggering engulfment of the bacteria (López *et al.*, 2012). The Translocon is a pore structure that inserts into the host cell membrane. A typical apparatus of the injectisome called the Needle Complex (NC), composed of rings (PrgKH and InvG) that are anchored to the inner and the outer membranes of the bacterium, and a needle-like structure (PrgIJ) that extends out of the surface of the bacterium shown in **Figure I-12** (Kimbrough and Miller, 2000). PrgI is essential for *Salmonella* entry into host cells, functioning in concert with PrgJ secretion and is required for the formation of the needle structure (Santos, Ferrari and Conte-Junior, 2019). InvG, is a member of the secretin family of proteins, allows exported substrates across the outer membrane (Kim *et al.*, 2013). A Type III Export Apparatus, housed within the inner membrane, is required to NC assembly and the secretion of effector proteins.

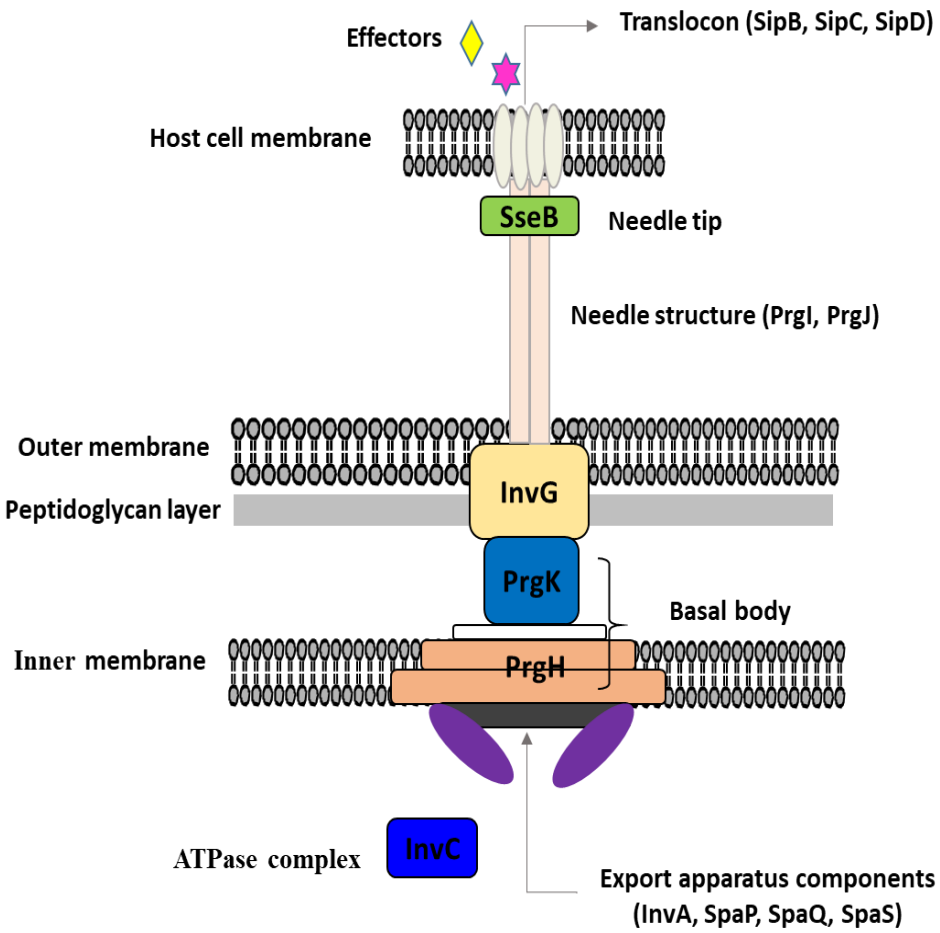


**Figure I-12 Structure and components of SPI-1 injectisome**

Adapted from Santos, Ferrari and Conte-Junior, 2019. A Translocon, which forms a translocation pore in the host cell membrane and translocates effector proteins into the host cytoplasm, formed by SipB, C, and D proteins; a needle structure, which extends beyond the surface of the bacterium, formed by PrgI and PrgJ proteins; an outer membrane rings, formed by InvG, located in outer membrane; and an inner membrane rings, formed by PrgK and PrgH, located in the inner membrane. An Export Apparatus housed within the inner membrane rings. An ATPase complex formed by InvC, located within the inner membrane to offer energy.

Once enter the epithelial cell, *Salmonella* uses the SPI-2 injectisome to survive and multiply within the *Salmonella*-containing vacuolar (SCV) space such as macrophages (Jennings, Thurston and Holden, 2017). Within the *ssa* operon encoded SPI-2 injectisome, the regulators are encoded by *ssr* operon, the corresponding chaperones are encoded by *ssc* genes, whereas the effectors are coded by *sse* gene. The effector protein SipC is responsible for the inhibition of phagolysosome formation, alongside effectors SseBCD and thus enables *Salmonella* to be able to survive within macrophages and dendritic cells (Halici *et al.*, 2008). Therefore, SPI-2 injectisome is essential for survival *in vivo* and systemic infections (Horstmann, 2017).

## I.2 Bacterial mechanosensing with flagella

When a motile bacterium approaches and adheres to a biotic or abiotic surface from a liquid environment, it undergoes a transition from a free-swimming or free-floating state to a sessile state, resulting in changes in the mechanical forces that act on it. The process of how bacteria sense and react to these mechanical stimuli, and how the signal is transmitted into cells termed surface-sensing or mechanosensing (Chawla *et al.*, 2020). The transition between planktonic to the sessile states is crucial for the bacteria as they spend a majority of their lifetime in surface-associated states in nature (Belas, 2014; Chawla *et al.*, 2020).

The surface-sensing or attachment-dependent behaviours involved in the transition of the motility appendage sates are widespread and conserved among many bacterial species (O'Toole and Wong, 2016; Mattingly *et al.*, 2018). Mechanosensory mechanisms require mechanosensors, like flagella, pili, and envelope proteins. To sense a surface, resistance during flagellar rotation of the type IV pili retraction and sensing surface proximity or shear forces of specific membrane-bound adhesins are crucial **Figure I-13** (Gordon and Wang, 2019).

Due to the special structures of their tips and potential various length scales, flagella and pili are sensitive to mechanical cues. When changing the viscosity of the growth media such as on soft agar plates, the mechanical load on the rotary flagellar motors is directly affected (**Figure I-13A**). Importantly, an increase in intracellular $H^+$ induces the up-regulation of c-di-GMP, resulting in the repression of flagella-dependent swarming motility and up-regulating T4P biogenesis as a result, whereas $Na^+$ supply increases the membrane potential, leading to the transition between reversible and irreversible attachment (González *et al.*, 2010). In contrast, when moving along a surface, bacteria are using twitching motility by extending *via* polymerisation/depolymerisation T4 pilus filaments (**Figure I-13B**) (Bisht *et al.*, 2017; Forest, 2019). T4P generates tension and starts to retract when attaching to a surface, and then co-localizes with the Chp chemosensory system to coordinate signalling *via* cyclic adenosine monophosphate (cAMP)-dependent virulence (Inclan *et al.*, 2016). cAMP signalling is required to upregulate T4P biogenesis for activation of virulence. Finally, when contacting surfaces, bacteria sense an adhesion force *via* different adhesins (pili, curli or other surface molecules (Jarrell *et al.*, 2011; Cooley *et al.*, 2013). When the cell envelope is distorted as a result of adhesion to the surface, the mechanical signal is transducted (Shimizu, Ichimura and Noda,

2015). Once membrane stress increase, the outer membrane protein NlpE activates the periplasmic stress pathways (CpxA–CpxR two-component system) as surface sensors (Otto and Silhavy, 2002), leading to the activation of virulence (**Figure I-13C**). Biofilm formation is also regulated by several signals including biological and chemical cues.

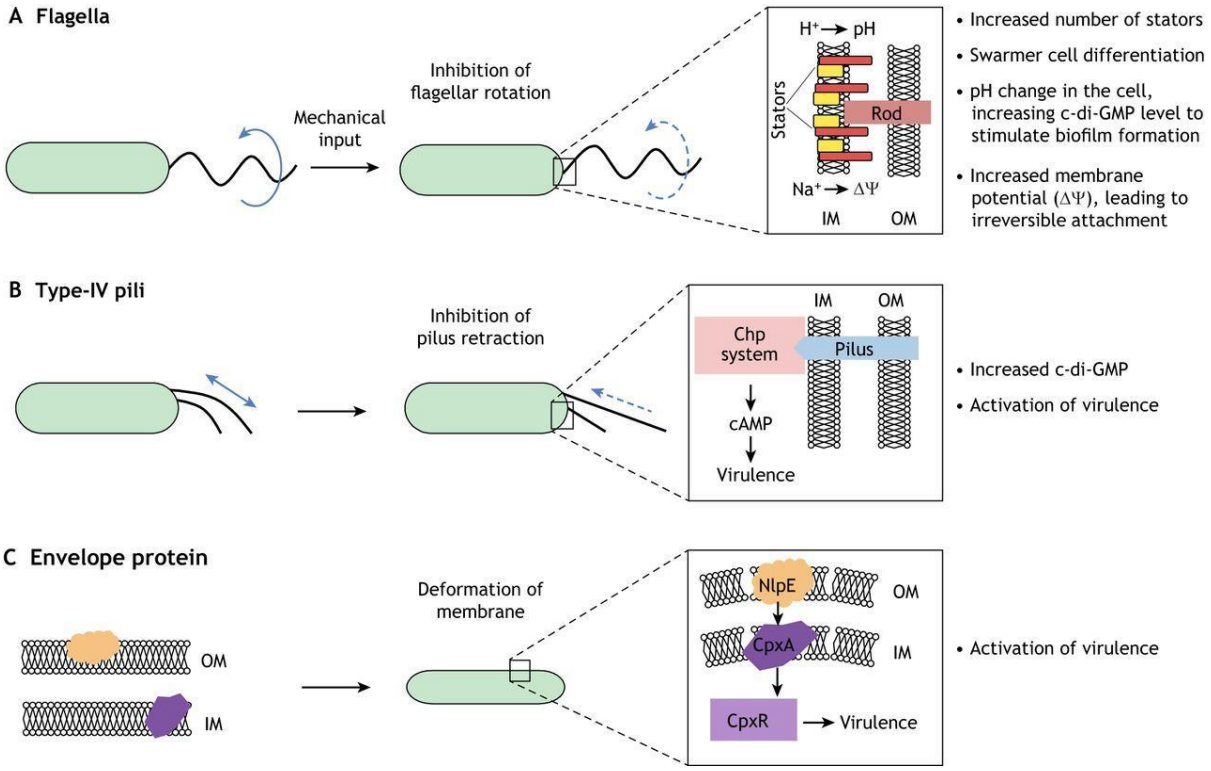


**Figure I-13 Bacterial mechanosensing elements and potential pathways and responses to mechanical inputs**
Source: Gordon and Wang, 2019. (A) Flagella. When increasing the viscosity of the liquid environment or contact with substrate surfaces, flagellar rotation is inhibited. This may increase the number of stators in the flagellar motor to trigger swarmer cell differentiation and interrupt the $H^+$ or $Na^+$ ion flux through the stators to stimulate or initiate biofilm formation. (B) T4P. Upon surface contact, the inhibition of pilus retraction generates tension in the pili, which is sensed by the Chp system, leading to cAMP-dependent upregulation of virulence. Shear stresses applied on the surface-attached bacteria also generate tension in the pili during pilus retraction, which elevates the level of cyclic diguanylate monophosphate (c-di-GMP). (C) Envelope protein. The adhesion force exerted by the surface and the shear stress yield a deformation of the bacterial cell membrane, which is sensed by the outer membrane protein NlpE, triggering the signal transduction through the CpxA–CpxR two-component system. CpxR is then involved in virulence activation. OM, outer membrane; IM, inner membrane.

Notably, the bacterial flagella-dependant mechanosensing is driven by flagellar electric transmembrane motors (composed of a rotor and membrane-embedded stators). The flagellar stator is likely the mechanosensitive protein complex of the motor (Che *et al.*, 2014). Flagellar stators (MotA and MotB) can be remodelled to recruit more stator units and the

binding stator-units to form $MotA_4MotB_2$ complex. The complex enhanced by the force it senses increases the flagellar power and modulates the torque and finally facilitates swarmer cell differentiation in high-viscosity resistance (Lele, Hosu and Berg, 2013; Chawla, Ford and Lele, 2017). The proton motive force is delivered by a torque generated from the multiunit stator to the rotor *via* electrostatic interactions between the rotor protein FliG and the stator protein MotA (Zhou, Lloyd and Blair, 1998). Rotation of the flagellar motor is powered by transmembrane ion gradients through $H^+$ or $Na^+$ channel (**Figure I-14**), resulting in interference in the rotation of the flagella.

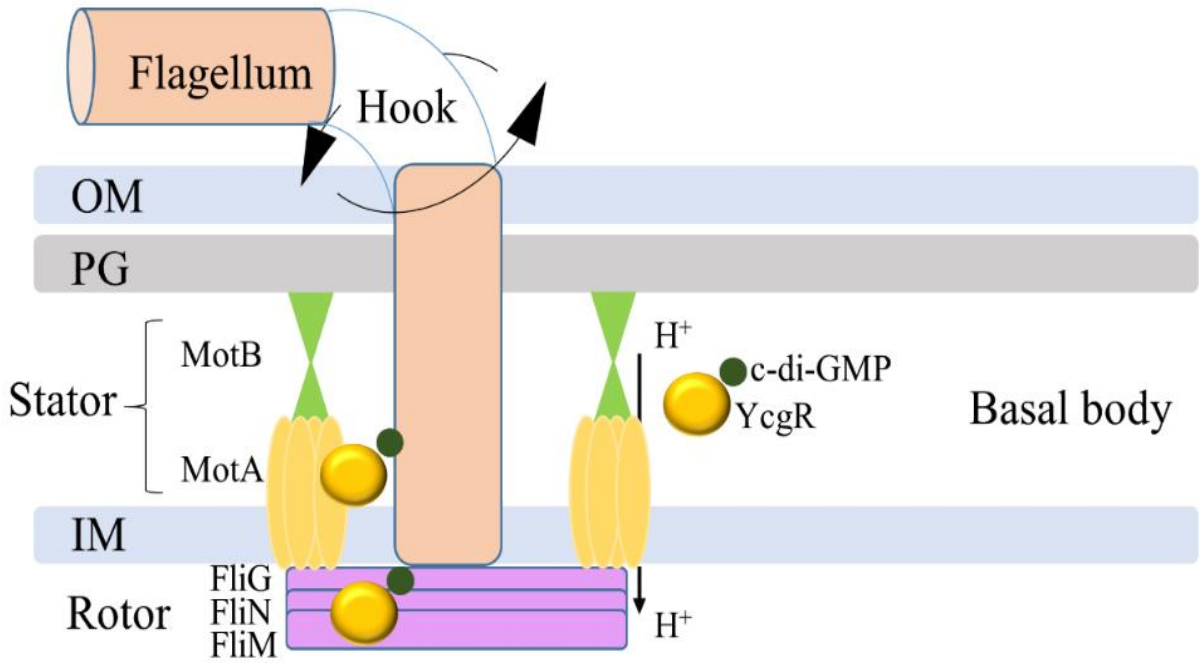


**Figure I-14 The mechanism of mechanosensing by flagellar motors**

Adapted from Belas, 2014. The motor is composed of the stator (MotA and MotB proteins) and the rotor (composed of protein FliG, FliM, and FliN). Ion ($H^+$ or $Na^+$) flow through the stator channel provides the power to rotate the flagellum. YcgR coupled with c-di-GMP are functional inhibitors of motor rotation. Abbreviations: IM, inner (or cytoplasmic) membrane; OM, outer membrane; PG, peptidoglycan.

The flagellar stators MotA and MotB form the $H^+$ channel and the homologous proteins PomA and PomB form the $Na^+$ channel (González *et al.*, 2010). Furthermore, the levels of messenger molecules such as c-di-GMP and cAMP can change to respond to chemical stimuli (Boehm *et al.*, 2010; Wang *et al.*, 2018). The second-messenger c-di-GMP is a global bacterial regulator for signal transduction in many cellular processes, including the transition from the motile to

sessile state to trigger surface colonization, biofilm formation and virulence (Galperin and Gomelsky, 2013; Luo *et al.*, 2015). For instance, when *Pseudomonas aeruginosa* encounters surfaces and senses shear force, the concentration of c-di-GMP increases within a few seconds, promoting surface colonization (Rodesney *et al.*, 2017). The protein YcgR, upon binding to c-di-GMP, interacts with the flagellar motor to control the motor rotation direction and speed and subsequently adjust its behaviour (Paul *et al.*, 2010; Wang *et al.*, 2018). There are some findings about the mechanisms of how the complex c-di-GMP/YcgR mediated bacterial motility and chemotaxis inhibition. The c-di-GMP/YcgR complex can inhibit motor rotation by interfering with the proper association of the MotA with FliG (Wolfe and Visick, 2008). YcgR mainly interacts with the motor-switch complex instead of the stators (Wang *et al.*, 2018). It also interacts with MotA directly to reduce bacterial swimming speed in correlation with c-di-GMP concentration (Boehm *et al.*, 2010). Other reports pointed out that YcgR interacts with switch-complex proteins FliG and FliM, and the interactions increase in the presence of c-di-GMP (Paul *et al.*, 2010). In addition, *Escherichia coli* (*E. coli*) flagella attachment on polydimethylsiloxane (PDMS) distinguishes stiff and soft surfaces with the help of MotB (Song and Ren, 2014; F. Song *et al.*, 2017).

## I.3 Protein methylation in bacteria

### I.3.1 Protein post-translational modifications in bacteria

Post-translational modifications (PTMs) are covalent modifications either during or after protein synthesis (Walsh, 2010). PTMs bring changes to protein structures and extend additional functions beyond the limits imposed by the 20 genetically encoded amino acids, which take place in almost all cellular dynamics ranging from signalling to metabolism (Cain *et al.*, 2014). PTMs were long considered an aberration for bacteria; however, they were described to be involved in crucial regulation for bacterial colonization (Pisithkul, Patel and Amador-Noguez, 2015). PTMs ensure cell survival and fitness in a wide range of extra- and intracellular environmental and nutritional stresses while in contact with abiotic (inert surface) or in association with living host cells (Broberg and Orth, 2010; Macek *et al.*, 2019). Therefore, due to the dynamic, reversible, or irreversible PTMs, the rapid adaptation of cells can be fine-tuned by the modifications of amino acids *via* hydroxyl, amino, or thiol on serine, threonine, tyrosine, histidine, aspartate, asparagine, lysine, arginine, and cysteine, or on C-/N- terminus

of a protein or polypeptide chains. The modifications can be for example, methyl, acetyl, phosphate groups or complex oligosaccharide structures (Dilweg and Dame, 2018; Christensen *et al.*, 2019; Chou, 2020) (**Figure I-15**).

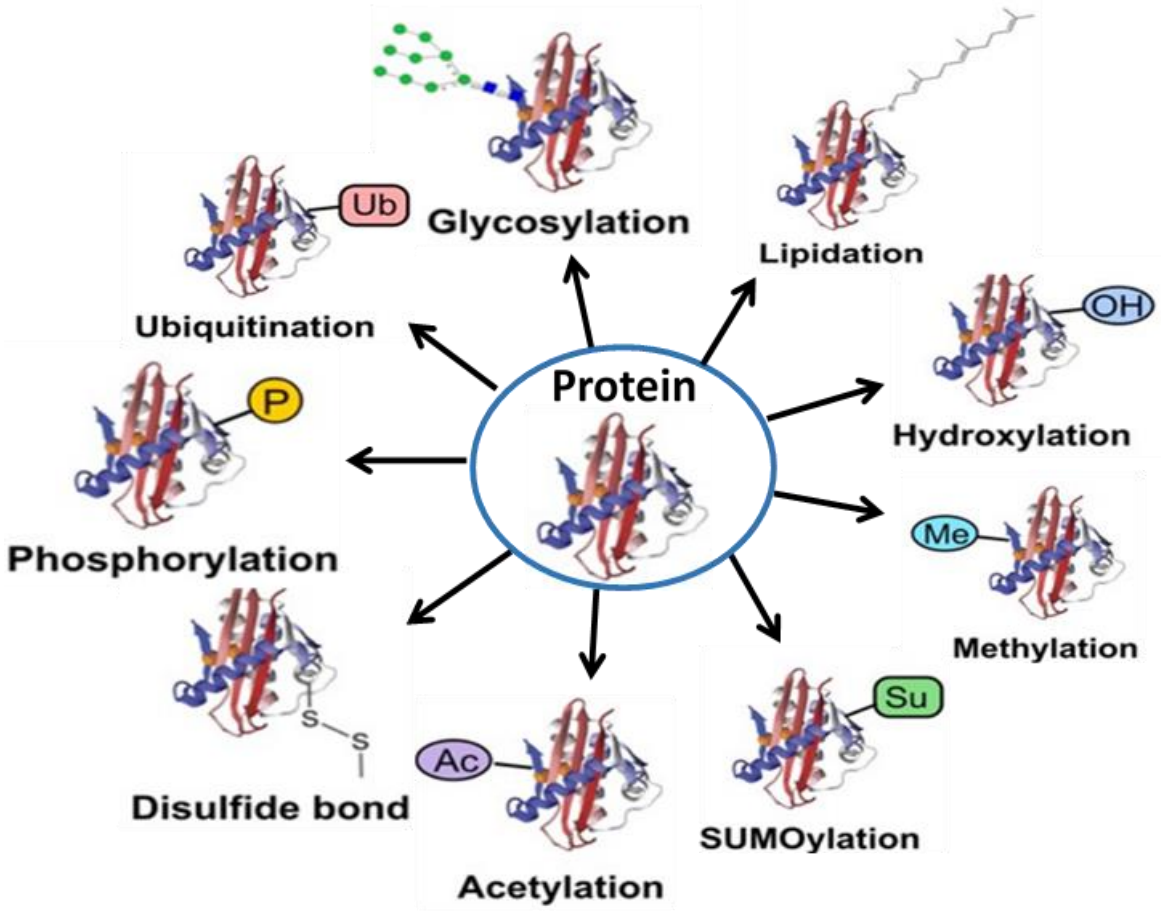


**Figure I-15 The common protein modifications in bacteria**

Source: Macek *et al.*, 2019. Multiple protein residues can be covalently modified with phosphoryl-, acetyl-, methyl-, oxidised, etc. Reactive groups on amino acid side chains are highlighted.

They are two types of modifications: covalent linkage and enzymatic cleavage (**Figure I-16**) (Walsh, Garneau-Tsodikova and Gatto, 2005; Deribe, Pawson and Dikic, 2010). The covalent modifications are associated with some specialized enzymes such as kinases and phosphatases in the case of phosphorylation, acetyltransferases and deacetylases in the case of acetylation, or ubiquitin ligases and deubiquitinases in the case of ubiquitin. These modifications are made in response to signal transduction pathways and regulatory processes by adding an electrophilic fragment of a substrate to a side chain residue in a protein (Carabetta and Hardouin, 2022). On the contrary, the proteolytic degradation process, an

irreversible process, degrades entire proteins to one or more amino acid residues during metabolic activities. All these modifications serve to invariably influence some structural aspects or functional roles of the protein targeted and therefore influence protein charge, molecular weight, stability, binding properties, conformations and functions for rapid response to diverse stimuli in bacterial cells (Macek et al., 2019). PTMs increase protein versatility during many biological functions including regulation of protein activities, subcellular localization, protein-protein interactions, or DNA-protein recognition (Grangeasse, Stülke and Mijakovic, 2015).

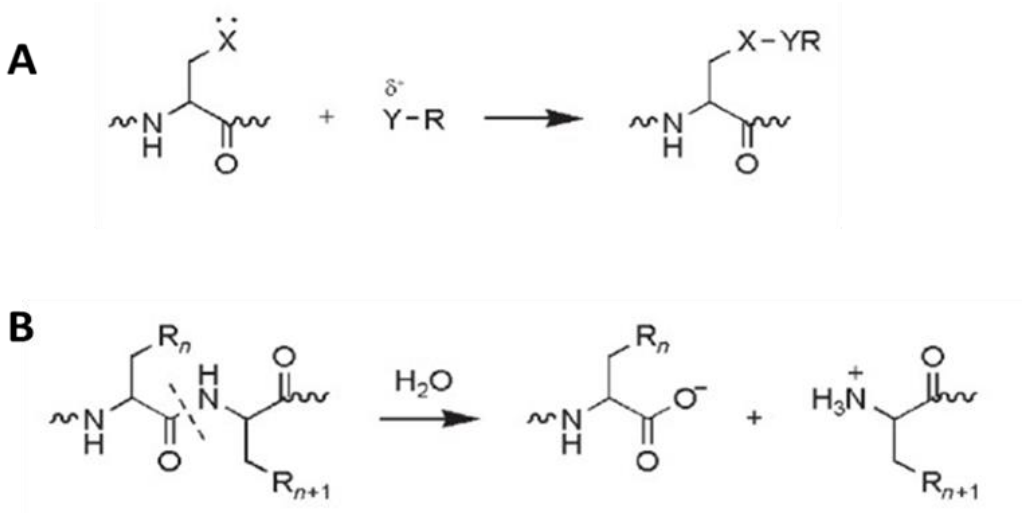


**Figure I-16 Two categories of posttranslational modifications of proteins**

Source: Walsh, Garneau-Tsodikova and Gatto, 2005. A) covalent modification of an amino acid side chain by an electrophilic fragment of a substrate; B) cleavage of a protein backbone at a peptide bond by protease

In the past decades, with the help of some specific PTM enrichment techniques and efficient multidimensional liquid chromatography (LC) separation strategy, the identification of a large extent of PTMs in proteins including multi-PTM sites and cooperative modifications in individual proteins has been reported (Huang *et al.*, 2014). By far, the most critical and the most time-consuming step is the enrichment of sufficient amounts of the target protein.

PTM-bearing peptides could be enriched from a vast number of unmodified peptides using affinity matrices covalently liked to a ligand specific for the target PTM, enabling the detection of relatively low-abundant PTMs *in vitro* (Zhao and Jensen, 2009; Černý et al., 2013). While useful, this method also suffers from various limitations for PTMs enrichment (Dunham, Mullin and Gingras, 2012; Zacharias *et al.*, 2021). For example, the availability of suitable

ligands is limited because the matrix materials are required to offer high stability, high surface-area to volume ratio and minimal non-specific binding. If a specific inhibitor is present, the PTM protein of interest cannot be fully captured. Moreover, some modification information about the type and location of PTMs on the protein may be obscured after affinity purification due to the possible removal of covalently attached PTMs after adding some detergent to elute the protein from the matrix. Therefore, the identification of one specific type of PTM which contains low-abundant modification sites requires effective PTM peptide enrichment and separation approaches.

Additionally, the purification of proteins of interest from protein complexes has been achieved by various affinity-based techniques, which rely on the close selective interaction of the target protein with an affinity tag such as His, MBP or GST tag (Bauer and Kuster, 2003; Waugh, 2005). However, these traditional affinity tags are often limited to the targeted analysis of a specific protein or a small group of proteins, but not to the non-targeted PTM analysis (Young, Britton and Robinson, 2012; Wood, 2014). Notably, affinity purification may lead to unpredictable changes. An affinity tag may alter protein conformation and change its physicochemical properties, alter its biological activity, and decrease protein yield and toxicity as a result (Kimple, Brill and Pasker, 2013). Given that, when the tag is removed enzymatically, the fragments of the target protein may also be cleaved even though at low efficiency, rendering it inactive or leading to degradation and consequent additional contamination of the protein with tag-removal agents (Waugh, 2011).

### I.3.2 Protein-lysine and arginine methylation

Among various protein modifications, protein methylation, catalysed by S-adenosyl-L-methionine (SAM, or AdoMet)-dependent methyltransferase, is one of the well-known common and most prevalent PTMs (Murn and Shi, 2017). To date, more than 200 methyltransferases have been found, including lysine and arginine methyltransferases in the human genome (Petrossian and Clarke, 2011). In contrast, knowledge about protein methylation in prokaryotes is extremely limited (Su *et al.*, 2021). In bacteria, only a few methyltransferases have been identified, such as PrmA and PrmB in *E. coli* and ArmA in *Salmonella enterica* (Granier *et al.*, 2011), and most of them are ribosomal protein modifiers (Lanouette *et al.*, 2014). However, for *Salmonella spp.*, only FliB is characterized (Burnens *et al.*, 1997). FliB post-translationally modifies lysine residues of flagellin on N-methyl-lysine

(Wang *et al.*, 2021). The methyl group is transferred from the methyl donor SAM to nucleophilic oxygen (*O*-), nitrogen (*N*-) and sulfur atoms by methyltransferase, resulting in the corresponding methylated derivatives on the side chain of polypeptides at the amino or carboxyl terminus. Six amino acids are targeted by *N*-methylation, including lysine, arginine, histidine, glutamine, glutamate, and asparagine, whereas *O*-methylation targets the carboxyl groups of glutamate and aspartate (Walsh, 2010).

Lysine and arginine are the most methylated residues (Zhang *et al.*, 2018). With over 5500 methylated proteins identified, lysine and arginine methylation in human cells have been well studied about regulating gene expression by altering chromatin structure and providing a binding platform for the recruitment of transcriptional regulators (Serre *et al.*, 2018). The lysine modification process involves two enzymes: lysine methyltransferases ('writer', KMTs) and lysine demethylases ('erasers', KDMs). Lysine residues can be respectively catalyzed by KMTs for the addition of one (MML), two (DML), or three (TML) methyl groups from the methyl donor AdoMet to the ε-amine of lysine residues (Cain *et al.*, 2014) (**Figure I-17**).

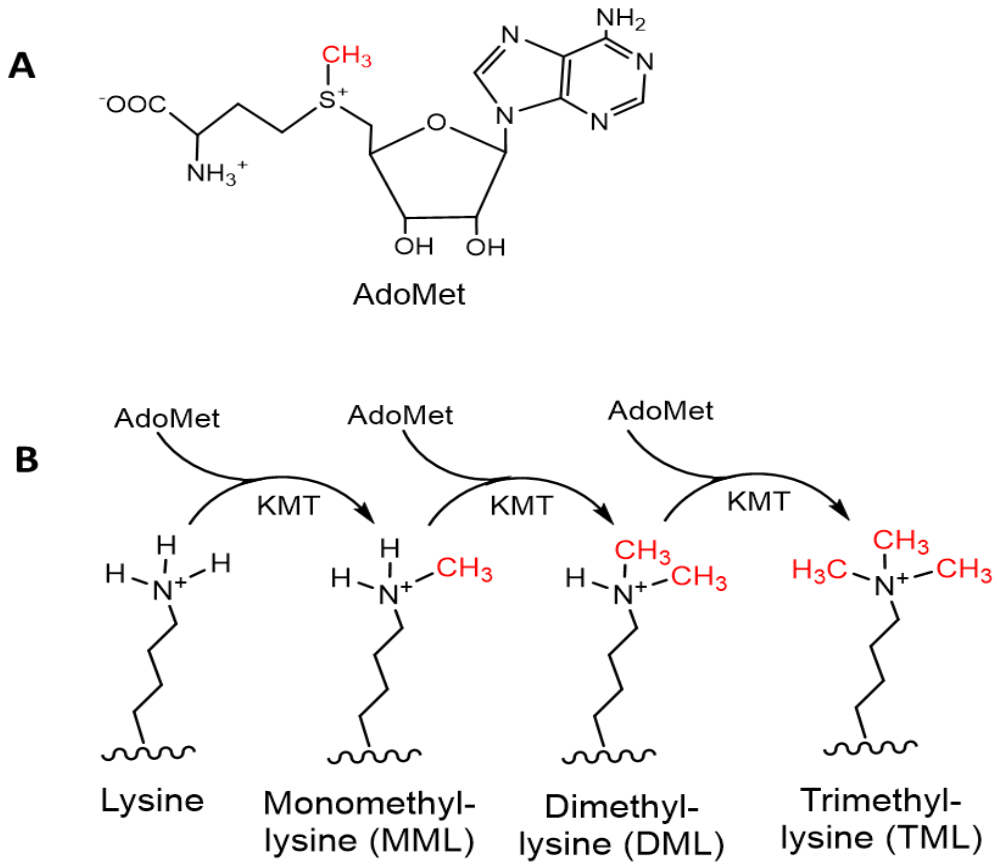


**Figure I-17 Lysine methylation by lysine-specific methyltransferases (KMTs)**

Inspired from Falnes *et al.*, 2016. (A) Chemical structure of the methyl donor AdoMet. (B) KMT-mediated methylation. A lysine residue can receive up to three methyl groups, leading to three possible methylation states mono-, di-, and tri-methyllysine (MML, DML and TML), respectively.

Besides methyl lysine, arginine residue can be mono-, asymmetrically, or symmetrically dimethylated (Soufi *et al.*, 2012) (**Figure I-18**). During the stepwise lysine methylation process, the addition of methyl groups to lysine introduces an increase in the residue's size and hydrophobicity when transitioning from the unmethylated to the methylated state. Whereas lysine demethylation, a counterpart of the methylation process, carries out removing methyl groups from lysine amino acid residues (Punnia-Moorthy *et al.*, 2021), thereby allowing dynamic and reversible regulation of histone and non-histone proteins methylation.

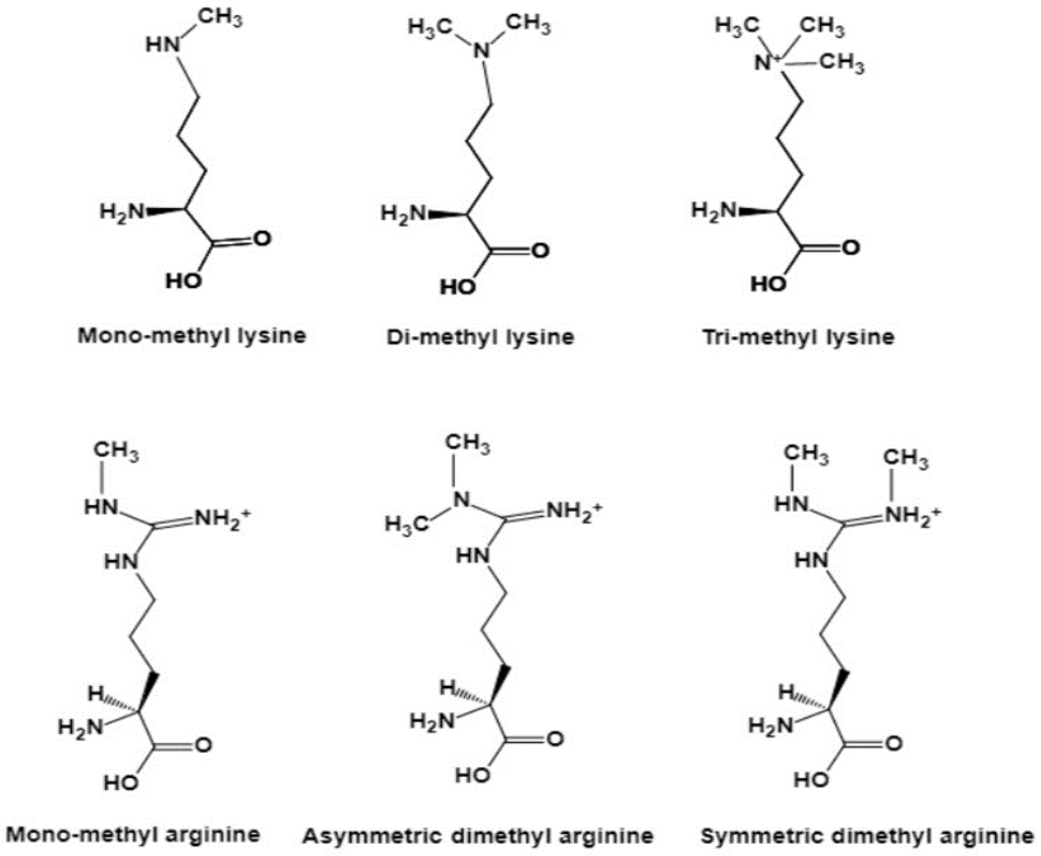


**Figure I-18 Structures of methylated lysine and arginine**

Lysine residues can be mono-, di-, and tri-methylated, whereas arginine can be mono-, asymmetrically-, or symmetrically- dimethylated.

Even though the first identification of methylated lysine was on the flagellar proteins of *S.* Typhimurium (Ambler and Rees, 1959), only one bacterial species has a characterized methylome: *Leptospira interrogans* with 155 methylated proteins and 40 methyllysine sites

(Cao *et al.*, 2010). Since this first work, these PTMs have been mainly studied in eukaryotes, focusing on histone protein methylation. However, in eukaryotic and prokaryotic cells, non-histone proteins are poorly described regarding their methylation and it remains challenging for scientists (Lanouette et al., 2014). Because histones are principal chromatin components in eukaryotes and most archaea, but are rare in bacteria, histones are generally considered to be absent from bacteria, except for their role as nucleoid components in the bacteria *Bdellovibrio bacteriovorus* and *Leptospira interrogans* (Hocher *et al.*, 2023). Numerous methyllysine-containing proteins have been identified in various bacterial species in recent years, as listed in **Table I-1**.

**Table I-1 Lysine methylation proteins in bacteria**

| Bacteria | Methyllysine state | Methyllysine sites | References |
|---|---|---|---|
| *Salmonella* Typhimurium | MML, DML, TML | 34 | (Horstmann *et al.*, 2020) |
| *Bacillus subtilis* | MML, TML | 4 | (Lauber, Running and Reilly, 2009) |
| *Thermus thermophilus* | MML, TML | 4 | (Cameron *et al.*, 2004) |
| *Escherichia coli* | MML, DML, TML | 84 | (Schmidt *et al.*, 2016) |
| *Pseudomonas aeruginosa* | MML, DML, TML | 15 | (Barbier *et al.*, 2013; Gaviard *et al.*, 2019) |
| *Sulfolobus spp.* | MML, DML, TML | 12-26 | (Vorontsov *et al.*, 2016) |
| *Thermoproteus tenax* | MML, DML | 30 | (Botting *et al.*, 2010) |
| *Mycobacterium spp.* | MML, DML | 13 | (Pethe *et al.*, 2002) |
| *Desulfovibrio vulgaris* | MML, DML, TML | 35 | (Gaucher *et al.*, 2008) |
| *Rickettsia spp.* | MML, DML, TML | 28 | (Abeykoon *et al.*, 2012) |
| *Synechocystis spp.* | TML | Unknown | (Kim *et al.*, 2011) |
| *Leptospira interrogans* | MML, DML, TML | 40 | (Cao *et al.*, 2010) |
| *Staphylococcus aureus* | TML | Unknown | (Ravipaty and Reilly, 2010) |
| *Acinetobacter baumannii* | TML | Unknown | (Li *et al.*, 2018) |
| *Agrobacterium tumefaciens* | MML, DML | Unknown | (Małecki *et al.*, 2016) |
| *Caulobacter crescentus* | MML, DML | 3 | (Running *et al.*, 2007) |
| *Rhodopseudomonas palustris* | MML, DML, TML | 13 | (Strader *et al.*, 2004) |

### I.3.3 Role of protein methylation in bacteria

Methylation reactions influence diverse cell processes, including transcriptional regulation, RNA processing, ribosome assembly, translation accuracy, protein nuclear trafficking and metabolism, and cellular signalling (Polevoda and Sherman, 2007). Due to the impact of lysine methylation on biological functions, the interests in its investigation in different types of cells

and functional states have taken attention over the years (Vorontsov *et al.*, 2016; Cornett *et al.*, 2019; Levy, 2019). Lysine methylation of histones has been proven to take roles in epigenetic regulation *via* chromatin compaction and gene transcription (Fei and Yang, 2009; Zhang, Wen and Shi, 2012). For example, in *E. coli*, lysine methylation in the histone-like protein HU helps to compact the bacterial chromosome and regulate gene expression (Ai, Lee and Schultz, 2010). In addition, methylation of elongation factor Tu (EF-Tu) in *E. coli* and *S*. Typhimurium with the occurrence of MML and DML at specific lysine sites decreases the GTPase activity, thereby affecting their growth phase (Van Noort *et al*., 1986). In contrast, methylated lysine from non-histones played a crucial role in protein function regulation, protein stability, protein-protein interaction, and protein activity regulation in different cellular processes (Kontaki and Talianidis, 2010; Wu, Connolly and Biggar, 2017). However, since the first pioneering work of Ambler and Rees, only recently methyllysine was uncovered to have an impact on bacterial physiology by (i) increasing the surface hydrophobicity of flagellin and subsequently facilitating bacterial adhesion, (ii) contributing to efficient gut colonization and (iii) contributing to host cell invasion (Ambler and Rees, 1959; Horstmann *et al.*, 2020). However, the origins and functions of methyllysine residues in cell biology are still poorly understood and remain challenging for the scientific community.

Previous studies have indicated that the deletion of *fliB* gene (encoding flagellin methylase) has no significant effect on flagellar motility and filament assembly (Frye *et al.*, 2006; Deditius *et al.*, 2015). However, regardless of invasion in the presence or absence of FliB, a functional methylated flagellar filament assembly is required to facilitate epithelial cell invasion (Horstmann *et al.*, 2020). Furthermore, the invasion defect is approximately 50% for the Δ*fliB* mutant strain, independent of the flagellin type or active bacterial motility. It proved that in *S*. Typhimurium, the flagellins (FljB and FliC) methylation has no impact on its swimming and swarming motility (Horstmann *et al.*, 2017). Additionally, methylation on lysine residues on *Aeromonas caviae* flagellin does not impact flagellar formation and motility either (Lowry *et al.*, 2022). Sun *et al*. also found that flagellin FlaB methylation was required neither for motility nor for flagellar assembly in *Shewanella oneidensis* (Sun *et al.*, 2013). However, due to the conservation in numerous bacterial species, flagellin methylations may play important roles in other phenotypes (De Maayer and Cowan, 2016). Methyllysines at surface-exposed domains or polypeptides might change the charge and result in avoiding host immune

responses. Mutants deficient in lysine methyltransferases showed a decreased virulence even avirulent in a mouse infection model, suggesting that lysine methylation plays a key role in *Rickettsia parkeri* pathogenesis (Engström *et al.*, 2021). Recently, it has been reported that the lysine residues within the variable D2 and D3 domains of filament are predominantly methylated, while they are not modified at D0 and D1 domains of *S*. Typhimurium (Horstmann *et al.*, 2020). The methylation improves bacterial adhesion on hydrophobic surfaces such as the host cell outer membrane and finally promotes host cell invasion to epithelial cells (Horstmann *et al.*, 2020). FliB-dependent methylation of flagella occurs in a broad range of bacterial species besides *Salmonella*, including *Yersinia*, *Enterobacteriaceae*, *Franconibacter, Pantoea*, and *Aeromonas* to promote adhesion to corresponding host cells (Horstmann *et al.*, 2020). However, nothing has been described so far about other proteins modified by FliB.

## I.4 Typical approaches for lysine methylation detection

Due to the small mass shift (14 Da) and the lack of charge difference between unmethylated and methylated residues, methylome information associated with different cellular processes is limited (Levy, 2019). The important roles of lysine methylation in diverse prokaryotic and eukaryotic cells require reliable approaches to identify methylation events and get more methylome information. The typical approaches for lysine methylation detection are including: (i) radio-labelled assays, (ii) antibody-based methods, (iii) fluorescence-based methods, (iv) protein and peptide assays, (v) mass spectrometry (MS)-based methods (Lanouette *et al.*, 2014). Identification of protein methylation *in vivo* can be directly achieved through MS analysis. However, lysine methylation occurs with similar physicochemical properties to non-methylated peptides and low abundance in the sample, hampering their detection, therefore, some enrichment steps are necessary before its identification by MS analysis (Mohammed and Heck, 2010; Sohtome *et al.*, 2021).

The most common approaches to enrich methyllysine-containing peptides or proteins are target-specific approaches involving affinity and/or chemical strategies. Among these approaches, the most direct one using radioactively labelled SAM ($^{3}$H-SAM) (Rubio *et al.*, 2017), allows the detection of peptides or full-length proteins containing labelled methylated lysine *in vivo* by performing ion-exchange chromatography, such as strong cation/anion exchange (SCX/SAX) chromatography or hydrophilic interaction liquid chromatography (HILIC)

(**Figure I-19A**). Common chromatographic approaches such as reversed-phase high-performance liquid chromatography (RP-HPLC) and ion exchange chromatography (IEX) are often used to separate peptides mainly based on their hydrophobicity (Zhang *et al.*, 2010) and surface charge (Amartely *et al*., 2018). Thus, it's difficult to enrich methylated peptides from cells and tissues using traditional chromatography (Polevoda and Sherman, 2007). In SCX chromatography, the separation is based on ionic character and specifically the peptide's net positive charge. Besides, tryptic methylated peptides usually carry 3 or more positive charges. However, the usage of $^{3}$H-SAM cannot specifically take place the methylation on lysine, due to other residues such as arginine, histidine, and aspartate are potential targets for methylation (Webb *et al.*, 2010). Under common SCX separation conditions, the histidine-containing peptides and unmodified peptides with miscleavage sites may cause interference as they also carry 3 or more positive charges (Wang, Wang and Ye, 2017). This was followed by improved approaches coupled with stable isotope labelling by amino acids in cell culture (SILAC)-based approaches (Deng, Erdjument-bromage and Neubert, 2020).

Antibody-based methods can be used to specifically discriminate between the proteins harbouring the same type of lysine methylation in cell lysates (Mishra, Tiwari and Gomes, 2017) by using specific anti-methyllysine antibodies (Cao and Garcia, 2016). They are also widely used to detect methylated proteins or peptides (Iwabata, Yoshida and Komatsu, 2005) in various assays such as Western blotting (immunoblotting), immunoprecipitation, and enzyme-linked immunosorbent assay (ELISA) (**Figure I-19B**). Different polyclonal antibodies have been produced for the enrichment of various PTMs (Hattori and Koide, 2018). Numerous 'pan-specific' antibody batches have been developed, i.e. antibodies that can detect all sequences that hold a specific PTM, without discriminating between different peptide sequences surrounding the PTM (Liang *et al.*, 2008; Hof, 2016). Up to date, several commercially available antibodies have been produced for methylated lysine residues detection, including anti-methylated lysine (di-, mono-methyl) antibody, pan anti-monomethyl (dimethyl, trimethyl) lysine polyclonal antibody, biotin anti- methylated lysine antibody, etc. However, most of these antibodies are MML- and DML-specific but are not TML specific, which leads to very low identified TML sites (Cao and Garcia, 2016).

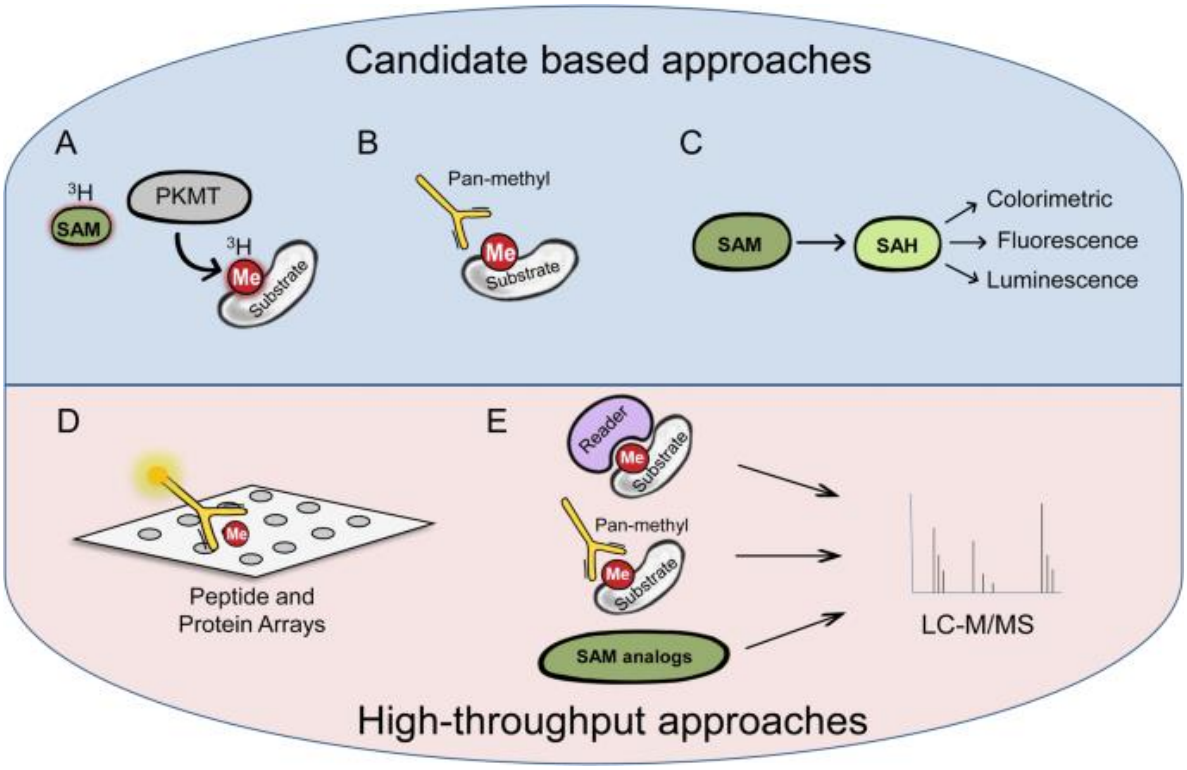


**Figure I-19 The most common approaches for lysine methylation detection**

Source: Levy, 2019. The scheme is divided into candidate-based (top part) and high-through- put (bottom part) approaches. (A) Radioactive in vitro methylation assay in the presence of $^3$H-SAM, lysine methyltransferase (PKMT) and a substrate of interest. (B) A pan-specific methyl antibodies-based method for methylated substrate recognition. (C) Different assays for the detection of methylated products which rely on the formation of S-adenosylhomocysteine (SAH). (D) Usage of peptide and protein arrays for screening thousands of potential candidate substrates. (E) Enrichment steps with pan-methyl antibodies, methyl-binding protein domains are required for mass spectrometry-based approach.

However, some antibodies are amino acid sequences specific to histones, but cannot distinguish between different levels of methylation (MML, DML, and TML) (Fuchs *et al.*, 2011). Only a few poorly specific antibodies against MML, DML, and TML motifs and/or a combination of chemical derivatizations have been developed to perform immunoaffinity purification of methylated peptides in the study of lysine methylation sites identification *in vivo* (Guo *et al.*, 2014; Wu *et al.*, 2015). Antibodies were also demonstrated highly influenced by neighbouring PTMs such as the neighbouring phosphorylation sites of histone (Rothbart *et al.*, 2015). Nevertheless, antibodies may cross-react with similar modifications or with non-modified forms of the same proteins such as DML with ethylation (Kampstra *et al.*, 2019). Cross-reactivity of antibodies may make it difficult to distinguish between meaningful PTM changes in cells, such as di- and trimethylation of yeast histones with opposing roles in

transcriptional regulation (Lothrop, Torres and Fuchs, 2013). Concerning protein methylation, the risk of co-purification of MML and DML-containing proteins with the use of the anti-methylated lysine antibody is high (Perez-Burgos *et al.*, 2003). In this case, the results should always be validated by the use of other methods such as MS to determine the exact location and degree of lysine methylation in a protein.

Only a subset of methylated peptides can be enriched using pan-specific antibodies because of their limitations: (i) difficult to produce on a large scale, (ii) low specificity because of small methyl moiety offering low antigenicity, (iii) poor sensitivity, (iv) low stability, and (v) low reproducibility between each batch (Cao, Arnaudo and Garcia, 2013). As a result, immunoblotting with pan-methyllysine antibodies does not allow the determination of the methylation sites on proteins and cannot be used for recognition of MML, DML, nor TML *in vivo* in some cases (Lanouette *et al.*, 2014). Furthermore, the use of animals and sometimes the requirement of killing animals to obtain antibodies should be subject to ethical review, which blocks its application (Tillotson, Cho and Shusta, 2013). As a result, several alternative approaches to antibody-based enrichment have been investigated, such as single-chain antibodies fragments (scFvs) (Ward and Swiatek, 2009), peptides displayed on protein domain scaffolded surfaces (Ward and Swiatek, 2009) and peptoids (synthetic peptides) (Reese *et al.*, 2020). However, each of these alternatives shared drawbacks such as low stability in varying conditions (ionic strength, temperature, and pH) or low affinity under many conditions (Phizicky *et al.*, 2003). Thus, other alternative approaches are required to improve target protein purification.

Additionally, methylated products such as S-adenosylhomocysteine (SAH) can be used in detection assays (Burgos *et al.*, 2017) (**Figure I-19C**). The resulting products can be quantified using colorimetric or fluorescent assays. In the peptide/protein array approach (Cornett *et al.*, 2018), a library of random peptides or protein domains is used to incubate with a given methyltransferase to screen the potential candidate substrates (**Figure I-19D**). The arrays are typically performed on-chip. The enzyme-based assays and protein microarray-based methods are also used even though not commonly. Enzyme-based assays can be used to detect and quantify lysine methylation in biological samples (Gale and Yan, 2015). For example, lysine-specific demethylase 1 (LSD1) can be used to specifically remove methyl groups from lysine residues (Chen *et al.*, 2006). The resulting products are then quantified

using a colorimetric or fluorescent assay. Protein microarray-based methods are arrays of immobilized proteins that can be used to detect protein-protein interactions and post-translational modifications (Levy *et al.*, 2011). Protein microarrays can be used to identify the binding partners of methylated lysine residues and to study the effects of lysine methylation on protein function.

Sometimes, several enrichment steps are combined for a single substrate to identify the presence and location of methyllysine (Carlson and Gozani, 2014) (**Figure I-19E**). The available pan-specific-methyllysine antibodies and methyllysine-binding domains can be either associated or alone to enrich methylated proteins for MS analysis. It enables the identification of the methylation sites and recognition of the methylated states. Methyllysine-binding domains have been proposed as an alternative method to enrich methyllysines (Iwabata, Yoshida and Komatsu, 2005; Carlson *et al.*, 2014). They are a large family of proteins consisting of multiple functional repeated elements, which bind differently to methylated lysines (Teske and Hadden, 2017). Some common examples of methyllysine-binding domains include chromodomains, the Tudor domain, and the malignant brain tumor (MBT) domain. For instance, the triple MBT (3xMBT) have been found to have pan-specificity for MML and DML (Moore *et al.*, 2013). However, this method does not distinguish between methylation of individual lysine residues within a protein or recognize TML in the binding pocket, nor can it distinguish between mono- and di-methylation (Carlson *et al.*, 2014).

Besides, the enrichment of methyllysine-containing proteins has also taken advantage of chemical biology methods. For example, a series of clickable azide- and alkyne-analogues of SAM (**Figure I-19E**) offering alkyne/azide tags (Chuh and Pratt, 2015), chemoenzymatic labelling by propargylic Se-adenosyl-L-selenomethionine (ProSeAM) (Sohtome *et al.*, 2021), calixarene-based *p*-sulfonatocalix [4] arene (PSC) strategy (Daze *et al.*, 2012) and chemical peptide derivatizations such as malondialdehyde (MDA) and o-phthalaldehyde (OPA) (Ning *et al.*, 2016) have been used for methylated proteins enrichment. But the derivatization reagents like MDA are unstable for storage and the highly acidic and/or basic conditions of MDA and OPA result in unwanted hydrolysis during enrichment treatment (Huang *et al.*, 2014). Nevertheless, unpredicted side reactions when contaminated from derivatization reagents produce complicated issues for proteomic analysis because of the aberrant mass shifts (Foettinger, Leitner and Lindner, 2006).

Overall, the detection approaches described above have their strengths and some limitations associated with their use for lysine methylation analysis, as listed in **Table I-2**.

**Table I-2 Various strategies for detecting methylated lysine**

| Strategies | Advantages | Disadvantages | References |
|---|---|---|---|
| Edman sequencing | Reliable and precise | Time-consuming and necessitates large amount of the target proteins, resulting in inapplicable to high-throughput approaches | (Schaefer *et al.*, 1987) |
| Radio-labelled assays | Radioactively labelled methyl donors either in culture media or lysate make it easily identify and locate | Does not allow the identification of specific methylation site; does not indicate what type of residue is labelled | (Webb *et al.*, 2010) |
| Immunoblotting | Precise and reliable | Pan-methyllysine antibodies not reliable; immunoblotting with pan-methyllysine antibodies does not allow the determination of the methylation site | (Cao, Arnaudo and Garcia, 2013; Cao and Garcia, 2016) |
| Mass spectrometry-based methods (SILAC; SCX;LC; IEX) | sensitive and reproducible; capable to determine the methylated site in dynamic changes | Hampered by the low abundance of methylated sites relative to their non-methylated counterpart; the small mass difference between a TML and an acetylated peptide cannot be separated by low-resolution mass spectrometers | (Ong, Mittler and Mann, 2004; Wang, Wang and Ye, 2017; Zhang *et al.*, 2018) |
| Methyllysine-binding protein domains | Systematically identify lysine methylation sites and map methyllysine-driven protein-protein interactions with high-confidence and high-resolution interactome | Rear effector proteins for recognizing specific methyllysine | (Liu *et al.*, 2013) |

The overall conclusion is that the drawbacks of these common approaches highlight the need for further research into other complementary methodologies for the detection of methyllysine-containing proteins/peptides that are more sensitive, specific and high-

throughput to identify state-specific and recognize distinct levels of methylation on lysine residues to obtain more methylome information.

## I.5 Aptamers, a new approach for molecules recognition

### I.5.1 History of aptamers

Due to intricate tertiary structures, nucleic acids have the potential to perform a variety of functions including specific ligand-binding. Based on this principle, three decades ago, several researchers first developed synthetic RNA motifs to specifically bind to molecular targets and revolutionized molecular recognition (McKeague and Derosa, 2012). These RNA structures, called aptamers, were first discovered in the early 1990s through an *in vitro* selection process called Systematic Evolution of Ligands by Exponential enrichment (SELEX) on eight nucleotides (Tuerk and Gold, 1990). The ligands termed "aptamers" deriving from the Latin word *aptus* which means "to fit", while *meros* (grec) denotes "particle" (Ellington and Szostak, 1990). It was first named by Andrew Ellington and Jack Szostak from the Ellington lab (Ellington and Szostak, 1990). Aptamers are short single-stranded oligonucleotides (ssDNA or RNA) that are able to bind to a specific target molecule with high affinity and specificity. Since their discovery, aptamers have opened up a new avenue for the development of highly specific and efficient tools through the SELEX methods (Gold *et al.*, 2012). The SELEX process starts with a large library of random oligonucleotides (theoretically $4^N$ individual sequences, ~$10^{14}$ molecules) containing single-stranded oligonucleotide sequences. They are then subjected to iterative rounds of selection, amplification by polymerase chain reaction (PCR) or reverse transcription-polymerase chain reaction (RT-PCR) (Jijakli *et al.*, 2016), to isolate the oligonucleotides that bind to the target molecule of interest with the highest affinity and specificity.

### I.5.2 General properties of aptamers

Aptamers have great potential to function as molecular recognition elements that mimic antibodies based on their variety of complex three-dimensional shapes in analytical systems for the detection, separation, or purification of target molecules (Ruscito and DeRosa, 2016; Röthlisberger and Hollenstein, 2018). Therefore, aptamers also are termed "chemical antibodies" as an alternative to antibodies (Dunn, Jimenez and Chaput, 2017). Compared to

traditional antibodies, aptamers offer several advantages. The *in vitro* aptamer selection process allows a wider range of conditions, including nonphysiological salt concentrations, temperatures (around 25°C) and physiological pH (pH 7.0-7.4) (Yan and Levy, 2009). They can be produced on larger scales *in vivo* and are easier to be synthesized and modified (Carothers *et al.*, 2011). In principle, aptamer production is a chemical process, it avoids the problem of biological contamination that can occur during antibody manufacturing and reduces the potential batch-to-batch variability that plagues antibody research (Dunn, Jimenez and Chaput, 2017). In addition, by folding into a functional structure such as hairpins, G-quartes, bulges, and pseudo-knots, aptamers are able to recognize and tightly bind their targets with high affinity and specificity in a broad variety of targets (Marimuthu *et al.*, 2012; Troisi and Sica, 2022). Based on their unique properties, aptamers have the great potential to be alternatives to traditional antibodies and be the ideal solution for various biomedical and biotechnological applications.

Aptamers are rather short (20–100 nucleotides (nt) long) nucleic acid sequences that are obtained by application of the SELEX *in vitro* selection. The initial libraries of oligonucleotides are created by a random central region with specific flanked sequences for primer extension reactions. Short randomized regions ($N_{20}$) will ensure complete coverage of the sequence space (i.e. more than one molecule of each sequence is represented in the pool) during the selection experiment, albeit at the expense of a reduction of possible structural motifs. In contrast, larger randomized sections ($N_{40}$) provide a higher complexity of possible three-dimensional structures and folds but only a small fraction of the sequence space will be covered during selection experiments (Velez *et al.*, 2012). Therefore, most selection experiments are carried out with randomized regions comprised between 20 and 60 nt, even though aptamers sequences as short as 8 nt (Kwon, Ahmad Raston and Gu, 2014) and as long as 228 nt (Li, Geyer and Sen, 1996) have been isolated.

For DNA or RNA aptamers selection, an initial synthesized random oligonucleotide library consists basically of three regions (**Figure I-20**).

(i) An inner 20-60 nt random sequence region, that serves as a putative target-binding domain, in which the four nucleotides are generally incorporated with equal probability or with a rich content of particular nucleotides, depending on the nature of the research. The most frequently used random region contains all four bases in an equal nucleotide distribution,

which was considered to provide the maximal sequence diversity (Blind and Blank, 2015). However, there are also some cases in the selection progress of RNA aptamers obtained an accumulation of pyrimidine-rich sequences and a loss of adenosine (Takahashi *et al.*, 2016). Slight biases in nucleotide composition, particularly in pyrimidine-rich (e.g. 30% of cytosine and guanine) random regions of RNA libraries, have been shown to form more stem structures, resulting in RNA sequences with higher predicted structural stability (Vorobyeva *et al.*, 2018). For example, in some bioinformatic cases, a guanine-rich library was predicted to contain a higher proportion of quadruplex-forming sequences than the standard library containing equimolar bases (Choi, Nayak and Bates, 2009). Therefore, a slightly higher cytosine and guanine content in the random region of the initial library can be considered acceptable.

(ii) Two constant regions (flanked regions) at both 5′- and 3′-sides of the oligonucleotide, which are used for the amplification of the selected sequences. Constant regions may contain restriction sites to facilitate the insertion of the random regions of selected aptamers in the multicloning site of a bacterial vector for sequencing.

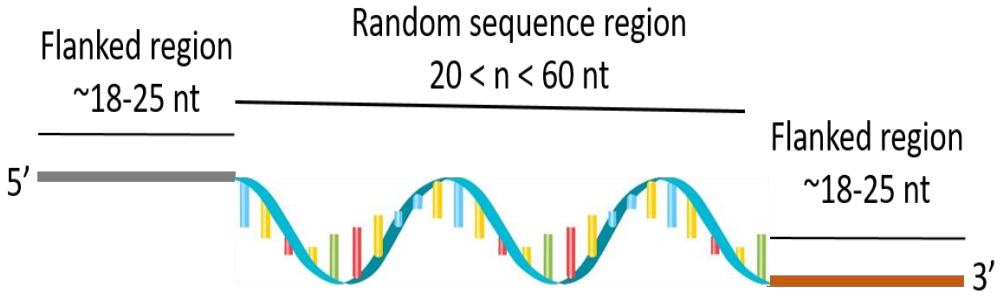


**Figure I-20 Schematic of consistent aptamer structures**

5’- and 3’- end are flanked regions that specific for amplification; central region was the random sequence region.

Furthermore, aptamers have a good stability due to their phosphodiester backbone structure. Aptamers can be reversibly denatured in different environments (Shastri *et al.*, 2015). Changing the conditions such as pH, temperature, ionic strength, or adding denaturants can cause the aptamers to be temporarily unfolded. However, when returned to the original binding conditions, aptamers can be refolded into a functional state by a simple annealing procedure of heating and cooling in an appropriate buffer. The use of aptamers in any application requires them to be stable, functional, and resistant to the enzymatic nucleases.

Chemical modifications also can increase the nuclease resistance and increase the diversity of the oligonucleotide pools.

### I.5.3 Different types of aptamers

Aptamers are mostly comprised of two types, DNA and RNA aptamers. They are attractive affinity ligands selected *in vitro* from a large random DNA or RNA library. Based on the differences between their structures and unique properties, their selection procedures are different. Individual steps are illustrated in **Figure I-21**. DNA aptamers and RNA aptamers are both synthetic oligonucleotides made up of 20-100nt, which are derived from a large library of random oligonucleotides (Lee *et al.*, 2004).

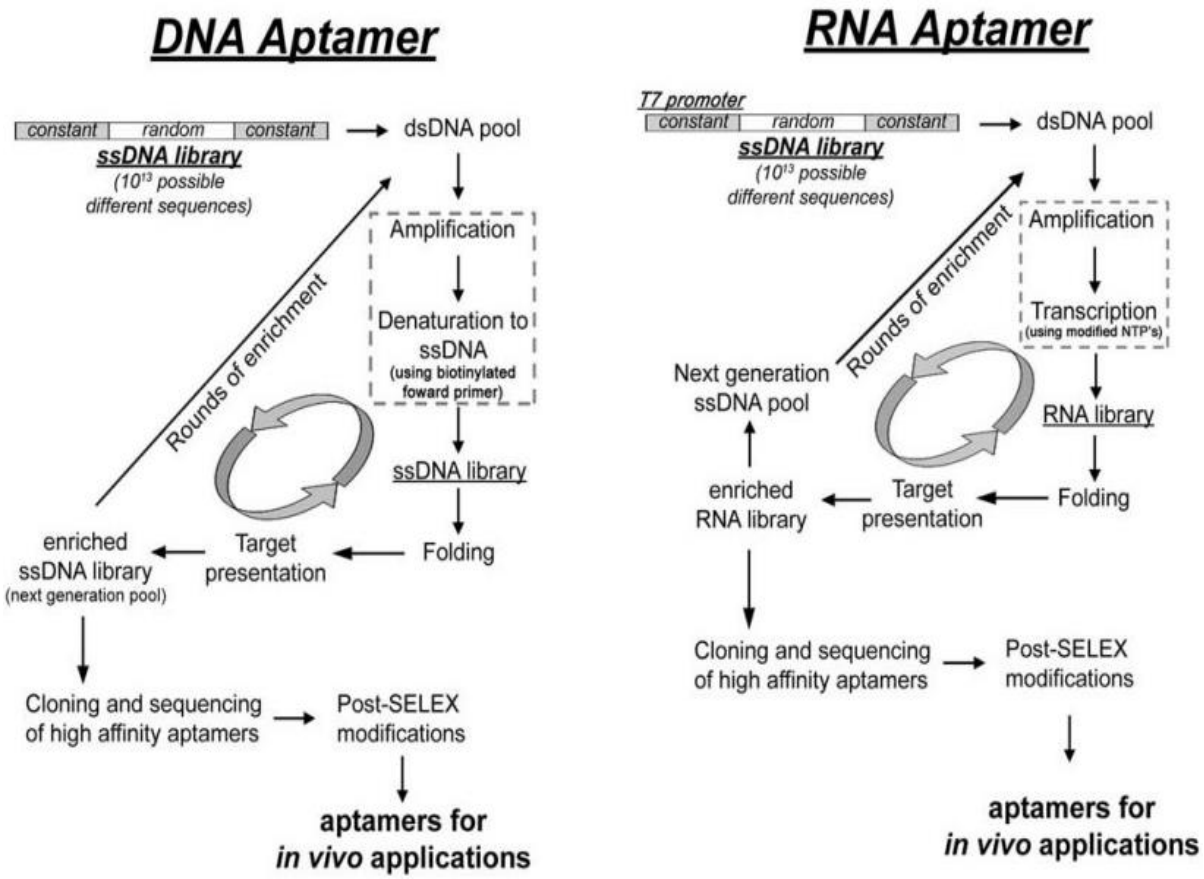


**Figure I-21 DNA and RNA aptamers selection for *in vivo* applications**

Source: Ulrich *et al.*, 2006. DNA and RNA aptamers are selected from a randomized oligonucleotide library by reiterative SELEX rounds. In case of the DNA aptamer (left side), the double-stranded DNA pool needs to be denaturated for purification of the single-stranded sense strand, which then is presented to its selection target. Following removal of unbound and low affinity bound DNA molecules, target-bound DNA molecules are eluted and amplified by PCR in the presence of a modified primer. Following denaturation, the modified sense strand can be purified by polyacrylamide gel electrophoresis and used for the next SELEX cycle. In the case of development of an RNA aptamer (right side), the double-stranded DNA pool is in vitro transcripted to the RNA

pool which is then used for SELEX. Eluted target binders are reversed transcripted to cDNA, amplified by PCR, and again in vitro transcripted to give the RNA pool used in the next SELEX cycle. RNA and DNA molecules can be protected against nuclease attacks during the selection process by incorporation of modified nucleotides using enzymatic reactions or can be chemically modified after the SELEX process; ss = single-stranded; ds = double-stranded; NTP = nucleoside-triphosphate.

However, there are some key differences in their structures and properties. ① Sugar moiety: The sugar moiety of DNA aptamers is deoxyribose, while the sugar moiety of RNA aptamers is ribose, as shown in **Figure Ⅰ-22**. The presence of a 2'-OH group in ribose makes RNA more flexible and prone to conformational changes than DNA. ② Stability: DNA aptamers are generally more stable than RNA aptamers due to the absence of the 2'-OH group in deoxyribose. The 2'-OH group in RNA can make the molecule more prone to hydrolysis, leading to lower stability compared to DNA. Due to their reactivity, the RNA aptamers may lead to the generation of cyclic-2',3'-phosphate, resulting in degradation (Yu *et al.*, 2016). However, RNA aptamers can form stable tertiary structures, due to G-U base pairs that enable high-affinity binding to targets.

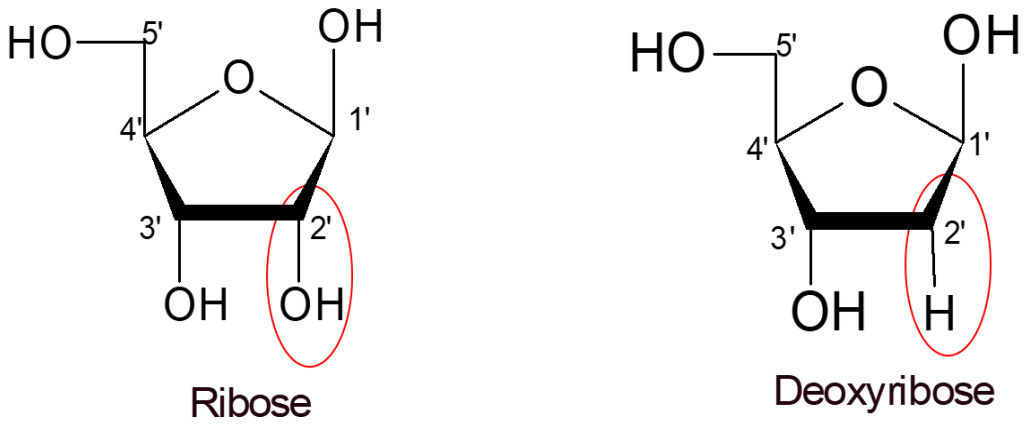


**Figure Ⅰ-22 The structure of ribose and deoxyribose compositing of RNA aptamers and DNA aptamers**
NOTE: The different part at 2'-H at deoxyribose, and 2'-OH at ribose are highlighted with red cycles.

③ Folding: DNA aptamers and RNA aptamers can both fold into complex 3D structures that enable specific binding to target molecules. However, RNA aptamers tend to be more flexible and can form more complex tertiary structures than DNA aptamers. ④ Aptamer selection: The selection of DNA aptamers and RNA aptamers involves similar processes, through SELEX procedures. However, RNA aptamers require additional precautions to stabilize them, such as the use of modified nucleotides, chelating agents, or higher salt concentrations. DNA *in*

*vitro* selection requires only a single enzymatic step (PCR) in comparison to the three enzymatic steps of RNA *in vitro* selection (reverse transcription to get cDNA, PCR for amplification, and transcription to get back the RNA sequences) (Vaught *et al.*, 2010; Aquino-Jarquin and Toscano-Garibay, 2011). Furthermore, an RNA aptamer has a T7-promoter site in one of the constant regions which were used for *in vitro* RNA aptamers selection (Ulrich *et al.*, 2006). While the ssDNA libraries can directly join in the procedure of DNA aptamer selections (Marimuthu *et al.*, 2012).

In summary, DNA aptamers and RNA aptamers have similar properties and functions but differ in their sugar moiety, stability, folding, enzymatic activity, and selection process. These differences can be exploited for specific applications in biotechnology, biomedical research, and diagnostics.

## I.5.4 Characterization of aptamers

### I.5.4.1 Structural characteristics of aptamers

Aptamers are broadly used for combinational selection because they can fold into well-defined structures and they are easily amplified by PCR or *in vitro* transcription (Famulok, Mayer and Blind, 2000). The various structures of aptamers play a crucial role in determining their function such as binding ability. Aptamers can fold into different structural forms, including primary, secondary, and tertiary structures.

The primary structure of aptamers refers to the sequence of nucleotides that make up the aptamer. Each nucleotide consists of three different elements: a nitrogen-containing base, a five-carbon sugar (deoxyribose in DNA; ribose in RNA) and phosphate group. Adenine (A), cytosine (C), and guanine (G) are the common nucleobases of nucleic acids. In contrast, thymine (T) is specific for DNA and uracil (U) for RNA. DNA aptamers are made up of several deoxyribonucleotides, while RNA aptamers are composited of various ribonucleotides. The nucleic acid sequences can be chemically synthesized following a 3’ to 5’ direction. Each nucleotide carried a negative charge on its phosphate group, therefore aptamers are highly negatively charged biopolymers (Pestourie, Tavitian and Duconge, 2005; Li *et al.*, 2015). *In vitro* selection can lead to the isolation of nucleic acids including RNA, ssDNA, modified RNA, and modified ssDNA (Famulok, Hartig and Mayer, 2007).

The secondary structure of an aptamer, referring to the local folding of the nucleotide chain, is determined by the base-pairing interactions between different regions of the nucleic acid sequence. A few studies have identified specific secondary structure elements among multiple self-hybridized aptamer structures (Pilehvar *et al.*, 2015). Aptamers can form different secondary structures, and they are predicted including (i) stem-loop structures, (ii) pseudoknots, (iii) G-quadruplexes, and (iv) various loops (**Figure I-23**).

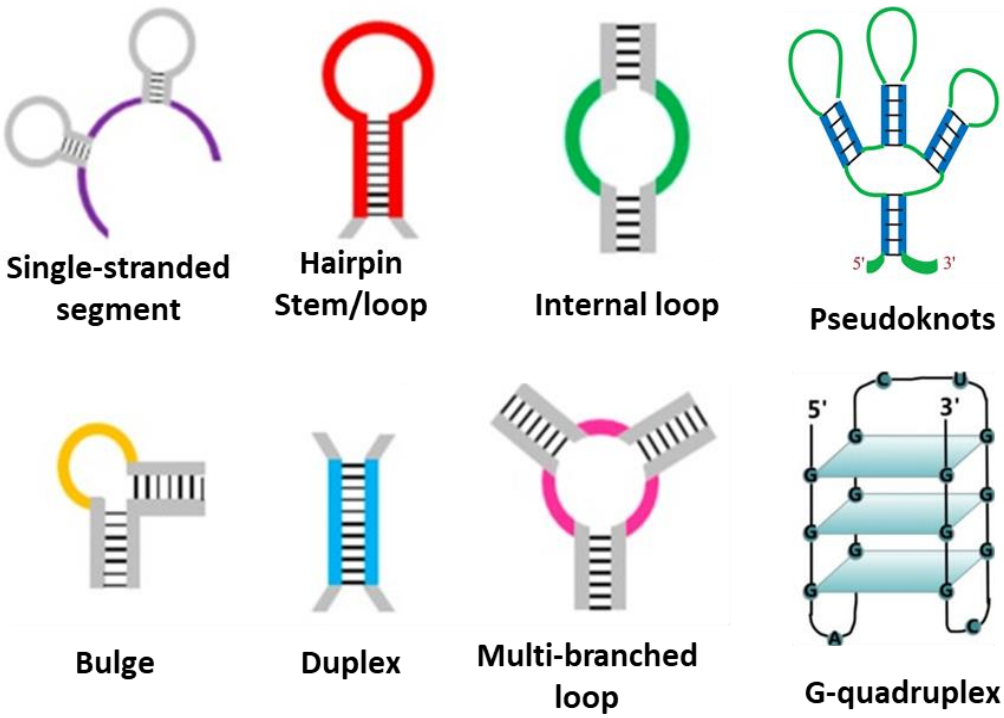


**Figure I-23 The predicted secondary structure elements of an aptamer**

Source: Sullivan *et al.*, 2019. Aptamers can be predicted into different secondary structure, namely single-stranded segment, hairpin stem/loop, internal loop, pesudoknots, bulge, duplex, multibranched loop, and G-quadruplex.

Stem-loop structures are formed by base-pairing between complementary regions of the sequence, leading to the formation of a stem and a loop, such as a hairpin structure. Pseudoknots are more complex structures that involve the formation of multiple stem-loops that are intertwined. G-quadruplexes are formed by the stacking of guanine bases in a planar arrangement, which can lead to the formation of a four-stranded helix such as the historically popular thrombin-binding DNA aptamer (Kelly, Feigon and Yeates, 1996; Nagatoishi *et al.*, 2011; Russo *et al.*, 2013). The dominant and suboptimal secondary structures of aptamers are predicted by various tools such as Zuker's Mfold ("M" induces "multiple") online web server

or RNAfold, under the principle of the free-energy minimization algorithm (Zuker, 2003). The secondary structure of an aptamer can have a significant impact on its binding affinity and specificity. For example, the formation of a stable stem-loop structure can help to stabilize the aptamer-target complex and increase binding affinity (Armstrong and Strouse, 2014). In contrast, the formation of a pseudoknot structure can result in a more flexible aptamer that is better able to adapt to different target conformations (Bjerregaard, Andreasen and Dupont, 2016).

The tertiary (3D) structure of an aptamer refers to the global folding of the nucleotide chain. The tertiary structure is determined by the interactions between different regions of the aptamer, such as hydrogen bonding, stacking, and electrostatic interactions. Aptamer's secondary structure contributes to the 3D structure prediction (Jeddi and Saiz, 2017). Some secondary elements will be employed in the prediction of 3D structures, including the helix and loops (**Figure I-24**) (Song *et al.*, 2020). Aptamers can form a variety of tertiary structures, including compact structures, extended structures, and complex structures. The tertiary structure can determine the aptamer's stability (Mayer, 2009), specificity, and sensitivity to environmental changes.

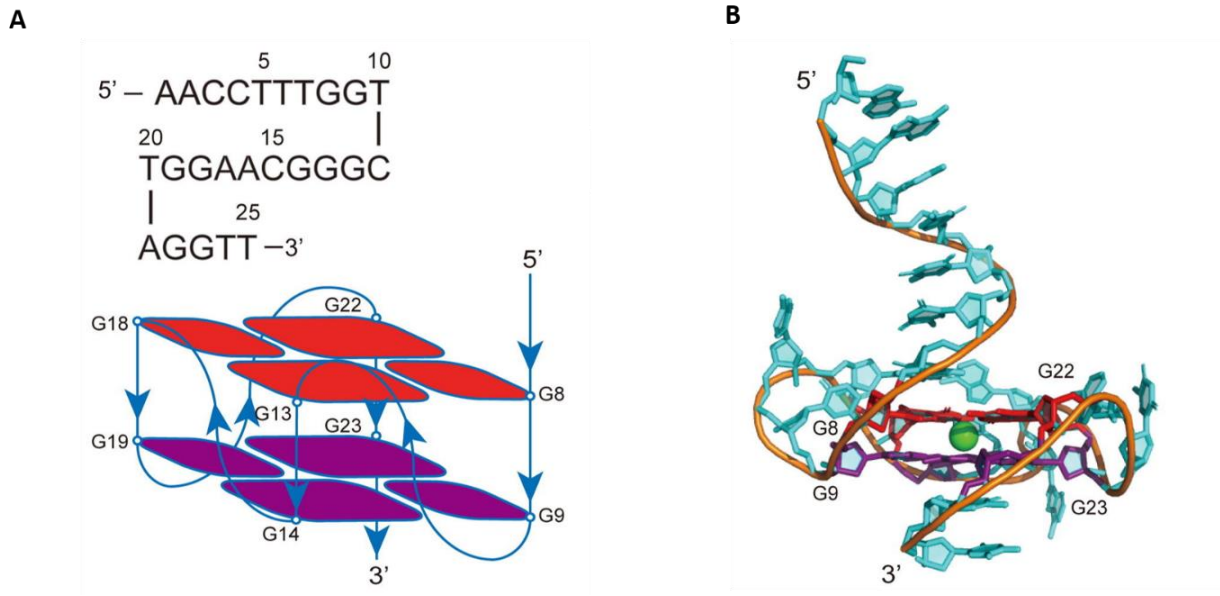


**Figure I-24 The predicted structure of a DNA aptamer**

Source: Song *et al.*, 2020. (A) The sequence and predicted G-quadruplexe-core pattern and (B) full-length 3D model of DNA aptamer for marine toxin gonyautoxin 1/4.

The structure of an aptamer can be characterized using techniques such as nuclear magnetic resonance (NMR) spectroscopy, X-ray crystallography, and circular dichroism (CD) spectroscopy (Sosnick, Fang and Shelton, 2000). CD spectroscopy is based on the differential absorption of left-and right-polarized light by the analytes. The CD spectrum of an aptamer is typically used to elucidate its possible secondary or tertiary structure (Yu *et al.*, 2021). Overall, the structure of aptamers is intimately linked to their function as molecular recognition elements. The precise structure of an aptamer determines its binding affinity and specificity for the target molecule. Changes in the aptamer's structure can affect its binding properties and overall function. Therefore, the design and optimization of aptamers for specific applications require a thorough understanding of their structure-function relationship.

### I.5.4.2 Affinity and specificity of aptamers

Aptamers are characterized by several parameters that determine their binding affinity, specificity, stability, and function. The most important property of an aptamer is how well it binds to its target molecule and distinguishes it from other non-specific molecules that may be present in a biological mixture. Thus, the key parameters of characterization are binding affinity and specificity (Dunn, Jimenez and Chaput, 2017). Binding affinity is typically determined as a solution equilibrium dissociation constant ($K_D$), which represents the concentration of the target molecule at which half of the aptamer molecules are bound. A lower value of $K_D$ indicates a higher binding affinity, whereas the specificity of an aptamer is determined by its ability to discriminate between the target molecule and other molecules in a complex mixture. The specificity is measured quantitatively as the ratio of $K_D$ for a cognate target to $K_D$ for a non-cognate target. Specificity is often reported for only a few off-target molecules that either have broad affinities for nucleic acids in general or are homologues of the targets. In general, $K_D$ values for most protein aptamers are in the low to sub-nanomolar range, whereas $K_D$ values for small-molecule aptamers are in the low to sub-micromolar range (McKeague and Derosa, 2012). The development of small-molecule aptamers with high affinity is therefore technically challenging. The majority of aptamers have been reported for binding affinity assays, but only a very small number have been reported for specificity assays (Hasegawa *et al.*, 2016).

Aptamer-target interactions are determined by the dynamic nature of aptamers and the characteristics of the targets (Deng *et al.*, 2014). Aptamers have been reported to bind their targets primarily through hydrogen bonding, electrostatic interactions, the hydrophobic effect, π- π stacking, van der Waals forces, or multiple combinations of these different forces (Tan *et al.*, 2016). To determine the binding interactions between aptamers and target molecules, various physicochemical methods have been applied, and each has its advantages and limitations (Cai *et al.*, 2018).

Surface plasmon resonance (SPR) is one of the most popular technologies to study aptamer-target binding interaction. Target molecules or aptamers are required to be immobilized on the biosensor chip first as a ligand. When analytes circulate, the refraction index will change resulting in the generation of the SPR signals (Wang and Zhou, 2008). This technology has key strengths since it allows (i) the monitoring of the interaction process in real-time, (ii) without any labelling, (iii) and high sensitivity. However, it suffers from some limitations hindering its widespread use. Firstly, SPR methods can suffer from non-specific absorption (Wu *et al.*, 2016), because almost any binding moiety on the biosensing chip can change the local refractive index. Secondly, the immobilization of one of the interaction partners can induce some structural modifications, even hide the epitope region, especially for small-molecule targets, thus influencing the binding (McKeague and Derosa, 2012). Finally, the binding parameters obtained by SPR do not necessarily correspond to those of the aptamer and ligand interacting freely in solution (Yu *et al.*, 2021).

Isothermal titration calorimetry (ITC) is another widely used method to investigate aptamer-target interactions. It's a powerful method to monitor the thermodynamics of the binding between aptamers and targets (Sakamoto, Ennifar and Nakamura, 2018). It can provide supportive data such as the reaction's stoichiometry and almost all the thermodynamic parameters, including the dissociation constant ($K_D$), the enthalpy change ΔH, the entropy change ΔS, the Gibbs free energy change ΔG, and the number of binding sites (Cai *et al.*, 2018). It eliminates the need for any chemical modifications or molecular labelling during titration analysis. However, a large quantity of samples is usually needed for ITC experiments and poor detection limits are sometimes obtained (Kobori *et al.*, 2007).

Microscale thermophoresis (MST) is a technique that uses fluorescent labelling of analytes to track the movement/diffusion of molecules along a temperature gradient (Thevendran and

Citartan, 2022). The MST signal can be continuously monitored in microcapillary tubes using fluorescence imaging as the irradiation progresses. Typically, MST detections are performed with a fixed concentration of target and a varying concentration of aptamer. As a free-in-solution based analysis, the MST approach provides a rapid enumeration of aptamer-target interactions in microscale volumes. Furthermore, it stands out for its ability to determine $K_D$ in complex samples such as human serum (Rangel et al., 2018). However, the compulsory requirement of fluorescently labelled molecules and highly exothermic aptamer reactions can add unnecessary complications (Thevendran and Citartan, 2022).

Dimethyl sulfate (DMS) footprinting is a classical method for studying RNA aptamers. DMS footprinting can report the accurate binding sites and investigate how the binding affects RNA (Tijerina, Mohr and Russell, 2007). By comparing the presence and absence of a bound ligand, the altered binding regions of the aptamer can be identified and localized (Spickler, Brunelle and Brakier-Gingras, 1997). It has been applied to monitor the binding process of RNAs to proteins and small ligands.

Currently, nuclear magnetic resonance (NMR) spectroscopy and X-ray crystallography have been used to study the binding. They are usually applied to detect the structural changes of the aptamer-target binding complexes (Warfield and Anderson, 2017). But both are limited to the research of aptamers-small molecules (<30-40 kDa). In addition, it can be difficult to obtain crystal structures of the binding complexes for X-ray crystallography.

Furthermore, aptamers can be chemically modified to enhance their binding affinity, specificity, and stability. Modification strategies include the addition of chemical groups to the nucleotides (Tolle and Mayer, 2013), the introduction of non-nucleotide moieties, or the conjugation of aptamers to other molecules. Modified aptamers can be characterized for their enhanced properties using the above-mentioned techniques.

The advantages and limitations of described methods are listed in **Table I-3** (Cai *et al.*, 2018).

**Table I-3 Summary of the analytical methods used to probe aptamer–target interactions**

| Methods | Principle | Advantages | Disadvantages |
|---|---|---|---|
| SPR | Main parameters are measured through changes in the refractive index when analytes bind to aptamers | Label-free, real-time, small quantities of analytes are needed | Limited sensitivity for small targets, limited detecting range, low-throughput |
| ITC | Heat is measured as the signal, which is released during the formation of the aptamer-target binding complex | Determines most thermodynamic parameters | Large sample quantities, low throughput, poor detection limits |
| MST | A microscopic temperature gradient is induced by an irradiating laser and the movement of the fluorescent molecules is detected and quantified during aptamer-target binding | Highly sensitive to molecular changes and temperature-dependent distribution; minimal samples are required. | Require fluorescent labelling for tracking molecular movements |
| DMS footprinting assays | DMS can methylate the N1 of the adenine and the N3 of the cytidine nucleotides, while the binding between RNA and target molecules can protect the involved nucleotides from methylation | Provides signals of the base-pairing of adenosine and cytidine nucleotides. The reaction is fast. The small size of DMS allows high spatial resolution. | Signal for accessibility of the phosphodiester backbone of the RNA and changes in global properties of the RNA are not provided |
| NMR | Nuclei in a magnetic field absorb and re-emit electromagnetic radiation | Little difference in the molecular structure can be detected | Limited to research on the relatively small molecules |
| X-ray | The pattern produced by the diffraction of X-rays through the closely spaced lattice of atoms in a crystal id recorded and then analyzed to reveal the nature of the lattice | A direct method that can be used to determine the structures of aptamer-target binding complexes | It is different to obtain crystal structures of the binding complexes |

SPR: surface plasmon resonance; CD: circular dichroism spectroscopy; ITC: isothermal titration calorimetry; DMS footprinting: dimethyl sulfate footprinting; NMR: nuclear magnetic resonance spectroscopy.

In summary, aptamers are characterized by their binding affinity, specificity, structure, stability, and modification. These characterizations can help researchers select and optimize aptamers for specific applications in various fields.

### I.5.5 Aptamer-based method for small molecule detection

Aptamers also have been applied to bind to and identify small molecules such as amino acids and various biological cofactors (McKeague and Derosa, 2012). The demand for the detection of small molecules (<900.0 g/mol) is increasing. For instance, metal ions for monitoring human health and markers for disease led to quick, reliable and sensitive detection methods being required (Ruscito and DeRosa, 2016). Moreover, the level of pathogens and heavy metals in water or food requires measuring to ensure food and water safety. Therefore, aptamers for small molecules can be applied to a large application in medicine, agriculture and environment analysis (Lyu, Khan and Wang, 2021). Until now, aptamers targeting small molecules such as ATP, thrombin, cocaine and theophylline has been used for sensoring or biosensing (Mascini, Palchetti and Tombelli, 2012). Due to their remarkably high selectivity, aptamers have always been considered ideal molecular recognition probes for small molecules (Famulok, 1999). For example, an RNA aptamer against theophylline was selected in 1994, establishing a new tool for small molecules recognition (Jenison *et al.*, 1994). Several additional aptamers have been isolated with a high affinity against small molecules such as guanine ($K_D$ of 5 nM, Mandal *et al.*, 2003), or oxytetracycline ($K_D$ of 9.6 nM, Niazi *et al.*, 2008). However, compared to the number of aptamers for larger molecules (protein, cells, etc.), there are very few for small molecules.

The *in vitro* selection experiments are conceptually similar but the specific experimental designs may differ considerably, based on (i) the nature and characteristics of the target molecule, and (ii) the selection strategies for separating target-bound sequences from unbound ones (Mckeague *et al.*, 2015). Several technical challenges associated with the SELEX experiment are considered to be involved in blocking the study of aptamers for small molecules. First of all, the size- or charge-mediated separation strategies are difficult to apply to small molecules because there is little difference in the molecular weight or charge of the aptamer-target complex compared to the aptamer alone (Blind and Blank, 2015). In this case, conventional SELEX involving the conjugation of a small-molecule target to a solid surface is performed using magnetic beads such as sepharose 4B beads (Liu *et al.*, 2018), acrylic beads, agarose/sepharose (Hamedani *et al.*, 2022), or an affinity column and platform (Chapuis-hugon *et al.*, 2011), to facilitate the separation process. Nevertheless, the lower the target loaded onto magnetic beads, the more competition among the sequences in the pool, which

could result in non-specific binding. In addition, the selection is performed using a conjugated target rather than a free one, which may negatively affect the affinity in the following application when the target is free in solution.

In order to avoid immobilization of the target on beads, alternative methods including structure-switching SELEX and capture-SELEX are performed (**Figure I-25**). In the structure-switching SELEX approach, a single strand of fluorescent oligonucleotides hybridizes to complementary DNA capture probes immobilized on magnetic beads (**Figure I-25A**). The aptamers are separated from immobilized oligonucleotides *via* a target-induced change in conformation. By this way, target remains free in solution (Nutiu and Li, 2003). The aptamer sequence, which changes conformation from a nucleic acid duplex to an aptamer-target complex upon binding to the target, is consequently released from the beads and produces a fluorescent signal (Feagin, Maganzini and Soh, 2018). In Capture-SELEX approach, without the need for target immobilization (Stoltenburg, Nikolaus and Strehlitz, 2012), beads are modified with a capture oligodeoxynucleotide complementary to a short docking sequence embedded in the random region of the library (**Figure I-25B**). When interacting with the target, a big change in the secondary and tertiary structure of the oligonucleotide takes place. However, due to many rounds are needed, it is time-consuming and arduous. In the process of Capture-SELEX, the abundance and diversity of the library may decrease. The binding sequences can only be separated from the matrix and other sequences in the library when the library undergoes a sizable conformational change upon target binding (Lyu, Khan and Wang, 2021). Therefore, this technology lacks sequence diversity while increasing displacement activity.

Based on their inherent structure-switching functionality, a sensor is easily established. Even though they are promising direct-selection strategies, the structure-switching SELEX and Capture-SELEX share some limitations. For instance, the immobilized oligonucleotide pool may hinder its downstream application due to changes in shape and conformation (Ruscito and DeRosa, 2016). The hybridization between the library and the docking strand is prone to spontaneous dissociation during the target elution step, and some sequences which unbound to the target are also dissociated from the support, resulting in low separation efficiency and more rounds to complete SELEX (Yu *et al.*, 2021).

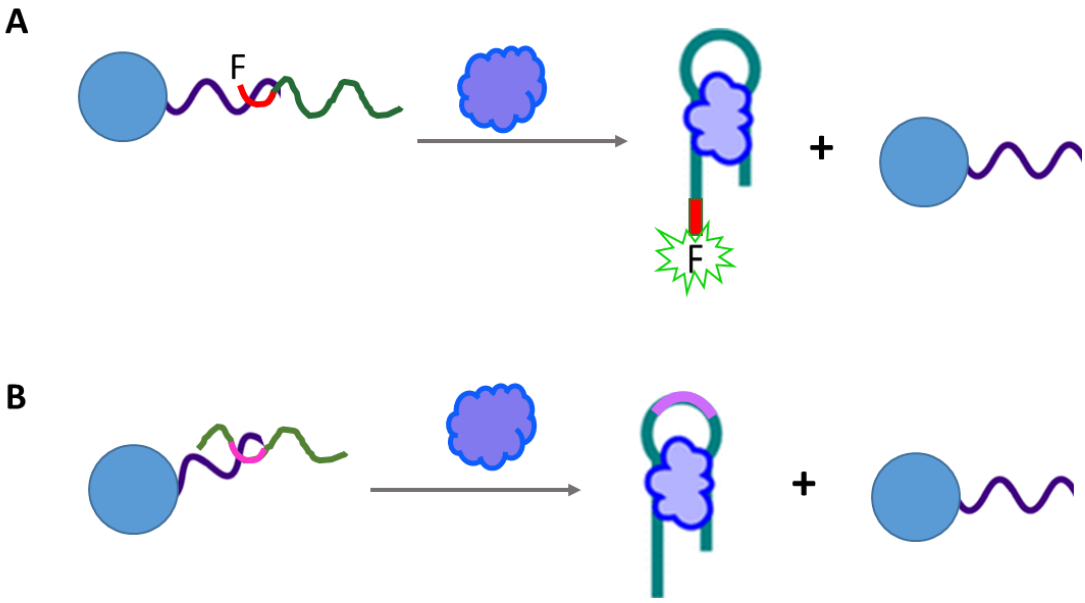


**Figure I-25 Strategies for selection of structure-switching aptamers**

Source: Feagin, Maganzini and Soh, 2018. (A) In structure-switching SELEX, a fluorophore-tagged oligonucleotide library (shown in green, highlighted with red fluorescent label) hybridizes to a short complementary DNA capture probe (shown in purple) conjugated to magnetic beads. Upon binding to the target, the sequences that undergo a large structural rearrangement are displaced from the capture strand and released from the dock. (B) In Capture-SELEX, the docking strand (shown in pink) within the random region of the oligonucleotide library hybridizes to a complementary DNA capture strand (shown in purple) coupled to the surface of the magnetic beads.

Moreover, Graphene oxide (GO)-SELEX was discovered for small molecules using the adsorption of graphene oxide with ssDNA without immobilizing targets (Nguyen *et al.*, 2014; Shi *et al.*, 2020). Differently, GO-SELEX adsorbs the non-target ssDNA, trapping oligonucleotides that are not bound to the target (Narlawar and Gandhi, 2021). But this procedure requires a high amount of GO to trap unbound oligonucleotides during the partitioning step of SELEX. Moreover, the adsorption of non-target bound ssDNA on GO surface rather than the selection of aptamers binding to the target (less frequent) results in the requirement of more SELEX cycles to achieve target-specific aptamer (Gu *et al.*, 2016).

Microfluidic SELEX (M-SELEX) technique, which combined capillary electrophoresis, microfluidic bead-based separation or sol-gel encapsulation, was performed in a microfluidic system that enabled automated systematic analysis of the evolution of ligands on-chip (Lai *et al.*, 2014). This method could handle small amounts of reagents cutting material costs and fewer rounds of selection compared to conventional methods, but the separation technique requires a special expertise (Ahmad *et al.*, 2011; Dembowski and Bowser, 2018).

Furthermore, other SELEX variations have been reported in order to reduce processing time or increase the process throughput such as Fluorescence-activated cell sorting (FACS)-SELEX (Wang *et al.*, 2014), Photo-SELEX (Brody and Gold, 2000), high-throughput sequencing (HTS)-SELEX (Komarova, Barkova and Kuznetsov, 2020) and *in silico* SELEX (Rabal *et al.*, 2016). Although a series of small molecule aptamers have been obtained by some of the selection methods mentioned above, each ligand SELEX development needs dedicated improvement.

Another challenge associated with the aptamer selection for small molecules is the lack of functional groups available for strong aptamer binding (Ruscito and DeRosa, 2016). Due to some small molecules containing similar structures with functional groups arranged only slightly different, it is difficult not only to select an aptamer that binds with high affinity but also that binds with high specificity. In this case, some organic compounds such as monosaccharide or organometallic receptors have been incorporated into a detection system using aptamers to promote the aptamer-target interaction: For example, Yand *et al*. used Shinkai's glucose fluorescent receptor to select aptamers capable of recognizing the monosaccharides glucose, fructose, and galactose (Yang *et al.*, 2014). After counter-selections against the receptor, a sensor could be established with a composition of a fluorescently-labelled aptamer. This technique, in which the receptors first form a complex with the targets, could also be applied to small molecules that do not contain suitable functional groups for binding during selection (Ruscito and DeRosa, 2016).

Recently, aptamer-based biosensors have been broadly utilized, involving a biological molecular recognition element and a physiochemical transducer to convert the binding event into a measurable signal (Sefah *et al.*, 2009). A biosensor that uses aptamers as the recognition element is called an aptasensor. It can be achieved through various mechanisms, such as electrochemical, optical, or piezoelectric transduction.

Overall, aptamer-based methods for small molecule detection offer several advantages, such as high specificity and sensitivity, ease of production and modification, and ability to detect a wide range of small molecules. They have potential applications in various fields, including clinical diagnostics, environmental monitoring, and food safety testing.

## I.6 Conclusions

*Salmonella* is a well-known bacterial pathogen that causes a wide range of diseases in both humans and animals. With several virulence factors including flagella, adhesins, and injectisomes, *Salmonella spp.* can colonise different hosts. It can sense and respond to mechanical cues in its environment, which allows it to adapt to changing conditions and survive in a variety of different host cells. One of the key mechanisms by which *Salmonella* senses mechanical cues is through the activity of mechanosensitive ion channels, which are thought to be involved in a range of cellular processes including signal transduction, and membrane remodelling. However, the flagella associated mechanosensing process within *S*. Typhimurium is complex and still not understood.

Another important aspect of *Salmonella spp.* biology is the process of protein methylation. Protein methylation is a PTM that involves the addition of methyl groups to specific amino acid residues of different proteins, and it is carried out by a family of enzymes known as protein methyltransferases. Lysine methylation has been shown to play a critical role in regulating various aspects of bacterial physiology, including adhesion, invasion, virulence, and adaptation to environmental cues. The process of flagellar chemotaxis also involves the methylation of chemoreceptors, which is regulated by a group of chemotaxis proteins, typically the methyltransferase CheR. Methylated chemotaxis proteins affect the ability of the bacteria to sense and respond to chemical stimuli in turn. In particular, methylation of the chemoreceptor by CheR is thought to increase the sensitivity of the bacteria to chemical gradients. Additionally, FliB-dependent methylation of flagella facilitates adhesion to hydrophobic host cell surfaces and may modulate the transition between free-swimming and attached states of bacteria. The fact that PTMs such as methylation can occur rapidly and help organisms to adapt to changes in their environment or behaviour so it fits with the need for fast adaptation for this transition. Therefore, it could be involved in the process of bacterial transition from planktonic to sessile state.

Our main target is to study these mechanisms in *S*. Typhimurium. To date, a variety of different tools and techniques have been developed for methylated lysine detection. However, due to their limitations and the lysine methylation low abundance, an efficient methyllysine enrichment approach is required. Aptamers are potentially an efficient tool to

target small molecules. Aptamer-based tools are expected to help us gain new insights into the molecular mechanisms underlying bacterial mechanosensing and protein methylation, and to develop new strategies for targeting these processes in the development of novel enrichment and purification approach.

In conclusion, with the help of aptamer-based tools to purify methylated proteins from *S*. Typhimurium, some important insights into complex mechanisms that allow bacteria to sense and respond to their environment could be provided. The development of new tools and techniques for studying these processes will undoubtedly continue to drive advances in our understanding of bacterial pathogenesis and provide new opportunities for the development of effective therapies to combat infectious diseases.

# Chapter II Selection of DNA aptamers against methyllysine by FluMag-SELEX

## II.1 Context

Since the first discovery of aptamers in the 1990s, they have been discribed to tightly and selectively bind to a broad range of targets, including metal ions, peptides, PTMs, mixtures of proteins, intact cells (Berezovski *et al.*, 2008; Raddatz *et al.*, 2008) and small organic molecules (with molecular weights from 100 to 10,000 Da) including several amino acids. Their binding abilities are due to their complex structures containing stem-loop, internal loops, etc. when binding with various targets (Mastronardi *et al.*, 2021). Until now, several aptamers have been discovered against a few amino acids, with $K_D$ generally ranging from mM to µM, as shown in **Table II-1** based on Mastronardi *et al*. (Mastronardi *et al.*, 2021).

**Table II-1 DNA and RNA aptamers selected for amino acid targets**

| Amino acid target | DNA/RNA aptamer | Apparent $K_D$ | Reference |
|---|---|---|---|
| L-arginine | DNA | 2.5 mM | (Harada and Frankel, 1995) |
| | RNA | 56-76 µM | (Famulok, 1994) |
| | RNA | 330 nM | (Geiger *et al.*, 1996) |
| L-citrulline | RNA | 62-68 µM | (Famulok, 1994) |
| D-citrulline | RNA | 180 µM | (Famulok, 1994) |
| D-arginine | RNA | 410 µM | (Famulok, 1994) |
| L-and D-glutamic acid | DNA | 580-810 µM | (Ohsawa *et al.*, 2008) |
| L-histidine | RNA | 8-54 µM | (Majerfeld, Puthenvedu and Yarus, 2005) |
| Isoleucine | RNA | 0.9 mM | (Legiewicz and Yarus, 2005) |
| L-isoleucine | RNA | 200-500 µM | (Allain *et al.*, 2000) |
| | RNA | 1-7 mM | (Lozupone *et al.*, 2003) |
| L-phenylalanine | RNA | 34-55 µM | (Illangasekare and Yarus, 2002) |
| L-tryptophan | DNA | 1.76 µM | (Yang *et al.*, 2011) |
| D-tryptophan | RNA | 18 µM | (Ellington, 1994) |
| L-tyrosine | RNA | 35 µM | (Mannironi *et al.*, 2000) |
| L-valine | RNA | 2.9 mM | (Hale and Schimmel, 1996) |
| L-serine | DNA | 2-7.9 µM | (Mastronardi *et al.*, 2021) |
| Trimethyllysine (TML) | DNA | 2.48 mM | This study |

Due to their extreme selectivity, aptamers are able to accurately discriminate closely related molecules with slight structural differences like functional groups and enantiomers of the same chiral molecule, as listed in **Table II-1** (Flinders *et al.*, 2004; Jo *et al.*, 2011). Moreover, some aptamers with modifications at 5' (-fluore and -biotin) conjugated to magnetic and fluorescent nanoparticles, as immobilized ligands in separation technologies, have been broadly used to enrich various target proteins at low concentrations (Herr *et al.*, 2006; Phillips *et al.*, 2008). Taken together, *in vitro* selection of aptamers could lead to specific binding agents for methyllysine. Hence, aptamers would be suitable for recognizing MML, DML and TML, respectively.

Since the discovery of the SELEX selection approach, aptamer technologies saw a significant development for a more efficient and cost-effective selection process due to the evolutions of technical equipment, analysis methods and chemical synthesis (Darmostuk *et al.*, 2015). For instance, capillary electrophoresis-SELEX (CE-SELEX) performs the selection process in the capillary and the separation was carried through an aptamer-target complex from unbound oligonucleotides according to their migration speeds caused by different charge-mass ratios in the electric field (Zhu *et al.*, 2019). The main limitation of CE-SELEX is that the equilibrium time must be strictly controlled and the difficulty of separating the free oligonucleotides from the complex formed by the binding of small ligands, due to the small differences in the mobility between them (Mosing and Bowser, 2009). Cell-SELEX uses whole cells as targets (Catuogno and Esposito, 2017; Kaur, 2018). It allows the selection of aptamers directed against the target according to their natural conformation, with appropriate modifications and orientations. Moreover, protein purification, which is time- and cost-reducing, is not necessary. Likewise, a large number of aptamers have been produced against bacterial cells, such as *Salmonella* Typhimurium, *Escherichia coli*, *Vibrio parahaemolyticus* and *Trypanosoma cruzi* using Cell-SELEX technology (Darmostuk *et al.*, 2015). However, during Cell-SELEX process, non-specific oligonucleotides can bind to cells and complex surface components of targets hinder aptamers identification.

FluMag-SELEX is a technique that combines fluorescence and magnetic bead-based SELEX to isolate aptamers. It is a selection method for fluorescence-labelled aptamers by binding the target to magnetic beads (Stoltenburg, Reinemann and Strehlitz, 2005). The use of magnetic beads and fluorescent labels allows a very small amount of target to be used for aptamer

selection and avoids radioactive labelling (Malhotra *et al.*, 2021). The use of fluorescent labels makes the enrichment process of the target-binding oligonucleotides visible and facilitates the step of purifying the relevant ssDNA out of the dsDNA PCR products. Besides, the fluorescent labelling of the selected oligonucleotides makes quantification easier by directly monitoring the fluorescence signal during selection (Malhotra *et al.*, 2021). FluMag-SELEX offers the potential for parallel and easy manual processing of multiple targets without the need for expensive instruments (Hao and Gu, 2021). This approach has successfully selected several ssDNA aptamers against ethanolamine (Mr=61.08), the smallest aptamer target described so far (Mann *et al.*, 2005). Therefore, FluMag-SELEX experiments can be suitable for aptamer selection against small targets such as methyllysine.

The overall goal of this work is to select an aptamer with affinity and specificity to methyllysine MML, DML and TML, respectively. The selections of the specific aptamers against MML, DML, and TML were separately performed using the FluMag-SELEX technology, through several repeated rounds of selection and enrichment processes (**Figure II-1**) (Stoltenburg, Reinemann and Strehlitz, 2005). The eluted ssDNA pools against the corresponding target from the last round were cloned and then the sequencing analysis was carried out. Subsequently, after aligning the sequences, the one with the highest redundancy was chosen for the characterization of interaction properties between the selected aptamer and its target, including affinity and specificity. The goal of this work should lead to the use of the selected aptamer against methylated lysine for future applications as a new purification tool to isolate and identify methyllysine-containing proteins or peptides.

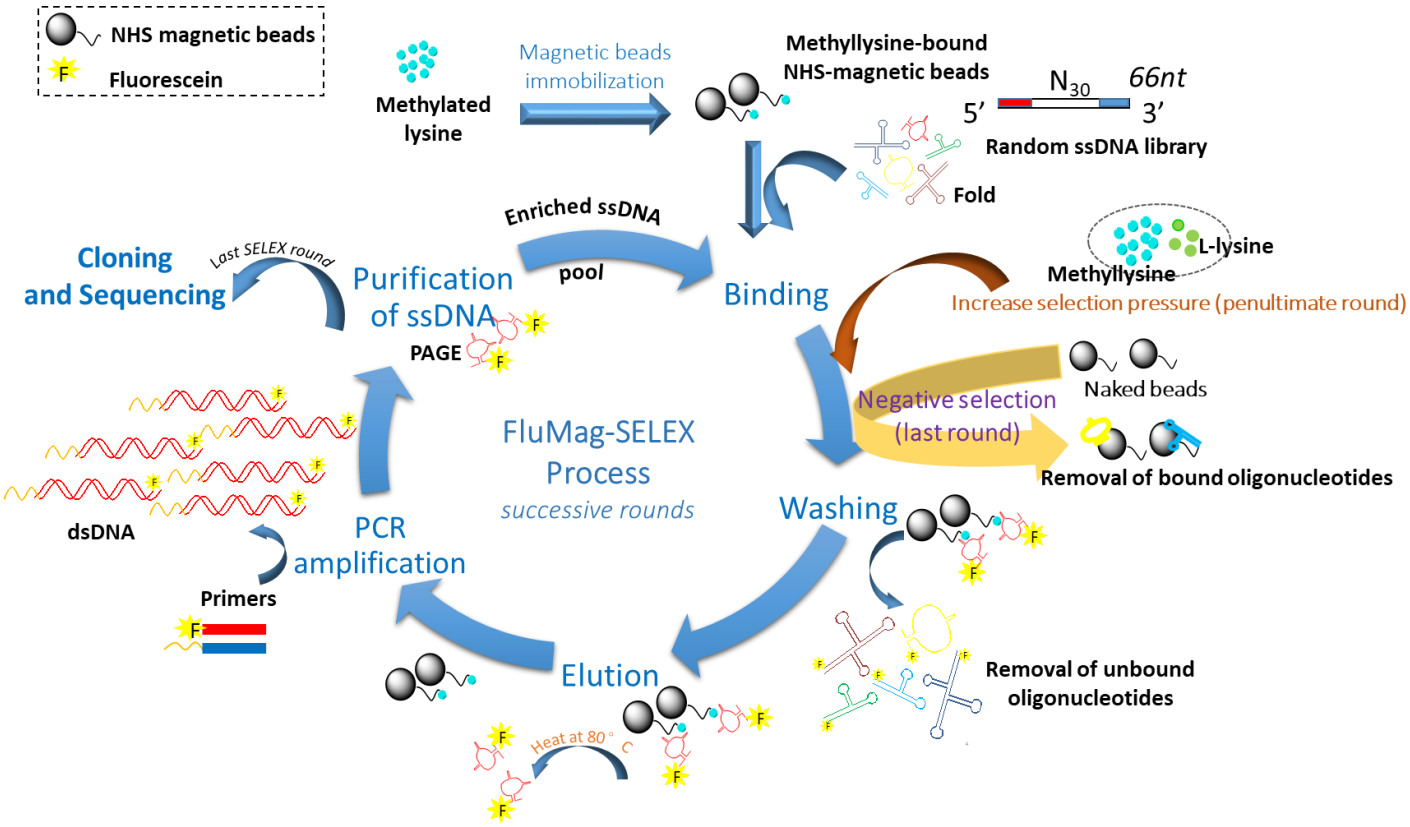


**Figure II-1 Schematic representation of the FluMag-SELEX procedure for the selection of DNA aptamers to methyllysines**

The FluMag-SELEX process for generating DNA aptamer for specific target molecules (here MML, DML and TML) immobilized on NHS-magnetic beads. The starting random ssDNA library consisting of oligonucleotides with a centrally randomized region of 30 nucleotides flanked by two specific regions was incubated with the target beads (methyllysine-bound NHS-magnetic beads) for binding. Unbound oligonucleotides were washed away, and the bound oligonucleotides were eluted from the target beads by heat treatment at 80°C. The eluted oligonucleotides were amplified by PCR using specially modified primers (forward primer modified with 5'-fluorescein (F, yellow star), and reverse primer modified with 5'-poly-dA20-HEGL (orange tail) to enable separation and recovery by denaturing urea-PAGE as described in materials and methods. The relevant ssDNA was subsequently purified from the double-stranded PCR products by PAGE and the resulting enriched ssDNA pool was used in the next SELEX round for binding with target beads. The fluorescein (F) labelled the selected oligonucleotides after the first SELEX round and thus enabled monitoring of the ssDNA purification. In the penultimate round, the selection pressure was increased by adding L-lysine and other types of methyllysine to the solution. In the last round, a counter selection was performed using naked beads and then the selected aptamers were cloned, and several monoclonal aptamers were characterized.

# II.2 Selection

## II.2.1 The oligonucleotide library

Starting point of the FluMag-SELEX process was a random ssDNA oligonucleotide library based on the original FluMag-SELEX strategy (Stoltenburg, Reinemann and Strehlitz, 2005). Taking

into account that short random regions of the oligonucleotide library may be better for a small target (Pan and Clawson, 2009), the SELEX library consisted of a multitude of ssDNA fragments comprising a central random region of 30 nucleotides (nt) (N) flanked by specific sequences of 18nt at the 5'- and 3'-end, which function as primer binding sites for the PCR: 5'-ATACCAGCTTATTCAATT–$N_{30}$-AGATAGTAAGTGCAATCT-3'. The total length is then 66nt with a medium molecular weight of 20391.4 g/mol. The theoretical diversity of this bank is $4^{30}$ or $1.15.10^{18}$. But, due to the size of samples and issues related to the synthesis processes, this diversity is rather estimated at $10^{14}$ to $10^{15}$ distinct oligonucleotides (Ni *et al.*, 2021). Knowing that previous selection work against a single amino acid as a target (for example Arg, in Gospodinov and Kunnev, 2020) leads to GC-rich sequences, the library was designed with a bias for G and C nucleotides performing an unbalanced distribution of the random region with 20%A-25%C-35%G-20%T.

The synthesis of the library has been outsourced and included a reverse phase chromatography-based (RP)-cartridge purification step. The synthesized library has further been validated by sequencing several clones in order to check if it met the requirements, in terms of diversity as well as the expected length. The sequencing results from 20 colonies for the SELEX library are listed in **Figure II-2**. Of all 20 successfully sequenced colonies, 18 showed the expected 30nt while 2 clones showed 28nt. It demonstrated that the oligonucleotide library was not 100% pure, resulting in several shorter ssDNA fragments retained in the original selection bank and subsequently joining the SELEX process. Indeed, RP-cartridge is based on the difference in hydrophobicity between the full-length product and truncated sequences, yielding 75-80% of purity, which explained that the library not only contained ssDNA fragments in good length but also probably in a shorter size.

Moreover, except for a few homologous clusters such as "GCC", "TCA", "TTA" and "CGT" that appeared in some two adjacent sequences at the 5'- or 3'-end, there's no redundancy among these sequences. Among the sequences, "N" indicated any possibility of A or T or G or C nucleotides, due to the inability of the machine to determine the bit values correctly when nested peaks appear during the sequencing process. But based on the known sequences of the fragment, whatever nucleotide it does not change the fact that they have no redundancies. Therefore, the diversity meets the requirements of the designed random library for several rounds of FluMag-SELEX.

```
                1         10        20        30
                |---------|---------|---------|
>blank-1        GGGGCGCGCAGAGATGGTCGACTTTTCCGT
>blank-2        GGAACCTCGNTCATTGTGCCTGGGACTCTN
>blank-3        GGTGGTGGCTTGGTTCATAAGGAGGTTTCG
>blank-4        GCCAATAATTTACGTAAATAGGTGTTCGTT
>blank-5        GCCTGTTATACGGTTGACTGGTGCCGATGT
>blank-6        GGACCACTGAAGGCACGCCGGCTTTTCCCN
>blank-7        GCGTTCTAGTCTAGGGGCTATCAATTCA
>blank-8        TAGGGCTAGGGCACCGAAGCATATCTCA
>blank-9        CCAAGTAGAGACATTAAGTACTTCAACACG
>blank-10       ACAGGATGATGCTGCGATTCGTTTTTGTTA
>blank-11       NNCGGNTGTCNGCGGGTCGCTGATCTTTTA
>blank-12       GGGAGGNNNAAGTTAGCTGGNNNNNACGCG
>blank-13       CGTAGCGAGTGTGANTGGTCGAGTCCGTGT
>blank-14       CGTGTCCGGCGCGACGCTGGCATCTTTAGG
>blank-15       GAAGCGGCAAAGTCTGCCAAGTCGTTCCTT
>blank-17       TGCAGATGGTGGGTACGGAGGGGTATGGGG
>blank-18       GTAGTGTGAAAGCCTTGTGGGTTCTAGGGC
>blank-19       ATAGGCGGGTATGACCTCCAAAGCTCGGCG
>blank-20       GCGGACTTAGTGGTATCAGGTCCAAACTCT
>blank-21       GGTCGTTCTACATCCCCNGCAGACGTTTCG
```

**Figure II-2 The obtained sequences of oligonucleotides library**

Letters in blue mark homologous clusters shared in two adjacent sequences at the 5'- or 3'-end.

## II.2.2 Coating of the magnetic beads

Ninhydrin solution was used for detecting unbound methyllysine in the solution. The linear relationships ($R^2$>0.99) between absorbance and L-lysine, MML, DML, and TML concentrations (10, 20, 30, 40, 50 µg/ml) were observed, respectively (**Figure II-3**). The absorbance of the ninhydrin reaction solution at 570 nm is linearly related to the amino acid concentration, suggesting that the traditional ninhydrin method is appropriate to quantify MML, DML, and TML.

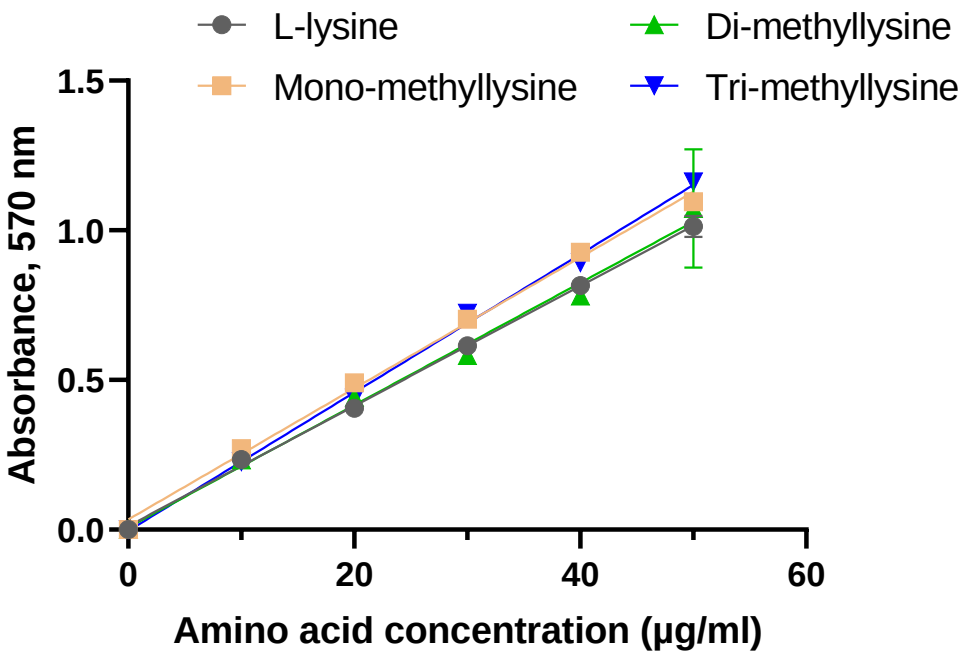


**Figure II-3 Relationships of lysine and methylated lysine concentration and absorbance measured by the ninhydrin method**

NOTE: All data are presented as mean ± standard error by duplicate determinations.

Since the commercial NHS magnetic beads were recommended to couple with 0.1-2.0 mg/ml protein solution, we performed 1, 3, 5, 10 mg/ml of MML, DML and TML to get the beads saturated. After incubation of a series of methylated lysines, the optimized concentration of methylated lysine (MML, DML and TML) was 3 mg/ml with an immobilized efficiency reached to highest level even though it's as low as around 20% as shown in **Figure II-4**. When the concentration was higher than 3 mg/ml, lower methylated lysine was coated with the beads, which illustrated that the activated sites on the beads were saturated.

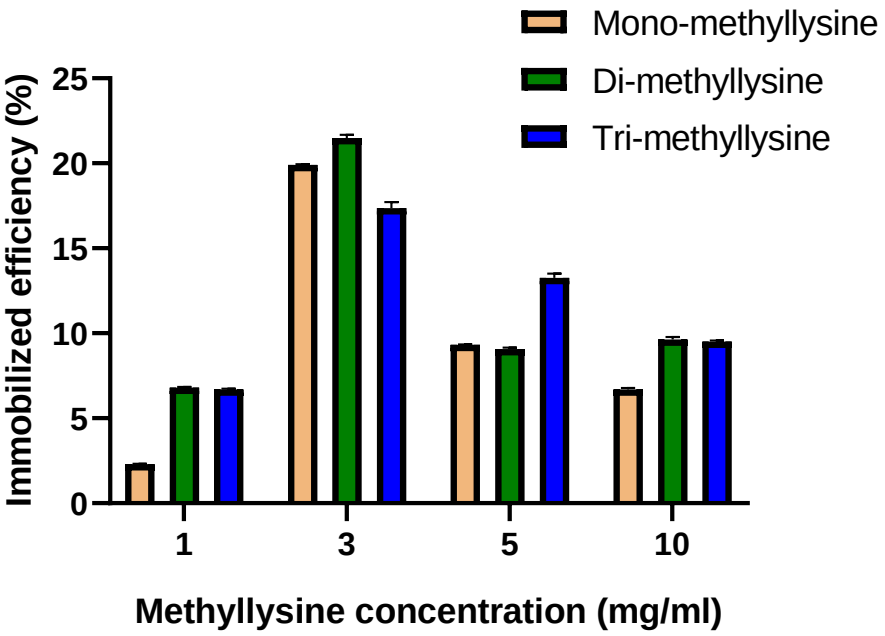


**Figure II-4 Relationships of methylated lysine concentrations and immobilized efficiency**

A constant NHS magnetic beads couple with 1, 3, 5, 10 mg/ml MML, DML, and TML. The immobilized efficiency was calculated by the ratio (coated methylated lysine*100/ total methylated lysine in the solution). All data are presented as mean ± standard error by duplicate determinations.

## II.2.3 Asymmetric amplification at each round

After the first round of the FluMag-SELEX selection, the selected DNA were labelled with fluorescein and a heavier Poly-$dA_{20}$ tail as described in the material and methods **VI.1.2**. Under a series of annealing temperatures from 47 to 60°C to optimize the PCR protocol, the best annealing temperature was defined at 47°C obtaining the expected band size (**Figure II-5A**). Therefore, the eluted DNAs were asymmetrically amplified under the annealing temperature 47°C in the following selection cycles. After the amplification step, the separation of the relevant DNA strands from the double-stranded PCR products was required by denaturing urea-PAGE (Flett and Interthal, 2013) as described in **Table VI-9**. The interest aptamer candidates are conjugated to fluorescein, whereas the complementary strand is heavier because of the poly-$dA_{20}$-hexaethylene glycol (HEGL) spacer, which was used for the separation of ssDNA from the double-stranded PCR products (Williams and Bartel, 1995). Under the UV, the fluorescent sense strand, corresponding to the selected aptamers, was removed from the gel (**Figure II-5B**), extracted and purified. To take a further check of the separation efficiency, methylene blue solution was used to stain the urea-PAGE. After

destaining with distilled water, the neo-synthesized strands with the Poly-dA20 sequence in 5', as well as excess sense/anti-sense primers can be visible (**Figure II-5C**).

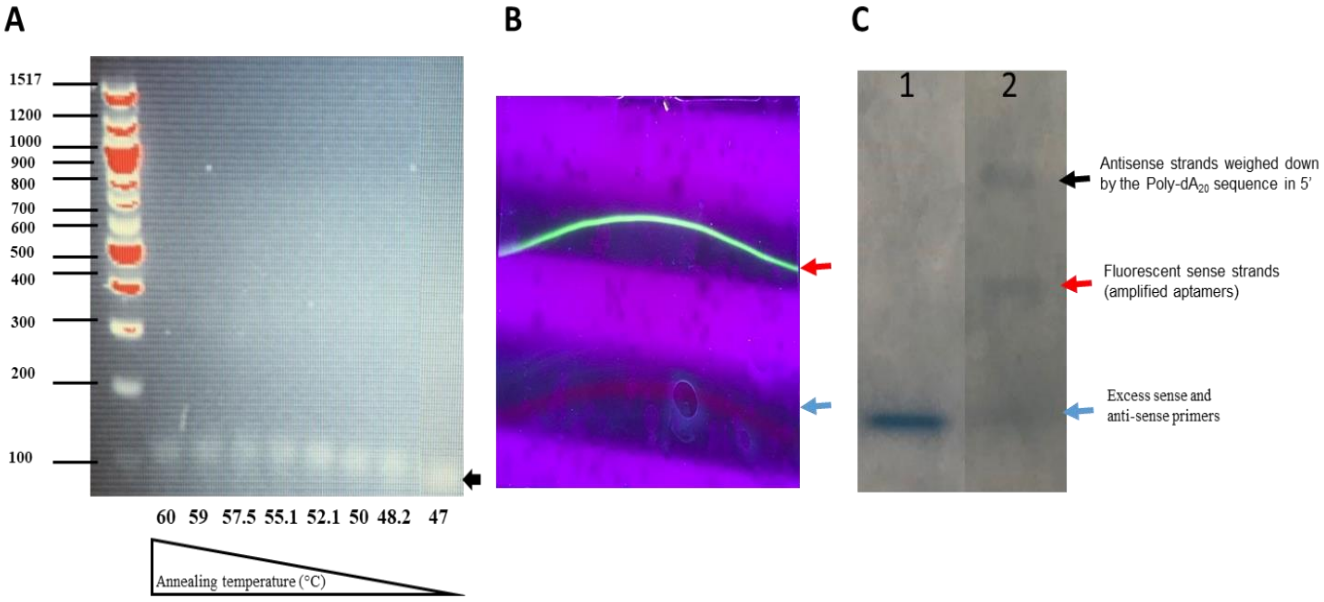


**Figure II-5 Electrophoresis of PCR products after asymmetric amplification**

(A) Electrophoresis of PCR products under different annealing temperatures on 5% agarose gel and stained with SYBR Safe DNA stain. The arrow indicates the expected size of the aptamer if retained. (B) Electrophoresis of PCR products on denaturing urea-PAGE under ultraviolet. The red arrow marked fluorescent sense strands and the blue arrow marked the excess primers. (C) Electrophoresis of PCR products on denaturing urea-PAGE of selected aptamers with methylene blue. The sense and antisense strands of the aptamers resulting from the PCR amplification were analyzed by electrophoresis in 20% PAGE-7M urea. Lane 1: mixture of primers Aptasensfluo and AptaantisensAAA; lane 2: PCR products after asymmetric amplification.

## II.2.4 Selection of aptamers targeting methylated lysine

During the selection process, we carried out several rounds of positive selections in which the oligonucleotides were mixed with NHS beads-coated with methylated lysine and one round of negative selection where the non-specific ssDNA were captured with naked NHS beads. The yield of the eluted ssDNA was measured after each positive selection round and negative selection round during the SELEX (**Figure II-6**). At the starting round, there were only a few eluted ssDNA pools. Gradually the amounts of ssDNA bound to MML- and DML-coated magnetic beads increased except for the 4$^{th}$ round, where the amount of oligonucleotides decreased slightly by around 10% (**Figure II-6A**) and less than 5% (**Figure II-6B**) for the MML

and DML, respectively. Whereas for TML, during all positive and negative selections, an increased yield of ssDNA was observed (**Figure II-6C**).

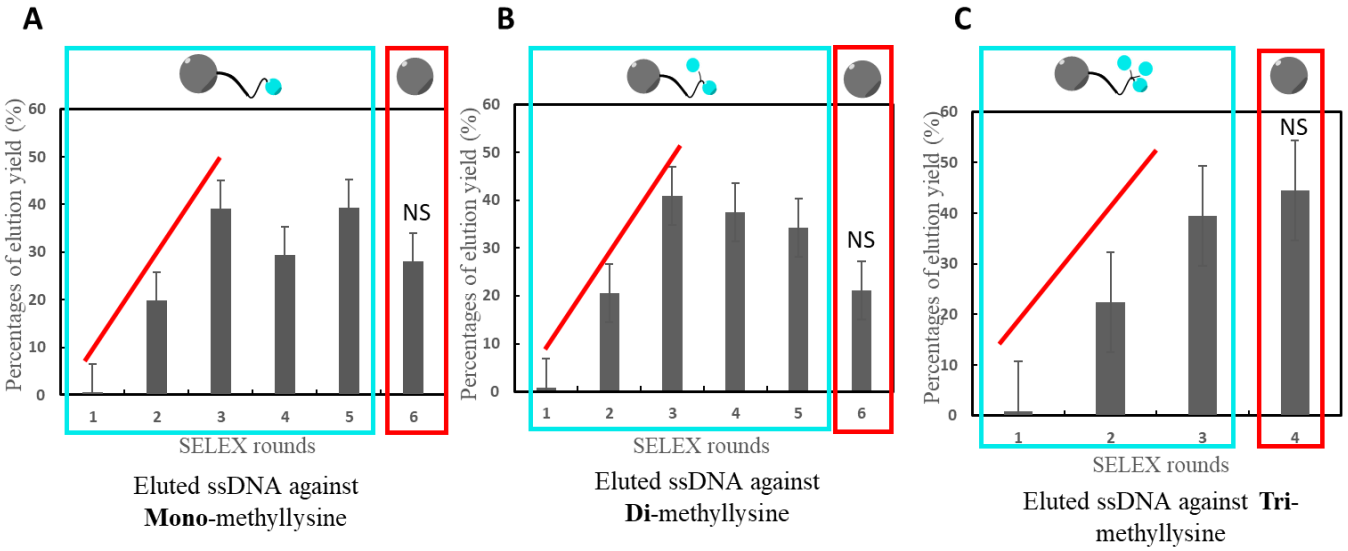


**Figure II-6 Aptamer enrichment during FluMag-SELEX process**

(A) Enrichment of MML-specific aptamers during the selection process. (B) Enrichment of DML-specific aptamers during the selection process. (C) Enrichment of TML-specific aptamers during the selection process. The red line illustrates an increasing trend. The positive selections are in a cyan square, and the negative selections are in a red square, respectively. The bar graph shows the yield of ssDNA eluted from methyllysine-coated NHS magnetic beads in each selection round. NS: negative selection. Error bars represent the standard deviation of the measurements of the eluted ssDNA in triplicate.

In order to eliminate oligonucleotides which are able to bind to unmethylated lysine (L-lysine) and other types of methylated lysine rather than the target, selection pressure was introduced in round 5 of the selection process by adding 0.1 mg/ml L-lysine, 0.1 mg/ml DML, and 0.1 mg/ml TML for MML; while by adding 0.1 mg/ml L-lysine, 0.1 mg/ml MML and 0.1 mg/ml TML for DML. Finally, for the selection of aptamers against TML, selection pressure was introduced in round 3 and induced by adding 0.1 mg/mL L-lysine, 0.1 mg/ml MML and 0.1 mg/ml DML simultaneously in the same binding buffer. Because TML was not readily available and with a high cost, fewer rounds were performed concerning the TML-aptamer selection. In addition, in the last round (i.e. round 6 for selection against MML and DML, but round 4 for selection against TML), a negative selection step with naked NHS magnetic beads was introduced to improve the specificity of the selected sequences by eliminating nonspecific binding oligonucleotides to the bead matrix (naked NHS magnetic beads). For MML and DML, the yield of eluted ssDNA decreased significantly, demonstrating the removal of a lot of non-specific oligonucleotides. Interestingly, no significant decrease during the

nonspecific step was observed for TML. This could be a consequence of two distinct phenomenons: (i) the size and even the charge of methylated groups in the TML could be the more favourable for establishing interactions with aptamers when compared to MML or DML, and/or (ii) the steric hindrance induced by the additional methyl group makes the beads surface less available, even if part of binding sites remains unoccupied. Nevertheless, the enrichment profiles obtained are characteristic and promising, which suggests that some selected sequences bind tightly to the immobilized MML, DML, and TML.

The resulting ssDNA pools from the last round selection were cloned using blunt-end ligation. We next performed colony picking and Sanger sequencing of a small number of colonies to give access to the most frequent clones (Darmostuk *et al.*, 2015). Subsequently, all sequences were aligned in order to group similar sequences. Here, in our study, the selected ssDNA pool from the final round of selection was cloned and 20 individual colonies were picked and sequenced. The core region sequences were aligned and analyzed with the software MultAlin. The online software *mfold* was used for the secondary structure prediction of the aptamer candidate with conserved core regions taking into account 100 mM [$Na^+$] and 2 mM [$Mg^{2+}$] (Stoltenburg, Schubert and Strehlitz, 2015).

For MML-specific aptamer selection, described in **Figure II-7A**, 13 clones showed the expected sequence length of 30nt, which was consistent with the random central region size. Whereas, the 7 other clones were 1-15nt shorter than the desired length. There are two explanations for this result, which may be due to (i) the oligonucleotide library being contaminated with many small DNA fragments, which were confirmed with the sequences of the initial oligonucleotides library indeed containing shorter DNA fragments; or (ii) due to some solvent or detergent used in DNA purification process, inducing oligonucleotides degradation and forming truncated aptamer (Lakhin, Tarantul and Gening, 2013).

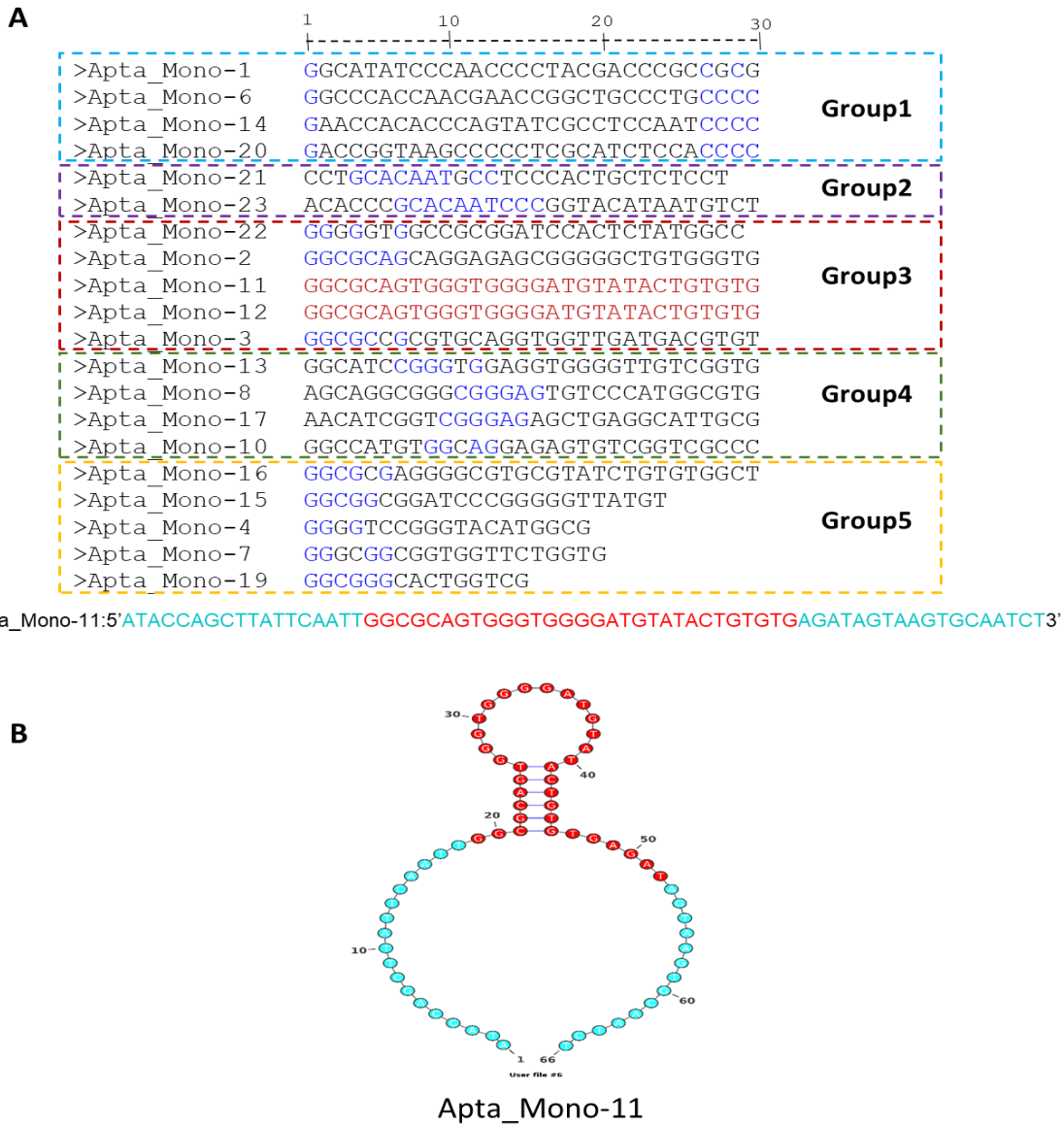


**Figure II-7 Identification of the eluted ssDNA for MML from the last selection round**

(A) The main groups of aptamers sequences obtained by FluMag-SELEX and aligned by online software MultAlin. Letters in blue marks homologous clusters shared in each group; Apta_Mono-11, 12, in dark red highlighted the redundant sequences. (B) Potential secondary structure of aptamer Apta_Mono-11 using *mfold*. The primer binding sites (18 nt each) at the 5'-and 3'-ends are highlighted in cyan and the consensus central region is highlighted in red.

The alignment illustrated in **Figure II-7A**, except for a few orphan clones, shows that the candidate aptamer sequences can be clustered in different sequence groups. We identified 5 distinct pools of similar sequences. Each sequence of a pool was unique, except for two clones sharing the same exact sequences in "group 3" (=Apta_Mono-11, 12, red frame Figure II.7A), demonstrating 10% redundancy in the sequences pool.

Concerning the other pools:

- "Group 1" (=Apta_Mono-1, 6, 14, 20), belongs to a cluster with a consecutive cytosines "CCCC" at 3'-end of the core region and with "G" start at 5'-end.
- "Group 2" (=Apta_Mono-21, 23), is composed of a consensus sequence "GCACAATCCC" near the 5'-end of the core region.
- "Group 3" (=Apta_Mono-22, 2, 11, 12, 3), in addition to two same clones (=Apta_Mono-11, 12, in dark red), sequences share a 7-nucleotide homologous cluster "GGCGCAG" at the 5'-end of the core region.
- "Group 4" (=Apta_Mono-13, 8, 17, 10), containes a short cluster of "CGGGAG" in the centre of the core region.
- "Group 5" (=Apta_Mono-16, 15, 4, 7, 19), shares a homologous fragment "GGCGG" at 5'-end of the inserts, respectively. The most redundant sequence was chosen and named Apta_Mono-11, it is composed of flanked sequences (18nt each) described at §VI.1.2 at the 5'- and 3'-end.

When focusing on the only fully redundant sequence (Apta_Mono-11/12), the predicted secondary structure illustrated in **Figure II-7B** demonstrated that, as expected, flanked sequences used for primers binding are not involved in a stem-loop structure or hairpin structure, whereas the internal region forms a stem-loop with 16 paired nucleotides involved in the stem, *versus* 14 nucleotides involved in a less structured loop circle, therefore probably having a more dynamic conformation.

Concerning the DML-specific aptamer selection, among all the 20 individual clones, the majority of the sequences are much shorter than the random region length and only 4 clones of the 18 successfully sequenced clones showed the expected sequence length of 30nt (**Figure II-8A**). Among them, two sequences Apta_Di-4 and Apta_Di- 6 share the same sequences. They are gathered in "group 2" (in dark red, red frame), including Apta_Di-16 which contains a short cluster "CCTCG" at 3'-end. It demonstrates around 11% redundancy of the sequences pool. Four other groups were identified:

- "Group 1" (=Apta_Di-1, 15), shares a short sequence "GCGGC" at the 5'-end of the core region.
- "Group 3" (=Apta_Di-8, 19, 12, 17), contains a consensus sequence "GTTGGTGTGT" at 3'-end of the core region.

- And “group 4” and “Group 5”, small groups with short sequence length (=Apta_Di-7, 21) and (=Apta_Di-22, 20), contain a cluster “GTGGTGTG” and “GGGTG” near the 3’-end, respectively.

Interestingly, all the sequences have rich content of guanosine, a characteristic that could influence the specificity of aptamers for dimethyl groups. Finally, the secondary structure model of the consensus sequence (Apta_Di-4/6, **Figure II-8B**) demonstrates that the core region tends to form two small stem-loop structures in a symmetrical structure.

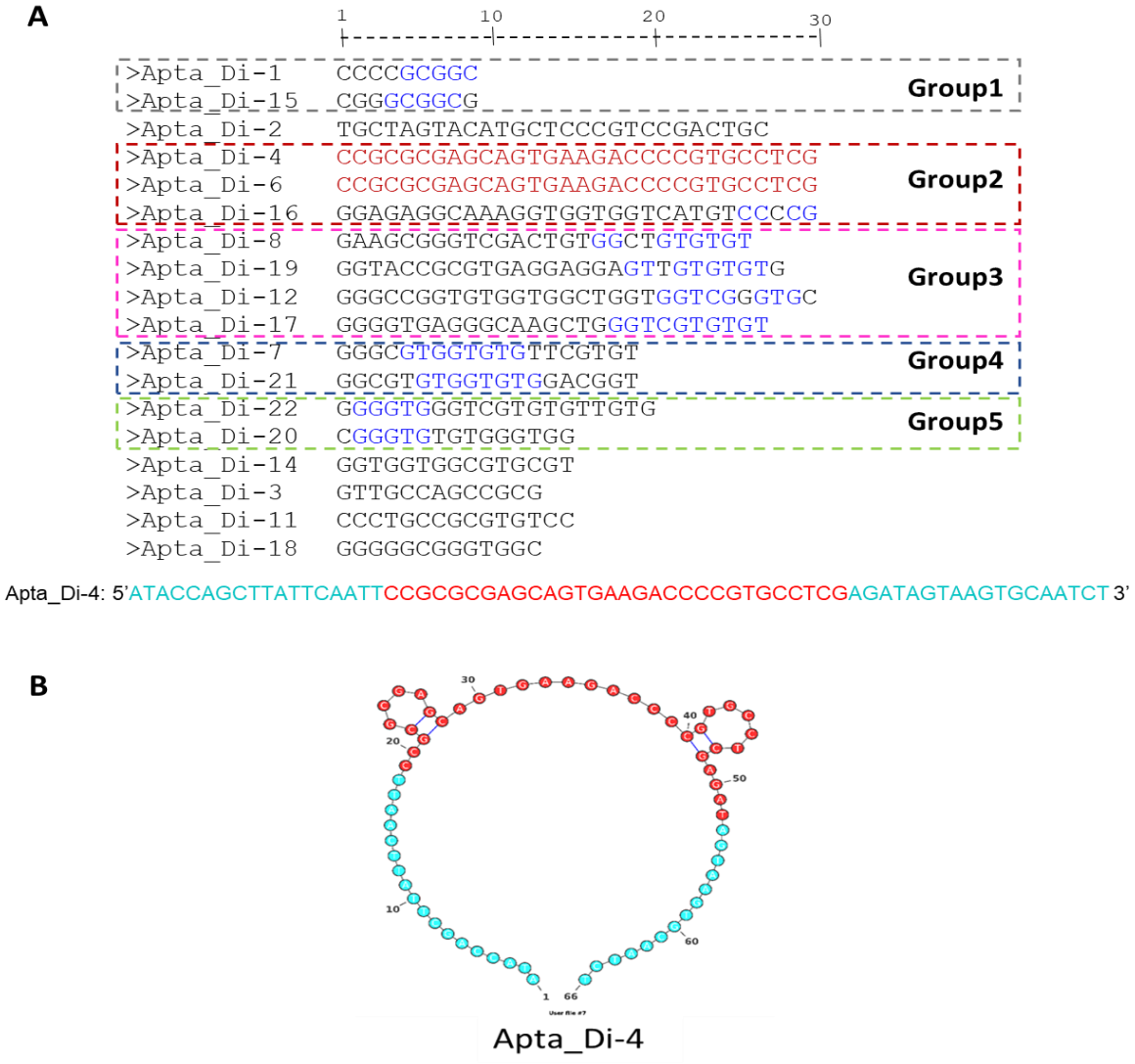


**Figure II-8 Identification of the eluted ssDNA for DML from the last selection round**

(A) The main groups of aptamers sequences obtained by FluMag-SELEX and aligned by online software MultAlin. Letters in blue marks homologous clusters shared in each group; Apta_Di-4, 6, in dark red highlighted the redundant sequences. (B) Potential secondary structure of aptamer Apta_Di-4 using mfold. The primer binding sites (18 nt each) at the 5’-and 3’-ends are highlighted in cyan and the consensus central region is highlighted in red.

The most promising result came from the sequences of the TML-specific aptamers (**Figure II-9**). Except for a few orphan clones, the clones could be identified as four different sequence groups (**Figure II-9A**). Six sequences of the 18 individual clones are pooled into “group 1” (=Apta_Tri-2, 6, 20, 15, 19, 12), with a high consensus, demonstrating a 33% redundancy of the sequences pool. Among them, four clones share the same sequence and the other two sequences differe by only two bases. “Group 2” gather sequences Apta_Tri-5, 11, 13 (purple frame) since they are composed of a 9 nt homologous fragment “GGATACCGG” near the 5’-end of the core region. “Group 3” (=Apta_Tri-7, 18, 14, 17) contains a consensus sequence “GACCCCG” near 3’-end of the inserts. Finally, the sequences of “Group4” (Apta_Tri-3, 9, 16) are significantly different from other clones with a guanosine-rich sequence at the 5’-end of the core region, whereas Apta_Tri-3, 9 share a short sequence “GACCCCG” in the core region. Apta_Tri-4 and Apta_Tri-1 contain a much shorter sequence of only 18nt and 15nt. The sequencing result indicates that the FluMag-SELEX selection for TML-specific sequences provides a very homogeneous aptamer pool. The most redundant sequence was conserved for further examinations and named Tri-6. Tri-6, with primer binding sites (18nt each) at the 5’ and 3’-end, has a length of 66 nt.

A secondary structure modelling analysis was performed (**Figure II-9B**). According to this computational structure prediction, similarly with Apta_Mono-11 and Apta_Di-4, the flanked sequences which were used for PCR amplification are not involved in a special conformation while the internal sequence region of 30nt possibly forms a small stem-loop. Such stem-loop structure may be especially important in determining the high recognition specificity and binding affinity due to the shape complementarity between the binding pocket and the target (Armstrong and Strouse, 2014; Qian *et al.*, 2022). This may be related to small-molecule binding, as structural analysis of several aptamers has revealed that the target-recognition elements recognize small-molecule targets like amino acids by fitting the targets in the binding pocket *via* well-defined intermolecular interactions (Edwards and Ferré-D’Amaré, 2006; Serganov, Huang and Patel, 2008).

Since the sequence of Tri-6 covered the highest redundancy compared to aptamers against MML and DML, we then focus on the characterization of Tri-6 in our following study.

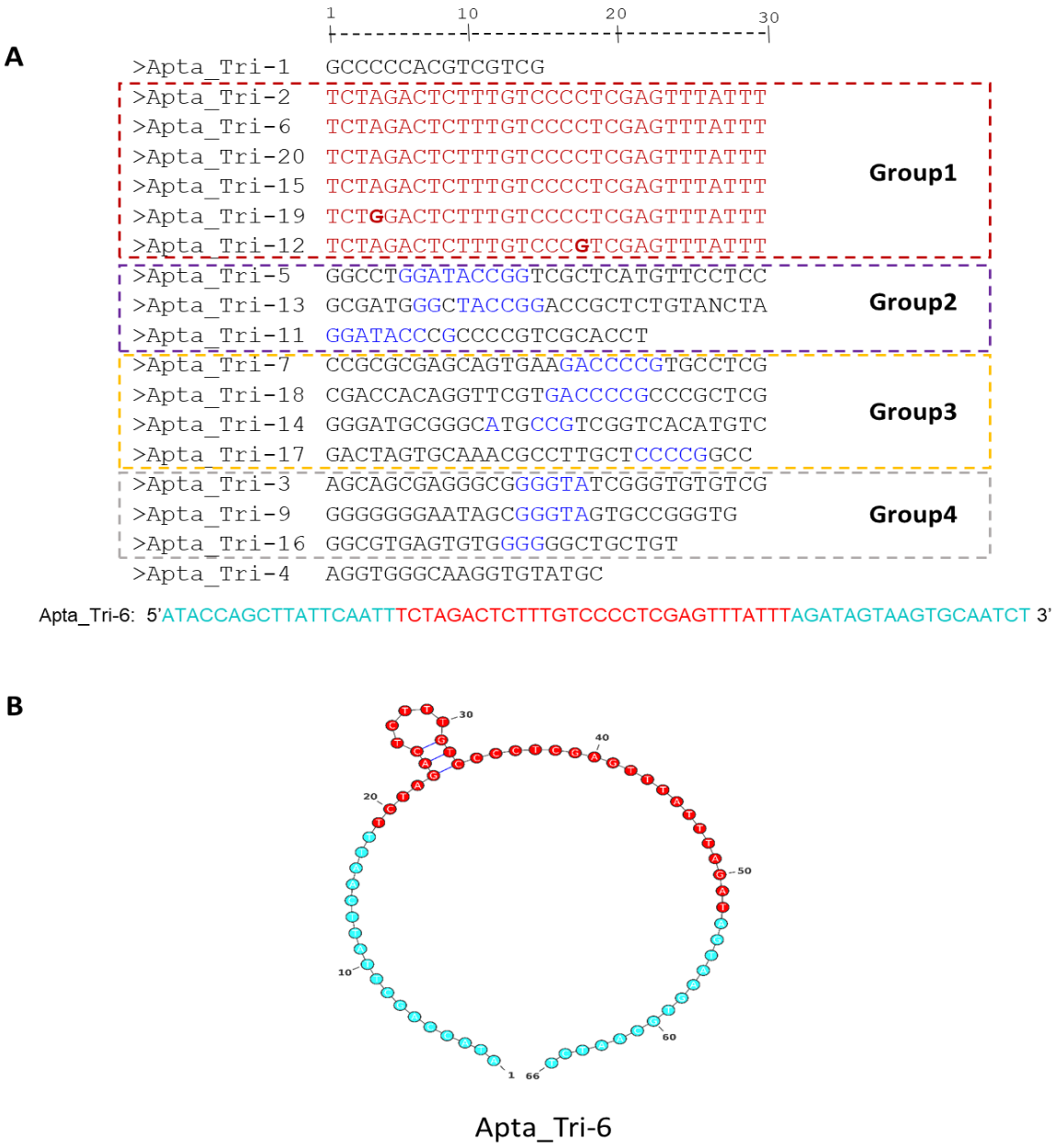


**Figure II-9 Identification of the eluted ssDNA for TML from the last selection round**

(A) The main groups of aptamers sequences obtained by FluMag-SELEX and aligned by online software MultAlin. Letters in blue marks homologous clusters shared in each group; Group1 sequences in dark red highlighted the redundant sequences, and unique different nucleotides are highlighted in bold. (B) Potential secondary structure of aptamer Apta_Tri-6 using mfold. The primer binding sites (18 nt each) at the 5'-and 3'-ends are highlighted in cyan and the consensus central region is highlighted in red.

## II.3 Characterization

The validation assays/strategies for estimating the aptamer-target interactions, including the binding affinity and specificity of the aptamers against their cognate targets, are required.

These methods differ by some determining binding parameters by the direct readout, some working in solution, whereas others require immobilization of either target or aptamer to a solid phase. As described in **Figure II-10**, the biophysical methods and technologies, including isothermal titration calorimetry (ITC), PCR with electrostatic analysis, and bead-based binding assays are used to determine the binding affinity and specificity of the TML aptamer.

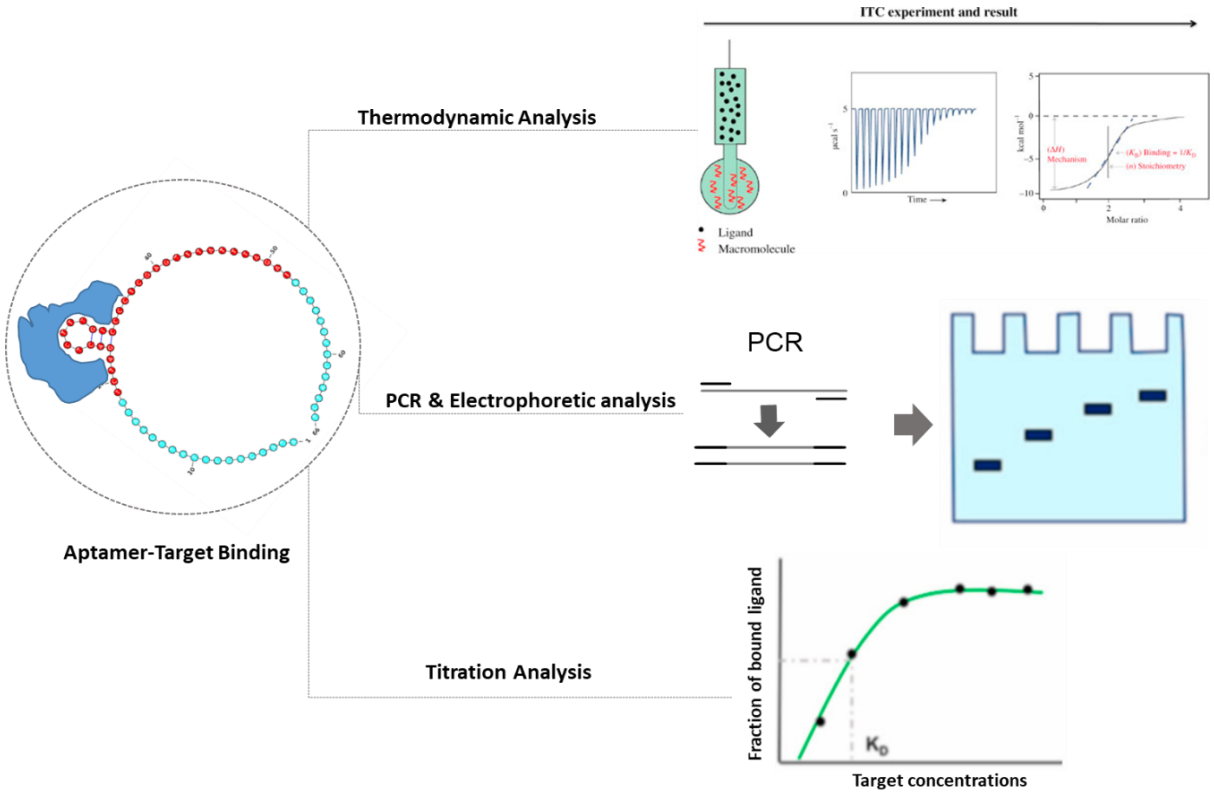


**Figure II-10 Schematic representation of the strategies to measure the characterizations of TML aptamer**
ITC measurement (Srivastava and Yadav, 2019) performed a thermodynamic analysis of TML and Tri-6/ Tri-Ctrl (top). Eluted aptamers Tri-6/Tri-Ctrl from TML-coated NHS beads were amplified with AP10 Eco and AP20 Eco and analyzed by electrophoresis (middle). A series of bead-based binding assays were performed to get the binding affinity (bottom).

## II.3.1 Interaction analyses of Tri-6 for TML using ITC measurement

The Isothermal Titration Calorimetry (ITC) measurement was first described by Wiseman *et al*. (Wiseman *et al.*, 1989). It's regarded as a standard characterization method that enables following the energetics of an association reaction between aptamer-target molecules. This method enables drawing a detailed thermodynamic picture of binding interactions of aptamer and not only cell targets but also small molecules (Herold *et al.*, 2011; Daems *et al.*, 2021). Experiments are performed by titrating a target into a solution containing the aptamer

in an ITC instrument such as the Nano-ITC instrument. The ITC technique is easy to perform a series of experiments to get the thermodynamic basis of aptamer-target binding interactions. It observes directly the heat change of a solution associated with a change of composition during the titration of a micromolecular component in the cell with increasing amounts of its binding partners (Johnson, 1990). The differences in heat between chemical equilibria along discrete steps of the titration are measured as the integral of the differential power applied to keep a sample and reference solution at the same temperature (Dellarole, Sánchez and De Prat Gay, 2010; Slavkovic and Johnson, 2018). The shape and midpoint of the resulting titration isotherm yield the binding information. As shown in **Figure II-11**, a typical ITC instrument is composed of a reference cell and a sample cell placed in an adiabatic jacket (**Figure II-11a**). These cells were maintained at a constant temperature (**Figure II-11a**; $\Delta T_1=0$). During the binding experiment, the ligand in the syringe is titrated into the sample cell by several injections (**Figure II-11b**).

When the binding event is an exothermic process, the temperature in the sample cell increases upon the addition of ligand causing a decrease of power to the heater around the sample cell. As a result, the raw experimental data consist of a series of negative spikes, where every spike corresponds to one ligand injection (**Figure II-11c**, top). Whereas for an endothermic reaction, the opposite occurs and a series of positive peaks results. These ligand injections are performed repeatedly and upon the ligand binding sites in the aptamer becoming saturated, the heat signal decreases until only the heat of dilution of the ligand is observed. Integration of this power supplied per unit of time yields the heat per mole of injectant with respect to the molar ratio (**Figure II-11c**, bottom). The parameters including enthalpy (ΔH), entropy (ΔS), reaction stoichiometry value (n), and equilibrium dissociation constant ($K_D$) were obtained by fitting the titration curves using the NanoAnalyze software.

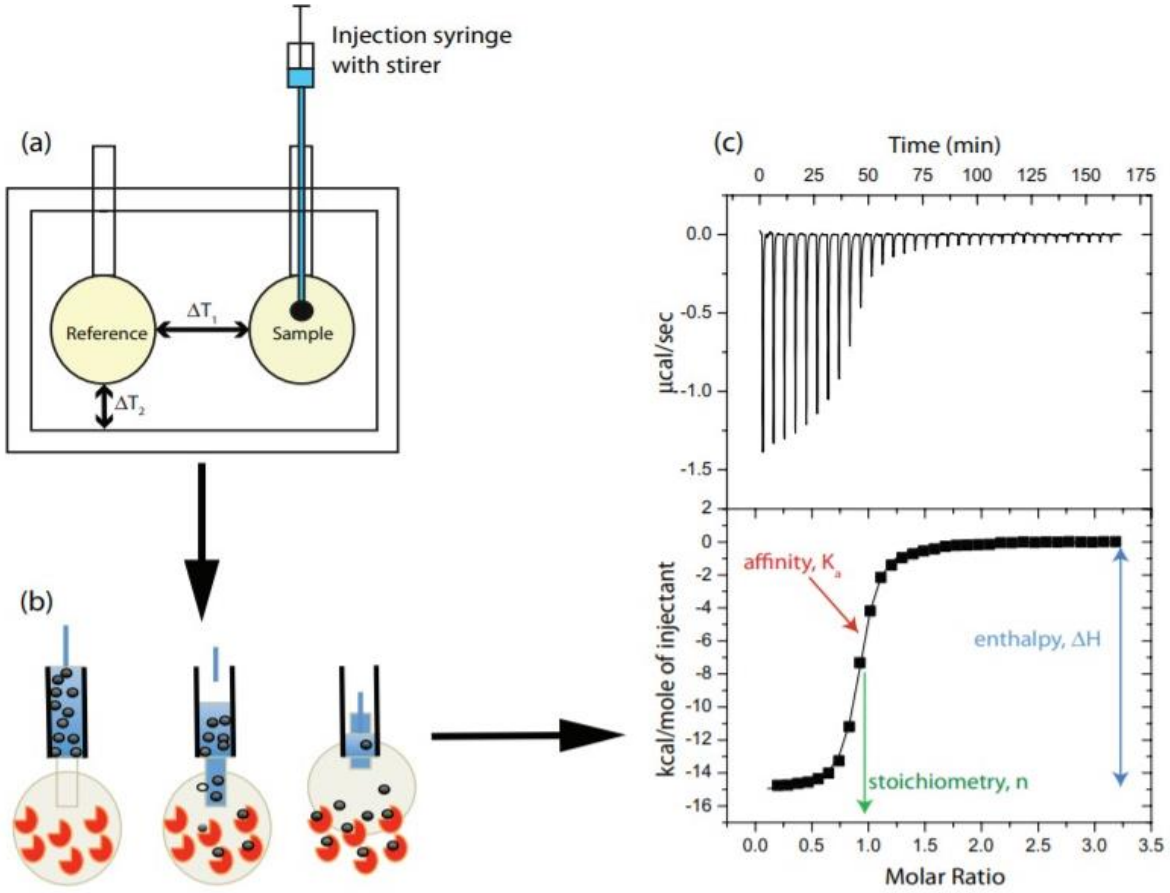


**Figure II-11 Schematic representation of the ITC technique for aptamer-small molecule interactions**

Source: Slavkovic and Johnson, 2018. (a) Aptamers and ligand in the ITC instrument. $\Delta T_1$ corresponds to the temperature between the two cells. The difference between cell and adiabatic jacket is referred to as $\Delta T_2$. Both $\Delta T_1$ and $\Delta T_2$ are zero during an experiment. (b) Depiction of binding during the gradual injection of the ligand into the sample cell containing selected aptamer and negative control, respectively. (c) Simulation of sample thermogram showing the interaction of target-binding with the corresponding aptamer. On the top is the heat from each injection with respect to time with the heat of dilution subtracted. On the bottom are the integrated heats for each injection (filled squares).

An ITC titration experiment was performed with the reference cell filled with binding buffer, while 500 µM TML in the syringe titrated into the sample cell that filled with 50 µM Tri-6 (**Figure II-12A**) and negative control with titration of 500 µM TML into 50 µM Tri-Ctrl (**Figure II-12B**), respectively. The titration curves relating to binding isotherm were obtained for Tri-6 and Tri-Ctrl bound to TML with a nearly equal affinity (apparent $K_D$ value of 27.16 ± 9.53 µM and 26.32±10.24 µM respectively) and binding stoichiometry (n= 1.51±0.52 and n= 1.54±0.45) (**Figure II-12**).

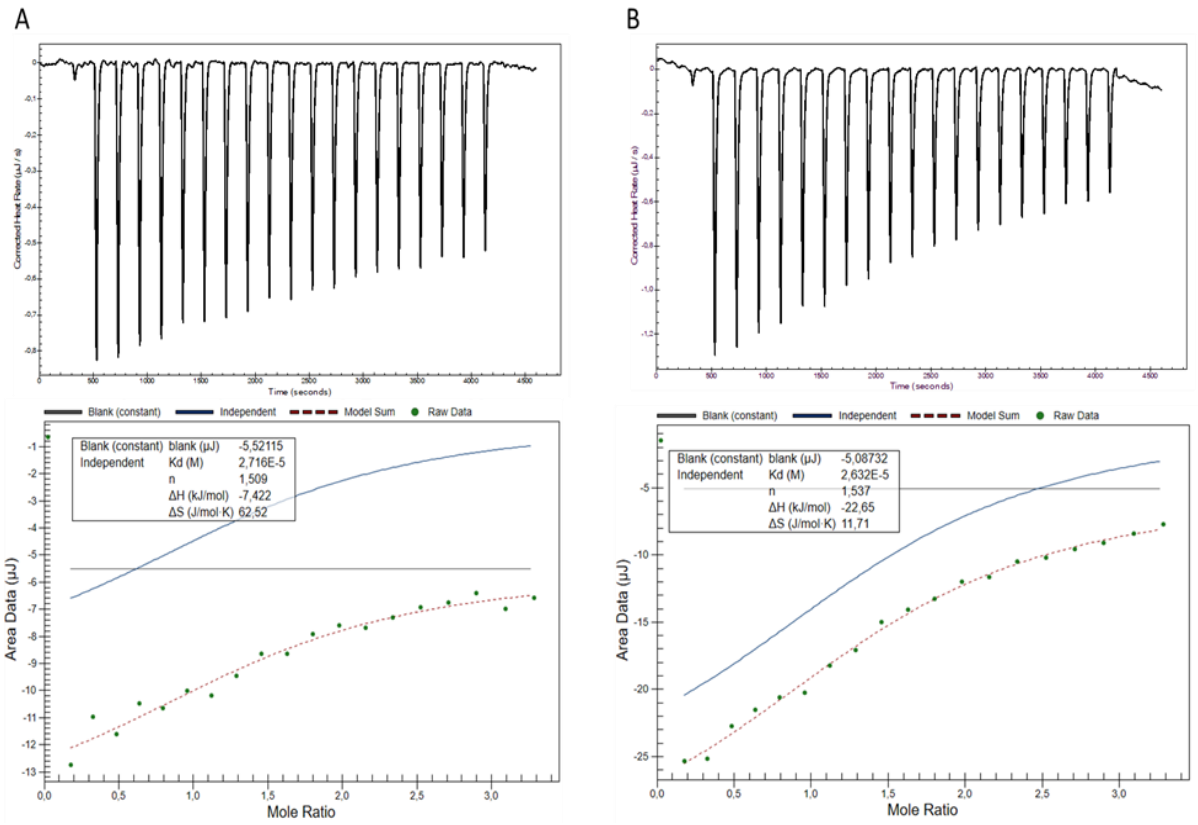


**Figure II-12 ITC data for TML binding to aptamers**

(A) 500 µM TML titrated into 50 µM Tri-6 at 25°C and (B) 500 µM TML titrated into 50 µM Tri-Ctrl at 25°C. The x-axis is the molar ratio of ligand added to total DNA aptamers. Binding thermodynamic parameters ($K_D$, n, ΔH, ΔS) are illustrated in the titration picture.

However, these two titrations performed very different thermodynamics. At the constant conditions, Tri-Ctrl bound with TML with a large enthalpy change (ΔH= -22.65 ± 5.23 kJ/mol) but a less entropy change (ΔS= 11.71 ± 4.46 J/mol·K), while the selected Tri-6 bound with a modest enthalpy change (ΔH= -7.42 ± 2.14 kJ/mol) but a significantly higher entropy change (ΔS= 62.52 ± 8.85 J/mol·K). The ΔS associated with the binding is divided into three entropic terms: $\Delta S = \Delta S_{water} + \Delta S_{conf} + \Delta S_{r/t}$, where $\Delta S_{water}$ represents the entropy change of water and ions arising mainly from the release of water and ions on the interaction surface upon binding; $\Delta S_{conf}$ represents the conformational entropy change caused by the changes in the conformational freedom of both the aptamer and the target upon binding; and $\Delta S_{r/t}$ represents the loss of rotational and translational degrees of freedom of the aptamer and target upon complex formation (Sakamoto, Ennifar and Nakamura, 2018). Therefore, we can

hypothesize that the increase in conformational flexibility of Tri-6 could contribute to the entropic change more than Tri-Ctrl. As mentioned, both aptamers exhibit negative heat capacity and a positive entropy, indicating that the conformational change of Tri-6 and Tri-Ctrl is in an endothermic process.

In addition, $K_D$ value ($K_D = k_{off}/k_{on}$, the ratio of the dissociation rate constant $k_{off}$ and the association rate constant $k_{on}$), a parameter describing the binding affinity, quantifies the equilibrium between a ligand being free in the solution and bound to a site in a target. The comparison of the $K_D$ value for Tri-6 and Tri-Ctrl showed that the binding affinities for TML are approximately equal, suggesting a low specificity of Tri-6 to TML under these ITC conditions. ITC conditions seem not suitable to study binding between Tri-6 and a so small ligand as TML, probably due to the conformational dynamics of Tri-6.

As described in a few other works, the use of ITC to study the binding of aptamers to small molecules like TML remains a challenge to reach the required levels of sensitivity (Mairal Lerga *et al.*, 2019). Moreover, when comparing to the distinct results got from the bead-based strategy, it is also possible that the coating of TML on beads induces conformational considerations making interaction with Tri-6 more favourable, by the opposition with a situation where both partners are free in solution. Indeed, Rangel *et al.* commented that immobilization of small-molecule targets can result in dramatic changes to chemical structure, which brought a key risk that the aptamers generated could only bind to the immobilized version of the target molecule but not bind to the free target in solution (Rangel *et al.*, 2018).

### II.3.2 Specificity characterization of Tri-6

Since ITC technology appeared not to be appropriate to demonstrate the interaction specificity between aptamers and small ligands such as TML or something else similar to TML, other approaches were considered. The selected ssDNA which has a high consensus sequence was expected with high specificity to its target TML compared to the negative control. Therefore, only the selected aptamer should specifically bind with TML-coated NHS magnetic beads and appear in the elution fractions. After PCR amplification using primers containing EcoRI site (AP10 Eco and AP20 Eco from **Table VI-1**, Chapter VI.1.2), the PCR products of the eluted aptamer are expected to illustrate on the agarose gel through gel electrophoresis (GE) following a general scheme shown in **Figure II-13**.

The bead-based binding assay is another ITC alternative strategy. It is one of the solid-phase assays, which analyze molecular interactions through surface immobilization of one analyte species while the other interacting molecules are in free state in the solution (Thevendran and Citartan, 2022). Generally, in affinity measurement using bead-based binding assays, varying concentrations of targets are titrated into a fixed concentration of aptamer-coated beads and the subsequent yield in signal intensities is measured in order to obtain the binding curve of the bound target/ligand fractions to determine the binding affinities (Frost *et al.*, 2015). When aptamer-targets complexes bound to the beads get saturated, the binding curve keeps flat. The resultant binding curve yields the aptamer's characteristic affinities (Orabi *et al.*, 2015). In our study, the selected aptamer Tri-6 was characterized by several binding assays according to the FluMag-SELEX conditions.

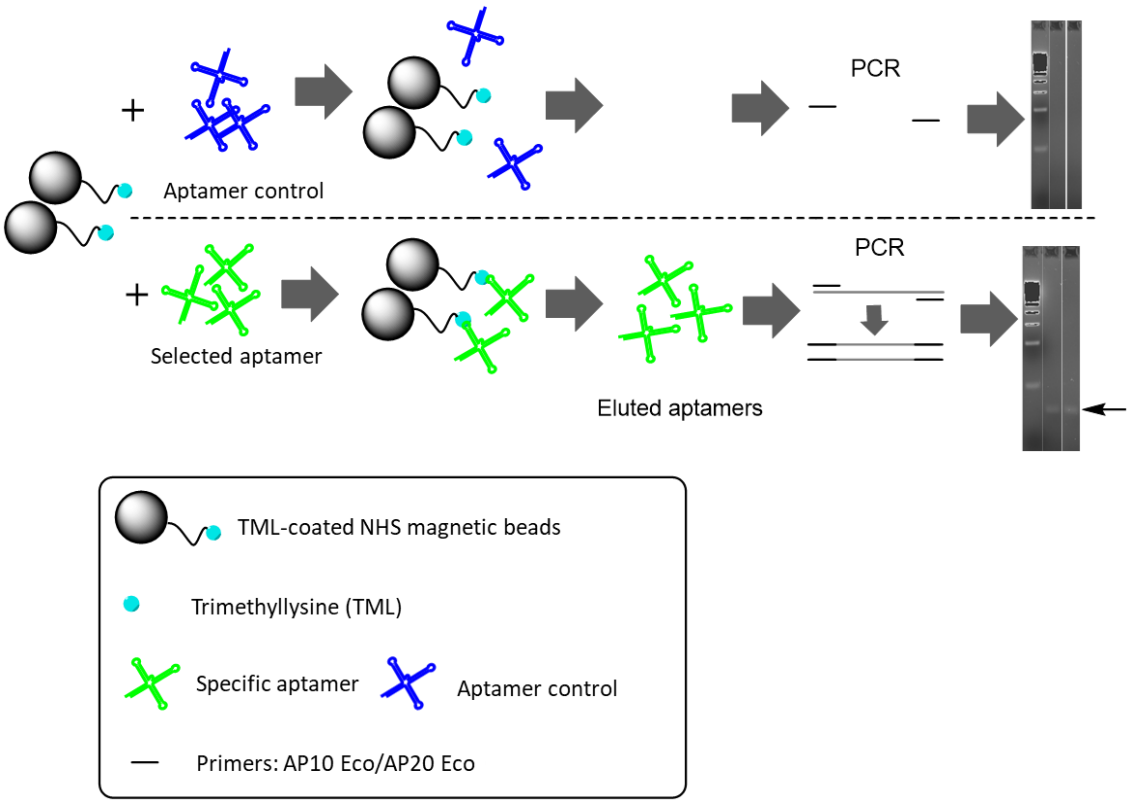


**Figure II-13 Schematic representation of the interaction characterization by PCR amplification**

TML-coated NHS beads were incubated with the selected aptamer and the negative control aptamer, respectively. After washing, only specific aptamer was expected in the elution fraction and subsequently appeared in the agarose gel. The arrow indicates the expected size of the aptamer.

Regarding the specificity and affinity of the obtained Tri-6, eluted aptamers were tested by GE for PCR products and bead-based binding assays, as shown in **Figure II-14**. Tri-6 and its negative control Tri-Ctrl were tested for their abilities to bind to TML. Firstly, after the binding of aptamers on TML-coated NHS beads similarly to FluMag-SELEX conditions described in chapter VI.2.3, PCR amplification of eluted aptamers was performed, followed by analysis by electrophoresis. From the 5% agarose gel, only eluted Tri-6 got amplified and the PCR products appeared as a band at the expected size (**Figure II-14**). Data validated the specificity of the interaction between Tri-6 to TML.

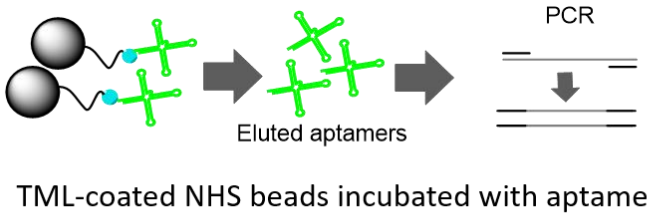


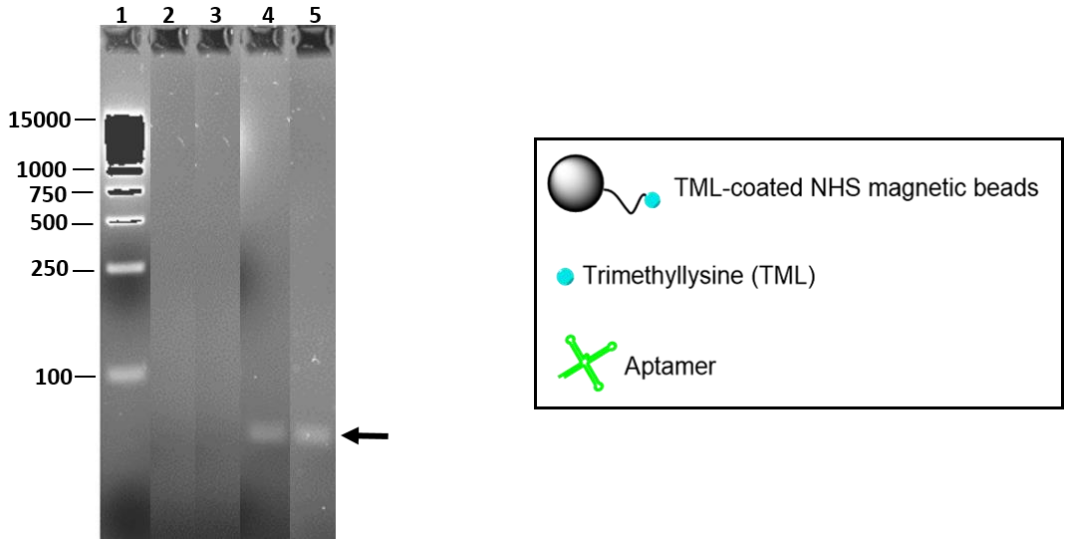


**Figure II-14 Agarose gel electrophoresis analysis of the PCR products of eluted aptamers**

Lane1: 1kb DNA ladder; Lane2: Eluted Tri-Ctrl incubated for 2 h; Lane3: Eluted Tri-Ctrl incubated for 4 h; Lane4: Eluted Tri-6 incubate for 2 h; Lane5: Eluted Tri-6 incubate for 4 h. The arrow indicates the expected size of the aptamer if retained.

## II.3.3 Affinity characterization of Tri-6 with TML

HILIC tandem mass spectrometry (HILIC-MS/MS) was broadly used to determine and quantify amino acids with the advantage that without derivatization or using any other sample preparation before the analysis and achieved the limits of detection (LODs) of 1-300 nmol/l (Qiu *et al.*, 2022). HILIC is usually used to separate polar and hydrophilic compounds (Hsieh

and The, 2008). In HILIC, the solutes between the more organic mobile phase and the aqueous layer will be partitioned and eluted depending on the number of polar groups and conformation of the sample (Rappold and Grant, 2011). Typically, HILIC performs a gradient separation by starting with a high percentage of an aqueous solvent and ending with a high portion of organic solvent (Maux, Nongonierma and Fitzgerald, 2015). TML is a polar and hydrophilic molecule, thus it could be separated by the HILIC column.

Mass spectrometric detection was performed under electrospray (positive)-quadrupole mass spectrometry (ESI(+)-MS) with extracted-ion chromatogram (EIC) for recovering the m/z values of the analytes. The peaks of TML and internal standard caffeine were obtained which are m/z 189.1 for TML and m/z 195.1 for caffeine.

We then used HILIC-MS/MS-based approach to estimate the affinity dissociation constant $K_D$. Taking into consideration of the bound TML in a low amount, a calibration curve based on the concentration of TML and the signal responses from the HILIC (**Figure II-15A**) was performed to determine the LOD of TML by HILIC-MS/MS (**Figure II-15B**). In the range of 0.1-25 µM of TML, the area of the signal peak at m/z 189.9 was linear. A concentration in the range of 0.2–8.0 mM TML was then applied to a series of individual binding assays with a constant number of Tri-6-streptavidin beads in a total volume of 500 µl binding buffer.

In each assay, an internal standard for calibration was used, caffeine with an m/z 195.1 in positive ionization mode (TML: m/z 189.1). Each elution fraction was measured and quantified by HILIC-MS/MS, the TML-specific peak appeared at 0.83 min, whereas the caffeine signal peak appeared at 4.32 min (**Figure II-16**).

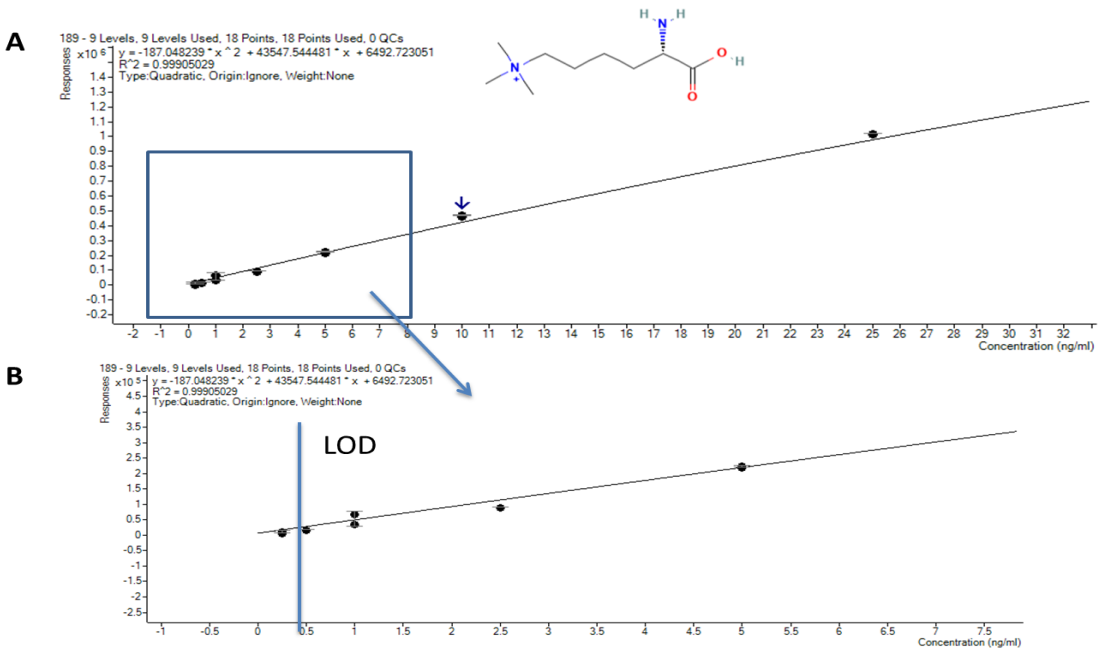


**Figure II-15 Calibration curves of TML measured by HILIC-MS/MS**

(A) The corresponding HILIC signal responses of TML at a range of 0.1-50 μM in binding buffer. (B) The LOD of TML detected by HILIC-MS/MS illustrated the magnification of the blue frame in Figure II-15A. The blue line marked the LOD point in the calibration curve. Each point was presented as a mean ± standard error by duplicate determination.

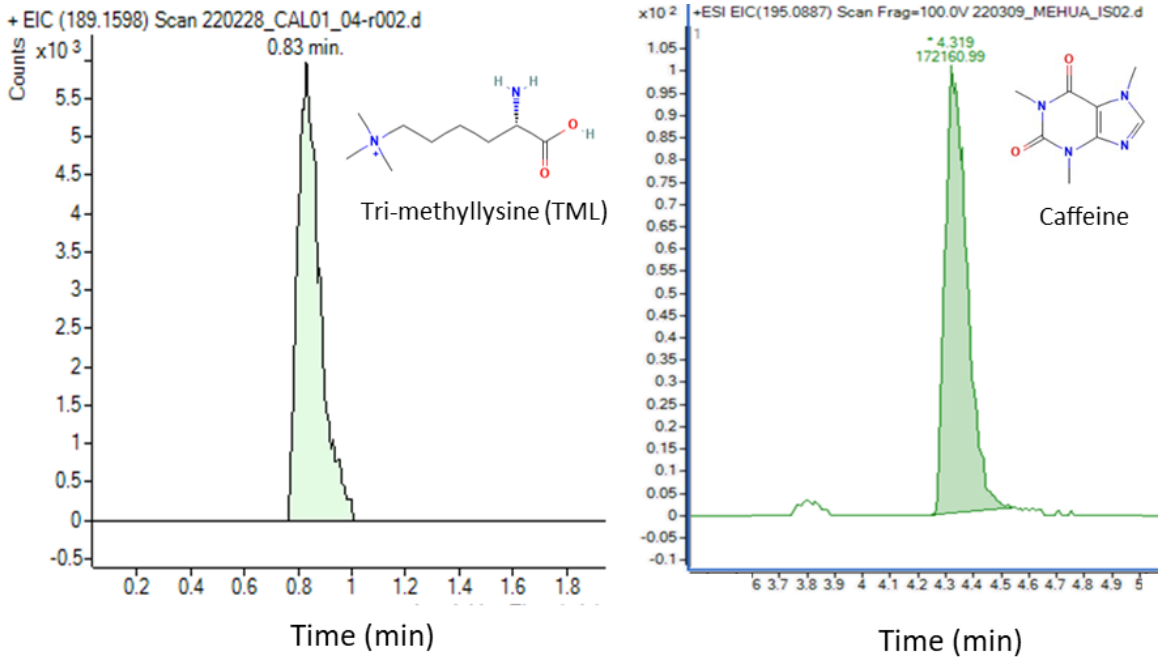


**Figure II-16 Signal of TML and internal standard (caffeine) measured by HILIC-MS/MS**

HILIC coupled with mass spectrometry analyzed each elution fraction and quantified the amount of TML, the specific TML peak appeared at 0.83 min (left) with a m/z 189.1, whereas the internal standard response peak appeared at 4.3 min (right) with a m/z 195.1.

Following, based on the high sensitivity of HILIC-MS/MS for TML as described above, we then used this approach to detect specificity and further define the affinity of Tri-6 with TML. 5'-biotin labelled Tri-6-biotin and Tri-Ctrl-biotin were independently immobilized with M-280 streptavidin beads respectively prior to binding with TML in a series of increasing concentrations. Excess aptamers ensured all the beads sites were saturated with both biotinylated aptamers. 1.78 mM of TML were incubated with Tri-6- or Tri-Ctrl-coated streptavidin beads. The amounts of unbound and bound TML in different washing and elution fractions were monitored using HILIC-MS/MS (**Figure II-17A**). Because almost absent TML was detected in the 3$^{rd}$ washing fraction, whatever the aptamer-coated beads used, we can conclude that washings were complete. Interestingly and as expected, a significant elution of TML was observed only when beads were coated with Tri-6 but not with Tri-Ctrl, validating the specificity of Tri-6.

These data were confirmed using higher concentrations of TML to check the dose response effect of the specific interaction of Tri-6 and TML (**Figure II-17B**). Indeed, when Tri-6 coated beads were incubated with TML 2.22 mM, 1.17 µM of TML were eluted from Tri-6-beads; while only 0.29 µM of TML were eluted from Tri-Ctrl-beads. These results are consistent with the removal of the large majority of TML as early as the washings only when Tri-Ctrl-beads were used. In a similar manner, when Tri-6 coated beads were incubated with 3.52 mM of TML, 3.15 µM of TML was eluted *versus* 0.69 µM of TML from the control beads.

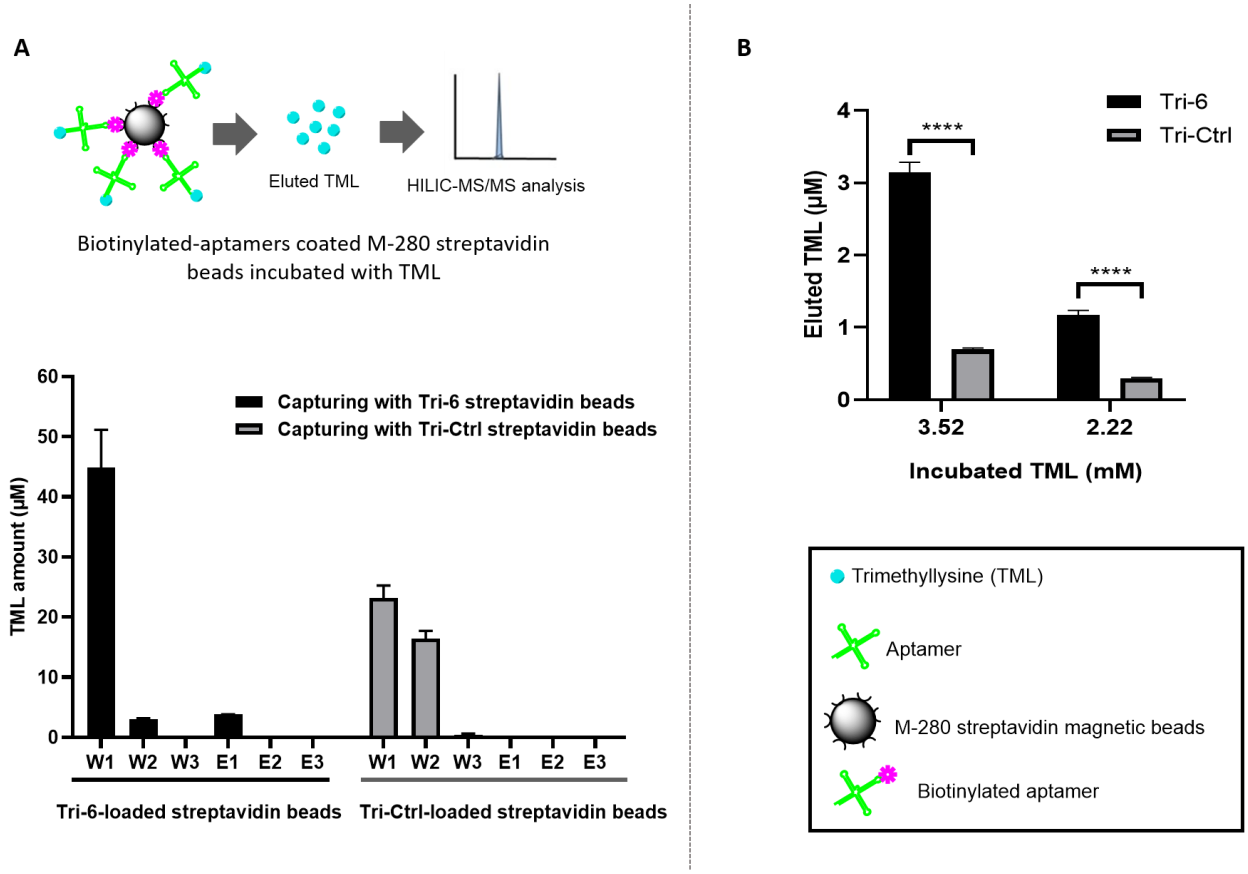


**Figure II-17 Specificity analysis of aptamer Tri-6 compared to negative control Tri-Ctrl**

(A) The amount of TML in washing (W1 to W3) and elution (E1 to E3) fractions after incubating 1.78 mM of TML with Tri-6-coated streptavidin beads and Tri-Ctrl-coated streptavidin beads, respectively. (B) The eluted TML after binding with 2.22 mM and 3.52 mM of TML with biotinylated Tri-6-coated streptavidin beads and biotinylated Tri-Ctrl-coated streptavidin beads, respectively. Statistical analyses: ANOVA tests with unpaired t-tests. All data are presented as mean ± standard error by duplicate determinations, "****" for $p<0.0001$.

Either through PCR data from captured aptamers thanks to immobilized TML, or through HILIC-MS/MS quantification, TML was specifically eluted from Tri-6-coated beads. Not only these results confirmed and highlighted the high specificity of Tri-6 for its target TML, giving a deeper insight into the functionality of the aptamer Tri-6, but they also provide the basis to characterize the affinity and thus define the $K_D$.

Bead-based binding assays according to the selection conditions revealed a concentration-dependent binding of TML to Tri-6-coated streptavidin beads (**Figure II-18**). Based on the different amounts of TML in elution fractions, a saturation binding curve was obtained and a $K_D$=2.48 ±0.14 mM was calculated by non-linear regression analysis by the "Binding Saturation-Specific binding with Hill slope" program (Arshavsky-Graham *et al.*, 2020). Given

the millimolar affinity constants obtained for Tri-6, it indicated weak binding interaction between aptamer Tri-6 and TML in the tested conditions.

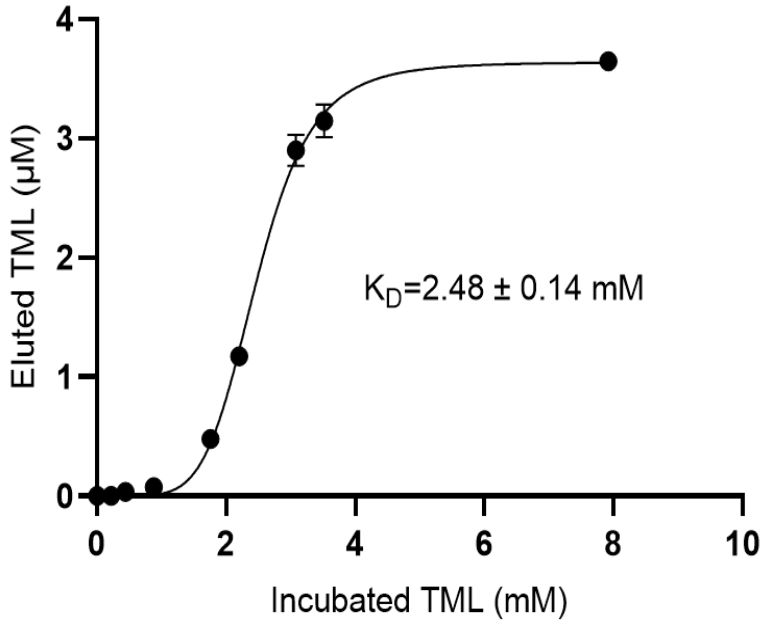


**Figure II-18 Binding curve of eluted TML was obtained by bead-based binding assays *via* HILIC-MS/MS**
The dissociation constant $K_D$ was calculated by nonlinear regression analysis with the GraphPad Prism 8.0 software. All data are presented as mean ± standard deviation bars in duplicate parallel determinations.

## II.4 Discussions and conclusions

Methylated lysine includes MML, DML, and TML occurring in both prokaryotic and eukaryotic cells (Cornett *et al.*, 2019). Lysine methylation of histone and non-histone proteins dynamically regulates the transduction pathways and plays important roles in diverse physical and pathological processes (Lanouette *et al.*, 2014). Lysine methylation has been recently discovered to be associated with bacterial pathogenesis by promoting bacterial adhesion to cell surfaces and gut colonization (Horstmann *et al.*, 2020). This indicates putative lysine methylation in many bacterial behaviours. Therefore, my project focused on the enrichment and purification of methyllysine-containing peptides from *S*. Typhimurium.

But due to poorly efficient specific enrichment approaches, there's limited information on proteins with lysine methylation. Large-scale studies reported on non-histone protein methylations are mainly focusing on arginine methylation because of better affinity obtained from the commercially available antibodies (Bremang *et al.*, 2013). To address the challenges

of high throughput methyllysine enrichment, we hypothesized that *in vitro* selected aptamers may have specificity and high methyl selectivity required for proteomic analysis. Compared to other enrichment approaches such as specific antibodies and methyllysine binding domains, aptamers have a similar, even higher, specificity and affinity and are easy to produce (Toh *et al.*, 2015; Ali, Elsherbiny and Emara, 2019).

During the aptamer selection process, isolation of the unbound sequences from target-bound sequences is a crucial step of a SELEX process. There's a drastic size difference between a small molecule target and the oligonucleotide. Therefore, it's especially a big challenge to select, characterize and apply aptamers for the detection of small-molecule targets like our research targets MML, DML, and TML due to the tiny changes of the aptamers before and after binding with the target when the selection process is performed only in solution (Ruscito and DeRosa, 2016). Small molecule targets are usually immobilized on solid supports, such as microplate wells, beads or columns to capture interesting aptamers. The immobilization of the target or oligonucleotide on the magnetic beads during selections as we described in this work enables easy handling and efficient separation of target-bound from unbound ligands (Stoltenburg, Reinemann and Strehlitz, 2005). But it also potentially introduces an additional challenge of non-specific binding to the beads. When the aptamers are immobilized on the beads, some functional groups provided by the solid support could interfere with the binding. This can make the aptamers either show an affinity for the target only in its immobilized form or show a different interaction affinity when the target is in solution (Szeitner *et al.*, 2014). In addition, Gu and co-workers pointed out that the possible difficulties using the immobilization strategy during selection could be that the immobilization process may change the original conformation of the target; the steric hindrance of the immobilized target may block the binding site, and nonspecific binding to a solid substrate may lead to nonspecific sequences (Gu *et al.*, 2016). Therefore, it's necessary to minimize the interference from the solid support with the application of control rounds with naked beads in the absence of the target, as we performed in the negative selection during the last round. By inserting a negative selection step into the selection cycles to remove non-specific binders, aptamers with very discrete specificities can be isolated (Yan and Levy, 2009). Furthermore, to increase the selectivity of the resulting aptamer candidates, the selection pressure has been reported to be performed by (i) decreasing the amount of the target or library, (ii) decreasing the target-library

incubation time, (iii) changing the incubation temperature, or (iv) increasing buffer ionic strength (Levine and Nilsen-Hamilton, 2007; Mckeague *et al.*, 2015). In our study, the stringency of the selection was performed by intensifying ligand competition in the penultimate round of selection. The oligonucleotides library was exposed to structurally similar molecules mixture of unmethylated L-lysine and other two corresponding methylated lysines, in order to improve the specificity and eliminate cross-reactive aptamers.

Repeating SELEX under identical conditions may lead to variable outcomes, which resulted from the randomness of the oligonucleotides library. A conventional aptamer selection procedure usually requires numerous repetitions (typically 5-20 rounds) of successive steps of SELEX-containing target binding (Tan et al., 2016). Generally, the oligonucleotide pool is composed of the best binding aptamer candidates after 8-15 cumbersome selection cycles, and more or less SELEX rounds are rarely performed in practice (Urmann and Walter, 2020). Herein, we presented 6 cycles FluMag-SELEX process for MML and DML aptamers selection separately while only 4 iterative rounds for TML aptamer selection. Interestingly, a great enrichment of the aptamers pool for the target of interest TML was observed, suggesting the successful selection of the obtained aptamers. Even though it's not the most frequent case, other teams have got interesting results with a few selection cycles for aptamer isolation (Mairal et al., 2008). For instance, small molecules of N-methyl mesoporphyrin aptamers have been obtained with $K_D$ ranging from nM to µM using CE-SELEX after only 3 rounds of selection (Yang and Bowser, 2013). In addition, Tang et al. shortened the selection process to just 4 rounds through CE-SELEX and obtained aptamers with high affinity and specificity to ricin toxin (Tang et al., 2006). They found that the reduced number of iterative cycles (only 2-4 rounds) of CE-SELEX not only faster aptamer producing procedure, but also decreased the deleterious effect of an extended number of PCR resulting from more selection rounds of conventional SELEX. Reinholt et al. exploited a multiplexed RNA aptamer selection to 19 different targets simultaneously by only 4 cycles using a microplate-based microcolumn device (Reinholt et al., 2016). In recent years, the occurrences of the single round of SELEX provide a new direction for improvements in SELEX efficiency for researchers. For example, Yang et al. created a novel one-round pressure controllable aptamers picking strategy by target competition to eliminate weakly bound or unbound sequences for each other (Yang et al., 2021).

Beyond the number of cycles, it has been suggested that a library of short sequences for smaller molecules could increase selection efficiency due to a short random region that could compensate for the size gap between the aptamer and small molecules (Neves et al., 2015).

Finally, as for the sequences of the selected oligonucleotide pools, there is a hypothesis that either the sequences with the highest enrichment may represent the best aptamer candidates; or they are possible to be represented the sequences that amplified more efficiently during PCR (Yu et al., 2021).

However, the majority of the sequences of the aptamer clones for MML, DML and TML could be identified into several groups with mostly identical sequences or shared similar structure motifs. All the aptamer candidates sharing consensus sequences were listed in **Figure II-19.**

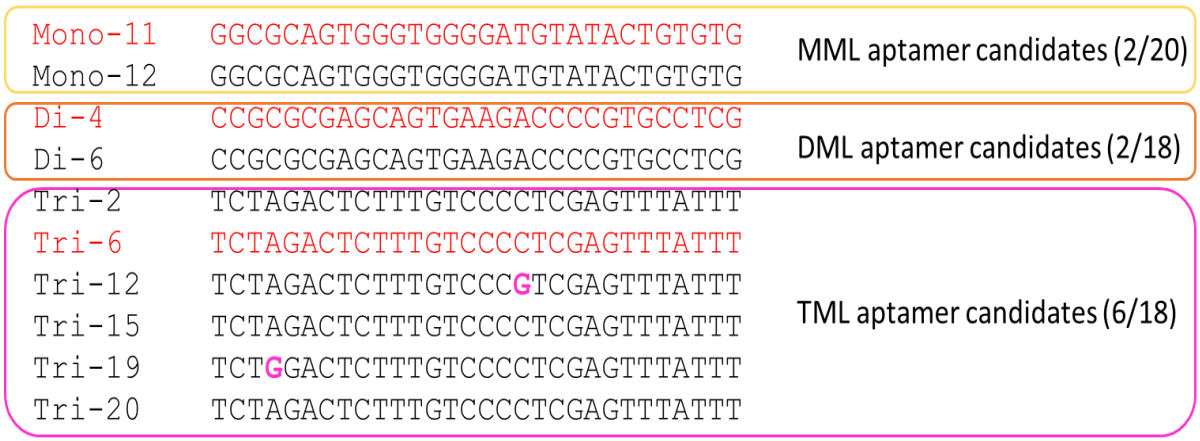


**Figure II-19 All aptamer candidates sharing consensus sequences against MML, DML and TML**

The selected sequences were highlighted in red colour. The aptamer candidates against MML are in a yellow frame, 2 consensus sequences in total 20 successfully sequenced fragments. The aptamer candidates against DML are in an orange frame, 2 consensus sequences in total 18 successfully sequenced fragments. The aptamer candidates against TML are in the pink frame, 6 consensus sequences in total 18 successfully sequenced fragments. The different nucleotides are highlighted in rose colour in bold.

As shown in Figure II-19, the candidate MML and DML aptamer sequences are overall rich in GC nucleotides. Both of them just have two identical sequences, compared to TML candidate aptamers which have 6 almost identical sequences including 4 identical sequences (Tri-2, 6, 15, 20). Interestingly, over just 4 selection rounds, a high redundancy (30%) of the sequences for TML was observed (Figure II-9A, group 1). A similar result came from the L-Tyrosinamide aptamer selection case, in which most of the selected aptamers shared a common consensus sequence of 38 nucleotides, for which a $K_D$ value in the µM was determined (Vianini, Palumbo and Gatto, 2001).

Nevertheless, the question of the size of the sequenced pool remains open to identify pertinent aptamers. Indeed, Kapakuwana *et al*. discovered all 108 sequences of the human α-thrombin aptamer candidates shared two major conversed motifs, which contained the consensus 15nt G-quadruplex (embedded in a conserved stem structure) (Kupakuwana *et al*., 2011). They identified that the top candidate in the motif could bond strongly to thrombin with $K_D$ ~12 nM. By limiting to only 20 clones for sequencing analysis, it could limit more possible aptamer candidates that contain high consensus motifs for MML and DML aptamers.

Once the aptamer candidate sequences have been obtained, it is important to characterize their binding affinity and their specificity (Yu *et al.*, 2021). Mostly, the characterization methods are based on several specialized instrumentations such as surface plasmon resonance (SPR) (Win, Klein and Smolke, 2006), ITC (Slavkovic and Johnson, 2018) and microscale thermophoresis (MST) (Entzian and Schubert, 2016). In the tested conditions and concerning this specific ligand-aptamer complex, the ITC approach was inappropriate. This could be due to (i) the change of the physiochemical properties of the small-molecule target between the immobilized target and the free target, and/or (ii) the structural dynamic properties inherent to aptamers. Indeed, it has been reported that the affinity of glutamic acid-binding aptamers exhibited different behaviours when conjugated to a small-molecule target and to a free target (Ohsawa *et al.*, 2008). The low binding enthalpy of small molecules also limits the small-molecule-aptamer interactions (Li, Li and Dong, 2007; Li *et al.*, 2020). Furthermore, the dynamic structural properties have been proved to affect the affinity and the specificity of the cocaine-binding aptamer when a structural switch or ligand-induced folding mechanism happens (Reinstein *et al.*, 2011). Finally, Yu and co-workers concluded about the limitations of ITC to study weak interactions between small molecules and aptamers. Specifically, they suggested that the potential number and strength of binding interactions between these molecules may be limited due to factors such as the small accessible surface areas and chemical moieties of small molecules, which may make it difficult to detect weak interactions at low concentrations in the ITC system (Yu *et al.*, 2021). It appears that ITC measurements to determine affinity between small ligands and aptamers are uncommon and remain a challenge.

Beads-based binding assay with the aid of LC-MS/MS approach (Mairal Lerga *et al.*, 2019) is an alternative approach. Indeed, LC-MS/MS has been used in numerous aptamer-ligands

interaction studies to provide highly sensitive, specific and accurate results (Pobran *et al.*, 2021). Additionally, Wang *et al*. found that HILIC-MS/MS analysis could be used precisely to quantify methylated lysine/arginine (Wang, Wang and Ye, 2017). It has been shown here that a series of bead-based binding assays can be used to effectively measure the interaction between TML and Tri-6. The eluted TML were measured by HILIC-MS/MS. Even if the $K_D$ value of 2.48 mM illustrated weak interaction between the selected aptamer and TML, our results show that Tri-6 is a specific aptamer for TML when compared to aptamer control at the same conditions. In such a context, DNA aptamer for TML appears as a new tool to specifically interact with methylated amino acids. In the following work, Tri-6 will be aimed to confirm if it could bind proteins or peptides displaying methylated lysines, making this tool pertinent for methyllysine-containing peptides research and the methylome study. Finally, a deeper understanding of the interaction and structure-function relations of the selected aptamer with its target opens the way for modifications aiming to improve the specificity and/or affinity of the aptamer. Understanding the essential role of this tiny modification will further extend our knowledge of protein methylation involved in diverse processes.

Conclusively, in this work, we first selected DNA aptamers against target methylated lysines. Due to the small size of the methyllysine and lack of efficient isolation methods, we developed dedicated methods to succeed.

To date, the aptamer Tri-6 we reported here, compared to the previously reported arginine aptamers (He *et al.*, 2021), is the only one developed against TML to our knowledge. The two other aptamers, Mono-11 and Di-4, recognizing MML and DML respectively, need to be further characterized. The described binding features of the selected aptamer Tri-6 make it suitable for analytical applications for the next step of work.

# Chapter III Applications of the aptamer-based method for enrichment and purification of methylated proteins

## III.1 Introduction

The proteome represents the complete set of proteins that are synthesized and modified by an organism (Müller *et al.*, 2020). A successful proteome analysis mainly aims at a large-scale study of the entire protein or/and peptides present in cells, tissues, or organs under specific conditions (Hui *et al.*, 2015; Smith and Kelleher, 2018). It mainly involves a variety of techniques, such as MS, protein microarrays, and bioinformatics (Nickerson *et al.*, 2023). The typical strategy for proteomic analysis consists of one or a combination of several steps including (i) extraction of proteins from the sample of interest; (ii) protein separation on the basis of their size, charge, and hydrophobicity; (iii) identification of the individual protein components obtaining the nature and position of any PTMs; (iv) measurement of proteins' dynamic quantitative change between control and treated samples obtaining their abundance; (v) bioinformatics analysis of the protein sequences interpreting the results in the context of biological pathways and networks; (vi) validation of the results with other techniques obtaining additional information on the expression, localization, and activity of the specific proteins. During proteomic analysis, protein separation and target protein purification play a critical role in achieving the identification of amino acid sequences and functional studies (Liu *et al.*, 2020). The proteomic data can (i) provide valuable insights into protein conformations indirectly by identifying peptides and protein fragments that are indicative of specific conformational states or by comparing the abundance of different protein isoforms; (ii) or provide a more comprehensive understanding of protein interactions in the context of biological networks (Gillet, Leitner and Aebersold, 2016).

Traditional proteomic analysis has been used in the past to yield clues to *S*. Typhimurium pathogenicity based on the identification analysis of proteins and the corresponding virulence genes (Deiwick and Pettenkofer-Institut, 1999). Recent advances in MS-based proteomics have helped in obtaining tens of thousands of unique PTMs sites by enabling high throughput characterization and quantification of proteins on eukaryotic and prokaryotic cells (Angel *et al*., 2012; Olsen and Mann, 2013). In particular, PTM-based regulations can occur at a single residue or multiple sites. However, even though MS-based proteomics has greatly advanced

our understanding of PTMs, there are still some major limitations to this approach. First of all, incomplete coverage of the proteome and biases towards the detection of certain types of PTMs may appear due to lower abundance and lower stoichiometry compared to unmodified proteins. The complexity and diversity of PTMs can lead to false positives and negatives in the data. Potential inaccuracies in quantification may occur because of the peptide ionization and chromatographic separation. Last but not least, the labile peptide-modification bond and the rapid PTM dynamics can induce a high variability in sample preparation, making the analysis of proteins impacted by PTMs more difficult than unmodified proteins (Prus *et al.*, 2019). Among all PTMs, because of the lack of efficient enrichment strategies, lysine methylations on non-histone proteins are especially difficult to detect. The dynamic concentration range of the proteome masks their signal during proteomic analysis which impedes the detection of these low-abundant methylated proteins (Wang, Wang and Ye, 2017).

There are two main analytical methods for proteomic analyses, the "top-down" and the "bottom-up"/shotgun approaches (Zhang *et al.*, 2013; Rourke *et al.*, 2019). The "top-down" approach relies on the analysis of intact proteins by MS and their characterization through the fragmentation of intact proteins within the mass spectrometer (**Figure III-1A**). Whereas, the "bottom-up" approach involves proteolytic digestion to provide peptide characterization analyses (**Figure III-1B**). When the "bottom-up" approach is carried out, proteins first undergo digestion through specific proteolytic enzymes, to next perform some specific enrichments for the peptides with corresponding modifications, and finally use MS to identify the peptide sequences (Gillet, Leitner and Aebersold, 2016). Compared to "top-down" workflow for proteomics research detecting complex proteins (typically >10,000 Da), the mass range of proteolytic peptides (typically 500-5000 Da) generated by trypsin digestion match more closely the MS instrumentation capabilities than large intact proteins (Botelho *et al.*, 2010). However, the intact protein separation techniques are at low-efficiency and require long ion accumulation, activation, and detection times, while bottom-up proteomics has the ability to achieve high-resolution separations (Kettman, Frey and Lefkovits, 2001). Therefore, in obtaining most large-scale PTM-mapping studies, the "bottom-up proteomics" approach

has been broadly used. In bottom-up proteomics, a significant amount of modified proteins were “fished out” using various PTM affinity-enrichment strategies (Curran *et al.*, 2015).

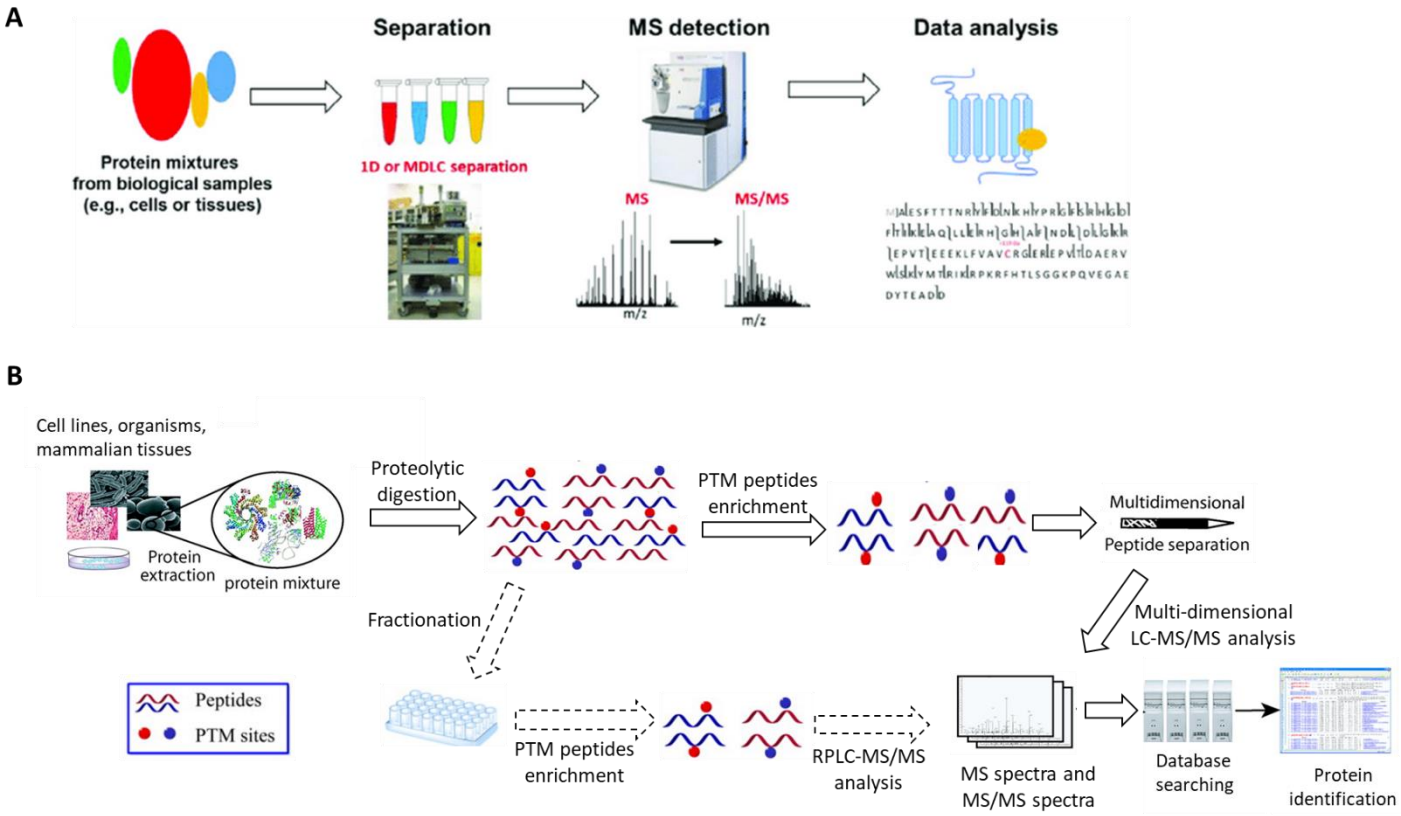


**Figure III-1 The flowcharts for large-scale PTM analysis by (A) top-down and (B) bottom-up proteomics**
(A) Top-down proteomics characterize intact proteins from biological samples without prior digestion into corresponding peptide species. The schematic workflow includes protein separation using multidimensional liquid chromatography (MDLC), mass spectrometer detection, and data analysis based on (Toby, Fornelli and Kelleher, 2016). (B) After enzymatic digestion, the protein mixture is directly digested into a peptides mixture and subsequently PTM peptides are enriched and separated by multidimensional separation methods and the peptides are then analyzed by mass spectrometry. Proteins are identified from the generated mass spectra using database searching based on (Fournier et al., 2007; Huang et al., 2014).

Both methyl-arginine and methyl-lysine occur in mammalian and bacterial cells using SAM as a methyl donor. The bacterium then uses SAM to methylate lysine residues on a variety of proteins, including those involved in virulence and host-pathogen interactions. For *S.* Typhimurium, the *de novo* methionine (Met) biosynthetic pathway is encoded by several genes, including *metA*, *metB*, *metC*, *metE*, *metH*, and *metK* (**Figure III-2**) (Colgan *et al.*, 2013; Husna *et al.*, 2018).

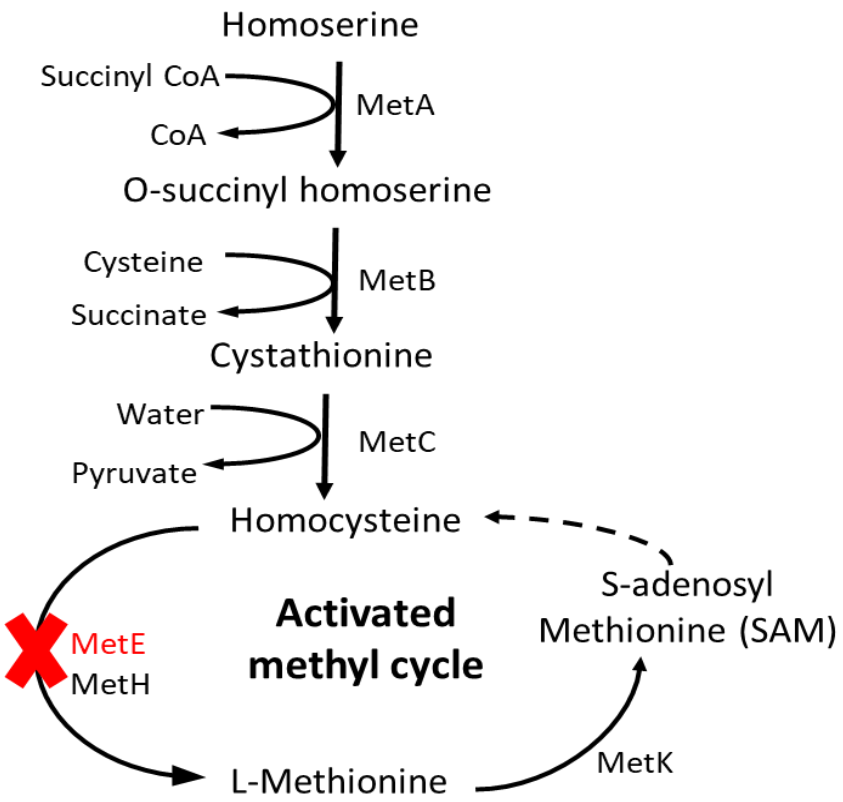


**Figure III-2 Schematic diagram of the biosynthetic pathway of Met with knockout *metE* gene in *S*. Typhimurium**

Source: Husna *et al.*, 2018**.** The first committed step of the pathway is catalyzed by homoserine transsuccinylase (MetA), which succinylates homoserine to form *O*-succmmmminyl-l-homoserine, which then undergoes a condensation reaction with cysteine to form l-cystathionine, catalyzed by cystathionine γ-synthase (MetB). Cystathionine β-lyase (MetC) catalyzes the conversion of l-cystathionine to l-homocysteine, pyruvate, and ammonia. The final biosynthetic step is catalyzed by distinct Met synthases, MetH and MetE, which are vitamin B12-dependent and -independent synthases, respectively. In *S. enterica*, Met is recycled through an activated methyl cycle. The primary methyl donor, SAM, is formed by the activation of Met through an ATP-dependent condensation reaction catalyzed by the SAM synthase (MetK). Catalytic enzymes metE is shown in red; arrows indicate the direction of catalytic reactions.

Met is required for the initiation of protein synthesis and is essential for *Salmonella* growth and survival. Strain *S*. Typhimurium Δ*metE* in this thesis is a mutant that has a deletion in the gene *metE*, which requires exogenous Met to transfer the methyl group to the primary methyl donor SAM for growth. Here, the strain Δ*metE* was cultured in the medium exogenously adding L-methionine in a minimal medium containing glucose as a carbon source help the tracking of the methyl group and identification of the methylation sites. Besides, human embryonic kidney (HEK) 293 cell lines have been described to carry out most of the PTMs, including large protein methylation events (Sabbir, 2019). As many as 8030 mono-methylated arginine sites within 3300 proteins in HEK293 cells have been identified using the high-pH

reversed-phase fractionation and immunoaffinity purification strategy (Larsen *et al*., 2016). Weiss *et al*. found an extremely lysine-rich (total 40 lysine residues) containing main methylation sites in the C-terminus of histone H1 of HEK293 cells (Weiss *et al.*, 2010). After that, Ning *et al*. identified 742 methylation events, including 305 MML, 28 DML, 66 TML, and also 77 mono- and 163 di-methylated arginine sites from HEK293 total lysate through MDA-OPA enrichment strategy (Ning *et al.*, 2016), suggesting that HEK293 cells could be used as a positive control for lysine methylation study, especially for TML sites identification.

Aptamers can recognize a specific conformational epitope on a protein with high affinity and specificity (Beloborodov *et al.*, 2018). The literature data suggested that when aptamers were selected for a protein target in a cell lysate, they could be immediately used as affinity probes for the purification of the target protein from the cell lysate (Javaherian *et al.*, 2009). Cell lysate mainly contains three groups of proteins that can interfere with aptamers as shown in **Figure III-3**: proteases and nucleases, highly abundant non-target proteins, and DNA-binding proteins. The presence of proteases and nucleases can degrade potential target proteins and aptamers, affecting their stability and binding capacity (Javaherian *et al.*, 2009). Highly abundant non-target proteins in the cell lysate may compete with aptamers for binding sites, resulting in non-specific binding. DNA-binding proteins, on the other hand, can bind to aptamer's sequences, leading to false-positive signals (Javaherian *et al.*, 2009). Very few protein-detecting aptamer sequences have been discovered and even fewer have been well characterized. Since 1999, the strategy based on aptamer-assisted protein purification has been introduced (Romig, Bell and Drolet, 1999), but only a few proof-of-concept studies have been conducted on the use of aptamers specifically for the proteomic approach and purified protein's activity has not been confirmed (Ahirwar and Nahar, 2015; Forier *et al.*, 2017). When synthetically modified with a linker such as an amine group, thiol group or biotin, aptamers can be linked non-covalently or covalently with a solid-phase substrate to promote the purification of associated proteins from a cell lysate (Balamurugan *et al.*, 2008). In these cases, magnetic carriers bearing an immobilized aptamer could capture the target protein and then use a single-step isolation to get a rapid and easy elution of the protein after contaminants removal (Safarik and Safarikova, 2004).

In this work, the purification procedure with the help of the selected TML aptamer was first applied to the crude cell lysate of strain *S*. Typhimurium Δ*metE*. After having shown the ability of this aptamer to enrich the crude extract from a positive control, i.e HEK293 cells, we tried to use it in order to specifically retain proteins and peptides bearing TML in the *Salmonella* samples. Both of these cells were prepared by sonication and followed a general scheme shown in **Figure III-3**. The biotinylated Tri-6 was immobilized onto M-280 streptavidin magnetic beads *via* 5'-terminal-biotin streptavidin interaction to try to maintain molecular flexibility and three-dimensional aptamer folding. Subsequently, the Tri-6-coated beads were incubated with the cell lysates containing the target proteins. The unbound components of the lysate were removed during the washing steps. The bound proteins were eluted by heating treatment or by a buffer containing a high concentration of a $MgCl_2$ which was inspired by (Beloborodov *et al.*, 2018).

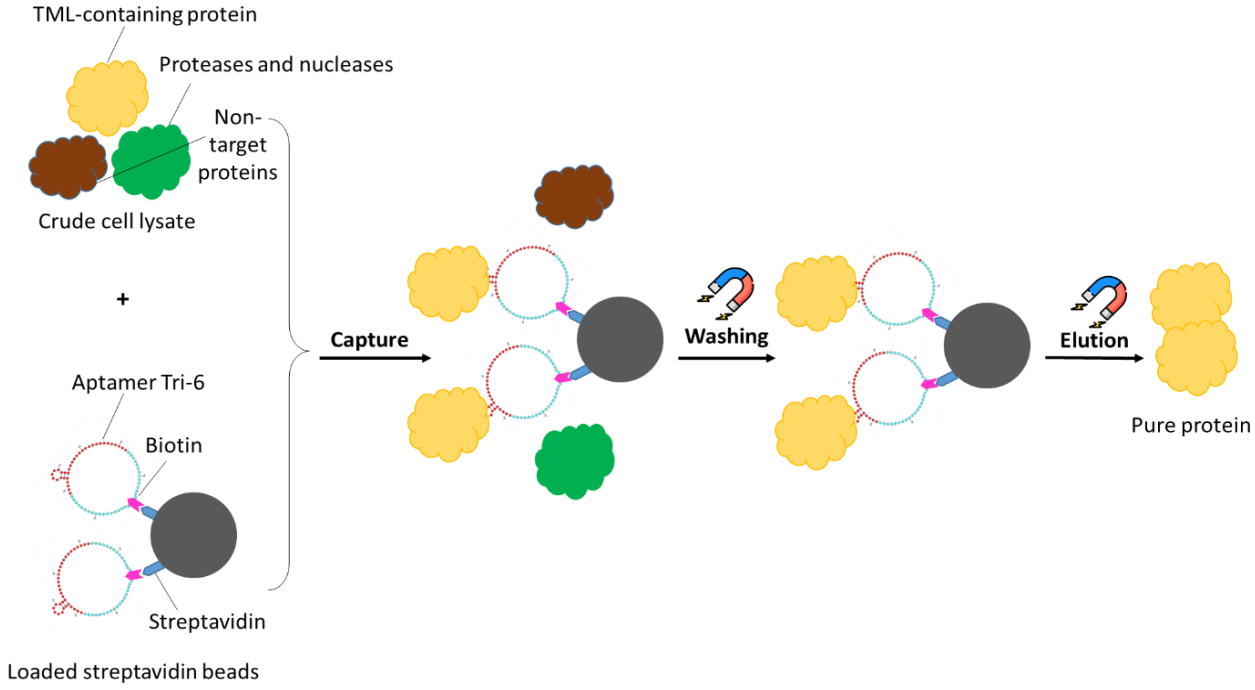


**Figure III-3 Schematic illustration of aptamer Tri-6-based purification method for capturing and elution of TML-containing proteins**

Multiple copies of protein- specific ssDNA aptamers are attached to magnetic beads through the streptavidin-biotin bridge. The aptamers serve as capture probes for the target protein in a crude cell lysate. Yellow cloud represents TML-containing proteins. The brown cloud represents highly abundant non-target proteins. The green cloud represents proteases and nucleases which could degrade the target protein and aptamers. The beads with captured target protein are separated from the lysate by a magnet and the unretained proteins are washed out. Finally, the target proteins are eluted with either $NH_4HCO_3$ solution supplemented with an additional strong electrolyte (NaCl or $MgCl_2$), or with heat treatment at 80°C.

## III.2 Results and discussions

### III.2.1 Purification of TML-containing protein from *S*. Typhimurium *ΔmetE*

The different fractions from *S*. Typhimurium *ΔmetE* cell lysate before and after incubation with Tri6-beads or naked-beads including crude cell extraction, washing fractions and elution fractions were analyzed by tricine-SDS-PAGE (**Figure III-4**). A large amount of unbound proteins was removed by 3 washes from Tri-6-beads and naked-beads (**Figure III-4**, lane 4 to lane 6), while the potentially specific bound proteins and beads-specific proteins were obtained from the Tri-6-bead and naked-bead surfaces after three successive elutions with heat-treatment (**Figure III-4**, lane 7 to lane 9), respectively. After three repeated elutions, essentially all bound proteins were eluted and the potential target proteins were mainly concentrated in the 1$^{st}$ elution fraction (**Figure III-4**, lane 7).

Because of the strong biotin-streptavidin bond in Tri-6-beads, heating at 80°C was expected to break the possible hydrophobic and electrostatic interaction between the TML-containing protein and Tri-6 to release the putative target proteins. Moreover, considering that high temperature may cause the eluted protein denaturation and degradation of some functional proteins, reducing the soluble elutes for subsequent experiments, while high ionic strength can induce a reversible structural alteration of the DNA aptamer to release the bound proteins without denaturation (Beloborodov *et al.*, 2018), a high concentration of $MgCl_2$ (2M) was used in parallel. However, the protein samples with high ion concentration can interfere with the separation of the proteins in the SDS-PAGE, resulting in a smearing of the protein bands, poor resolution, difficulty in visualizing the protein bands, and thus masking part of the signal (Gallagher, 2012). Therefore, elutes in high $MgCl_2$ were not analysed by tricine-SDS-PAGE in this work.

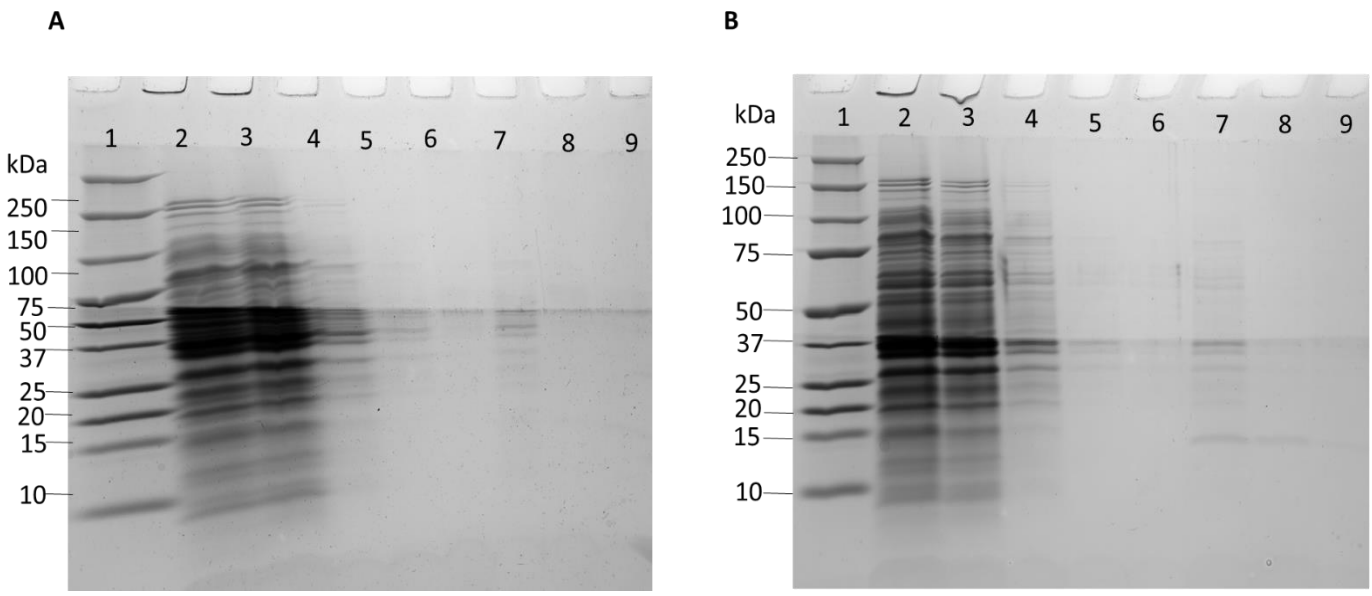


**Figure III-4 SDS-PAGE of different fractions before and after incubation of *S.* Typhimurium Δ*metE* with Tri6-beads (A) and naked beads (B)**

The lanes correspond to the following: protein ladder (lane 1), crude cell extraction (lane 2), remaining solution after incubation (lane 3), 1st -3rd washing fraction (lane 4-lane 6), 1st -3rd elution fraction (lane 7-lane 9).

In order to initially analyze the size of the potential specific and nonspecific proteins for Tri-6, we focused on the first eluted fractions from Tri-6 and nake-beads, respectively, as shown in **Figure III-5**. The SDS-PAGE obtained is illustrating the eluted proteins ranging from 37-75 kDa from Tri-6-beads (**Figure III-5**, lane 3). The negative control experiments were performed with naked beads in order to determine the nonspecific interactions between protein and streptavidin beads (**Figure III-5**, lane 4). The eluted proteins obtained with the nanaked beads range froma and 50-100 kDa. Markedly, the band at around 15 kDa appeared in the three elution fractions (**Figure III-4B**, lane 7 to lane 9) (only the first elution fraction shown in **Figure III-5**, lane 4) but neither observed at washing fractions nor during the elutions from Tri-6-beads.

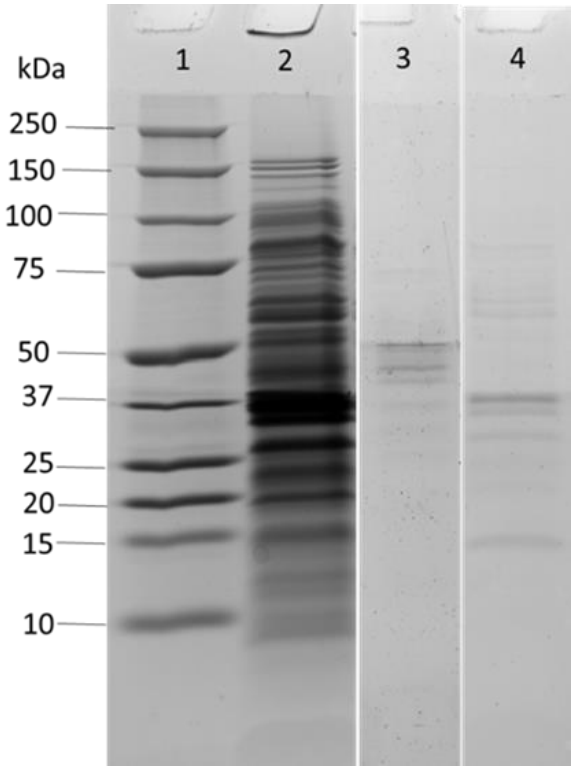


**Figure III-5 Aptamer facilitated purification of TML-containing protein from *S.* Typhimurium *ΔmetE***

The lanes correspond to the following (from left to right): molecular weight markers (lane 1), crude cell lysate of *S*. Typhimurium *ΔmetE* (lane 2), the 1st elution fraction from the Tri-6 beads (lane 3), the 1st elution fraction from the naked-beads (lane 4).

The protein concentrations of different fractions including the total crude cell lysate and the mixture of the 1st elution from naked and Tri-6 beads through heat treatment and high salt (2M $MgCl_2$ solution) treatment were detected by BCA assays (detailed in Chapter VI.4.4), as listed in **Table III-1**. The concentrations of the proteins eluted from the Tri-6 beads were listed from duplicate parallel determinations and marked as "Tri-6-1" and "Tri-6-2" in the **Table III-1**. These data showed that more proteins targeted streptavidin beads than Tri-6, regardless of the type of elution treatment, suggesting that more bead-specific proteins rather than Tri-6-specific proteins were present in the protein samples.

**Table III-1 BCA assays for protein concentrations of different fractions from *S*. Typhimurium *ΔmetE***

| Protein fractions | Concentration (μg/ml) |
|---|---|
| Crude cell lysate | 2488,67± 180,36 |
| 1st elute from naked beads by heat treatment | 105,83± 0,05 |
| 1st elute from Tri-6-1 by heat treatment | 93,33±0,01 |
| 1st elute from Tri-6-2 by heat treatment | 76,67±0,01 |
| 1st elute from Tri-6-1 by salt treatment | 73,33±0,02 |
| 1st elute from Tri-6-2 by salt treatment | 76,67±0,03 |

## III.2.2 Purification of TML-containing protein from HEK293 cells

Due to the lack of proteome information for the strain *S*. Typhimurium *ΔmetE*, a protein extract known to contain a large amount of TML sites is required. Therefore, the HEK293 cells, whose proteome information is well defined, were used as a positive control and then analysed by tricine-SDS-PAGE. The HEK293 cell lysate before and after incubation with Tri-6-beads were analysed by electrophoresis (**Figure III-6**).

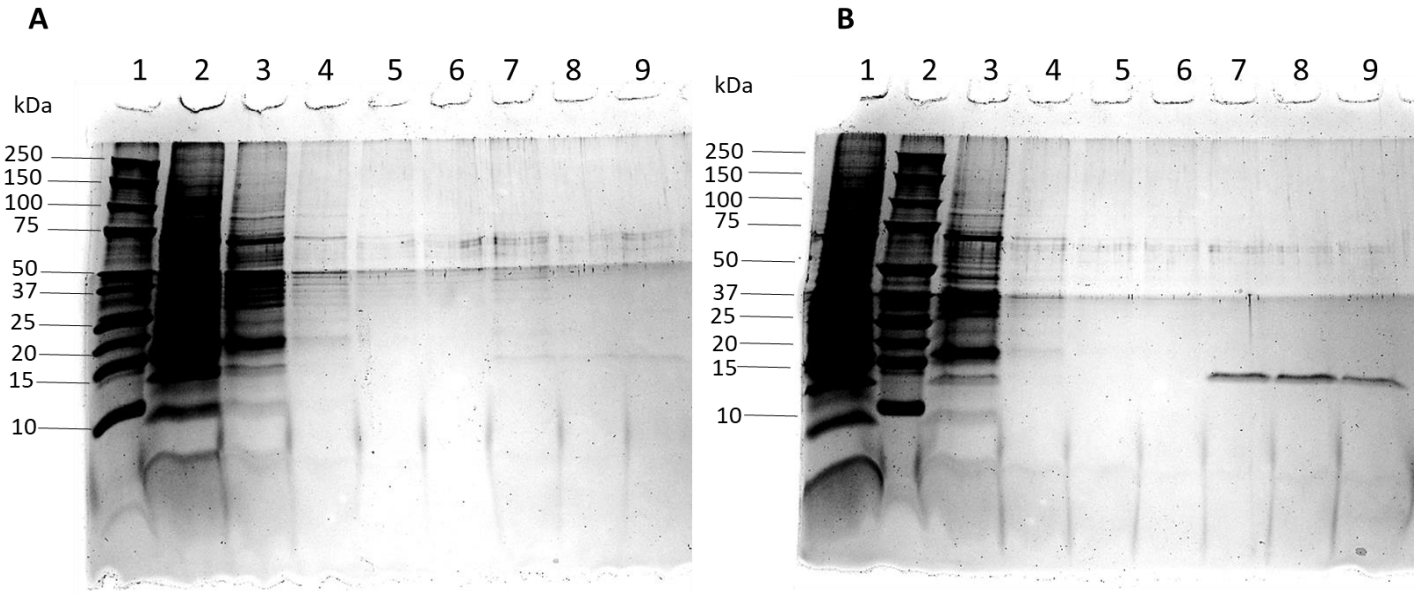


**Figure III-6 SDS-PAGE of different fractions before and after incubation of HEK293 cells with Tri6-beads (A) and naked-beads (B)**

The lanes correspond to the following: protein ladder (lane 1 for A, lane 2 for B), crude cell extraction (lane 2 for A, lane 1 for B), remaining solution after incubation (lane 3), 1st -3rd washing fraction (lane 4-lane 6), 1st -3rd elution fraction (lane 7-lane 9).

Similar results with *S*. Typhimurium were obtained for the 3 washing fractions (**Figure III-4**, lane 4 to lane 6). All the proteins were gradually decreased when increasing the number of washes. A large number of unbound proteins was removed by 3 washes (**Figure III-6**, lane 4 to lane 6) and they are found mainly at a range of 15-100 kDa. Moreover, the use of aptamer-free beads (naked beads) suggests a background noise due to the unspecific binding of proteins on beads, both from *S*. Typhimurium and from HEK293 cell lysate.

In addition, Figure III-7 illustrates that the eluted proteins range from 15-75 kDa (**Figure III-7**). Nevertheless, a few bands around 50 kDa appears to be specifically eluted from Tri-6 when compared to naked beads. In contrast, the non-specific binding was confirmed when compared with naked beads, showing proteins at a range of 50-75 kDa (**Figure III-7**, lane 4), and even a stronger band between 15 and 20 kDa.

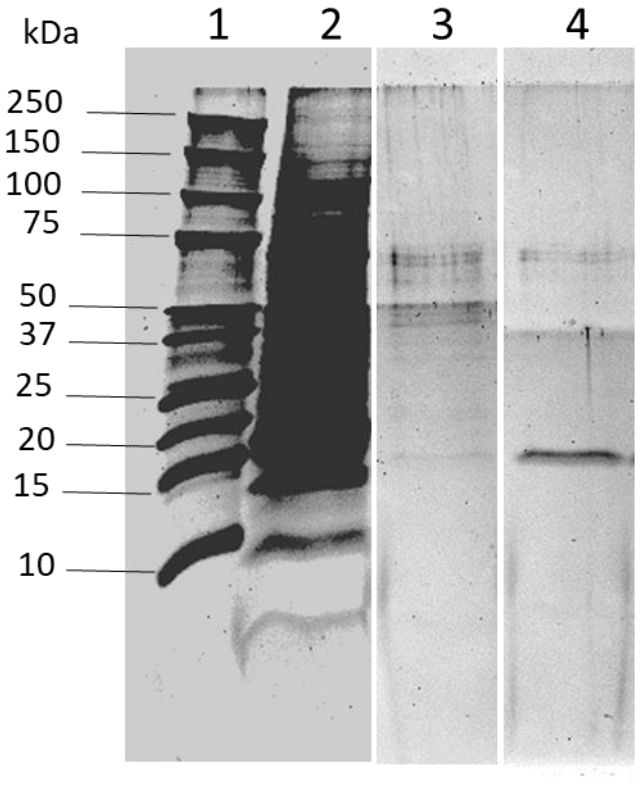


**Figure III-7 Aptamer-assisted protein purification of TML-containing protein from HEK293 cells**
The lanes correspond to the molecular weight markers (lane 1), crude cell lysate of HEK293 cell (lane 2), the 1st elution fraction from the Tri-6-beads (lane 3), and the 1st elution fraction from the naked-beads (lane 4).

In **Table III-2**, all the concentrations of the 1st elution fractions are listed which were measured including the two elution types (heat treatment and high salt treatment) described

above for *S*. Typhimurium. These data illustrate that more proteins were eluted by heat treatment than by high $Mg^{2+}$ salt treatment, regardless of the types of incubation.

**Table III- 2 BCA assay for protein concentrations of different fractions from HEK293 cells**

| Protein fractions | Concentration (µg/ml) |
|---|---|
| Crude cell lysate | 1947,5±31,82 |
| 1st elute from naked beads by heat treatment | 24,11± 0,04 |
| 1st elute from Tri-6 by heat treatment | 41,12± 1,21 |
| 1st elute from naked beads by salt treatment | 10,81±0,03 |
| 1st elute from Tri-6 by salt treatment | 10,01±0,02 |

## III.2.3 Proteomic analysis of the purified proteins

### III.2.3.1 Methodology

The proteomic analyses were performed by liquid chromatography-tandem mass spectrometry (LC-MS/MS), which enables the identification and quantification of a wide range of proteins and their PTMs at a high level of sensitivity and accuracy (Paul Zolg *et al.*, 2018). After purifications of the proteins by the Tri-6-beads, the potential TML-containing proteins were followed by trypsin and lys-C cleavages, desalted with HLB cartridge (60mg beads, Waters cat. no. WAT094226), separated by LC, and then ionized through electrospray ionization (ESI)-Orbitrap Q-Exactive at the Proteomics and modified peptides platform (P3M) (https://pasteur-lille.fr/en/center-of-research/technological-platforms/p3m-proteomics-and-modified-proteins-analysis-platform/) for mass analysis (**Figure III-8**). The precursor ions with the highest signal intensities are selected to undergo fragmentation and re-analyzed as product ions by a second mass analyzer using Proteome Discoverer SEQUEST (Thermo Scientific). The m/z of the precursor and product ions were then aligned to UniProt and EMBL's European Bioinformatics Institute (EMBL-EBI) databases that contain a given set of protein spectra. The database contains the predicted spectra of the sample's known proteome. All raw files were searched with monomethyl(K/R), dimethyl(K/R), trimethyl(K), oxidation of methionine, carbamidomethylation, and acetylation at the *N*-terminal of proteins. The precursor spectrum was compared to the target database to generate a list of

matches, then the confidence of these matches was scored by aligning the product ion spectrum to the matches' predicted fragmentation pattern. Finally, the identified peptides containing methylation sites were quantified to determine their abundance values using a 1% site-specific FDR filtering, and analyzed using bioinformatic tools to identify the biological processes and the proteome functions. This work was done by the P3M (the Institute Pasteur of Lille, France).

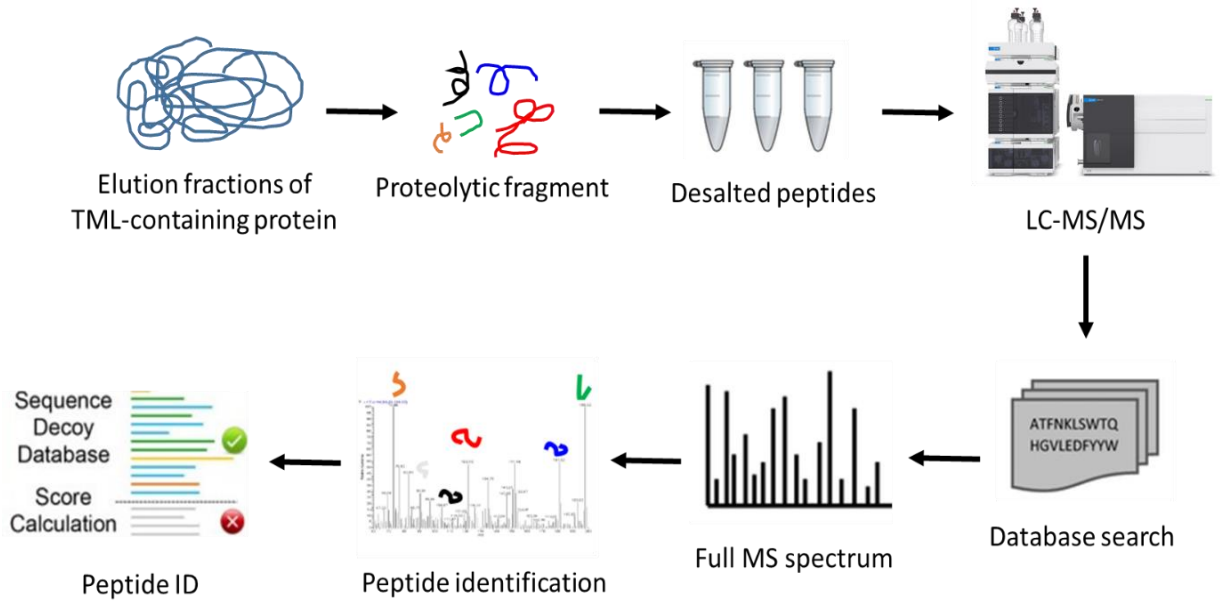


**Figure III-8 Schematic workflow of the procedure of proteomic analysis for protein separation, identification, and data analysis**

## III.2.3.2 Identification of methylated peptides from *S*. Typhimurium *ΔmetE*

Considering the inevitable loss of large amounts of protein during the cleavage and desalting steps, we pooled all the elution fractions obtained from the above two elution treatments for the following proteomic analysis. The workflow was first applied to *S*. Typhimurium *ΔmetE* lysate. Across all experiments, we identified 19 methylation sites on 5 proteins in 21 methylation events with the Peptide Spectral Matches (PSMs) site confidence $\geq$ 0.5. LC-MS/MS analysis results of the eluted and digested proteins revealed that peptides containing methylated lysine from *S*. Typhimurium are more frequently identified when using Tri-6 beads rather than naked beads, as shown in **Figure III-9A**. It suggests that Tri-6 specifically recognized certain methyllysine sites on *Salmonella* proteins. The number of methyl and non-methyl PSMs of the proteins eluted from Tri-6 and naked beads were used to calculate the

specificity. Here, we calculated the specificity by the ratio of methyl peptides recognized by the aptamer versus all peptides, methylated or not, retained on naked beads. When the total protein extract is considered, this ratio is about 141/105. When focusing on the identified methylated proteins, including isochorismate, the ratio is 1/0, 27/26 in 50S ribosomal protein L7, 12/7 in 50S ribosomal protein L3, 52/38 in elongation factor Tu, and 49/34 in Flagellin FljB, respectively. When compared with peptides retained on naked beads, data suggest that more identified peptides containing modifications of methylation and oxidation were enriched by Tri-6.

These results suggest a lack of specificity, but other explanations for the retention of proteins on both Tri-6 and naked beads have to be considered. It may result from the proteins with different states (unmethylated or methylated) of lysine residues at certain sites that bind to Tri-6 and naked beads. During cell processes, the same amino acid can be modified heterogeneously on the same protein. For example, at a specific lysine site, some are unmethylated whereas others are mono-, di- or tri-methylated (Biggar and Li, 2015). It is, therefore, possible that the protein with the unmethylated lysine bound to the naked beads, while the methylated version was retained on Tri-6 beads. To confirm this possibility, more precise detections such as MS are required to identify the methylated state of the same protein eluted from naked beads. Moreover, the naked beads may not be the most appropriate negative control. The strong absorption of such support can interfere with the separation of proteins and can lead to strong background noise. It would be interesting to use beads coated with irrelevant aptamers, which contain the same nucleotide composition but in a different order, instead of naked beads as a negative control.

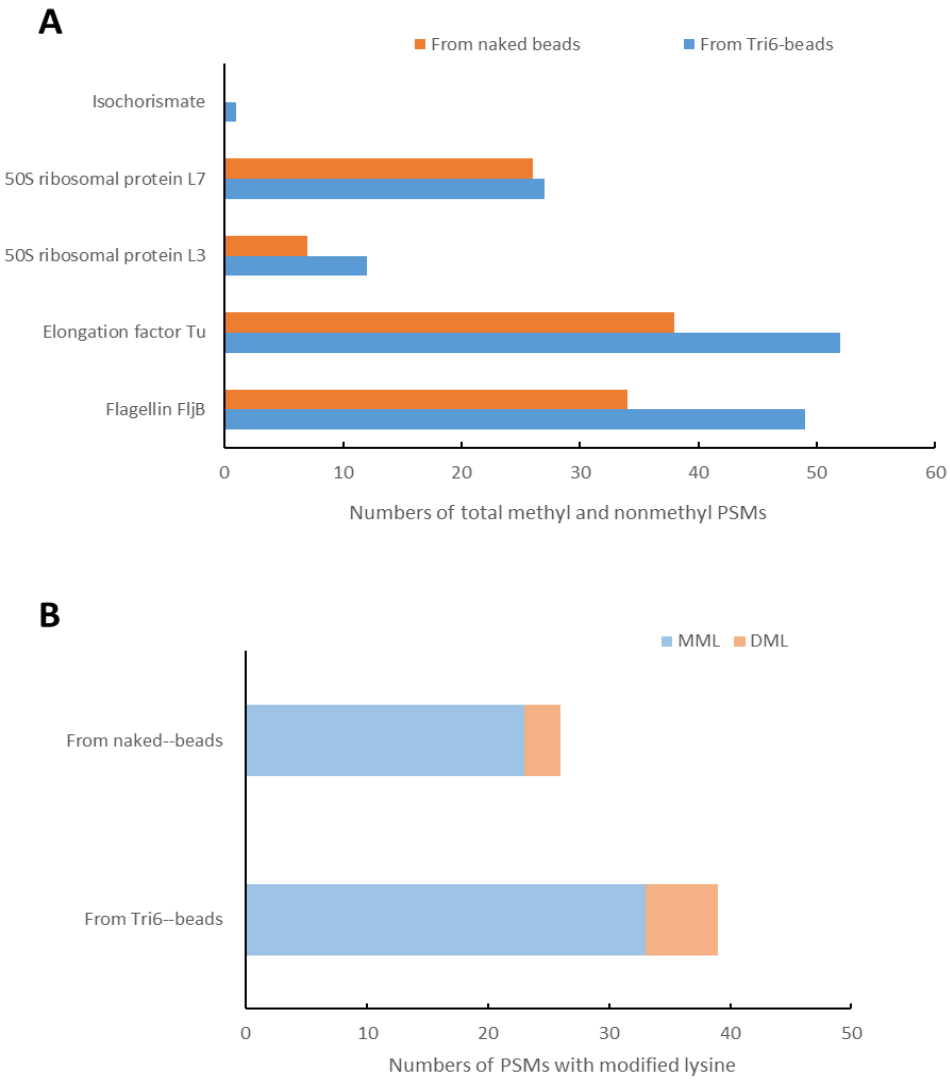


**Figure III-9 Quantity of peptides derived from *Salmonella* retained on Tri-6 or naked beads, according to the protein from which they were found**

(A) Number of total methyl and non methyl PSMs of the methylated proteins eluted from Tri-6 and naked beads.
(B) Number of methylation sites of methyl peptides from Tri-6 and naked beads.

Notably, only MML and DML sites but no TML site were identified from Tri-6 nor naked beads (**Figure III-9B**), suggesting that there are no TML sites in *S*. Typhimurium *ΔmetE* samples. To validate this conclusion, a sample with known TML sites is required and would allow verifying the recognition of TML sites in proteins using Tri-6 beads.

In the methylated peptides, the methylation sites in the corresponding identified peptides described above illustrated that one methylation site in 50S ribosomal protein L3 and L7 separately are not specific for Tri-6 (**Figure III-10**). Interestingly, the unique DML site in isochorismate only appeared in the protein fraction purified with Tri-6. The methylated peptides containing 10 MML sites which are specific for Tri-6 in flagellin FljB and EF-Tu

contained 3 MML and 2 DML sites, reinforcing our confidence in the specificity of Tri-6 for lysine methylation sites but not for the TML site. Whether this is due to the lack of TML sites in *S*. Typhimurium *ΔmetE* or to the non-specificity of selected Tri-6 to TML-containing peptides needs to be verified by a further positive experiment.

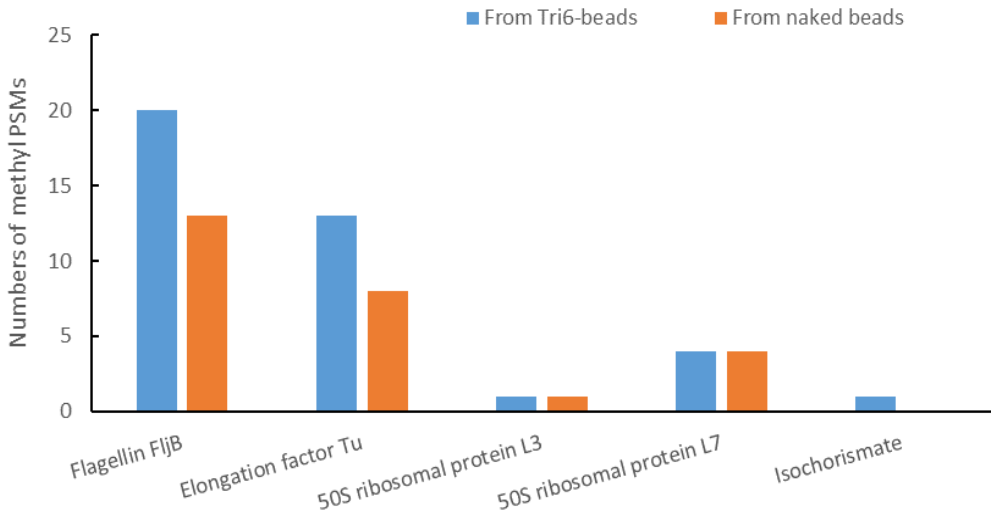


**Figure III-10 Number of methyl PSMs showing the indicated *Salmonella* proteins specifically retained on Tri-6 beads or naked beads, according to the protein from which they are derived**

In the aptamer-specific methylation events (13 mono-methyl and 3 di-methyl), 2 lysine residues showed mono- and di-methylation on the same Lys site in EF-Tu proteins (**Figure III-11**). The overlap of unique methyl peptides enriched by Tri-6 bounded beads confirmed the dynamic regulation of protein methylation (Biggar and Li, 2015).

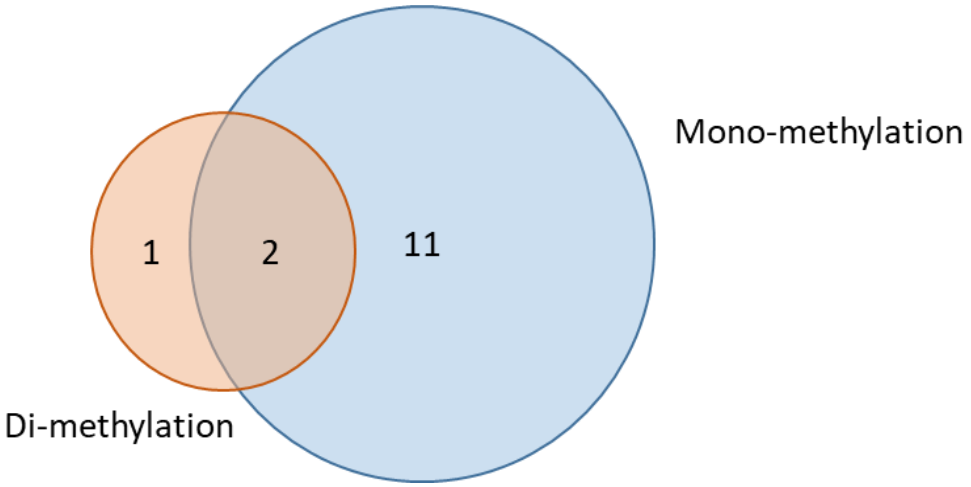


**Figure III-11 Overlap of identified mono/di-methyllysine peptides on the same lysine residues of *S*. Typhimurium *ΔmetE***

### III.2.3.3 Identification of methylated peptides from HEK293 cells

The HEK293 cells were applied as a positive control subsequently. The proteins eluted from Tri6-coated and naked beads after digestion were analyzed by proteomics. Considering all the peptides, all 1473 identified peptides from 414 proteins including 374 human proteins were identified. 11 unique methylation sites, including 6 MML, 3 DML, and 2 TML sites on 8 proteins were identified, suggesting that around 2.1% (8/374) of the identified HEK293 proteins containing methylated lysine were enriched using the Tri-6-bound beads. The result indicated that no matter what kind of proteins containing methylated lysine, the quantity of peptides retained on Tri6-beads is much higher than peptides retained on naked-beads (**Figure III-12**). The methylated centrosomal protein and heat shock 70 kDa protein 1A were identified to be specific for Tri-6.

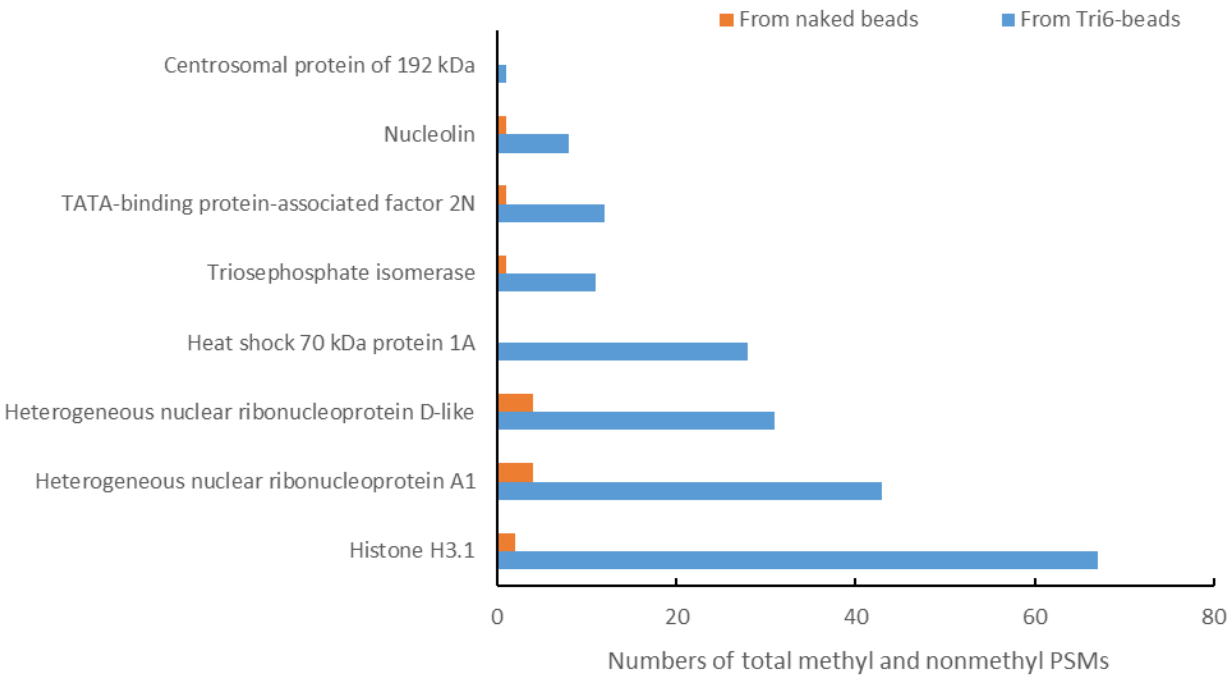


**Figure III-12 Quantity of proteins derived from HEK293 cells retained on Tri-6 and naked beads, according to the protein from which they are derived**

Furthermore, except for one PSM TML in peptide "**K**(trimethyl)SAPATGGVK" in histone H3.1 protein, the methyl PSMs showed that all the identified methylated peptides were from Tri-6-beads rather than naked beads, verifying the specificity of Tri-6 for methyllysine in proteins, as shown in **Figure III-13**.

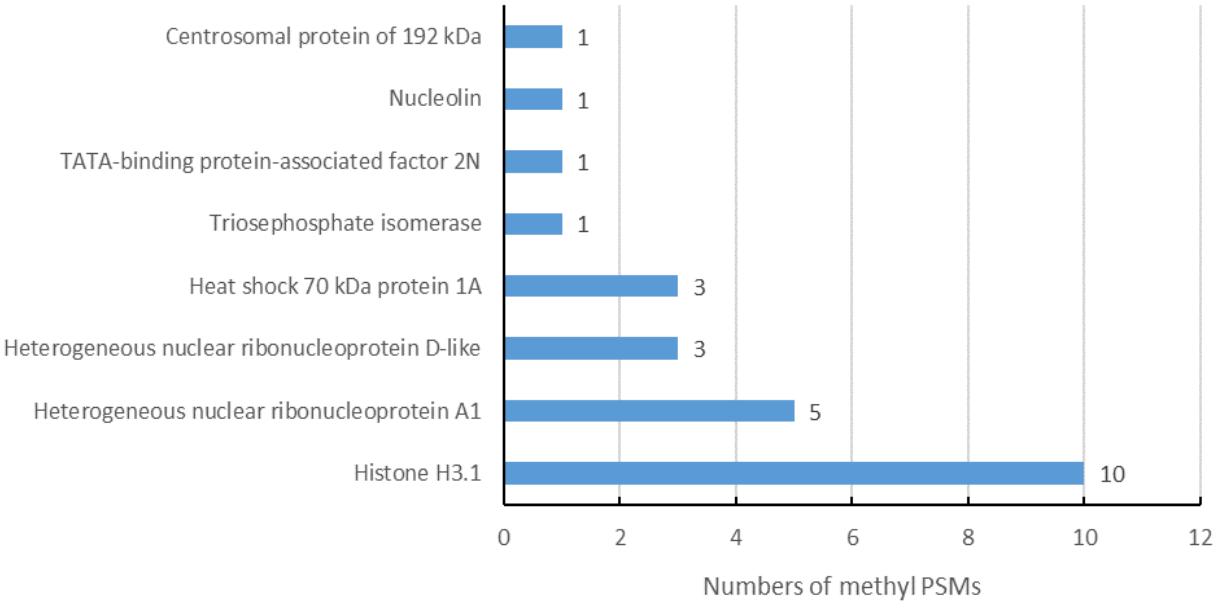


**Figure III-13 Numbers of methyl PSMs in the identified peptides of HEK293 cells enriched by Tri-6**

Among the methylated proteins, the highest amount of the methylation sites appeared in histone (3 methylation sites) and then in heterogeneous nuclear ribonucleoproteins (hnRNPs) (2 methylation sites), suggesting that lysine methylation may play a critical role in regulating corresponding gene expression and protein functions in HEK293 cells.

The methylated peptides which are specific for Tri-6 in HEK293 cells contained 14 MML PSMs, 7 DML PSMs and 2 TML PSMs (**Figure III-14A**). In the aptamer specific methylation events, similar results as described for *S*. Typhimurium, a few lysine residues showed multiple methylation types (**Figure III-14B**), which were consistent with the previous paper (Ning *et al.*, 2016). Lysine in peptide "SAPAKTGGV**K**KPHR" (overlap methyllysine site in red bold) showed mono- and di-methylation, whereas in peptide "**K**SAPATGGVKKPHR" showed mono-, di-, and tri-methylation, and these overlap methylation events only happened in histone H3.1 (H3C12), confirming the dynamic lysine methylation of histone in HEK293 cells.

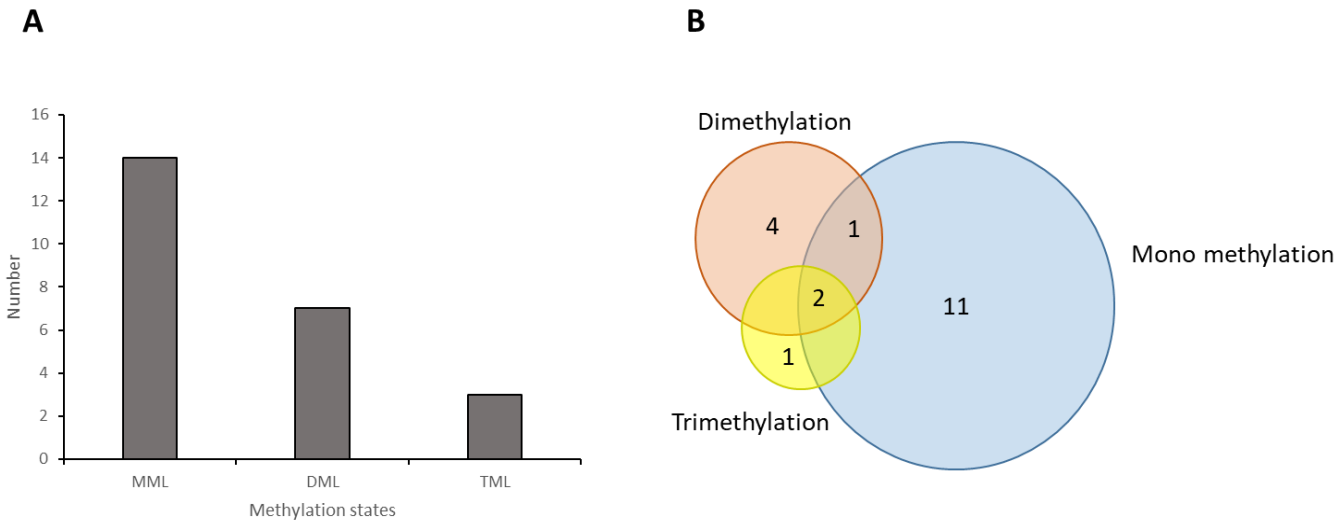


**Figure III-14 Identified lysine methylations in the enriched proteins of HEK293 cells**

(A) Tri-6-specific methylation sites were identified from the enriched proteins of HEK293 cells. (B) Overlap of methylation events identified on the same lysine site.

18 methylation events were identified from enrichment by Tri6-beads of the HEK293 lysates as starting material. Alignment of the identified peptide sequences with the latest HEK293 (Ning *et al.*, 2016) and 293T cell (Hartel *et al.*, 2019) methylated peptides was performed and around 28% (5/18) of methylation events of the methyl proteome was newly discovered after the enrichment with Tri-6 in this study. Several new methylation events were found, including mono-methylated K15 (GFAFVTFDDHDSVD**K**) of HNRNPA1; mono-methylated K3 (LD**K**AQIHDLVLVGGSTR) of HSPA1A; mono-methylated K3 (EALNSCN**K**) of nucleolin; mono-methylated K13 (IIYGGSVTGATC**K**) of TPI1; and tri-methylated K8 (LIGEALG**K**N) of CEP192.

Especially, the methylation events on histone H3, heat shock protein 1A and HNRNPDL are consistent with the previously reported chemistry-based enrichment method using malondialdehyde and ortho-phthalaldehyde (MDA-OPA reaction) (Ning *et al.*, 2016) and complementary enrichment using high pH SCX and immunoaffinity purification (IAP) (Hartel *et al.*, 2019) (**Figure III-15**).

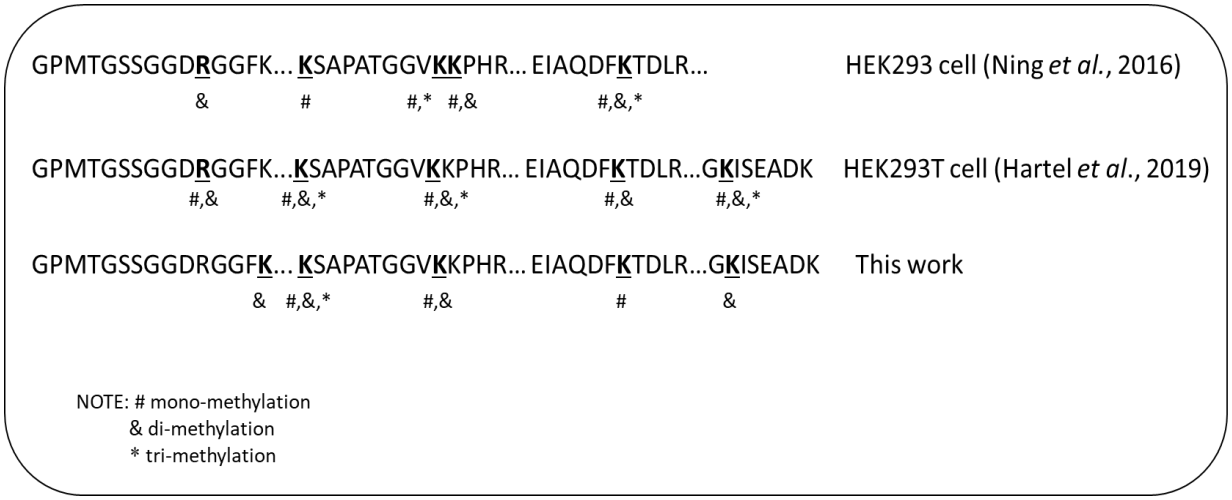


**Figure III-15 Cross-cell comparison of lysine methylation in HEK293 cells**

Comparison of lysine methylations in HEK293 cells enriched by Tri-6 in this work and previous MDA-OPA approach and in HEK293T cells enriched by the combining SCX and immunoaffinity approaches. Date of MDA-OPA approach from Ning *et al*., 2016 and data of combination of SCX and immunoaffinity from Hartel *et al*., 2019. Methylated K and R residues are indicated in bold and underlined. The symbol "#" stands for mono-methylation, "&" for di-methylation and "*" for tri-methylation.

Peptides containing monomethylated K1, K10, K11 and dimethylated K10 (**K**SAPATGGV**KK**) were conserved with previously described (Ning *et al.*, 2016; Hartel *et al*., 2019). Mono-methylated K7 (EIAQDF**K**TDLR) and dimethylated K2 (G**K**ISEADK) were also inconsistent with these two documents. Interestingly, as **Figure III-15** showed, the dimethylated site K15 of a peptide from TATA-binding protein-associated factor 2N (TAF15) (GPMTGSSGGDRGGF**K**) in our work was only found dimethylated R11 in Ning's work (Ning *et al.*, 2016). Trimethylated and dimethylated K1 (**K**SAPATGGVKKPHR) was newly found from HEK293 cells in our enriched peptides. Taken together, these results got on the positive control we used highlight the interest of our enrichment tool, which may be considered complementary to existing tools.

# Chapter IV Enrichment of methylated peptides using high pH SCXtip

## IV.1 Introduction of SCXtip method

The identification and quantification of methylated peptides require a highly efficient enrichment approach to separate the methylated peptides from diverse background peptides (Wang, Wang and Ye, 2017). Therefore, the enrichment of methylated peptides from a complex biological sample is a major challenge in the field of proteomics.

With the development of chromatography-based approaches such as SCX (Bremang *et al.*, 2013) and HILIC (Uhlmann *et al.*, 2012), remarkable progress has been achieved in the field of methyl proteome analysis. Conventional SCX separation was usually conducted at low pH of around 2-3. These low pH conditions allow the stationary phase (a positively charged resin) to retain positively charged peptides, while negatively charged molecules are eluted, resulting in histidine residues (pKa 1.8) being retained by the SCX resin. In contrast, when the solution pH is higher than 7.6, histidine residues would have negative charges and be washed out from the SCX resin (Wang et al., 2016). As a result, under high pH SCX conditions (typically between 8-10), the stationary phase is negatively charged and negatively charged histidine is eluted, reducing the interference from histidine-containing peptides. Additionally, the digestion of the proteins by the combined usage of three enzymes (trypsin, Lys-C and Arg-C) could greatly reduce the proportion of miscleavage peptides (Olsen, Ong and Mann, 2004; Szapacs and Budamgunta, 2013; Wu *et al.*, 2018), causing an improvement of specificity to the methylated peptide enrichments (Wang, Wang and Ye, 2017). Thus, the high pH SCX separation with the help of efficient protein digestion can increase the identification confidence level.

To improve the confidence of methylation identification, heavy Methyl Stable Isotope Labelling by Amino Acids in Cell Culture (hM-SILAC) was adopted as an alternative orthogonal methyl-peptide validation strategy (Wang, Wang and Ye, 2017). The hM-SILAC is a quantitative proteomics technique in which cells are grown in culture media containing heavy methyl amino acids (Wang and Ye, 2018). As the cells grow and divide, these heavy amino acids are incorporated into newly synthesized proteins, resulting in a population of proteins that are uniformly labelled with heavy methyl groups. For example, when $^{13}CD_3$-methionine ($^{13}CD_3$-Met) is used in the cell media, heavy-methyl groups ($^{13}CD_3$) are introduced into lysine and arginine residues and generate a distinctive mass shift of 18 Da per methyl group (Carlson

and Gozani, 2014). One of the advantages of hM-SILAC is its ability to enrich low-abundance proteins in complex biological samples, which may be undetectable by conventional proteomic approaches (Deng, Erdjument-bromage and Neubert, 2020).

Wang and co-workers developed a simple SCX method using a high pH SCXtip, which has no requirement of a complex chromatography system and can be performed in parallel (Wang *et al.*, 2016; Wang and Ye, 2018). The SCXtips stands for “strong cation exchange tip” and involves the use of small pipette tips with SCX resin and a manual liquid handling system for the separation of positively charged analytes in a sample matrix. High pH refers to the use of a high pH buffer ranging from 9-12 during the extraction process. At this pH range, the positively charged peptides containing methylated lysine or arginine can be retained on the resin, while the negatively charged or neutral interferents are excluded. The extraction process using high SCXtips typically involves several steps, including conditioning, sample loading, washing, and elution (Wang and Ye, 2018). In the conditioning step, the SCX resin is activated, the sample is then loaded onto the SCXtip, and the interferents are removed by washing with a low pH buffer. Finally, the analytes are eluted from the stationary phase. As described in this study, we have followed the workflow tandem chromatography strategy (**Figure IV-1**) by combining hM-SILAC cultivation but on bacteria, high pH SCXtip and LC-MS/MS analysis.

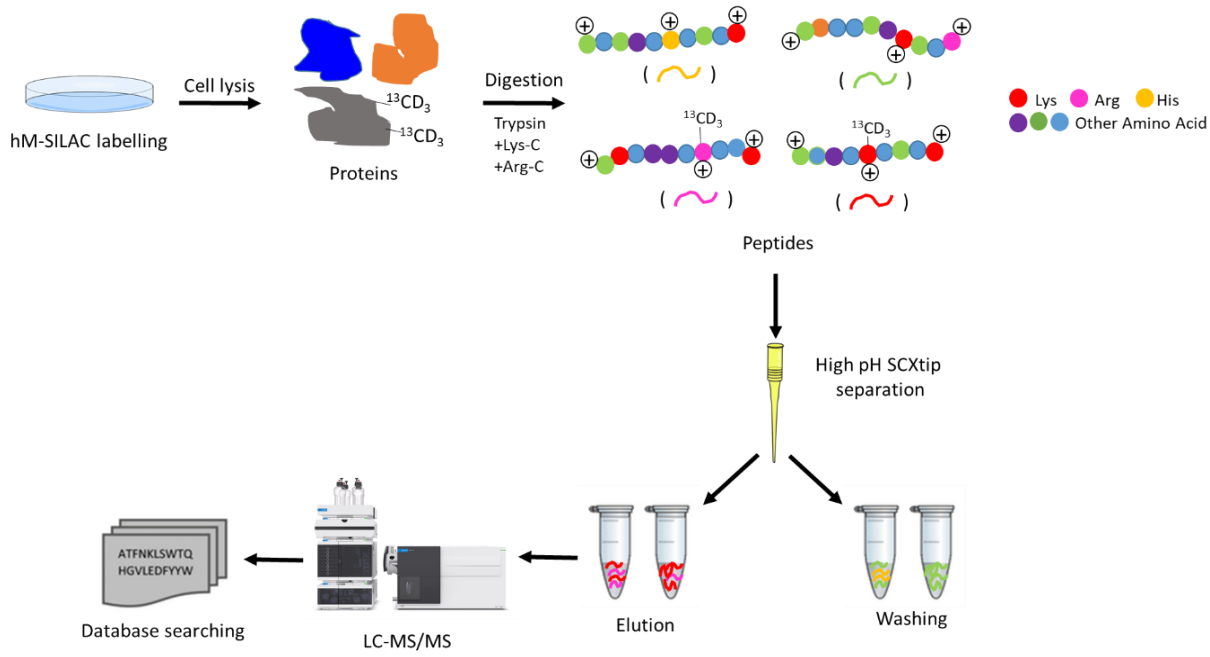


**Figure IV-1 Workflow for the analysis of protein methylation in heavy methionine-labelled cells**

Based on Wang and Ye, 2018. Methylated lysine/arginine was labelled with $^{13}CD_3$-methionine added to the medium. The extracted proteins were digested with multiple endopeptidases and the resulting peptides were separated with high pH SCXtip into different fractions. The different fractions were subsequently analyzed by LC-MS/MS.

# IV.2 Results and discussions

## IV.2.1 Enriching methylated peptides from *S.* Typhimurium strains

The *S.* Typhimurium *ΔmetE* and the double mutants *ΔmetEΔmotAB*, and *ΔmetEΔfliB* strains were cultured in the DEME medium with $^{13}CD_3$-Met and performed digestion with trypsin, Lys-C and Arg-C before high-pH SCXtip enrichment. The *S.* Typhimurium *ΔmetE* was used as wild type (WT); *ΔmetEΔmotAB* has flagella but is non-motile; and *ΔmetEΔfliB* is lack of methylase FliB. For the enriched peptides, after 1-2 elution, the peptides almost eluted from the SCXtip and a very low amount of peptides were obtained from 3-5 elution, as shown in **Figure IV-2**. Compared to *ΔmetE* (WT) and *ΔmetEΔmotAB*, less peptides (lose around 50%) of *ΔmetEΔfliB* get enriched in 1-2 elution fraction, demonstrating that less ($^{13}CD_3$)-labelled sites in *ΔmetEΔfliB* strain. Therefore, it's most likely due to around half of the identified peptides is methylase FliB-dependent, resulting in half peptides being modified with $^{13}CD_3$. Compare to *ΔmetE*, fewer protein expressions in *ΔmetEΔmotAB* and *ΔmetEΔfliB*, suggesting that around 2000 peptides expressed the genes function for motility and methylase.

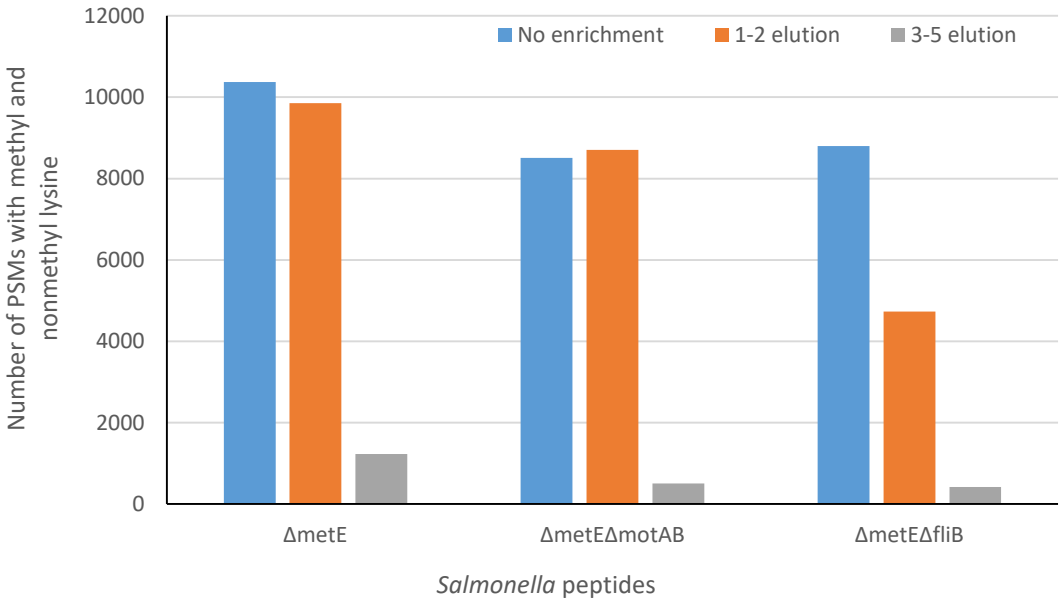


**Figure IV-2 Different fractions of *S*. Typhimurium peptides enriched *via* high-pH SCXtips**

On average, 10369 WT (*ΔmetE*) peptides, 8701 *ΔmetEΔmotAB* and 8799 *ΔmetEΔfliB* peptides from unique 1604 proteins were identified. For these *Salmonella* proteins, 19 methylated proteins were associated with 64 methylation events containing 59 methyl peptides in *ΔmetE*, 134 methyl peptides in *ΔmetEΔmotAB*, and 46 methyl peptides in *ΔmetEΔfliB*. The distribution of the identification of the peptide using SCXtip for methylation enrichment is described in **Figure IV-3A**.

Most methylated peptides Additionally, the enriched methylated peptides were identified distribution of MML, DML, and MMA (mono-methyl arginine) PSMs in all detected strains and DMA (di-methyl arginine) also appeared in strain *ΔmetE* and *ΔmetEΔmotAB* but not in *ΔmetEΔfliB* (**Figure IV-3B**). Approximately twice as many methylated peptides were enriched from *ΔmetEΔmotAB* than from *ΔmetE* and *ΔmetEΔfliB*, suggesting that 2 times the number of peptides are involved in *Salmonella* motility and that they are FliB independent. Interestingly, DML, MMA, and DMA events were relatively low for all types of tested strains, demonstrating that in these cases, methylation levels may not directly relate to bacterial function such as bacterial motility in this work.

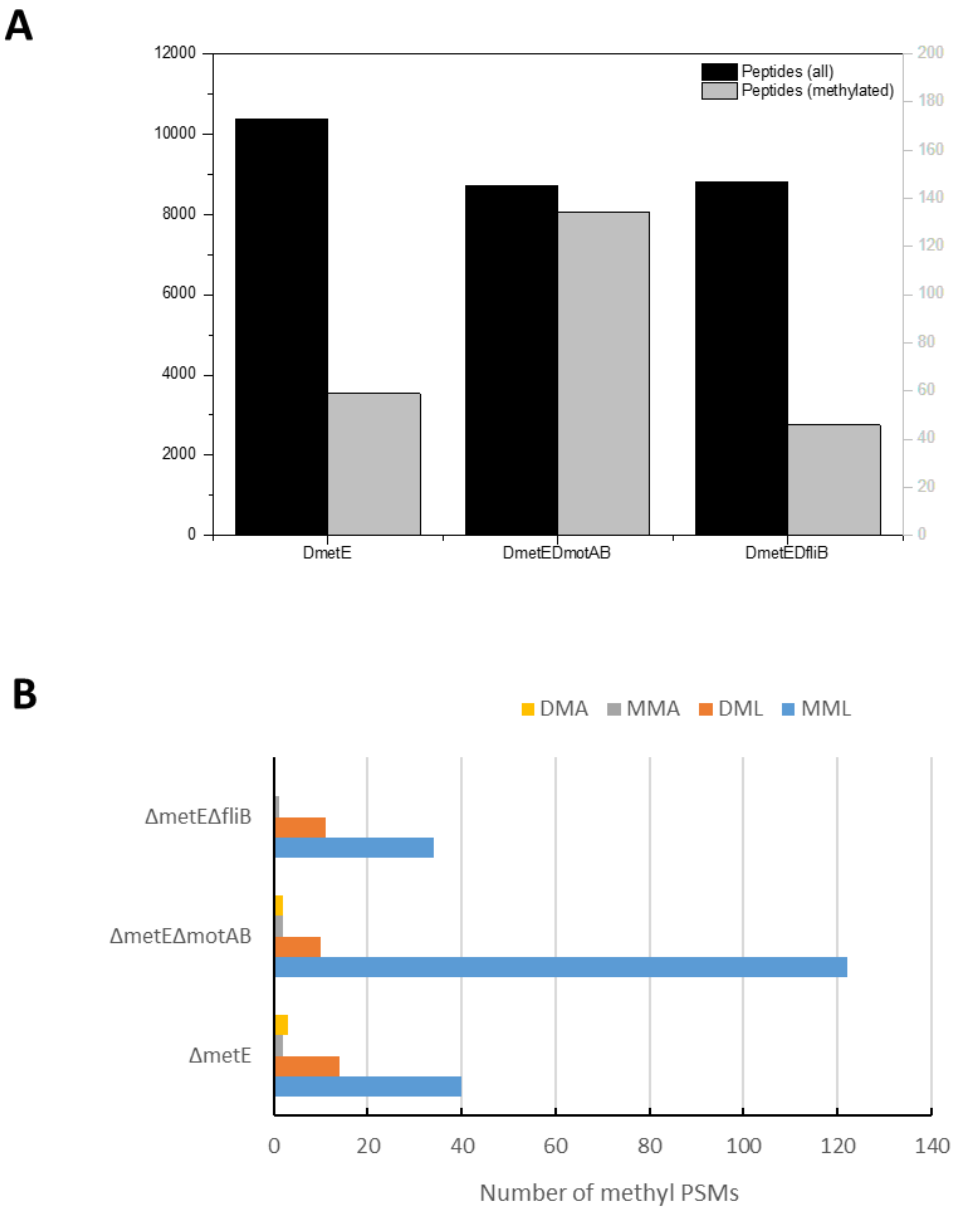


**Figure IV-3 Distribution of the peptides and methylated peptides identification from SCXtip for methylation enrichment in strain *ΔmetE*, *ΔmetEΔmotAB* and *ΔmetEΔfliB*, respectively**

(A) The number of methyl and non-methyl PSMs of the enriched peptides. (B) Number of methylation states per PSM for each methyl peptide.

## IV.2.2 Bioinformatics analysis of identified methylome

As for the identified methylated peptides from 19 different proteins enriched from different strains (**Figure IV-4**), 23 unique methylation sites in *ΔmetE*, 51 unique methylation sites in *ΔmetEΔmotAB*, and 18 unique sites in *ΔmetEΔfliB*. The majority of these methylation sites were found monomethylated, except 7 dimethyl-lysine sites, 5 mono-methyl arginine, and 1 dimethyl-arginine site. The dimethyl-arginine site in FliA only appeared in strain *ΔmetE* and

*ΔmetEΔmotAB* but not in *ΔmetEΔfliB*, suggesting that dimethylation of FliA is FliB-dependent. In addition, as for dimethyl-lysine sites, except for two in elongation factor Tu and one site in 50S ribosomal protein L7/L12, the others were only found in strain *ΔmetEΔmotAB*, including three sites in FljB, one site in hydroxy acid dehydrogenase and one site in an uncharacterized protein. The elongation factor Tu plays an important role in virulence-associated functions including adhesion to the host extracellular surface (Harvey *et al.*, 2019); and 50S ribosomal proteins are required for ribosomal translation (Korobeinikova, Garber and Gongadze, 2012) thus both are essential for bacterial survival. The methylated sites are conserved with mono-methyl and di-methyl sites in all strains used.

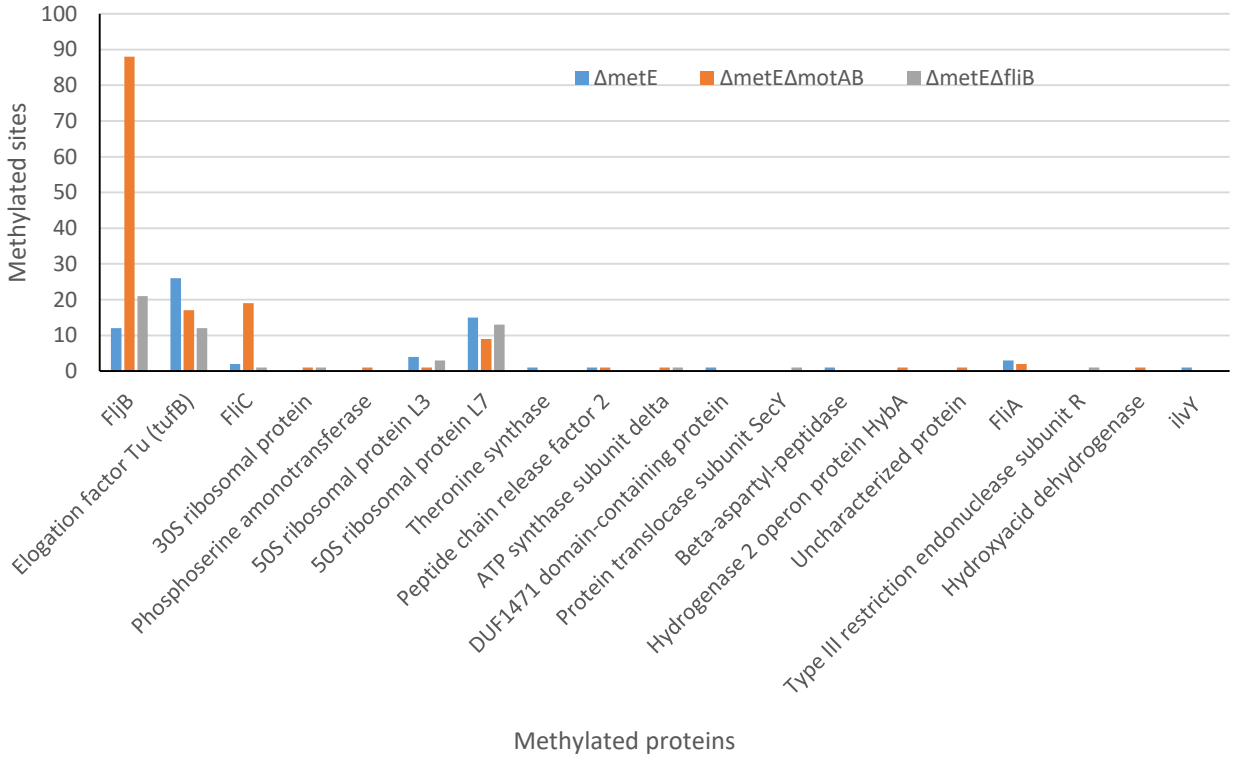


**Figure IV-4 The identified methylated sites in the corresponding proteins from strains *ΔmetE*, *ΔmetEΔmotAB* and *ΔmetEΔfliB***

Notably, one lysine in FljB, two in TufB, one in FliC, and one arginine site in PrfB were methylated only in the presence of the methylase FliB. Moreover, the methylated lysine sites were identified including one in DUF1471 domain-containing protein, one in beta-aspartyl-peptidase, and one in the HTH-type transcriptional activator Ilvy (Ilvy). In addition, one arginine site in threonine synthase, are only detected in the strain *ΔmetE*. These proteins can be only methylated when MotAB and FliB are expressed or it's a matter of detection in the

double mutants. This result has to be confirmed by repeating this experiment. DUF1471 domain-containing proteins were found to be related to stress response and inhibit biofilm formation (Eletsky *et al*., 2014; Horng *et al*., 2022). Strain *ΔmetEΔmotAB* is flagellated but is unable to swim *via* flagella, it can adhere more on itself or on the surface to form biofilm.

The number of methylation sites in flagellin FljB and FliC is the highest in strain *ΔmetEΔmotAB*, compared to strain *ΔmetE* and *ΔmetEΔfliB* as shown in **Figure IV-5**. The methylated FljB in strain *ΔmetEΔmotAB* contained 88 methyl PSMs (including 3 DML and one MMA PSMs), which was approximately 7 times more than strain *ΔmetE* and almost 4 times more than strain *ΔmetEΔfliB*. In contrast, methylated FliC in strain *ΔmetEΔmotAB* contained 19 methylation events (including one MMA site), which was almost 10 times more than strain *ΔmetE* and 19 times more than strain *ΔmetEΔfliB*.

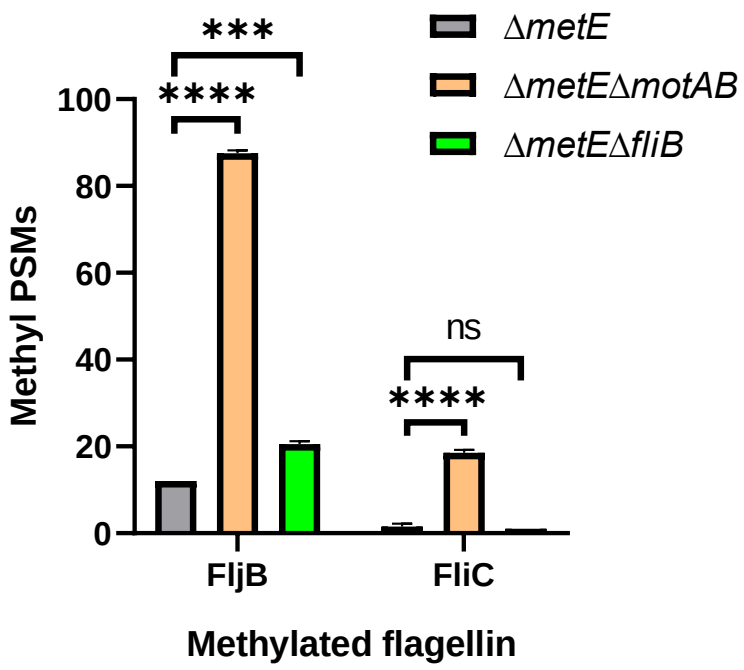


**Figure IV-5 The number of methyl PSMs in methylated flagellins from strains *ΔmetE*, *ΔmetEΔmotAB* and *ΔmetEΔfliB***

Statistical significances were determined by a two-tailed Student's t test (****=p<0.0001, ***=p<0.001, ns=p>0.05).

We observed the only methylation site from peptide "AALTAAGVTGTASVV**K**" in flagellin FliC in strain *ΔmetE* and *ΔmetEΔfliB* is the same one, suggesting that this methylated lysine site did not depend on the methylase FliB. Except for this lysine site, other methylation sites in

FliC only appeared in strain *ΔmetEΔmotAB*. The methylated FliC increased the hydrophobicity of the flagellar surface probably promoting the adhesion of *Salmonella* to compensate for its motor defects, which could also explain the high amount of methylation site in FljB in strain *ΔmetEΔmotAB*. Furthermore, the observation that the methylation site in flagellin FljB and FliC is much higher in strain *ΔmetEΔmotAB* compared to strain *ΔmetE* or *ΔmetEΔfliB* may be due to the fact that the absence of motility gene (motAB) results in a change in the bacterial lifestyle that triggers the expression of genes involved in lysine methylation. This change may also lead to the expression of other proteins that contribute to lysine methylation in FljB and FliC. Another possible explanation is that the higher lysine methylation site in FljB or FliC is due to the presence of other methylases in the *ΔmetEΔmotAB* strain that can compensate for the lack of FliB. The higher lysine methylation sites in strain *ΔmetEΔmotAB* may affect the bacterial cell's ability to colonize surfaces and acquire nutrients. As for the specific lysine methylation sites in *ΔmetEΔmotAB* strain in several unique proteins including phosphoserine aminotransferase, ATP synthase subunit, HybA, and hydroxyl acid dehydrogenase, it suggested they are methylase-dependent and they must be motility-related proteins. A comparison of peptides from all strains shows that the strain *ΔmetEΔmotAB* has these lysine methylation sites, that are not present in the *ΔmetE* nor *ΔmetEΔfliB* strain. The absence of motAB genes involved in flagellar motility could alter the intracellular environment and affect the activity of methyltransferases that act on these proteins. Additionally, two specific methylation sites in the *ΔmetEΔfliB* strain that are not present in the *ΔmetE* and *ΔmetEΔmotAB* strains, including a lysine methylation site in the SecY subunit and an arginine-methylation site in the Type III restriction endonuclease subunit.

### IV.2.3 Alignment of the methylated peptide sequences

By alignment of the peptide sequences of FljB and FliC with the sequences containing methylation sites matching the Big-1 domains (Horstmann et al., 2020), most of them obtained consensus methylation sites as shown in **Table IV-1**. The Big-1 domain was noted as crucial bacterial pathogenicity mediating host-cell invasion or adherence. A large number of methylation sites in the identified FljB and FliC, suggesting a similar role for bacterial flagellins in strain *ΔmetE*, *ΔmetEΔfliB* and *ΔmetEΔmotAB*. The highest number of methylation site matching the Big-1 domain in strain *ΔmetEΔmotAB* also demonstrates that the motAB did

not affect bacterial invasion or adherence, on the contrary, *ΔmotAB* promote bacterial adherence and invasion.

**Table Ⅳ-1 The methylation sites matching the Big-1 domain aligned with the previous profile**

| Site | Sequence | Methylation type | Strain *ΔmetE* | Strain *ΔmetEΔmotAB* | Strain *ΔmetEΔfliB* |
|---|---|---|---|---|---|
| FljB | DTPAVVSADA**K** | MML | 3 | 7 | 2 |
| | YFVTIGGFTGADAA**K** | MML | 0 | 3 | 0 |
| | AATGGTNGTASVTGGAV**K** | MML | 1 | 3 | 2 |
| | YYAADYDEATGAIKA**K** | MML | 2 | 13 | 3 |
| | AQPELAEAAA**K** | MML | 3 | 7 | 7 |
| | NALIAGGVDATDANGAELV**K** | MML | 1 | 5 | 1 |
| | AYANNGTTLDVSGLDDAAI**K** | MML | 1 | 3 | 1 |
| | TAANQLGGVDG**K**TEVVTIDGK | MML | 0 | 2 | 1 |
| | NGDYEVNVATDGTVTLAAGAT**K** | MML | 0 | 11 | 0 |
| | TTENPLQ**K**IDAALAQVDALR | MML | 0 | 1 | 0 |
| | TTSYTAADGTT**K**TAANQLGGVDGK | MML, DML | 4 | 12 | 4 |
| FliC | NVQVANADLTEA**K** | MML | 0 | 1 | 0 |
| | AALTAAGVTGTASVV**K** | MML | 1 | 4 | 1 |
| | YTADDGTS**K**TALNK | MML | 0 | 3 | 0 |
| | LGGADG**K**TEVVSIGGK | MML | 0 | 1 | 0 |
| | AQPDLAEAAATTTENPLQ**K** | MML | 0 | 2 | 0 |
| | VTVTGGTG**K**DGYYEVSVDK | MML | 0 | 2 | 0 |
| | DGSISINTT**K**YTADDGTSK | MML | 0 | 2 | 1 |

The methylated lysine of each sequence is indicated in red, in bold. The consensus peptides and sites were highlighted in yellow frames.

Alignment of all the identified methylated peptide sequences of strain *ΔmetE* obtained from Tri-6 beads and high pH SCXtip enrichment strategies, no TML sites were found, which verified our hypothesis that there are indeed no TML sites in strain *ΔmetE* as described in Chapter Ⅲ. Especially, 6 lysine methylation sites associated with 4 methylation events appeared only in the methylated peptides from Tri6-beads enrichment, including mono-methylation in peptides “TIEGGYAL**K**”, “AATGGTNGTASVTGGAV**K** “and “NGDYEVNVATDGTVTLAAGAT**K**” in flagellin FljB and di-methylation in peptide “LLASQ**K**DR “in isochorismate synthase. Except for these unique lysine methylation sites, compared to the methylation sites in this study, 65.5% of lysine methylation sites were identified through Tri-6 enrichment, which illustrates that

our method using Tri-6-beads is complementary to high pH SCXtips meth for enriching methylated peptides.

Additionally, the peptides with the same sequence but different methylation forms from strain *ΔmetE* were enriched by high pH SCXtips and identified in this study. In our dataset, two methylation forms including mono- and di-methylation were simultaneously identified on 19 lysine residues in FljB, EF-Tu, and 50S ribosomal protein L7/L12 (**Figure IV-6**), which was more than from Tri6-beads enriched.

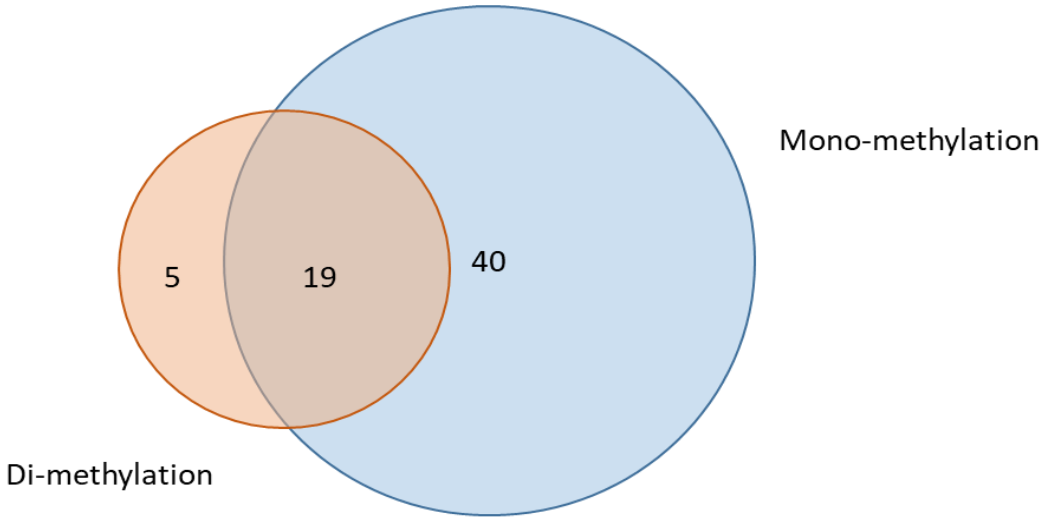


**Figure IV-6 Overlap of identified mono- and di-methylated lysine sites in strain *ΔmetE***

## IV.3 Conclusions

In summary, the high pH SCXtips approach was developed to enrich methylated peptides from digested proteins of *S.* Typhimurium *ΔmetE*, *ΔmetEΔmotAB*, and *ΔmetEΔfliB* strains. Compared to our previously developed enrichment strategy using Tri-6, only partial results were obtained for methyl proteomics analyses. A total of 19 methylated proteins, 59 methylation sites in *ΔmetE*, 134 methylation sites in *ΔmetEΔmotAB* and 46 sites in *ΔmetEΔfliB* were identified. Methylation events that happened to Lys or Arg in the strains could be related to some corresponding gene regulation to flagellar motility and virulence-associated functions. A lot of flagellin FljB and FliC performing methylation are FliB-independent, suggesting that the methylation of flagella is not strictly controlled by methylase encoded by FliB gene.

# Chapter V Discussion and Perspectives

*S*. Typhimurium is a pathogenic bacterium that causes salmonellosis, a common foodborne illness. It possesses several virulence factors that enable it to colonize and cause disease in the host. Among them, T3SS is a specialized apparatus that allows the bacterium to inject effector proteins directly into the host cells, enabling the bacterium to survive and replicate. Additionally, various adhesins such as fimbriae, pili, and outer membrane proteins, can help bacteria attach to and invade host cells. Notably, the flagella of *S*. Typhimurium play a critical role in bacterial virulence by moving and surface-sensing the environmental stimuli. Therefore, understanding the mechanisms of *Salmonella spp*. mechanosensing could provide insights to develop novel strategies for combating *Salmonella* infections.

During bacterial chemotaxis, the methyltransferase CheR regulates the activities of the corresponding chemoreceptors CheA and CheW (Levit, Liu and Stock, 1998) and negatively regulates the kinase sensors and response regulators PhoQ and PhoP (Su *et al.*, 2021). These mechanisms ensure that *S*. Typhimurium responds to attractants or repellents. Methylation of the receptors is associated with an increased tendency of the flagellar motor to rotate from CCW to CW state (Blair, 1995; Sourjik and Wingreen, 2012). When the bacteria adhere to the surface, the cells move toward the surface, attach to the substrate with flagella and T4P, and ultimately initiate biofilm formation (Karmakar, 2021). Moreover, the methyltransferase FliB is involved in the methylation of the filament proteins by modifying FliC and FljB. FliB-dependent methylations have been shown to facilitate adhesion to surface-exposed hydrophobic molecules and thus invasion of epithelial cells (Horstmann *et al.*, 2020). Up to date, FliB has been only described to methylate the flagellins FliC and FljB. Nothing is known about other proteins modified by FliB in *S*. Typhimurium so far. To answer this question and to study the relationship between lysine methylation and bacterial mechanosensing, more specific methods to enrich methylated proteins were required.

In this thesis, we have developed a new tool targeting methyllysine to enrich methylated proteins from *S*. Typhimurium and its mutants and used an existing strategy (high pH SCXtips) to justify this work. Firstly, for specific aptamers selection, MML, DML and TML were used as targets. We chose methylated lysines (MML, DML, and TML, respectively) as target rather than synthesised peptides or whole proteins. This deliberated choice was made because no

prior knowledge about methylated peptides or proteins was known for *Salmonella spp.* and no data was available for related bacterial species. However, the synthesised peptides containing amino acid residues with PTM have been used in the past with success to select acetylated proteins aptamers (Williams *et al*., 2009). But no synthesised peptides associated with methylated lysines have been used so far. Moreover, some aptamers against other PTMs, such as glycan-targeted aptamers, have been obtained successfully to identify glycopeptides and glycosylation sites with magnetic bead-based SELEX as well (Li *et al*., 2008). Finally, the choice of using only methylated lysines to select aptamers was motivated by one study describing aptamers able to discriminate two molecules only with one methyl group (Jenison *et al.*, 1994). Even if the authors of this work used RNA instead of a DNA library, the better stabilities of DNA aptamers led to our choice.

*In vitro* selection of aptamers by FluMag-SELEX implies the immobilization of a soluble target on a surface (Stoltenburg, Reinemann and Strehlitz, 2005), here magnetic beads. The bad side of this method could be masking the potential targeted sites (methyl groups). Likewise, if choosing to immobilize the aptamers could lead to altering their native conformations in comparison to their free states in solution. However, this methodology is amenable to common laboratory practices. Our strategy involving modified amino acids as targets coated on beads during the selection process, can avoid this conformation drawback. Furthermore, we employed the carboxylic function to immobilize the targets to ensure the best exposition of the methyl group(s).

The buffers were with low concentrations of $Mg^{2+}$, $K^{+}$, and $Ca^{2+}$ to mimic physiological conditions. To greatly reduce non-specific absorption to wash away the unbound and the weakly bound particles from the selection pool as much as possible, a buffer containing 0.02% Tween 20 was used (Cho *et al.*, 2006). In this thesis, we have used the elution buffer containing 3.5 M urea and an 80°C treatment to separate the binding DNA sequences from the beads (Stoltenburg, Reinemann and Strehlitz, 2005). Salt composition and concentration, pH, temperature and incubation time were similar to the conditions described in Stoltenburg *et al*. While it worked for other teams, our targets were not the same and these conditions could have induced bias during our selection. In the future, systematic work should be performed including an easy way to test different conditions and their impacts on the aptamer selections. It could be performed by incubating the library in several conditions and

then sequenced by next-generation sequencing (NGS), a tool becoming more available but still with a non-negligible cost. Such a technology allows to check the convergence of consensus sequences during the selection process (Miller *et al*., 2010; Blind and Blank, 2015).

Within this project, we utilized negative selection rounds to eliminate sequences that bind to unwanted targets by exposing the aptamer library to naked beads (without target molecules). For instance, Kolovskaya *et al*. performed a selection of DNA aptamers for *S*. Typhimurium or *S. enteritidis via* Cell-SELEX by starting with a negative selection (Kolovskaya *et al.*, 2013). Several examples showed that multiple negative rounds were performed alternatively with positive selection (Li *et al.*, 2020) or repeated negative cycles were performed (Stoltenburg, Reinemann and Strehlitz, 2005). The decision of whether to perform only one round or multiple rounds of negative selection depends on various factors such as the complexity of the target molecule and the size of the library. In our case, the targets MML, DML and TML are structurally simple molecules, and the oligonucleotide library is only 66nt in length. Therefore, performing only one round of negative selection has been considered sufficient to remove unspecific binders. Nonetheless, to strengthen our selection, the pressure was increased by adding 0.1 mg/ml free lysine including L-lysine in the buffer during the penultimate round. 10% (2/20) and 11% (2/18) redundancy of the selected DNA sequences were obtained respectively for MML and DML through 5 rounds of positive selections including free L-lysine pressure and one round of negative selection. Nevertheless, more selection rounds including more negative rounds during the SELEX procedure would have helped us to gain more aptamer candidates. Notably, the result of 33% (6/18) redundancy of aptamers against TML obtained after only 3 rounds of positive selections and one of negative selection is surprising but could be explained by a higher impact of the selection pressure induced by L-lysine when TML is the target, due to higher capacity of TML to form H bonds when compared with MML, DML, or even unmethylated lysine. Moreover, the size and hydrophobicity of the target increase during the lysine methylation process (Luo, 2018), which also is in favour of a successful selection.

After several rounds of positive selections and one round of negative selection against MML, DML, and TML, aptamer candidates Mono-11, Di-4 and Tri-6 were isolated from 20 colonies for further characterizations. Because higher redundancy of the selected oligonucleotide pools was obtained for TML, the affinity and specificity of the selected aptamer Tri-6 were

first assessed by ITC. This technique is one of the most used for affinity detection to characterize interaction with small molecules. However, the $K_D$ value of Tri-6 and its negative control are close (27.16 ± 9.53 µM and 26.32±10.24 µM, respectively), indicating a low specificity between Tri-6 and TML. On the contrary, bead-based assays using biotinylated Tri-6-beads and Tri-Ctrl-beads validated the specificity of Tri-6, and allowed us to evaluate the affinity with a $K_D$ of 2.48±0.14 mM. The discrepancies between these two methods can be attributed to the Tri-6 free state while performing ITC in comparison to the conjugated state with the bead experiments for mass spectrometry detection. It's more appropriate to measure the affinity in the same state than during the selection. Notably, selection using immobillized ssDNA libraries rather than target molecules on a matrix could achieve higher affinity in some cases, for example for small molecules such as metal ions (Cd, Zn, etc.) without enough sites for immobilization (Wu *et al*., 2014). In addition, the weak affinity makes affinity quantification challenging. The use of different approaches to quantify this affinity could be performed in the future with SPR, MST, or competitive ELISA to improve the measurements. Some optimizations of the sequence based on bioinformatic approaches could improve Tri-6 affinity, likewise, buffers and other experimental conditions (Ducongé, 2022).

Nevertheless, focusing only on the high redundancy sequences may lead to the loss of highly selective aptamer candidates that are present in low abundance (Quang, Perret and Ducongé, 2016). The full sequencing data analyses can help to gain more information on the diversity of aptamer pools by not neglecting low-abundance aptamer sequences. Thus, characterization studies of Mono-11 and Di-4 and other aptamers obtained from the selected oligonucleotide pools in Figure II-8A, Figure II-9A, and Figure II-10A can be performed to gain more options for specific aptamers against MML, DML, and TML. However, considering the time to be devoted to the other part of the project, this part of the work was not approached and will be the subject of future projects.

To test whether the selected Tri-6 can recognize methylation sites in bacteria or human cells, the aptamer-based tool was then applied to complex protein mixes. Applications of aptamers for protein detection and purification have been developed over the years based on their unique 3D structure for molecular recognition (Walter, Stahl and Scheper, 2012).

We were not sure if *S*. Typhimurium could harbour any TML, therefore a well-studied cell model as a positive control known to contain a high amount of methyllysine was used, HEK293 cells (Ning *et al.*, 2016; Hartel *et al.*, 2019). 19 methylation sites in *S*. Typhimurium *ΔmetE* from 5 unique proteins and 11 methylation sites in HEK293 cells from 8 unique proteins were identified by Tri-6. A comparison of the binding methylated proteins from Tri-6-beads and naked-beads eluting from a *Salmonella* strain and HEK293 cells suggested that Tri-6 can specifically recognize lysine methylation sites in both cells but at a low level. Compared to previous works (Ning *et al.*, 2016; Hartel *et al.*, 2019), lower enriched methylated proteins were identified by Tri-6. This low efficiency could be imputed to the incubation of entire proteins with the aptamers coated to the beads. For this reason, a new experiment with tryptic peptides from HEK293 was done. We hypothesise that the complex structures of proteins from the crude cell lysates may mask most of the methyllysine sites (Walter, Stahl and Scheper, 2012). The results are in progress and could not be included in this manuscript. Nevertheless, we are expecting the related data to conclude about the efficacity of Tri-6 for the proteins modified with TML.

Besides, several factors that may interfere with optimal aptamer folding when they are immobilized should be considered for future improvements. For example, when aptamers are immobilized at a too high density, their folding can be impacted (Walter, Stahl and Scheper, 2012). To circumvent this limitation, the introduction of a spacer arm such as a carbon chain (C3-C18) or oligothymidine between the aptamer molecule and the solid surface could be considered in future developments (Urmann and Walter, 2020). Furthermore, the concentration of Tri-6 for immobilization could be optimized to ensure sufficient aptamer binding sites with correct folding on the bead surface.

A complementary strategy using high pH SCXtips for the enrichment of methylated peptides from complex cell lysates has been developed recently (Wang and Ye, 2018). This methodology combined hM-SILAC cultivation as used here with the methionine auxotrophy (*metE* mutation) and SCXtips. One of the main drawbacks of this method is the three washing and five elution steps needed for enrichment and purification are particularly laborious. The eluted peptides were then analyzed by proteomic in collaboration with the Institute Pasteur de Lille. Despite the purification steps, many unmethylated peptides were still detected and

required the injection of more simplified fractions, leading to numerous injections and therefore expensive experiments.

The most promising result obtained from the high pH SCXtips experiment is the identification of FliA as a substrate for the methylase FliB. FliB is only known to modify the two flagellins from *Salmonella spp.* FliA is known as an alternative sigma factor ($\sigma^{28}$) specific for flagellar operons (Ohnishi *et al*., 1990). It's therefore possible to have methylation by FliB on FliA which is found on the same operon (Frye *et al*., 2006). FliA, transcribes and regulates class 3 flagellar genes expression, which are proteins required for filament formation, motility, and chemotaxis as follows: FlgMN, FlgKL, FliB, FliC, FliDST, FljBA, MotABcheAW, TarcheRBYZ, Tsr and Aer (Minamino *et al*., 2021). How FliA methylation can influence flagellar synthesis is an existing question to be answered in the future, but FliB mutant has been found to have no impact on flagellar number or length (Horstmann et al., 2020). However, FliA was found *via* only one peptide leading to the question if it's a trustable result or a mistake of the algorithm to identify the peptide. Further work will consist of confirming or not the absence of MML on FliA in *ΔfliB* before pursuing this aspect. Regarding the surface sensing aspect of this work, we tried to compare the methylome of *ΔmetE* and *ΔmetE Δmot AB* as MotAB is needed for flagellar movement which is mandatory for surface sensing by flagellar rotation obstruction (Belas et al., 2014). But because of the verification and improvement needed to obtain more reliable results, we could not reach interpretable data.

Taken together, these strategies after optimization can be promising for methylated protein purification *in vivo*. As a general perspective for this thesis, future works should focus on aptamer optimizations.

# Chapter VI Material and Methods

## VI.1 Materials

### VI.1.1 Chemicals and instruments

L-lysine, $N^{\varepsilon}$-Methyl-L-lysine hydrochloride (MML), $N^{\varepsilon}$,$N^{\varepsilon}$-Dimethyl-L-lysine monohydrochloride (DML), $N^{\varepsilon}$,$N^{\varepsilon}$,$N^{\varepsilon}$-Trimethyllysine hydrochloride (TML), as experimental target or negative control, were purchased from Sigma-Aldrich, France. Pierce™ NHS-activated magnetic beads and streptavidin-coupled magnetic beads (Dynabeads™ M-280 Streptavidin) were obtained from ThermoFisher SCIENTIFIC, France. Chemicals for selection and cell lysate solutions and media, and equipment including ITC instrument, spectrophotometer, gel electrophoresis instrument, HILIC-MS/MS (Aglient Mass Spec Instruments) and sonicator were provided by the GEC lab, UTC. Other chemicals and equipment for peptide purification and desalting were provided by the Unité de glycobiologie structurale et fonctionnelle, Université de Lille. Proteomic analysis was performed by the Proteomics and modified peptides platform (P3M), Institut Pasteur de Lille.

### VI.1.2 Oligonucleotides, primers, and plasmids

The random oligonucleotide library referred to as ‘‘BANK’’, was synthesized by Eurogentec, Belgium. This library consisted of a multitude of ssDNA fragments comprising a central random region of 30 nucleotides (nt) flanked by two specific sequences of 18nt for PCR amplification: 5’-ATACCAGCTTATTCAATT–$N_{30}$-AGATAGTAAGTGCAATCT-3’. Random region ($N_{30}$) of the library was designed with 20%A-25%C-35%G-20%T. Primers that were used for PCR during the aptamer selection process with fluorescein isothiocyanate (FITC) and poly-$dA_{20}$ label (with a hexaethylene glycol (HEGL) chemical spacer) at 5’-end and for cloning with EcoRI site at 5’-end (eurofins, Germany) were listed in **Table VI-1**.

**Table VI-1 Primers for aptamers selection and cloning**

| | Primers | Sequences |
|---|---|---|
| Amplification during FluMag-SELEX | Aptasensfluo | 5’-[FITC] ATACCAGCTTATTCAATT-3’ |
| | AptaantisensAAA | 5’-poly-$dA_{20}$-HEGL-AGATTGCACTTACTATCT-3’ |
| Amplification for cloning | AP10 Eco | 5’-ATACCAGCGAATTCAATT-3’ |
| | AP20Eco | 5’-AGATTGGAATTCCTATCT-3’ |

Note: The yellow frame indicated the EcoRI site in the primer sequences.

The selected oligonucleotides from the last round were amplified with the primers containing modifications with AP10 Eco and AP20 Eco and cloned into the pCR-Blunt vector. The ssDNA with high consensus sequence against TML and its negative control (eurofins, Germany) for its characterization studies were listed in **Table VI-2**.

**Table VI-2 Sequences of aptamers for characterization study**

| Aptamers | Sequences |
|---|---|
| Tri-6 | 5'-ATACCAGCTTATTCAATTTCTAGACTCTTTGTCCCCTCGAGTTTATTTAGATAGTAAGTGCAATCT-3' |
| Tri-Ctrl | 5'-ATACCAGCTTATTCAATTTTGATTCTATCTTTCATGCCATCGTGCTCTAGATAGTAAGTGCAATCT-3' |
| Tri-6-biotin | 5'biotin-ATACCAGCTTATTCAATTTCTAGACTCTTTGTCCCCTCGAGTTTATTTAGATAGTAAGTGCAATCT-3' |
| Tri-Ctrl-biotin | 5'biotin-ATACCAGCTTATTCAATTTTGATTCTATCTTTCATGCCATCGTGCTCTAGATAGTAAGTGCAATCT-3' |

Note: The fragments in blue color are specific sequences for PCR amplification.

## VI.1.3 Bacterial strains and eukaryotic cell lines

All bacterial strains and eukaryotic cell lines used in this thesis are listed in **Table VI-3**.

**Table VI-3 Bacterial strains and eukaryotic cell lines used in this thesis**

| Strain | Genotype | Reference |
|---|---|---|
| *E.coli* TOP10 | Cloning strain | (Vanschoenbeek *et al.*, 2015) |
| *Salmonella enterica* serovar Typhyimurium LT2 | | |
| EM11429 | *ΔmetE*::FKF (*ΔmetE*) | This thesis |
| EM11430 | *ΔmetE ΔfliC* | This thesis |
| EM11431 | *ΔmetE ΔfliB* | This thesis |
| EM11432 | *ΔmetE Δmot AB* | This thesis |
| HEK293 cell line | | (Ning *et al.*, 2016) |

NOTE: EM stands for Erhardt Marc, the professor at Humboldt University of Berlin, who made these mutants for this work.

## VI.1.4 Reagents and solutions

### VI.1.4.1 Buffers for immobilization of NHS-activated beads

- Wash buffer A: ice-cold 1mM HCl
- Coupling buffer: 50 mM borate, pH 8.5
- Wash buffer B: 0.1 M glycine, pH 2.0
- Quenching buffer: 3 M ethanolamine, pH 9.0
- Storage buffer: 50 mM borate with 0.05% sodium azide, pH 8.5

### VI.1.4.2 Buffers for immobilization of M-280 streptavidin beads

- Binding and washing (B&W) buffer (2×): 10 mM Tris-HCl (pH 7.5), 1 mM ethylenediaminetetraacetic acid (EDTA), 2 M NaCl

### VI.1.4.3 Ninihydrin solution

Ninihydrin (0.4 g) and hydrindantin (0.06 g) were dissolved in 15 ml DMSO under a stream of nitrogen gas. After adding 5 ml sodium acetate buffer (4 mol/l, pH 6), the mixture (ninhydrin/DMSO) was bubbled with nitrogen for at least 2 min to obtain the ninhydrin solution. This solution was sealed and stored in a refrigerator (4°C) ready to be used.

### VI.1.4.4 Solutions for FluMag-SELEX

- Binding/selection buffer: 100 mM NaCl, 20 mM Tris-HCl pH 7.6, 2 mM $MgCl_2$, 5 mM KCl, 1 mM $CaCl_2$, 0.02% Tween 20.
- Elution buffer: 40 mM Tris-HCl pH 8, 10 mM EDTA, 3.5 M urea, 0.02% Tween 20.
- 0.25% linear polyacrylamide (Gaillard and Strauss, 1990): 5% acrylamide solution (no bis-acrylamide) in 40 mM Tris-HCl, 20 mM Na acetate, 1 mM EDTA, pH 7.8. 1/100 vol. of 10% ammonium persulfate (m/v) and 1/1000 vol. TEMED (v/v) polymerize for 30 min. When the solution become viscous, precipitate the polymer with 2.5 vol. ethanol, centrifuge, and redissolve the pellet in 20 vol. of water by shaking overnight. Finally, the 0.25% linear polyacrylamide solution was obtained and stored at -20°C.
- TE buffer pH 7.4: 10 mM Tri-HCl pH7.4, 1mM EDTA pH8.0.

### VI.1.4.5 Solutions for bacterial strains and HEK293 cell line

#### VI.1.4.5.1 Solutions for *S.* Typhymurium strains

- Resuspension buffer: 50mM $NH_4HCO_3$, pH 8.2.
- Lysis buffer for enrichment using aptamer-beads: 50 mM $NH_4HCO_3$ (pH 8.2), 1% (v/v) protease inhibitor cocktail (Roche, ref 05056489001).
- Lysis buffer for enrichment using high pH SCXtips: 8 M urea, 50 mM Tris-HCl (pH 7.5), 1% (v/v) Triton X-100, 65 mM dithiothreitol (DTT), 1% (v/v) protease inhibitor cocktail.
- Activation buffer, 10×: 50 mM Tris-HCl (pH 7.6-7.9), 50 mM DTT, 2mM EDTA
- BRUB buffer, 5mM: 5mM acetic acid, 5 mM phosphoric acid, 5 mM boric acid, adjust pH with 1M NaOH for the need of SCXtip buffers.

- Desalting solvents:
  - ➔ a) loading buffer: 1% (v/v) trifluoroacetic acid (TFC)
  - ➔ b) washing buffer: 0.1% (v/v) TFC
  - ➔ c) elution buffer: 80% (v/v) acetonitrile, 0.1% (v/v) TFC
- SCXtip buffers:
  - ➔ a) loading buffer: 60% (v/v) acetonitrile, 40% (v/v) 5 mM BRUB buffer, pH 2.5
  - ➔ b) washing buffer: 80% (v/v) acetonitrile, 20% (v/v) 5 mM BRUB buffer, pH 9
  - ➔ c) elution buffer 1: 60% (v/v) acetonitrile, 40% (v/v) 5 mM BRUB buffer, pH 9
  - ➔ d) elution buffer 2: 60% (v/v) acetonitrile, 40% (v/v) 5 mM BRUB buffer, pH 10
  - ➔ e) elution buffer 3: 60% (v/v) acetonitrile, 40% (v/v) 5 mM BRUB buffer, pH 11
  - ➔ f) elution buffer 4: 30% (v/v) acetonitrile, 70% (v/v) 5 mM BRUB buffer, pH 12
  - ➔ g) elution buffer 5: 5 mM BRUB buffer (pH 12), 1 M NaCl
- RP-HPLC solvents:
  - ➔ a) buffer A: 0.1% (v/v) formic acid
  - ➔ b) buffer B: 80% (v/v) acetonitrile and 0.1% (v/v) formic acid

VI.1.4.5.2 Solutions for HEK293 cell line

- PBS buffer: 8 g/l NaCl, 0.2 g/l KCl, 1.44 g/l $Na_2HPO_4$, 0.245 g/l, $KH_2PO_4$, pH 7.4.
- Lysis buffer: PBS buffer+ 1% (v/v) protease inhibitor cocktail (Roche, ref 05056489001).
- RIPA buffer: 25 mM Tris-HCl (pH 7.6), 150 mM NaCl, 1% NP-40, 1% sodium deoxycholate, 0.5% SDS.

## VI.1.5 Media and supplements

All media and their compositions are listed in **Table VI-4** and were autoclaved before usage. Media supplements are listed in **Table VI-5**. Heat-sensitive components were sterile-filtered by passing them through a 0.22 µm filter and added to the autoclaved medium.

**Table VI-4 Media compositions**

| Medium | Composition (in dd$H_2O$) |
|---|---|
| LB (lysogeny broth) medium | 10 g/l tryptone, 5 g/l yeast extract, 5 g /l NaCl, (15 g/l agar) |
| S.O.C medium | 20 g/l tryptone, 5 g/l yeast extract, 10 mM NaCl, 2.5 mM KCl, 10 mM MgCl2, 10 mM MgSO4, 20 mM glucose |
| M9 minimal medium (for 100 ml) | 10 ml M9 salts (10×) (75.2 g/l $Na_2HPO_4$, 30 g/l $KH_2PO_4$, 5 g/l NaCl, 5 g/l $NH_4Cl$), 10 µl 1 M $CaCl_2$, 200 µl 1 M $MgCl_2$, 2 ml 20% glucose |
| Dulbecco's modified eagle medium (DMEM) | 4 mM L-glutamine, 4500 mg/l glucose, 1 mM sodium pyruvate, 1500 mg/l $NaHCO_3$ |
| hM-SILAC medium | M9 minimal medium, 100 µM L-methionine-(methyl-$^{13}C$, $D_3$), 10% (v/v)dialyzed fetal bovine serum |

**Table VI-5 Supplements used in the medium**

| Supplement | Stock concentration | Final concentration |
|---|---|---|
| Kanamycin | 50 mg/ml | 50 µg/ml |
| D-glucose | 40% (w/v) | 0.2% |
| L-methionine | 250 mM | 200 µM |
| L-methionine-(methyl-$^{13}CD_3$) | 250 mM | 200 µM |
| Fetal bovine serum | | 10% (v/v) |

## VI.2 Aptamer selection and characterization of selected aptamer

### VI.2.1 Immobilization of NHS activated beads

The procedure for methyllysine immobilization was following the manufacturer's instructions (https://www.thermofisher.com/order/catalog/product/fr/en/88826). 150 µl of NHS magnetic beads were mixed with 1 ml of ice-cold wash buffer A. Subsequently, 150 µl of methylated lysine solution (1, 3, 5, 10 mg/ml of methylated lysine) in coupling buffer was added into the beads and incubated for 1-2 h at room temperature on a rotator at 50 rpm. 1 ml of wash buffer B was added to the beads and repeated washing one more time with the wash buffer B, followed by washing with 1 ml of ultrapure water. Then 1 ml of quenching buffer was added to the beads and mixed for 2 h at room temperature on a rotator at 50 rpm. The beads were following washed with 1 ml of purified water and washed with 1 ml of storage

buffer. Finally, the beads were suspended in 300 µl of storage buffer and were stored at 4°C until needed.

The commercial NHS-activated magnetic beads conjugated with optimal concentration of MML, DML, and TML were used for positive selection, while lysine (not methylated) or naked beads were used for negative selections.

### VI.2.2 Immobilization coupling efficiency detection

In order to make the binding sites on the magnetic beads saturated as much as possible with the targets (MML, DML, TML), the binding capacity assays were performed. The immobilization coupling efficiency detection was by Ninhydrin method (Sun *et al.*, 2006). The immobilized efficiency was calculated using the following formula:

$$\text{Immobilized efficiency} = \frac{\text{Total methyllsine} - \text{Leftover methyllysine}}{\text{Total methyllysine}} * 100$$

Methyllysine solution (10, 20, 30, 40, 50 µg/ml, 1 ml) and ninhydrin solution (1 ml) were put in screw-capped test tubes and heated in a boiling water bath for 10 min, respectively. After heating, the tubes were immediately cooled in an ice-bath for 10 min. Then, 5 ml of 50% alcohol was added into each tube and thoroughly mixed with a vortex mixer for 15 sec. Then the reaction mixture was measured at 570 nm to get the absorbance. Two independent experiments duplicated were conducted and the reported values were the means.

### VI.2.3 DNA aptamer selections by FluMag-SELEX

As illustrated in Figure II-1, the selection of DNA aptamer for methyllysine was based on the FluMag-SELEX procedure (Stoltenburg, Reinemann and Strehlitz, 2005, 2007; Stoltenburg, Schubert and Strehlitz, 2015). Before each SELEX round, the oligonucleotides pool was pre-heated in binding/selection buffer. 3 nmol of oligonucleotides library in the first round and, in each of the following rounds, the constant quantity of selected oligonucleotides from the previous round in a total volume of 500 µl binding buffer, respectively, were folded by heating at 90°C for 10 min, immediately cooling at 4°C for 15 min, and a finally with a short incubation (5–8 min) at room temperature before its application in the binding reaction. An aliquot of $1.5\times10^8$ methyllysine-coated NHS magnetic beads and naked NHS magnetic beads were washed five times with binding buffer. Subsequently, the washed magnetic beads were then

re-suspended in the 500 µl of the folded oligonucleotide pool in each round. After incubation of this mixture at 21°C for 2 h with mild shaking at 300 rpm, the unbound oligonucleotides were removed by five washing steps with 500 µl binding buffer, using the magnetic stand to separate the supernatant from the beads. The beads were mixed with 200 µl elution buffer and the bound oligonucleotides were eluted by heating the binding complex at 80°C for 7 min, centrifuging at 13,000 rpm for 15 min and the supernatant was removed with the help of magnetic stand and carried out in triplicate. Subsequently, every 200µl of the eluted oligonucleotides were precipitated by 500 µl of a solution of ethanol containing 6 µl of 0.25% linear polyacrylamide (Gaillard and Strauss, 1990). The precipitated ssDNA was then re-suspended in 20 µl dd$H_2O$ and the amount of recovered ssDNA was quantified using Nano-drop. The eluted ssDNA were amplified in 15 parallel PCR reactions. As a result, dsDNA products were obtained with a fluorescein modification at the 5'-end of the relevant sense strand and a poly-dA20 extension at the 5'-end of the antisens strand. 5% agarose gel was used to monitor the successful amplification and the correct size of the amplified DNA. The different-sized DNA strands of PCR products were separated in a preparative denaturing urea-PAGE (polyacrylamide gel electrophoresis) in TBE buffer to get purified ssDNA.

By using a UV-transilluminator, the fluorescein-labeled DNA strand could be identified and cut. The corresponding DNA strand was eluted from the gel with 3 ml of 2 mM Na-EDTA, 300 mM sodium acetate, pH 7.8, at 80°C for 45 min, with mild shaking at 300 rpm. After centrifugation at 10,000 g for 10 min to remove the gel residues, the supernatant was transferred to a 15 ml tube and then precipitated with 6 ml of ethanol and 100 µl of 0.25% linear polyacrylamide at -80°C for 2h. After centrifugation at 10,000 g for 10 min at 4°C, the supernatant was removed carefully. The pellet was washed with 70% ethanol (v/v) and re-suspended in 50 µl of MQ-water and ready for the next selection round.

From the 2$^{nd}$ to 3$^{rd}$ round for TML (from 2$^{nd}$ to 4$^{th}$ round for MML and DML), around 200 pmol ssDNA was used and transferred in the binding reaction. After centrifugation and magnetic stand, the coated beads were removed from the supernatant and eluted with 200 µl of elution buffer each time. The eluted ssDNA was precipitated with ethanol and re-suspended in 15-20 µl of MQ-water. Subsequently, the eluted ssDNA was amplified with Aptasensfluo and AptaantisensAAA by PCR. The DNA in the different SELEX fractions (binding solution, washing solutions, and solution of DNA eluted from target beads after ethanol precipitation) of each

round was measured and quantified the concentration. In the 3rd round, to enhance the specificity of the selected oligonucleotides for TML (in the 4th round for MML and DML), the selection pressure was increased by adding 0.1 mg/ml free lysine, 0.1 mg/ml other two forms of methyllysines. Additionally, to remove nonspecific binding oligonucleotides, a negative selection step was introduced at the 4th round (for MML and DML at 5th round) with unmodified NHS beads (naked magnetic beads) at 21°C for 30 min. After washing, the coated beads were discarded, and the supernatant was taken out and amplified as described above by PCR reactions with primers containing EcoRI site (AP10 Eco and AP20 Eco). The enrichment of target-specific aptamers was monitored during the selection process by calculating the ratio of eluted DNA after the elution step to the total quantity of oligonucleotides incubated with beads using the following formula:

$$\text{Elution yield of pools} = \frac{\text{Quantity of eluted DNA}}{\text{Total quantity of DNA incubated with beads}} * 100$$

The PCR products were purified with a PCR purification kit and subsequently cloned into the pCR®-Blunt vector using Zero Blunt® PCR Cloning Kit. The resulting recombinant vectors were transformed into *Escherichia coli* TOP10 cells. For each target methylated lysine, 20 clones were picked out and the recombinant plasmids were prepared using the QIAprep Spin Miniprep Kit for further sequencing analysis. The obtained transformants were analyzed using M13 forward primer (M13rev-29) and the sequences were aligned using MultAlin (http://multalin.toulouse.inra.fr/multalin/). The secondary structure analysis was performed by means of the free-energy minimization algorithm according to Zuker (Zuker, 2003) using the DNA folding form in software online *mfold* (http://mfold.rna.albany.edu/?q=mfold) (SantaLucia, 1998; Stoltenburg, Reinemann and Strehlitz, 2005).

### VI.2.4 Isolation and *in vitro* modification of nucleic acids

#### VI.2.4.1 Polymerase Chain Reaction

Each round eluted ssDNA were amplified by polymerase chain reaction (PCR). For construction of PCR reaction, Taq DNA polymerase with 10× PCR Buffer (Roche, France) were used. Standard PCR reactions and cycling conditions are listed in **Table VI-6** and **Table VI-7**. Annealing temperatures were decided by a series of gradient annealing parallels according to

the used oligonucleotide bank. Elongation time were determined according to the DNA template size and DNA polymerase.

**Table VI-6 Standard PCR reaction**

| Component | Final concentration |
|---|---|
| 10×PCR Buffer | 1× |
| Primers each (see Table VI-1) | 0.5 µM |
| 25 mM dNTP mix (5mM each; NEB) | 0.1 mM |
| Taq polymerase (2.5 U) | 0.25 µl |
| ssDNA template | 1-500 ng |
| $ddH_2O$ | ad 25 µl |

**Table VI-7 PCR cycling conditions**

| Cycle* | Taq polymerase |
|---|---|
| 1. Initial denaturing | 5 min, 94°C |
| 2. Denaturing | 30 sec, 94°C |
| 3. Annealing | 45 sec, 47°C |
| 4. Elongation | 1 min, 72°C |
| 5. Final elongation | 7 min, 72°C |
| 6. Hold on at 4°C | |

*Step 2 to step 4 were repeated for 30 cycles.

### VI.2.4.2 Agarose gel electrophoresis

Correct amplification of PCR products was checked by agarose gel electrophoresis. Thus, the DNA products were loaded on a 5% agarose (w/v) TAE gel (40 mM Tris base, 20 mM acetic acid, 1 mM EDTA). The PCR products were mixed with 6× loading dye (NEB) before loading. The mixture was performed in 1× TAE buffer at 100 V for around 30 min. The 100 bp DNA Ladder (ThermoFisher) was used as a marker. Migrated DNA bands were stained with SYBR Safe DNA gel stain (ThermoFisher), observed *via* UV transillumination (Bio-Rad) and analyzed by the Image Lab software (Bio-Rad).

### VI.2.4.3 Separation of dsDNA by denaturing urea-PAGE

It was required to separate the relevant DNA strands from the double-stranded PCR products to get ssDNA for next round SELEX cycle. For this purpose, denaturing urea-PAGE was used

under TBE running buffer (Tris-base 89 mM, boric acid 89 mM, EDTA 2 mM pH8.0), and the fluorescein-labelled DNA strand could be obtained. All PCR products (25 µl) were precipitated with 50 µl of ethanol in the presence of 10 µl of 0.25% linear polyacrylamide at -80°C for 30 min and re-suspended in 60 µl TE buffer, pH 7.4. The obtained solution was mixed with 60 µl of 2x denaturing loading buffer (listed in **Table VI-8**), heated at 95°C for 5 min and subsequently cooled down to room temperature before use. The total 120 µl mixed solution were loaded into 0.75 mm thin denaturing urea-PAGE (listed in **Table VI-9**) with a unique loading hole. The electrophoresis (Bio-Rad) condition was set at 150 V for 10 min and then 200 V for 30 min.

**Table VI-8 2× Denaturing loading buffer**

| Component | Amount (10 ml total) |
|---|---|
| Formamide | 9.5 ml |
| EDTA-KOH, 500 µM, pH 8.0 | 360 µl |
| SDS, 10% (v/v) | 25 µl |
| Bromophenol blue | 5 mg |
| $ddH_2O$ | ad 10 ml |

**Table VI- 9 Denaturing urea-PAGE**

| Component | Amount (total 10 ml) |
|---|---|
| 40% PAA solution (acrylamide: bisacrylamide=29 :1) | 5ml (final 20%) |
| Urea | 5 g (final 7 M) |
| 10× TBE buffer | 1 ml (final 1×) |
| 10% APS (w/v) | 80 µl |
| TEMED | 10 µl |
| Formamide | 2 ml |
| $ddH_2O$ | ad 10 ml |

EDTA: ethylenediaminetetraacetic acid; SDS: sodium dodecyl sulfate; PAA: polyacrylamide gel; APS: ammonium persulfate; TEMED: tetramethylethylenediamine

### VI.2.4.4 Measurement of DNA concentration

DNA was measured by absorbance at 260 nm by a nano-spectrophotometer (NanoDropTM 2000, ThermoFisher). DNA purity was determined according to 260/280 nm and 260/230 nm ratios.

### VI.2.4.5 PCR products purification, molecular cloning, and transformation

Before cloning to the vector, it's necessary to purify and concentrate the PCR products. The PCR products purification was performed using QIAquick PCR Purification Kit (QIAGEN) as described in the user manual. Subsequently, purified blunt-ended PCR products and pCR®-Blunt vector with a 10:1 molar ratio were performed ligation using Zero Blunt® PCR Cloning Kit (Invitrogen) according to the manufacturer's protocol. The ligation reaction and condition are listed in **Table VI-10**. 2 µl of each ligation reaction were transformed directly into *Escherichia coli* TOP10 cells (50-µl vial of One Shot® TOP10 cells). Then the cells were under heat shock at 42°C for 45 sec and subsequently incubated in 250 µl of S.O.C medium for 1 h. The transformed cells were spread on LB plates containing 50 µg/ml kanamycin and incubated overnight at 37°C. The transformants were tested by sequencing of the isolated plasmids.

**Table VI-10 Ligation reaction**

| Component | Volume (10 µl total) |
|---|---|
| pCR®-Blunt vector (25 ng) | 1 µl |
| PCR product (4.71 ng) | 1-5 µl |
| 5× ExpressLink™ T4 DNA Ligase Buffer | 2 µl |
| Sterile water | ad 9 µl |
| ExpressLink™ T4 DNA Ligase (5 U/µl) | 1 µl |

Note: Incubate the ligation reaction at 22°C for 2h, and store the ligations at -20°C until ready for transformation.

### VI.2.4.6 Isolation of plasmids and sequencing

For each target methylated lysine, 20 clones were picked out and cultured in 5 ml of LB medium containing 50 µg/ml kanamycin overnight. The recombinant plasmids were isolated using the QIAprep Spin Miniprep Kit (QIAGEN) as described in the user manual. Finally, the plasmids were performed Sanger sequencing using M13 forward primer (M13rev-29) at Eurofins Scientific (Genomics, Germany). The sequencing results were analyzed using MultAlin (http://multalin.toulouse.inra.fr/multalin/) and online software *mfold* (http://mfold.rna.albany.edu/?q=mfold).

## VI.2.5 Characterization of the selected aptamer

### VI.2.5.1 ITC measurement

The binding interaction was performed between the selected aptamer Tri-6 and TML at 25°C with a Nano-ITC instrument (TA Instruments, Waters). A degassing station (TA Instruments) for degassing and vacuum cleaning, which contacted with ITC instrument. 2.5% Decon 90™ (v/v) in deionized water was used for cleaning the ITC sample cell.

Tri-6/Tri-Ctrl and TML were dissolved in deionized water to prepare stock at 100 µM and 1 mM, respectively. During an experiment, Tri-6 and Tri-Ctrl were diluted into 50 µM final, while TML was diluted into 500 µM final with binding buffer. Before loading the solution into the reference cell, sample cell and syringe, all the solutions need to be degassed. Then a blank run with binding buffer in the reference cell and 500 µM TML in the syringe was performed and subtracted from the experimental run to account for heat of dilution of the TML solution. When the heat signal keeps constant, the reference cell was filled with 350 µl of binding buffer, 350 µl of 50 µM Tri-6/Tri-Ctrl was in sample cell, and 50 µl of 500 µM TML in the syringe was titrated into the sample cell. The first injection of 0.5 µl preceded 20 injections of 2.5 µl. The time interval between injections was 150 s. The syringe rotational speed was 250 rpm. All the parameters here and results were analyzed using ITCRun and NanoAnalyze software (TA Instruments, Waters).

### VI.2.5.2 PCR amplification for interaction characterization

A fresh aliquot of $1\times10^8$ TML-coated NHS magnetic beads mixed with 1 nmol Tri-6 and Tri-Ctrl separately according to the FluMag-SELEX conditions. All incubation steps were performed at room temperature. After the binding reaction, 5 washings with 200 µl binding buffer were performed. The bound aptamers were then eluted by incubating the aptamer–TML complex twice in 200 µl binding buffer containing 0.05% Tween 20 at 80°C for 10 min with mild shaking. The amount of aptamer DNA eluted from the beads was determined by NanoDrop 2000 (Bio-Rad) and then amplified by PCR reactions with primers containing EcoRI site (AP10 Eco and AP20 Eco). The PCR conditions were listed in **Table VI-11** according to the Tm value of the primers. Subsequently, 5% agarose gel was used to monitor the PCR product.

**Table VI-11 PCR cycling conditions**

| Cycle* | Taq polymerase |
|---|---|
| 1. Initial denaturing | 5 min, 94°C |
| 2. Denaturing | 30 sec, 94°C |
| 3. Annealing | 45 sec, 49°C |
| 4. Elongation | 1 min, 72°C |
| 5. Final elongation | 7 min, 72°C |
| 6. Hold on at 4°C | |

*Step 2 to step 4 were repeated for 30 cycles.

### VI.2.5.3 Bead-based binding assays

The individual aptamers with a 5'-biotin label (Tri-6-biotin and Tri-Ctrl-biotin) were pre-heated as described in §VI.2.3 before adding it to the washed beads. Before each assay, a fresh aliquot of $1 \times 10^7$ aptamer-coated M-280 streptavidin beads (Tri-6-coated streptavidin beads and Tri-Ctrl-coated streptavidin beads) was washed three times with 300 µl binding buffer. Subsequently, the incubation of the TML to Tri-6-coated streptavidin beads and Tri-Ctrl-coated streptavidin beads were performed at 21°C for 2h with mild shaking, respectively. The unbound TML was removed by 3 washings and following through three times elution by incubating the binding complexes in 200 µl binding buffer at 80 °C for 10 min with mild shaking. During each binding procedure, the volume of TML, number of washes, and the elution time were kept constant. The concentration of TML eluted from the beads was determined by HILIC-MS/MS detection and calculation using a calibration curve.

To determine the affinity ($K_D$) of the aptamer Tri-6, different concentrations of TML in a range of 0.2–8.0 mM in binding buffer were mixed with a constant number of Tri-6-coated streptavidin beads ($1 \times 10^7$ beads) in individual tubes in order to obtain a significant signal to evaluate binding. On the basis of these data, a saturation curve was obtained and the dissociation constant $K_D$ was calculated by non-linear regression analysis using GraphPad Prism 8 (https://www.graphpad.com/scientific-software/prism/).

### VI.2.5.4 HILIC-MS/MS assays

The amount of TML in washing and elution fractions 200 µl were determined and quantified by HILIC-MS/MS. The mobile phases were composed of water with 0.1% (v/v) trifluoroacetic acid (TFA) (A) and methanol (B) at a flow rate of 0.3 ml/min and with an injection volume of

2 µl. The chromatographic separations were achieved by HILIC chromatography using the Accucore AQ C18 HPLC column under gradient LC conditions. Gradient LC flow started with 98%A-2%B for 2 min, then decreased to 85%A in 3 min and finally turned to 5%A in 10 min followed by 1 min equilibration. Thus, the total chromatographic run time was 15 min. The column was maintained at 30°C.

ESI (+) was used for the mass spectrometric quantification of TML and internal standard caffeine. The acquisition was made in full scan mode between 85 m/z and 275 m/z. A series of TML at 0.1, 0.25, 0.5, 1.0, 2.5, 5, 10, 25, 50 µM were used for in-run calibration. Based on these data, a saturation curve was obtained and the dissociation constant $K_D$ was calculated by non-linear regression analysis using GraphPad Prism 8.0 (https://www.graphpad.com/).

## VI.3 Cultivation of biological material

### VI.3.1 Cultivation and storage of bacteria

All mutant strains were constructed on the *S*. Typhimurium LT2 and lack theMet biosynthetic pathway (Δ*metE*) (Husna *et al.*, 2018) genetic background. *S*. Typhimurium Δ*metE* (EM11429), Δ*metE*Δ*flic* (EM11430), Δ*metE*Δ*fliB* (EM11431), and Δ*metE*Δ*motAB* (EM11432) were pre-cultured in 10 ml of LB broth overnight, and 100 µl of the overnight culture was subcultured into 10 ml of fresh LB broth and grown at 37°C with 180 rpm shaking for 3-4 h until the optical density reaches $OD_{600}$ 0.6-0.8, if not stated otherwise. Then the cultures were transferred to M9 minimal medium containing 100 µM L-methionine or L-methionine-(methyl-$^{13}CD_3$) and grown at 37°C at 180 rpm overnight. The cultured S. Typhimurium strains were stored in LB with 10% glycerol at -80°C.

### VI.3.2 Cultivation and storage of HEK293

HEK293 cells (www.atcc.org), were originally derived from human embryonic kidney (HEK) cells following exposure to sheared fragments of human adenovious type 5 (Ad5) DNA (Thomas and Smart, 2005), grown in tissue culture. HEK293 cells were grown on 80% confluence in 15cm culture dishes in DMEM supplemented with 10% fetal bovine serum, in a humidified 37°C, 5% $CO_2$ incubator, as described in the culture procedure of HEK cells (Ning *et al.*, 2016). Growth media was replaced every 2-3 days. After the cells have detached, they are spun down and resuspended in 80% DMEM supplemented with 15% fetal bovine serum

and 5% DMSO. Then store the cells overnight at -80°C and transfer the vial to liquid nitrogen for a long time.

## VI.4 Protein extraction and analysis

### VI.4.1 Preparation of cell lysate

The first step of proteomic analysis is protein extraction from the cells. The *S*. Typhimurium *ΔmetE*, *ΔmetEΔmotAB*, and *ΔmetEΔfliB* cells were pelleted by centrifugation at 14000 g for 15min at 4°C. The supernatant was removed, and the pellets were resuspended in 10 ml of the resuspension buffer ($NH_4HCO_3$ (50mM), pH 8.2), that contained a protease inhibitors cocktail tablet (Roche, ref. 05056489001) for 10 ml solution. Then break the cells with glass-bead in a bead beater Precellys 24 (VWR, France) with 0.1 mm glass beads, at 6800 rpm, 3×30 sec. Next, the mixture was centrifuged for 20 min at 14000g at 4°C. The supernatant was collected, DTT was added (20 mM final) and the mix was incubated for 2 h at 37°C with gentle agitation. Finally, the protein solution was kept at 4°C.

The cell pellet of HEK293 cells was washed twice with 2 ml PBS (pH 7.4) and centrifuged at 15000 g for 10 min. The supernatant was removed, and the pellets were resuspended in 1.5 ml of the resuspension buffer (PBS+ protease inhibitor). The cells were broken at 3-sec pulse and 3-sec intervals (for 1 min) on ice using 30% power on Sonic Dismembrator 500 w/Bioblock Scientific 75115 Sonicator. Next, the cell debris was centrifuged for 20 min at 15000 g at 4°C. The supernatant was collected and precipitated by adding 5× volume of cold acetone at -20°C overnight followed by two washes with 500 µl of cold acetone as well. The protein pellet was then dissolved in 1 ml of 50 mM $NH_4HCO_3$ and quantified by BCA protein assay kit, as described in Chapter VI.4.4. The DTT (20 mM final) was added to the protein solution and incubated for 2 h at 37°C with gentle agitation. Finally, the crude HEK293 cell lysate was kept at 4°C until needed.

### VI.4.2 TML-containing protein purification by aptamer-beads

The TML-containing proteins were performed through a “pull-down” enrichment procedure as following. 200 µl of the supernatant of *S*. Typhimurium Δ*metE* and HEK293 cell lysates were mixed with 200 µl of Tri-6-coated streptavidin beads suspension, respectively. The capture was performed at continuous gentle rotation overnight at room temperature. After the

incubation, the magnetic beads with the biotinylated aptamer Tri-6 and proteins were pulled down using a magnet. The beads were removed and sequentially washed three times with 200 µl of aptamer binding buffer (see Chapter VI.1.4.4). To elute the bound proteins, the coated beads were re-suspended three times in 100 µl of aptamer binding buffer and treated at 80°C for 10 min. After heat treatment, magnetic beads were pulled down by a magnet. The protein concentrations of the different fractions were measured by BCA assay according to the manufacturer's instructions in Chapter VI.4.4.

Taking into account that heat treatment could destroy the proteins for further MS analysis, we also tried another way to get elution of the immobilized protein, with high salt concentration. After the incubation of biotinylated Tri-6 with M-280 streptavidin beads, the beads were collected and washed three times with 200 µl of resuspension buffer ($NH_4HCO_3$ (50 mM), pH 8.2). To elute the bounded proteins, the beads were incubated (20 min each) with 100 µl of aptamer binding buffer containing 2M $MgCl_2$ at room temperature three times. The eluted fractions were collected and the protein concentrations were measured as described above.

200 µl of naked streptavidin beads suspension were used for the negative control experiments for heat treatment and high salt, respectively. All the washing and elution fractions above were stored at -20°C for further proteomic analyses.

### VI.4.3 SDS-PAGE analysis

The unbound fraction, three washing fractions, and supernatants of bound fractions were analyzed on SDS-PAGE with Coomassie blue staining. In order to separate the protein in a larger range, the sodium dodecyl sulfate-polyacrylamide gel electrophoresis (SDS-PAGE) assay was conducted in the freshly made 4-16.7% N-(2-Hydroxy-1,1-bis (hydroxymethyl) ethyl) glycine (tricine)-SDS-PAGE (see Table **VI-12**) (Schägger and von Jagow, 1987), which was capable of the separation of proteins in the range from 1-100 kDa. Tricine facilitates the separation of low-molecular-mass proteins especially for size at 1-20 kDa, at lower acrylamide concentration than typical glycine-SDS-PAGE systems.

**Table VI-12 Stock solution for SDS-PAGE**

| Buffer | Tris (M) | Tricine (M) | pH | SDS (%) |
|---|---|---|---|---|
| Anode buffer | 0.2 | - | 8.9 | - |
| Cathode buffer | 0.1 | 0.1 | 8.25 | 0.1 |
| Gel buffer | 3.0 | - | 8.45 | 0.3 |
| Acrylamide/bisacrylamide mixture 40% T,3% C | Percentage acrylamide (w/v) | | Percentage bisacrylamide (w/v) | |
| | 37.5 | | 2.5 | |

The short-pore-gel (10×14×0.07 cm) was composed of separating gel overlaid by a spacer gel (2-3 cm) that again was overlaid by the stacking gel (1-2 cm) (see **Table VI-13**). During the SDS-PAGE assay, 20 µl of cell lysate and TML-containing eluted fractions were mixed with 7 µl of 4×SDS-PAGE loading buffer (62.5 mM Tris, 10% Glycerol, 0.05% Bromophenol Blue, 2% SDS and 5% 2-mercaptoethanol) and 20 µL of each mixture was injected into the gel-plate vials. SDS-PAGE electrophoresis was conducted at 150 V for 20 min and then 200 V for 1 h. Precision plus protein™ all blue prestained protein standards (Bio-Rad) worked as a protein marker. Ready Blue™ Protein Gel Stain containing Coomassie blue dye was used to visualize the protein bands and destained with pure water for 30 min.

**Table VI- 13 Composition of separating, spacer and stacking gels**

| Composition | Stacking gel (4% T, 3% C) | "Spacer" gel (10% T, 3% C) | Separating gel (16.5% T, 3% C) |
|---|---|---|---|
| Acrylamide/Bisacrylamide solution (40% T,3% C) | 312.5 µl | 937.5 µl | 3.125 ml |
| Gel buffer | 775 µl | 1.25 ml | 2.5 ml |
| Glycerol | - | - | 1 g |
| 10% APS | 31.25 µl | 37.5 µl | 75 µl |
| $H_2O$ | 2 ml | 1.5 ml | 1 ml |
| Volume final | 3.125 ml | 3.75 ml | 7.5 ml |

Note: T denotes the total percentage concentration of both acrylamide and bisacrylamide. C denotes the percentage concentration of the crosslinker relative to the total concentration T. 10% APS devotes 10% (v/v) ammonium persulphate solution. TEMED: Tetramethylethylenediamine.

### VI.4.4 Analysis of protein concentration

The BCA assays was used to determine the protein concentrations by performing with a series of bovine serum albumin (BSA) (Bio-Rad) at concentration of 0, 50, 100, 200, 300, 400, 500, 1000 µg/ml to create a calibration curve following the Pierce BCA Protein Assay Kit. The BCA working reagent was composed of Pierce BCA protein assay reagent A and Copper (II) sulfate solution (reagent B) (Thermo Scientific) with a ratio of 50:1 (v/v). 10 µl of protein samples and the standard BSA mixed with 200 µl BCA working reagent in a 96-well plate in duplicates and then incubated at 37°C for 30 min and measured with a spectrophotometer set at 560 nm.

## VI.5 Experimental section for protein enrichment using SCXtips

### VI.5.1 Digestion of the cell lysates of *S*. Typhimurium strains

The *S*. Typhimurium *ΔmetE*, *ΔmetEΔmotAB*, and *ΔmetEΔfliB* cell lysates prepared above were mixed with iodoacetamide (IAA) (40 mM final) and incubated for 30 min in the dark at room temperature. Then the solution was removed to a 10kDa MWCO filter (Sigma-Aldrich, ref. UFC801008) and centrifuged for 15 min at 1,4000g to remove the protease inhibitor in the urea lysis buffer. After three washing with 50mM $NH_4HCO_3$ (pH 8.2), 400 µl of 50mM $NH_4HCO_3$ (pH 8.2) was added to the 10-kDa ultrafiltration tubes to dissolve the proteins and then incubated the proteins with typsin and lysyl endopeptidase (lys-C) (mass spectrometry, ThermoFisher) at an enzyme-to-protein ratio of 1:50 overight at 37°C on the columns. The 10-kDa MWCO filter was then centrifuged for 15 min at 1,4000g and the filtrate was collected in a fresh tube. The filters after two washes with 200 µl of 50mM $NH_4HCO_3$ (pH 8.2), all the filtrates were removed to 10× activation buffer (1× final) with 500 mM $CaCl_2$ (5 mM final) and incubated the lysate mixture with clostripain (arg-C) at an enzyme-to-protein ratio of 1:50 overight at 37°C. Finally, the digested sample was placed on ice with TFA (final 1% (v/v)) to quench the activity of arg-C.

### VI.5.2 Desalting the sample

The tryptic peptides sample obtained above was desalted by Hydrophilic-Lipophilic Balance (HLB) extraction cartridge (60 mg beads, Waters, cat. no. WAT094226) through washing 3 times with 1 ml 0.1% (v/v) TFA and 3 times eluting with 300 µl 80% acetonitrile/0.1% TFA (v/v). Finally, the eluted peptide samples were lyophilized until needed.

### VI.5.3 Preparation of SCXtip

The solution containing solid SCX beads were carefully suspended in methanol and the slurry was transferred to the 200 µl pipet tip which was prepared with degreasing cotton. Then the SCXtip was then washed with 200 µl 5mM BRUB buffer (pH 12) (VI.1.4.5.1) and equilibrated by 3 times washing with 200 µl loading buffer (SCXtip buffers, VI.1.4.5.1). Finally, the tips were stored at 4°C before use.

### VI.5.4 Enrichment of methylated peptides using high pH SCXtips

The dry, desalted peptides samples above were resuspended in 600 µl loading buffer (SCXtip buffers, VI.1.4.5.1). Then the samples were loaded into the prepared SCXtip above and centrifuged at 500g for 30 min to achieve complete binding. After binding, the SCXtips were carried out 3 times washes with 200 µl washing buffer *via* centrifugation at 1000g for 15 min and subsequently 3 times washes with 200 µl different elution buffers (including elution buffer 1, 2, 3, 4, 5) to sequentially elute the peptides. Finally, the each elute was lyophilized and then resolved in 150 µl 1% (v/v) TFA.

The obtained peptides in TFA were then desalted by HLB extraction cartridge (60 mg). All the elutes above were pooled 1-2 together and 3-4-5 together into the HLB cartridge and washed and eluted 3 times with 50 µl 80% acetonitrile/0.1% TFA (v/v) following the desalting procedure as described in § Chapter VI.5.2. Finally, the elutes were combined to around 150 µl into 2 tubes and lyophilized until LC-MS/MS analysis.

### VI.5.5 LC-MS/MS analysis

The Lc-MS/MS system was containing a nano-HPLC Dionex UltiMate 3000 (Thermo Scientific) and a Q-Exactive mass spectrometer. The lyophilized peptides obtained above were dissolved in 20 µl 0.1% TFA (v/v) and loaded into the LC-MS/MS system. Finally, raw MS output data was processed onto MaxQuant computational proteomics platform at http://www.maxquant.org/ for possible peptide sequence database searching.

# References


Abeykoon, A. H. *et al.* (2012) 'Two protein lysine methyltransferases methylate outer membrane protein B from *Rickettsia*', *Journal of Bacteriology*, 194(23), pp. 6410–6418. doi: 10.1128/JB.01379-12.

Agbor, Terence A and Mccormick, B. A. (2011) '*Salmonella* effectors: important players modulating host cell function during infection', *Cellular Microbiology*, 13(12), pp. 1858–1869. doi: 10.1111/j.1462-5822.2011.01701.x.

Ahmad, K. M. *et al.* (2011) 'Probing the limits of aptamer affinity with a microfluidic SELEX platform', *PLoS ONE*, 6(11), pp. 27051–21059. doi: 10.1371/journal.pone.0027051.

Ahirwar, R. and Nahar, P. (2015) 'Development of an aptamer-affinity chromatography for efficient single step purification of Concanavalin A from *Canavalia ensiformis*', *Journal of Chromatography B*, 997, pp. 105–109. doi: 10.1016/j.jchromb.2015.06.003.

Ai, H. W., Lee, J. W. and Schultz, P. G. (2010) 'A method to site-specifically introduce methyllysine into proteins in *E. coli*', *Chemical Communications*, 46(30), pp. 5506–5508. doi: 10.1039/c0cc00108b.

Aizawa, S.-I. (2015) 'Flagella', *Molecular Medical Microbiology*, pp. 125–146. doi: 10.1016/B978-0-12-397169-2.00007-X.

Akira, S., Uematsu, S. and Takeuchi, O. (2006) 'Pathogen recognition and innate immunity', *Cell*, 124(4), pp. 783–801. doi: 10.1016/j.cell.2006.02.015.

Aleksic, S., Heinzerling, F. and Bockemühl, J. (1996) 'Human infection caused by salmonellae of subspecies II to VI in Germany, 1977-1992', *Zentralblatt fur Bakteriologie*, 283(3), pp. 391–398. doi: 10.1016/S0934-8840(96)80074-0.

Allain, F. H. T. *et al.* (2000) 'Solution structure of the two N-terminal RNA-binding domains of nucleolin and NMR study of the interaction with its RNA target', *Journal of Molecular Biology*, 303(2), pp. 227–241. doi: 10.1006/jmbi.2000.4118.

Allerberger, F. *et al.* (2003) 'Occurrence of *Salmonella enterica* serovar Dublin in Austria', *Wiener Medizische Wochenschrift*, 157(7–8), pp. 148–152. doi: 10.1046/j.1563-258x.2003.03015.x.

Ali, M. H., Elsherbiny, M. E. and Emara, M. (2019) 'Updates on aptamer research', *International Journal of Molecular Sciences*, 20(10), pp. 1–23. doi: 10.3390/ijms20102511.

Amartely, H. *et al*. (2018) 'Coupling multi angle light scattering to Ion Exchange chromatography (IEX-MALS) for protein characterization', *Scientific Reports*, 8(1), pp. 1–9. doi: 10.1038/s41598-018-25246-6.

Ambler, R. P. and and Rees, M. W. (1959) 'Epsilon-N-Methyl-lysine in bacterial flagellar protein', *Nature*, 184(4679), pp. 56–57. doi: doi:10.1038/184056b0.

Andino, A. and Hanning, I. (2015) '*Salmonella enterica*: survival, colonization, and virulence differences among serovars', *Scientific World Journal*, 520179, pp. 1–16. doi: 10.1155/2015/520179.

Angel, T. E. et al. (2012) 'Mass spectrometry-based proteomics: existing capabilities and future directions', *Chemical Society Reviews*, 41(10), pp. 3912–3928. doi: 10.1039/c2cs15331a.

Antommattei, F. M., Munzner, J. B. and Weis, R. M. (2004) 'Ligand-specific activation of *Escherichia coli* chemoreceptor transmethylation', *Journal of Bacteriology*, 186(22), pp. 7556–7563. doi: 10.1128/JB.186.22.7556-7563.2004.

Aquino-Jarquin, G. and Toscano-Garibay, J. D. (2011) 'RNA aptamer evolution: two decades

of selection', *International Journal of Molecular Sciences*, 12(12), pp. 9155–9171. doi: 10.3390/ijms12129155.

Armstrong, R. E. and Strouse, G. F. (2014) 'Rationally manipulating aptamer binding affinities in a stem-loop molecular beacon', *Bioconjugate Chemistry*, 25(10), pp. 1769–1776. doi: 10.1021/bc500286r.

Arshavsky-Graham, S. *et al.* (2020) 'Aptamers *vs*. antibodies as capture probes in optical porous silicon biosensors', *Analyst*, 145(14), pp. 4991–5003. doi: 10.1039/d0an00178c.

Azriel, S. *et al.* (2017) 'The Typhi colonization factor (Tcf) is encoded by multiple non-typhoidal *Salmonella serovars* but exhibits a varying expression profile and interchanging contribution to intestinal colonization', *Virulence*, 8(8), pp. 1791–1807. doi: 10.1080/21505594.2017.1380766.

Balamurugan, S. *et al.* (2008) 'Surface immobilization methods for aptamer diagnostic applications', *Analytical and Bioanalytical Chemistry*, 390(4), pp. 1009–1021. doi: 10.1007/s00216-007-1587-2.

Barbier, M. *et al.* (2013) 'Lysine trimethylation of EF-Tu mimics platelet-activating factor to initiate *Pseudomonas aeruginosa pneumonia*', *mBio*, 4(3), pp. 1–8. doi: 10.1128/mBio.00207-13.

Bauer, A. and Kuster, B. (2003) 'Affinity purification-mass spectrometry powerful tools for the characterization of protein complexes', *European Journal of Biochemistry*, 270(4), pp. 570–578. doi: 10.1046/j.1432-1033.2003.03428.x.

Beatson, S. A., Minamino, T. and Pallen, M. J. (2006) 'Variation in bacterial flafellins: from sequence to structure', *Trends in Microbiology*, 14(4), pp. 149–151. doi: 10.1016/j.tim.2006.02.008.

Belas, R. (2014) 'Biofilms, flagella, and mechanosensing of surfaces by bacteria', *Trends in Microbiology*, 22(9), pp. 517–527. doi: 10.1016/j.tim.2014.05.002.

Beloborodov, Stanislav S *et al.* (2018) 'Aptamer facilitated purification of functional proteins', *Journal of Chromatography B*, 1073, pp. 201–206. doi: 10.1016/j.jchromb.2017.12.024.

Bell, R. L. *et al.* (2016) 'Recent and emerging innovations in *Salmonella* detection: a food and environmental perspective', *Microbial biotechnology*, 9(3), pp. 279–292. doi: 10.1111/1751-7915.12359.

Berezovski, M. V *et al.* (2008) 'Aptamer-facilitated biomarker discovery (AptaBiD)', *ACS Publications*, 130(28), pp. 9137–9143. doi: 10.1021/ja801951p.

Besser, J. M. (2018) '*Salmonella* epidemiology: a whirlwind of change', *Food Microbiology*, 71, pp. 55–59. doi: 10.1016/j.fm.2017.08.018.

Bi, S. and Sourjik, V. (2018) 'Stimulus sensing and signal processing in bacterial chemotaxis', *Current Opinion in Microbiology*, 45, pp. 22–29. doi: 10.1016/j.mib.2018.02.002.

Bierschenk, D., Boucher, D. and Schroder, K. (2017) '*Salmonella*-induced inflammasome activation in humans', *Molecular Immunology*, 86, pp. 38–43. doi: 10.1016/j.molimm.2016.11.009.

Biggar, K. K. and Li, S. S. C. (2015) 'Non-histone protein methylation as a regulator of cellular signalling and function', *Nature Reviews Molecular Cell Biology*, 16(1), pp. 5–17. doi: 10.1038/nrm3915.

Bischofberger, M. and van der Goot, F. G. (2008) 'Exotoxin secretion: getting out to find the way in', *Cell Host and Microbe*, 3(1), pp. 7–8. doi: 10.1016/j.chom.2007.12.003.

Bisht, K. *et al.* (2017) 'Twitching motility of bacteria with type-IV pili: fractal walks, first passage time, and their consequences on microcolonies', *Physical Review E*, 96(5), pp. 1–7. doi: 10.1103/PhysRevE.96.052411.

Bjerregaard, N., Andreasen, P. A. and Dupont, D. M. (2016) 'Expected and unexpected features of protein-binding RNA aptamers', *Wiley Interdisciplinary Reviews: RNA*, 7(6), pp. 744–757. doi: 10.1002/wrna.1360.

Blair, D. F. (1995) 'How bacteria sense and swim', *Annual Review of Microbiology*, 49(1), pp. 489–522. doi: 10.1146/annurev.micro.49.1.489.

Blind, M. and Blank, M. (2015) 'Aptamer selection technology and recent advances', *Molecular Therapy - Nucleic Acids*, 4(1), pp. 223–230. doi: 10.1038/mtna.2014.74.

Boehm, A. *et al.* (2010) 'Second messenger-mediated adjustment of bacterial swimming velocity', *Cell*, 141(1), pp. 107–116. doi: 10.1016/j.cell.2010.01.018.

Bonifield, H. R. and Hughes, K. T. (2003) 'Flagellar phase variation in *Salmonella enterica* is mediated by a posttranscriptional control mechanism', *Journal of Bacteriology*, 185(12), pp. 3567–3574. doi: 10.1128/JB.185.12.3567-3574.2003.

Botelho, D. *et al.* (2010) 'Top-down and bottom-up proteomics of SDS-containing solutions following mass-based separation', *Journal of Proteome Research*, 9(6), pp. 2863–2870. doi: 10.1021/pr900949p.

Botting, C. H. *et al.* (2010) 'Extensive lysine methylation in hyperthermophilic crenarchaea: Potential implications for protein stability and recombinant enzymes', *Archaea*, 8(5), pp. 1–6. doi: 10.1155/2010/106341.

Bremang, M. *et al.* (2013) 'Mass spectrometry-based identification and characterisation of lysine and arginine methylation in the human proteome', *Molecular BioSystems*, 9(9), pp. 2231–2247. doi: 10.1039/c3mb00009e.

Brenner, F. W. *et al.* (2000) '*Salmonella* nomenclature', *Journal of clinical microbiology*, 38(7), pp. 2465–2467. doi: 10.1525/abt.2021.83.8.495.

Briegel, A. *et al.* (2012) 'Bacterial chemoreceptor arrays are hexagonally packed trimers of receptor dimers networked by rings of kinase and coupling proteins', *Proceedings of the National Academy of Sciences of the United States of America*, 109(10), pp. 3766–3771. doi: 10.1073/pnas.1115719109.

Broberg, C. A. and Orth, K. (2010) 'Tipping the balance by manipulating post-translational modifications', *Current Opinion in Microbiology*, 13(1), pp. 34–40. doi: 10.1016/j.mib.2009.12.004.

Brody, E. N. and Gold, L. (2000) 'Aptamers as therapeutic and diagnostic agents', *Review in Molecular Biotechnology*, 74(1), pp. 5–13. doi: 10.1016/S1389-0352(99)00004-5.

Bulmer, D. M. *et al.* (2012) 'The bacterial cytoskeleton modulates motility, type 3 secretion, and colonization in *Salmonella*', *PLoS Pathogens*, 8(1), pp. 13–15. doi: 10.1371/journal.ppat.1002500.

Burgos, E. S. *et al.* (2017) 'A simplified characterization of S-adenosyl-L-methionine-consuming enzymes with 1-Step EZ-MTase: a universal and straightforward coupled-assay for *in vitro* and *in vivo* setting', *Chemical Science*, 8(9), pp. 6601–6612. doi: 10.1039/c7sc02830j.

Burnens, A. P. *et al.* (1997) 'The flagellin N-methylase gene fliB and an adjacent serovar-specific IS200 element in *Salmonella typhimurium*', *Microbiology*, 143(5), pp. 1539–1547. doi: 10.1099/00221287-143-5-1539.

Bylda, C. *et al.* (2014) 'Recent advances in sample preparation techniques to overcome difficulties encountered during quantitative analysis of small molecules from biofluids using LC-MS/MS', *Analyst*, 139(10), pp. 2265–2276. doi: 10.1039/c4an00094c.

Cai, S. *et al.* (2018) 'Investigations on the interface of nucleic acid aptamers and binding targets', *Analyst*, 143(22), pp. 5317–5338. doi: 10.1039/c8an01467a.

Cain, J. A., Solis, N. and Cordwell, S. J. (2014) 'Beyond gene expression: the impact of protein post-translational modifications in bacteria', *Journal of Proteomics*, pp. 265–286. doi: 10.1016/j.jprot.2013.08.012.

Cameron, D. M. *et al.* (2004) 'Thermus thermophilus L11 methyltransferase, PrmA, is dispensable for growth and preferentially modifies free ribosomal protein L11 prior to ribosome assembly', *Journal of Bacteriology*, 186(17), pp. 5819–5825. doi: 10.1128/JB.186.17.5819-5825.2004.

Cantoni, G. L. (1975) 'Biological methylation: selected aspects.', *Annual review of biochemistry*, 44(1), pp. 435–451. doi: 10.1146/annurev.bi.44.070175.002251.

Cao, X. J. *et al.* (2010) 'High-coverage proteome analysis reveals the first insight of protein modification systems in the pathogenic spirochete Leptospira interrogans', *Cell Research*, 20(2), pp. 197–210. doi: 10.1038/cr.2009.127.

Cao, X. J., Arnaudo, A. M. and Garcia, B. A. (2013) 'Large-scale global identification of protein lysine methylation *in vivo*', *Epigenetics*, 8(5), pp. 477–485. doi: 10.4161/epi.24547.

Cao, X. J. and Garcia, B. A. (2016) 'Global proteomics analysis of protein lysine methylation', *Current Protocols in Protein Science*, 2016, pp. 24.8.1-24.8.19. doi: 10.1002/cpps.16.

Carabetta, V. J. and Hardouin, J. (2022) 'Editorial: bacterial post-translational modifications', *Frontiers in Microbiology*, 13, pp. 1–2. doi: 10.3389/fmicb.2022.874602.

Carlson, S. M. *et al.* (2014) 'Proteome-wide enrichment of proteins modified by lysine methylation', *Nature Protocols*, 9(1), pp. 37–50. doi: 10.1038/nprot.2013.164.

Carlson, S. M. and Gozani, O. (2014) 'Emerging technologies to map the protein methylome', *Journal of Molecular Biology*, 426(20), pp. 3350–3362. doi: 10.1016/j.jmb.2014.04.024.

Carothers, J. M. *et al.* (2011) 'Model-driven engineering of RNA devices to quantitatively program gene expression', *Science*, 334(6063), pp. 1716–1719. doi: 10.1126/science.1212209.

Catuogno, S. and Esposito, C. L. (2017) 'Aptamer cell-based selection: overview and advances', *Biomedicines*, 5(3), pp. 49–67. doi: 10.3390/biomedicines5030049.

Černý, M. *et al*. (2013) 'Advances in purification and separation of posttranslationally modified proteins', *Journal of Proteomics*, 92, pp. 2–27. doi: 10.1016/j.jprot.2013.05.040.

Chakravortty, D. *et al.* (2005) 'Formation of a novel surface structure encoded by *Salmonella* Pathogenicity Island 2', *EMBO Journal*, 24(11), pp. 2043–2052. doi: 10.1038/sj.emboj.7600676.

Chapuis-hugon, F. *et al.* (2011) 'New extraction sorbent based on aptamers for the determination of ochratoxin A in red wine', *Analytical and Bioanalytical Chemistry*, 400(5), pp. 1199–1207. doi: 10.1007/s00216-010-4574-y.

Chawla, R. *et al.* (2020) 'A skeptic's guide to bacterial mechanosensing', *Journal of Molecular Biology*, 432(2), pp. 523–533. doi: 10.1016/j.jmb.2019.09.004.

Chawla, R., Ford, K. M. and Lele, P. P. (2017) 'Torque, but not FliL, regulates mechanosensitive flagellar motor- function', *Scientific Reports*, 7(1), pp. 5565–5574. doi: 10.1038/s41598-017-05521-8.

Che, Y. *et al.* (2014) 'Load-sensitive coupling of proton translocation and torque generation in the bacterial flagellar motor', *Molecular Microbiology*, 91(1), pp. 175–184. doi: 10.1111/mmi.12453.

Chen, Y. *et al.* (2006) 'Crystal structure of human histone lysine-specific demethlase 1 (LSD1)', *Proceedings of the National Academy of Sciences of the United States of America*, 103(38), pp. 13956–13961. doi: 10.1073/pnas.0606381103.

Cho, E. J. *et al.* (2006) 'Optimization of aptamer microarray technology for multiple protein targets', *Analytica Chimica Acta*, 564(1), pp. 82–90. doi: 10.1016/j.aca.2005.12.038.

Choi, E. W., Nayak, L. V. and Bates, P. J. (2009) 'Cancer-selective antiproliferative activity is a general property of some G-rich oligodeoxynucleotides', *Nucleic Acids Research*, 38(5), pp. 1623–1635. doi: 10.1093/nar/gkp1088.

Chou, K. C. (2020) 'Progresses in predicting post-translational podification', *International Journal of Peptide Research and Therapeutics*, pp. 873–888. doi: 10.1007/s10989-019-09893-5.

Christensen, D. G. *et al.* (2019) 'Post-translational protein acetylation: an elegant mechanism for bacteria to dynamically regulate metabolic functions', *Frontiers in Microbiology*, 10(JULY), p. 1604. doi: 10.3389/fmicb.2019.01604.

Chuh, K. N. and Pratt, M. R. (2015) 'Chemical methods for the proteome-wide identification of posttranslationally modified proteins', *Current Opinion in Chemical Biology*, 24, pp. 27–37. doi: 10.1016/j.cbpa.2014.10.020.

Clare, B. (2021) 'Inflammasome activation by *Salmonella*', *Current Opinion in Microbiology*, 64, pp. 27–32. doi: 10.1016/j.mib.2021.09.004.

Clarke, S. *et al.* (1980) '*In vitro* methylation of bacterial chemotaxis proteins: characterization of protein methyltransferase activity in crude extracts of *Salmonella typhimurium*', *Journal of Supramolecular and Cellular Biochemistry*, 13(3), pp. 315–328. doi: 10.1002/jss.400130305.

Coburn, B., Grassl, G. A. and Finlay, B. B. (2007) '*Salmonella*, the host and disease: a brief review', *Immunology and Cell Biology*, 85(2), pp. 112–118. doi: 10.1038/sj.icb.7100007.

Colgan, A. *et al.* (2013) 'An infection-relevant transcriptomic compendium for *Salmonella enterica* Serovar Typhimurium', *Cell Host & Microbe*, 14(6), pp. 683–695. doi: 10.1016/j.chom.2013.11.010.

Colin, R. and Sourjik, V. (2017) 'Emergent properties of bacterial chemotaxis pathway', *Current Opinion in Microbiology*. Elsevier Ltd, 39, pp. 24–33. doi: 10.1016/j.mib.2017.07.004.

Collinson, S. K. *et al.* (1993) 'Thin, aggregative fimbriae mediate binding of *Salmonella enteritidis* to fibronectin', *Journal of Bacteriology*, 175(1), pp. 12–18. doi: 10.1128/jb.175.1.12-18.1993.

Cooley, B. J. *et al.* (2013) 'The extracellular polysaccharide Pel makes the attachment of *P. aeruginosa* to surfaces symmetric and short-ranged', *Soft Matter*, 9(14), pp. 3871–3876. doi: 10.1039/c3sm27638d.

Cornett, E. M. *et al.* (2018) 'A functional proteomics platform to reveal the sequence determinants of lysine methyltransferase substrate selectivity', *Science Advances*, 4(11), pp. 2623–2634. doi: 10.1126/sciadv.aav2623.

Cornett, E. M. *et al.* (2019) 'Lysine methylation regulators moonlighting outside the epigenome', *Molecular Cell*, 75(6), pp. 1092–1101. doi: 10.1016/j.molcel.2019.08.026.

Craig, L. and Li, J. (2008) 'Type IV pili: paradoxes in form and function', *Current Opinion in Structural Biology*, 18(2), pp. 267–277. doi: 10.1016/j.sbi.2007.12.009.

Cremon, C. *et al.* (2014) '*Salmonella* gastroenteritis during childhood is a risk factor for irritable bowel syndrome in adulthood', *Gastroenterology*, 147(1), pp. 69–77. doi: 10.1053/j.gastro.2014.03.013.

Curran, T. G. *et al.* (2015) 'MARQUIS: a multiplex method for absolute quantification of peptides and posttranslational modifications', *Nature Communications*, 6, pp. 5924–

5935. doi: 10.1038/ncomms6924.
Daems, E. *et al.* (2021) 'Mapping the gaps in chemical analysis for the characterisation of aptamer-target interactions', *TrAC Trends in Analytical Chemistry*, 142, p. 116311. doi: 10.1016/j.trac.2021.116311.
Damton, N. C. *et al.* (2010) 'Dynamics of bacterial swarming', *Biophysical Journal*, 98(10), pp. 2082–2090. doi: 10.1016/j.bpj.2010.01.053.
Darmostuk, M. *et al.* (2015) 'Current approaches in SELEX: an update to aptamer selection technology', *Biotechnology Advances*, 33(6), pp. 1141–1161. doi: 10.1016/j.biotechadv.2015.02.008.
Deditius, J. A. *et al.* (2015) 'Characterization of novel factors involved in swimming and swarming motility in *Salmonella enterica* serovar typhimurium', *PLoS ONE*, 10(8), pp. 1–15. doi: 10.1371/journal.pone.0135351.
Deng, J., Erdjument-bromage, H. and Neubert, T. A. (2020) 'Quantitative comparison of proteomes using SILAC', *Current Protocols in Protein Science*, 95(1), pp. 1–21. doi: 10.1002/cpps.74.
Dembowski, S. K. and Bowser, M. T. (2018) 'Microfluidic methods for aptamer selection and characterization', *Analyst*, 143(1), pp. 21–32. doi: 10.1039/c7an01046j.
Deng, B. *et al.* (2014) 'Aptamer binding assays for proteins: the thrombin example-a review', *Analytica Chimica Acta*, 837, pp. 1–15. doi: 10.1016/j.aca.2014.04.055.
Deiwick, J. and Pettenkofer-institut, M. Von (1999) 'Regulation of virulence genes by environmental signals in *Salmonella typhimurium*', *Electrophoresis*, 20(4–5), pp. 813–817. doi: 10.1002/(sici)1522-2683(19990101)20:4/5%3C813::aid-elps813%3E3.0.co;2-q.
Deribe, Y. L., Pawson, T. and Dikic, I. (2010) 'Post-translational modifications in signal integration', *Nature Structural and Molecular Biology*, 17(6), pp. 666–672. doi: 10.1038/nsmb.1842.
Diepold, A. and Wagner, S. (2014) 'Assembly of the bacterial type III secretion machinery', *FEMS Microbiology Reviews*, 38(4), pp. 802–822. doi: 10.1111/1574-6976.12061.
Dilweg, I. W. and Dame, R. T. (2018) 'Post-translational modification of nucleoidassociated proteins: an extra layer of functional modulation in bacteria?', *Biochemical Society Transactions*, pp. 1381–1392. doi: 10.1042/BST20180488.
Duan, Q. *et al.* (2013) 'Flagella and bacterial pathogenicity', *Journal of Basic Microbiology*, 53(1), pp. 1–8. doi: 10.1002/jobm.201100335.
Ducongé, F. (2020) 'Improvement of aptamers by high-throughput sequencing of Doped-SELEX', *Nucleic Acid Aptamers*, 2570, pp. 85-102. doi: 10.1007/978-1-0716-2695-5_7.
Dufour, Y. S. *et al.* (2014) 'Limits of Feedback Control in Bacterial Chemotaxis', *PLoS Computational Biology*, 10(6), pp. 1–11. doi: 10.1371/journal.pcbi.1003694.
Dufresne, K., Saulnier-Bellemare, J. and Daigle, F. (2018) 'Functional analysis of the chaperone-usher fimbrial gene clusters of *Salmonella enterica* serovar Typhi', *Frontiers in Cellular and Infection Microbiology*, 8, pp. 1–13. doi: 10.3389/fcimb.2018.00026.
Dunham, W. H., Mullin, M. and Gingras, A. C. (2012) 'Affinity-purification coupled to mass spectrometry: basic principles and strategies', *Proteomics*, 12(10), pp. 1576–1590. doi: 10.1002/pmic.201100523.
Dunn, M. R., Jimenez, R. M. and Chaput, J. C. (2017) 'Analysis of aptamer discovery and technology', *Nature Reviews Chemistry*, 1(10), p. 76. doi: 10.1038/S41570-017-0076.
Edwards, T. E. and Ferré-D'Amaré, A. R. (2006) 'Crystal structures of the *thi*-box riboswitch

bound to thiamine pyrophosphate analogs reveal adaptive RNA-small molecule recognition', *Structure*, 14(9), pp. 1459–1468. doi: 10.1016/j.str.2006.07.008.

Eletsky, A. *et al*. (2014) 'Structural and functional characterization of DUF1471 domains of *Salmonella* proteins SrfN, YdgH/SssB, and YahO', *PLoS ONE*, 9(7), pp. 1–15. doi: 10.1371/journal.pone.0101787.

Ellington, A. D. and Szostak, J. W. (1990) '*In vitro* selection of RNA molecules that bind specific ligands', *Nature*, 346(6287), pp. 818–822. doi: 10.1038/346818a0.

Ellington, A. D. (1994) 'RNA Selection: Aptamers achieve the desired recognition recognition', *Current Biology*, 4(5), pp. 427–429. doi: 10.1016/S0960-9822(00)00093-2.

Eng, S. K. *et al.* (2015) '*Salmonella*: a review on pathogenesis, epidemiology and antibiotic resistance', *Frontiers in Life Science*, 8(3), pp. 284–293. doi: 10.1080/21553769.2015.1051243.

Engström, P. *et al.* (2021) 'Lysine methylation shields an intracellular pathogen from ubiquitylation and autophagy', *Science Advances*, 7(26), p. 2517. doi: 10.1126/sciadv.abg2517.

Entzian, C. and Schubert, T. (2016) 'Studying small molecule-aptamer interactions using MicroScale Thermophoresis (MST)', *Methods*, 97(2016), pp. 27–34. doi: 10.1016/j.ymeth.2015.08.023.

Erhardt, M. *et al.* (2011) 'An infrequent molecular ruler controls flagellar hook length in *Salmonella enterica*', *EMBO Journal*, 30(14), pp. 2948–2961. doi: 10.1038/emboj.2011.185.

Evans, M. L. and Chapman, M. R. (2014) 'Curli biogenesis: order out of disorder', *Biochimica et Biophysica Acta - Molecular Cell Research*, 1843(8), pp. 1551–1558. doi: 10.1016/j.bbamcr.2013.09.010.

Falnes, P. Q. *et al.* (2016) 'Protein lysine methylation by seven-β-strand methyltransferases', *Biochemical Journal*, 473(14), pp. 1995–2009. doi: 10.1042/BCJ20160117.

Famulok, M. (1994) 'Molecular recognition of amino acids by RNA-aptamers: an L-citrulline binding RNA motif and its evolution into an L-arginine binder', *Journal of the American Chemical Society*, 116(5), pp. 1698–1706. doi: 10.1021/ja00084a010.

Famulok, M. (1999) 'Oligonucleotide aptamers that recognize small molecules', *Current Opinion in Structural Biology*, 9(3), pp. 324–329. doi: 10.1016/S0959-440X(99)80043-8.

Famulok, M., Hartig, J. S. and Mayer, G. (2007) 'Functional aptamers and aptazymes in biotechnology, diagnostics, and therapy', *Chemical Reviews*, 107(9), pp. 3715–3743. doi: 10.1021/cr0306743.

Famulok, M., Mayer, G. and Blind, M. (2000) 'Nucleic acid aptamers from selection in vitro to applications *in vivo*', *Accounts of Chemical Research*, 33(9), pp. 591–599. doi: 10.1021/ar960167q.

Feagin, T. A., Maganzini, N. and Soh, H. T. (2018) 'Strategies for creating structure-switching aptamers', *ACS Sensors*, 3(9), pp. 1611–1615. doi: 10.1021/acssensors.8b00516.

Feasey, N. A. *et al.* (2012) 'Invasive non-typhoidal salmonella disease: an emerging and neglected tropical disease in Africa', *The Lancet*, 379(9835), pp. 2489–2499. doi: 10.1016/S0140-6736(11)61752-2.

Fei, L. A. N. and Yang, S. H. I. (2009) 'Epigenetic regulation: methylation of histone and non-histone proteins', *Science in Cjina Series C: Life Sciences*, 52(4), pp. 311–322. doi: 10.1007/s11427-009-0054-z.

Flinders, J. *et al.* (2004) 'Recognition of planar and nonplanar ligands in the malachite green-

RNA aptamer complex', *Chembiochem*, 5(1), pp. 62–72. doi: 10.1002/cbic.200300701.
Finlay, B. B. and Brumell, J. H. (2000) '*Salmonella* interactions with host cells: *In vitro* to *in vivo*', *Philosophical Transactions of the Royal Society B: Biological Sciences*, 355(1397), pp. 623–631. doi: 10.1098/rstb.2000.0603.
Forest, K. T. (2019) 'Type IV pili: dynamics, biophysics and functional consequences', *Nature Reviews Microbiology*, 17(7), pp. 429–440. doi: 10.1038/s41579-019-0195-4.
Forier, C. *et al.* (2017) 'DNA aptamer affinity ligands for highly selective purification of human plasma-related proteins from multiple sources', *Journal of Chromatography A*, 1489, pp. 39–50. doi: 10.1016/j.chroma.2017.01.031.
Fournier, M. L. *et al.* (2007) 'Multidimensional separations-based shotgun proteomics', *Chemical Reviews*, 107(816), pp. 3654–3686. doi: 10.1021/cr068279a.
Frost, N. R. *et al.* (2015) 'An in solution assay for interrogation of affinity and rational minimer design for small molecule-binding aptamers', *Analyst*, 140(19), pp. 6643–6651. doi: 10.1039/c5an01075f.
Frye, J. *et al*. (2006) 'Identification of new flagellar genes of *Salmonella enterica* serovar typhimurium', *Journal of Bacteriology*, 188(6), pp. 2233–2243. doi: 10.1128/JB.188.6.2233-2243.2006.
Fuchs, S. M. *et al.* (2011) 'Influence of combinatorial histone modifications on antibody and effector protein recognition', *Current Biology*, 21(1), pp. 53–58. doi: 10.1016/j.cub.2010.11.058.
Fujii, T. *et al.* (2017) 'Identical folds used for distinct mechanical functions of the bacterial flagellar rod and hook', *Nature Communications*, 8(1), p. 14276. doi: 10.1038/ncomms14276.
Fujii, T., Kato, T. and Namba, K. (2009) 'Specific arrangement of α-helical coiled coils in the core domain of the bacterial flagellar hook for the universal joint function', *Structure*, 17(11), pp. 1485–1493. doi: 10.1016/j.str.2009.08.017.
Gaillard, C. and Strauss, F. (1990) 'Ethanol precipitation of DNA with linear polyacrylamide as carrier', *Nucleic Acids Research*, 18(2), p. 378. doi: 10.1093/nar/18.2.378.
Gal-Mor, O. (2019) 'Persistent infection and long-term carriage of typhoidal and nontyphoidal Salmonellae', *Clinical Microbiology Reviews*, 32(1), pp. 1–31. doi: 10.1128/CMR.00088-18.
Galán, J. E. (2021) '*Salmonella* Typhimurium and inflammation: a pathogen-centric affair', *Nature Reviews Microbiology*, 19(11), pp. 716–725. doi: 10.1038/s41579-021-00561-4.
Gale, M. and Yan, Q. (2015) 'High-throughput screening to identify inhibitors of lysine demethylases', *Epigenomics*, 7(1), pp. 57–65. doi: 10.2217/epi.14.63.
Gallagher, S. R. (2012) 'SDS-polyacrylamide gel electrophoresis (SDS-PAGE)', *Current Protocols in Essential Laboratory Techniques*, 2012(SUPPL.6), pp. 1–28. doi: 10.1002/9780470089941.et0703s06.
Galperin, M. Y. and Gomelsky, M. (2013) 'Cyclic di-GMP: the first 25 years of a universal bacterial second messenger', *Microbiology and Molecular Biology Reviews*, 77(1), pp. 1–52. doi: 10.1128/MMBR.00043-12.
Gart, E. V. *et al.* (2016) '*Salmonella typhimurium* and multidirectional communication in the gut', *Frontiers in Microbiology*, 7(22), pp. 1–18. doi: 10.3389/fmicb.2016.01827.
Gast, R. K. *et al.* (2017) 'Colonization of internal organs by *Salmonella* serovars Heidelberg and Typhimurium in experimentally infected laying hens housed in enriched colony cages at different stocking densities', *Poultry Science*, 96(5), pp. 1402–1409. doi:

10.3382/ps/pew375.
Gaucher, S. P. *et al.* (2008) 'Post-translational modifications of *Desulfovibrio vulgaris* hildenborough sulfate reduction pathway proteins', *Journal of Proteome Research*, 7(6), pp. 2320–2331. doi: 10.1021/pr700772s.
Gaviard, C. *et al.* (2019) 'LasB and CbpD virulence factors of *Pseudomonas aeruginosa* carry multiple post-translational modifications on their Lysine residues', *Journal of Proteome Research*, 18(3), pp. 923–933. doi: 10.1021/acs.jproteome.8b00556.
Geiger, A. *et al.* (1996) 'RNA aptamers that bind L-arginine with sub-micromolar dissociation constants and high enantioselectivity', *Nucleic Acid Research*, 24(6), pp. 1029–1036. doi: 10.1093/nar/24.6.1029.
Gerlach, R. G. and Hensel, M. (2007) 'Protein secretion systems and adhesins: the molecular armory of Gram-negative pathogens', *International Journal of Medical Microbiology*, 297(6), pp. 401–415. doi: 10.1016/j.ijmm.2007.03.017.
Gillet, L. C., Leitner, A. and Aebersold, R. (2016) 'Mass spectrometry applied to bottom-up proteomics: entering the high-throughput era for hypothesis testing', *Analytical Chemistry*, 9, pp. 449–472. doi: 10.1146/annurev-anchem-071015-041535.
Gold, L. *et al.* (2012) 'Aptamers and the RNA world, past and present', *Cold Spring Harbor Perspectives in Biology*, 4(3), pp. 1–11. doi: 10.1101/cshperspect.a003582.
Gonzales, A. M., Wilde, S. and Roland, K. L. (2017) 'New insights into the roles of long polar fimbriae and Stg fimbriae in *Salmonella* interactions with enterocytes and M cells', *Infection and Immunity*, 85(9), pp. e00172-17. doi: 10.1128/IAI.00172-17.
González, J. F. *et al.* (2019) 'Human bile-mediated regulation of *salmonella* curli fimbriae', *Journal of Bacteriology*, 201(18), pp. 1–32. doi: 10.1128/JB.00055-19.
González, Y. *et al.* (2010) '$Na^+$- and $H^+$-dependent motility in the coral pathogen *Vibrio shilonii*', *FEMS Microbiology Letters*, 312(2), pp. 142–150. doi: 10.1111/j.1574-6968.2010.02110.x.
Gordon, M. A. *et al.* (2008) 'Epidemics of invasive *Salmonella enterica* serovar enteritidis and *S. enterica* serovar typhimurium infection associated with multidrug resistance among adults and children in Malawi', *Clinical Infectious Diseases*, 46(7), pp. 963–969. doi: 10.1086/529146.
Gordon, V. D. and Wang, L. (2019) 'Bacterial mechanosensing: the force will be with you, always', *Journal of Cell Science*, 132(7), pp. 1–9. doi: 10.1242/jcs.227694.
Gospodinov, A. and Kunnev, D. (2020) 'Universal codons with enrichment from GC to AU nucleotide composition reveal a chronological assignment from early to late along with LUCA formation', *Life*, 10(6), pp. 1–22. doi: 10.3390/life10060081.
Grangeasse, C., Stülke, J. and Mijakovic, I. (2015) 'Regulatory potential of post-translational modifications in bacteria', *Frontiers in Microbiology*, 6, pp. 2014–2015. doi: 10.3389/fmicb.2015.00500.
Granier, S. A. *et al.* (2011) 'ArmA methyltransferase in a monophasic *Salmonella enterica* isolate from food', *Antimicrobial Agents and Chemotherapy*, 55(11), pp. 5262–5266. doi: 10.1128/AAC.00308-11.
Griffith, R. W., Carlson, S. A. and Krull, A. C. (2019) 'Salmonellosis', *Diseases of Swine, Eleventh Edition*. doi: 10.1002/9781119350927.ch59.
Grognot, M. and Taute, K. M. (2021) 'More than propellers: how flagella shape bacterial motility behaviors', *Current Opinion in Microbiology*, 61, pp. 73–81. doi: 10.1016/j.mib.2021.02.005.
Grzymajło, K. *et al.* (2013) 'FimH adhesin from host unrestricted *Salmonella* Enteritidis binds

to different glycoprotein ligands expressed by enterocytes from sheep, pig and cattle than FimH adhesins from host restricted *Salmonella* Abortus-ovis, *Salmonella* Choleraesuis and *Salmonella* Dublin', *Veterinary Microbiology*, 166(3–4), pp. 550–557. doi: 10.1016/j.vetmic.2013.07.004.

Gu, H. *et al.* (2016) 'Graphene oxide-assisted non- immobilized SELEX of okdaic acid aptamer and the analytical application of aptasensor', *Scientific Reports*, 6, p. 21665. doi: 10.1038/srep21665.

Gulig, P. A. (1990) 'Virulence plasmids of *Salmonella typhimurium* and other salmonellae', *Microbial Pathogenesis*, 8(1), pp. 3–11. doi: 10.1016/0882-4010(90)90003-9.

Guo, A. *et al.* (2014) 'Immunoaffinity enrichment and mass spectrometry analysis of protein methylation', *Molecular and Cellular Proteomics*, 13(1), pp. 372–387. doi: 10.1074/mcp. O113.027870.

Günster, R. A. *et al.* (2017) 'SseK1 and SseK3 T3SS effectors inhibit NF-kB signalling and necroptotic cell death in *Salmonella*-infected macrophages', *Cellular Microbiology*, 85(3), pp. 1–18. doi: 10.1128/IAI.00010-17.

Gut, A. M. *et al.* (2018) '*Salmonella* infection – prevention and treatment by antibiotics and probiotic yeasts: a review', *Microbiology society*, 164(11), pp. 1327–1344. doi: 10.1099/mic.0.000709.

Hale, S. P. and Schimmel, P. (1996) 'Protein synthesis editing by a DNA aptamer', *Proceedings of the National Academy of Sciences*, 93(7), pp. 2755–2758. doi: 10.1073/pnas.93.7.2755.

Halici, S. *et al.* (2008) 'Functional analysis of the *Salmonella* pathogenicity island 2-mediated inhibition of antigen presentation in dendritic cells', *Infection and Immunity*, 76(11), pp. 4924–4933. doi: 10.1128/IAI.00531-08.

Hamedani, N. S. *et al.* (2022) 'Aptamer loaded superparamagnetic beads for selective capturing and gentle release of activated protein C', *Scientific Reports*, 12(1), p. 7091. doi: 10.1038/s41598-022-11198-5.

Haneda, T. *et al.* (2012) '*Salmonella* type III effector SpvC, a phosphothreonine lyase, contributes to reduction in inflammatory response during intestinal phase of infection', *Cellular Microbiology*, 14(4), pp. 485–499. doi: 10.1111/j.1462-5822.2011.01733.x.

Hansmeier, N. *et al.* (2017) 'Functional expression of the entire adhesiome of *Salmonella enterica* serotype Typhimurium', *Scientific Reports*, 7(1), pp. 1–12. doi: 10.1038/s41598-017-10598-2.

Hao, L. and Gu, H. (2021) 'Introduction of aptamer, SELEX, and different SELEX variants', *Aptamers for Medical Applications*, pp. 1-30. doi: 10.1007/978-981-33-4838-7.

Harada, K. and Frankel, A. D. (1995) 'Identification of two novel arginine binding DNAs', *The EMBO Jounal*, 14(23), pp. 5798–5811. doi: 10.1002/j.1460-2075.1995.tb00268.x.

Haraga, A., Ohlson, M. B. and Miller, S. I. (2008) 'Salmonellae interplay with host cells', *Nature Reviews Microbiology*, 6(1), pp. 53–66. doi: 10.1038/nrmicro1788.

Hartel, N. G. *et al*. (2019) 'Deep protein methylation profiling by combined chemical and immunoaffinity approaches reveals novel PRMT1 targets', *Molecular and Cellular Proteomics*, 18(11), pp. 2149–2164. doi: 10.1074/mcp.RA119.001625.

Harvey, K. L. *et al.* (2019) 'The diverse functional roles of elongation factor tu (Ef-tu) in microbial pathogenesis', *Frontiers in Microbiology*, 10(OCT), pp. 1–19. doi: 10.3389/fmicb.2019.02351.

Hasegawa, H. *et al.* (2016) 'Methods for improving aptamer binding affinity', *Molecules*, 21(4).

doi: 10.3390/molecules21040421.
Hazelbauer, G. L., Falke, J. J. and Parkinson, J. S. (2008) 'Bacterial chemoreceptors: high-performance signaling in networked arrays', *Trends in Biochemical Sciences*, 33(1), pp. 9–19. doi: 10.1016/j.tibs.2007.09.014.
He, Y. *et al.* (2021) 'An electrochemical impedimetric sensing platform based on a peptide aptamer identified by high-throughput molecular docking for sensitive L-arginine detection', *Bioelectrochemistry*, 137, p. 107634. doi: 10.1016/j.bioelechem.2020.107634.
Hermann, T. and Patel, D. J. (2000) 'Adaptive recognition by nucleic acid aptamers', *Science*, 287(5454), pp. 820–825. doi: 10.1126/science.287.5454.820.
Herold, J. M. *et al.* (2011) 'Small-molecule ligands of methyl-lysine binding proteins', *Journal of Medicinal Chemistry*, 54(7), pp. 2504–2511. doi: 10.1021/jm200045v.
Herr, J. K. *et al.* (2006) 'Aptamer-conjugated nanoparticles for selective collection and detection of cancer cells', *Analytical Chemistry*, 78(9), pp. 2918–2924. doi: 10.1021/ac052015r.
Herrmann, H. and Aebi, U. (2000) 'Intermediate filaments and their associates: multi-talented structural elements specifying cytoarchitecture and cytodynamics', *Current Opinion in Cell Biology*, 12(1), pp. 79–90. doi: 10.1016/S0955-0674(99)00060-5.
Hiraoka, K. D. *et al.* (2017) 'Straight and rigid flagellar hook made by insertion of the FlgG specific sequence into FlgE', *Scientific Reports*, 7(1), p. 46723. doi: 10.1038/srep46723.
Hocher, A. *et al.* (2023) 'Histone-organized chromatin in bacteria', *BioRxiv*, pp. 2023–01. doi: 10.1101/2023.01.26.525422.
Hof, F. (2016) 'Host-guest chemistry that directly targets lysine methylation: synthetic host molecules as alternatives to bio-reagents', *Chemical Communications*, 52(66), pp. 10093–10108. doi: 10.1039/c6cc04771h.
Horng, Y. T. *et al*. (2022) 'A protein containing the DUF1471 domain regulates biofilm formation and capsule production in *Klebsiella pneumoniae*', *Journal of Microbiology, Immunology and Infection*, 55(6P2), pp. 1246–1254. doi: 10.1016/j.jmii.2021.11.005.
Horstmann, J. A. *et al.* (2017) 'Flagellin phase-dependent swimming on epithelial cell surfaces contributes to productive *Salmonella* gut colonisation', *Cellular Microbiology*, 19(8), pp. 1–14. doi: 10.1111/cmi.12739.
Horstmann, J. A. (2017) *The Role of Flagella and Bacterial Motility in Virulence of Salmonella*. doi: 10.1111/cmi.12739.
Horstmann, J. A. *et al.* (2020) 'Methylation of *Salmonella* Typhimurium flagella promotes bacterial adhesion and host cell invasion', *Nature Communications*, 11(1), pp. 1–11. doi: 10.1038/s41467-020-15738-3.
Horváth, P. *et al.* (2019) 'Structure of *Salmonella* flagellar hook reveals intermolecular domain interactions for the universal joint function', *Biomolecules*, 9(9), p. 462. doi: 10.3390/biom9090462.
Hsieh, Y. and The, S. (2008) 'Potential of HILIC-MS in quantitative bioanalysis of drugs and drug metabolites', *Journal of separation science*, 31(9), pp. 1481–1491. doi: 10.1002/jssc.200700451.
Huang, Z. *et al.* (2019) 'Cross talk between chemosensory pathways that modulate', *Molecular Biology and Physiology*, 10(1), pp. 1–15. doi: 10.1128/mBio.02876-18.
Huang, J. *et al.* (2014) 'Enrichment and separation techniques for large-scale proteomics analysis of the protein post-translational modifications', *Journal of Chromatography A*. Elsevier B.V., 1372, pp. 1–17. doi: 10.1016/j.chroma.2014.10.107.

Hui, S. *et al.* (2015) 'Quantitative proteomic analysis reveals a simple strategy of global resource allocation in bacteria', *Molecular Systems Biology*, 11(2), p. 784. doi: 10.15252/msb.20145697.

Humphries, A. D. *et al.* (2003) 'The use of flow cytometry to detect expression of subunits encoded by 11 *Salmonella enterica* serotype Typhimurium fimbrial operons', *Molecular Microbiology*, 48(5), pp. 1357–1376. doi: 10.1046/j.1365-2958.2003.03507.x.

Husna, A. U. *et al.* (2018) 'Methionine biosynthesis and transport are functionally redundant for the growth and virulence of *Salmonella* Typhimurium', *Journal of Biological Chemistry*, 293(24), pp. 9506–9519. doi: 10.1074/jbc.RA118.002592.

Ibrahim, G. M. and Morin, P. M. (2018) '*Salmonella* serotyping using whole genome sequencing', *Frontiers in Microbiology*, 9, pp. 2993–3001. doi: 10.3389/fmicb.2018.02993.

Illangasekare, M. and Yarus, M. (2002) 'Phenylalanine-binding RNAs and genetic code evolution', *Journal of Molecular Evolution*, 54(3), pp. 298–311. doi: 10.1007/s00239.

Inclan, Y. F. *et al.* (2016) 'A scaffold protein connects type IV pili with the Chp chemosensory system to mediate activation of virulence signaling in *Pseudomonas aeruginosa*', *Molecular Microbiology*, 101(4), pp. 590–605. doi: 10.1111/mmi.13410.

Inoue, Y. *et al.* (2019) 'Mutational analysis of the C-terminal cytoplasmic domain of FlhB, a transmembrane component of the flagellar type III protein export apparatus in *Salmonella*', *Genes to Cells*, 24(6), pp. 408–421. doi: 10.1111/gtc.12684.

Iwabata, H., Yoshida, M. and Komatsu, Y. (2005) 'Proteomic analysis of organ-specific post-translational lysine-acetylation and -methylation in mice by use of anti-acetyllysine and -methyllysine mouse monoclonal antibodies', *Proteomics*, 5(18), pp. 4653–4664. doi: 10.1002/pmic.200500042.

Jarrell, K. F. *et al.* (2011) 'Flagella and pili are both necessary for efficient attachment of *Methanococcus maripaludis* surfaces', *FEMS Microbiology Letters*, 319(1), pp. 44–50. doi: 10.1111/j.1574-6968.2011.02264.x.

Javaherian, S. *et al.* (2009) 'Selection of aptamers for a protein target in cell lysate and their application to protein purification', *Nucleic Acids Research*, 37(8), pp. 1–10. doi: 10.1093/nar/gkp176.

Jeddi, I. and Saiz, L. (2017) 'Three-dimensional modeling of single stranded DNA hairpins for aptamer-based biosensors', *Scientific Reports*, 7(1), pp. 1–13. doi: 10.1038/s41598-017-01348-5.

Jenison, R. D. *et al.* (1994) 'High-resolution molecular discrimination by RNA', *Science*, 263(5152), pp. 1425–1429. doi: 10.1126/science.7510417.

Jennings, E., Thurston, T. L. M. and Holden, D. W. (2017) '*Salmonella* SPI-2 Type III Secretion System Effectors: molecular mechanisms and physiological consequences', *Cell Host and Microbe*, 22(2), pp. 217–231. doi: 10.1016/j.chom.207.107.009.

Jijakli, K. *et al.* (2016) 'The *in vitro* selection world', *Methods*, 106, pp. 3–13. doi: 10.1016/j.ymeth.2016.06.003.

Jo, M. *et al.* (2011) 'Development of single-stranded DNA aptamers for specific bisphenol a detection', *Oligonucleotides*, 21(2), pp. 85–91. doi: 10.1089/oli.2010.0267.

Jones, B. B. D., Ghori, N. and Falkow, S. (1994) '*Salmonella typhlrnurium* initiates murine infection by penetrating and destroying the specialized epithelial M Cells of the Peyer' s Patches', *Journal of experimental medicine*, 180(1), pp. 15–23. doi: 10.1084/jem.180.1.15.

Jong, H. K. De *et al.* (2012) 'Host–pathogen interaction in invasive salmonellosis', *PLoS Pathogens*, 8(10), pp. 1–9. doi: 10.1371/journal.ppat.1002933.

Kagambèga, A. *et al.* (2011) 'Prevalence of *Salmonella enterica* and the hygienic indicator *Escherichia coli* in raw meat at markets in Ouagadougou, Burkina Faso', *Journal of Food Protection*, 74(9), pp. 1547–1551. doi: 10.4315/0362-028X.JFP-11-124.

Kampstra, A. S. B. *et al.* (2019) 'Different classes of anti-modified protein antibodies are induced on exposure to antigens expressing only one type of modification', *Annals of the Rheumatic Diseases*, 78(7), pp. 908–916. doi: 10.1136/annrheumdis-2018-214950.

Karmakar, R. (2021) 'State of the art of bacterial chemotaxis', *Journal of Basic Microbiology*, 61(5), pp. 366–379. doi: 10.1002/jobm.202000661.

Kaur, H. (2018) 'General developments in cell-SELEX technology for aptamer selection', *BBA-General Subjects*, 1862(10), pp. 2323–2329. doi: 10.1016/j.bbagen.2018.07.029.

Kawamoto, A. *et al.* (2013) 'Common and distinct structural features of *Salmonella* injectisome and flagellar basal body', *Scientific Reports*, 3(1), p. 3369. doi: 10.1038/srep03369.

Kelly, J. A., Feigon, J. and Yeates, T. O. (1996) 'Reconciliation of the X-ray and NMR structures of the thrombin-binding aptamer d(GGTTGGTGTGGTTGG)', *Journal of Molecular Biology*, 256(3), pp. 417–422. doi: 10.1006/jmbi.1996.0097.

Kettman, J. R., Frey, J. R. and Lefkovits, I. (2001) 'Proteome, transcriptome and genome: top down or bottom up analysis?', *Biomolecular Engineering*, 18, pp. 207–212. doi: 10.1016/S1389-0344(01)00096-X.

Khan, I. H., Reese, T. S. and Khan, S. (1992) 'The cytoplasmic component of the bacterial flagellar motor', *Proceedings of the National Academy of Sciences*, 89(13), pp. 5956–5960. doi: 10.1073/pnas.89.13.5956.

Kim, J. S. *et al.* (2013) 'Molecular characterization of the InvE regulator in the secretion of type III secretion translocases in *Salmonella enterica* serovar Typhimurium', *Microbiology (United Kingdom)*, 159(PART3), pp. 446–461. doi: 10.1099/mic.0.061689-0.

Kim, M. *et al.* (2018) 'Crystal structure of *Bacillus cereus* flagellin and structure-guided fusion-protein designs', *Scientific Reports*, 8(1), pp. 1–10. doi: 10.1038/s41598-018-24254-w.

Kim, S. I. *et al.* (2018) 'Secretion of *Salmonella* pathogenicity island 1-encoded type III secretion system effectors by outer membrane vesicles in *Salmonella enterica* serovar Typhimurium', *Frontiers in Microbiology*, 9, pp. 1–13. doi: 10.3389/fmicb.2018.02810.

Kim, Y. H. *et al.* (2011) 'Identification of trimethylation at C-terminal lysine of pilin in the cyanobacterium Synechocystis PCC 6803', *Biochemical and Biophysical Research Communications*, 404(2), pp. 587–592. doi: 10.1016/j.bbrc.2010.11.133.

Kimbrough, T. G. and Miller, S. I. (2000) 'Contribution of *Salmonella typhimurium* type III secretion components to needle complex formation', *Proceedings of the National Academy of Sciences of the United States of America*, 97(20), pp. 11008–11013. doi: 10.1073/pnas.200209497.

Kimbrough, T. G. and Miller, S. I. (2002) 'Assembly of the type III secretion needle complex of *Salmonella* typhimurium', *Microbes and Infection*, 4(1), pp. 75–82. doi: 10.1016/S1286-4579(01)01512-X.

Kimple, M. E., Brill, A. L. and Pasker, R. L. (2013) 'Overview of affinity tags for protein purification', *Current Protocols in Protein Science*, 9(9), pp. 1–23. doi: 10.1002/0471140864.ps0909s73.

Kirk, M. D. *et al.* (2015) 'World Health Organization estimates of the global and regional disease burden of 22 foodborne bacterial, protozoal, and viral diseases, 2010: a data

synthesis', *PLoS Medicine*, 12(12), pp. 1–21. doi: 10.1371/journal.pmed.1001921.
Kobori, T. *et al.* (2007) 'Applications of isothermal titration calorimetry in RNA biochemistryand biophysics', *Research on Biomolecules*, 87(5-6), pp. 293–301. doi: 10.1002/bip.20816.
Kolovskaya, O. S. *et al.* (2013) 'Development of bacteriostatic DNA aptamers for salmonella', *Journal of Medicinal Chemistry*, 56(4), pp. 1564–1572. doi: 10.1021/jm301856j.
Komarova, N., Barkova, D. and Kuznetsov, A. (2020) 'Implementation of high-throughput sequencing (HTS) in aptamer selection technology', *International Journal of Molecular Sciences*, 21(22), pp. 8774–8796. doi: 10.3390/ijms21228774.
Kontaki, H. and Talianidis, I. (2010) 'Lysine methylation regulates E2F1-induced cell death', *Molecular Cell*, 39(1), pp. 152–160. doi: 10.1016/j.molcel.2010.06.006.
Korobeinikova, A. V., Garber, M. B. and Gongadze, G. M. (2012) 'Ribosomal proteins: structure, function, and evolution', *Biochemistry (Moscow)*, 77(6), pp. 562–574. doi: 10.1134/S0006297912060028.
Krell, T. *et al.* (2011) 'Diversity at its best: bacterial taxis', *Environmental Microbiology*, 13(5), pp. 1115–1124. doi: 10.1111/j.1462-2920.2010.02383.x.
Krembel, A. K., Neumann, S. and Sourjik, V. (2015) 'Universal response-adaptation relation in bacterial chemotaxis', *Journal of Bacteriology*, 197(2), pp. 307–313. doi: 10.1128/JB.02171-14.
Kupakuwana, G. V. *et al.* (2011) 'Acyclic identification of aptamers for human alpha-thrombin using over-represented libraries and deep sequencing', *PLoS ONE*, 6(5), p. 19395. doi: 10.1371/journal.pone.0019395.
Kwon, Y. S., Ahmad Raston, N. H. and Gu, M. B. (2014) 'An ultra-sensitive colorimetric detection of tetracyclines using the shortest aptamer with highly enhanced affinity', *Chemical Communications*, 50(1), pp. 40–42. doi: 10.1039/c3cc47108j.
Lai, H.-C. *et al.* (2014) 'Influenza A virus-specific aptamers screened by using an integrated microfluidic system', *Lab on a Chip*, 14(12), pp. 2002–2015. doi: 10.1039/c4lc00187g.
Lanouette, S. *et al.* (2014) 'The functional diversity of protein lysine methylation', *Molecular Systems Biology*, 10(4), p. 724. doi: 10.1002/msb.134974.
Larock, D. L., Chaudhary, A. and Miller, S. I. (2015) 'Salmonellae interactions with host processes', *Nature Publishing Group*, 13(4), pp. 191–205. doi: 10.1038/nrmicro3420.
Larsen, S. C. et al. (2016) 'Proteome-wide analysis of arginine monomethylation reveals widespread occurrence in human cells', *Science Signaling*, 9(443), pp. 1–15. doi: 10.1126/scisignal.aaf7329.
Lauber, M. A., Running, W. E. and Reilly, J. P. (2009) '*B. subtilis* ribosomal proteins: structural homology and post-translational modifications', *Journal of Proteome Research*, 8(9), pp. 4193–4206. doi: 10.1021/pr801114k.
Lauteri, C. *et al.* (2022) 'Overcoming multidrug resistance in *Salmonella spp*. isolates obtained from the swine food chain by using essential oils: an *in vitro* study', *Frontiers in Microbiology*, 12(9), pp. 1–11. doi: 10.3389/fmicb.2021.808286.
Lee, J. F. *et al.* (2004) 'Aptamer database', *Nucleic Acids Research*, 32(95–100), pp. 95–100. doi: 10.1093/nar/gkh094.
Legiewicz, M. and Yarus, M. (2005) 'A more complex isoleucine aptamer with a cognate triplet', *Journal of Biological Chemistry*, 280(20), pp. 19815–19822. doi: 10.1074/jbc.M502329200.
Lele, P. P., Hosu, B. G. and Berg, H. C. (2013) 'Dynamics of mechanosensing in the bacterial flagellar motor', *Biophysics and Computational biology*, 110(29), pp. 11839–11844. doi:

10.1073/pnas.1305885110.
Levine, H. A. and Nilsen-Hamilton, M. (2007) 'A mathematical analysis of SELEX', *Computational Biology and Chemistry*, 31(1), pp. 11–35. doi: 10.1016/j.compbiolchem.2006.10.002.
Levit, M. N., Liu, Y. and Stock, J. B. (1998) 'Stimulus response coupling in bacterial chemotaxis: receptor dimers in signalling arrays', *Molecular Microbiology*, 30(3), pp. 459–466. doi: 10.1046/j.1365-2958.1998.01066.x.
Levy, D. *et al.* (2011) 'A proteomic approach for the identification of novel lysine methyltransferase substrates', *Epigenetics and Chromatin*, 4(1), pp. 1–12. doi: 10.1186/1756-8935-4-19.
Levy, D. (2019) 'Lysine methylation signaling of non-histone proteins in the nucleus', *Cellular and Molecular Life Sciences*, 76(15), pp. 2873–2883. doi: 10.1007/s00018-019-03142-0.
Li, F. *et al.* (2015) 'Aptamers facilitating amplified detection of biomolecules', *Analytical Chemistry*, 87(1), pp. 274–292. doi: 10.1021/ac5037236.
Li, M. *et al*. (2008) 'Selecting aptamers for a glycoprotein through the incorporation of the boronic acid moiety', *Journal of the American Chemical Society*, 130(38), pp. 12636–12638. doi: 10.1021/ja801510d.
Li, T., Li, B. and Dong, S. (2007) 'Adaptive recognition of small molecules by nucleic acid aptamers through a label-free approach', *Chemistry - A European Journal*, 13(23), pp. 6718–6723. doi: 10.1002/chem.200700068.
Li, W. *et al.* (2020) 'Efficient screening of glycan-specific aptamers using a glycosylated peptide as a scaffold', *Analytical Chemistry*, 93(2), pp. 956–963. doi: 10.1021/acs.analchem.0c03675.
Li, Y. *et al.* (2018) 'Type Ⅰ IFN operates pyroptosis and necroptosis during multidrug-resistant *A. baumannii* infection', *Cell Death and Differentiation*, 25(7), pp. 1304–1318. doi: 10.1038/s41418-017-0041-z.
Li, Y., Geyer, C. R. and Sen, D. (1996) 'Recognition of anionic porphyrins by DNA aptamers', *Biochemistry*, 35(21), pp. 6911–6922. doi: 10.1021/bi960038h.
Li, Y. *et al.* (2020) 'Engineering base-excised aptamers for highly specific recognition of adenosine', *Chemical Science*, 11(10), pp. 2735–2743. doi: 10.1039/d0sc00086h.
Liang, Z. *et al.* (2008) 'Development of pan-specific antibody against trimethyllysine for protein research', *Proteome Science*, 6(2), pp. 4–11. doi: 10.1186/1477-5956-6-2.
Liu, H. *et al.* (2018) 'An oligosorbent-based aptamer affinity column for selective extraction of aflatoxin $B_2$ prior to HPLC with fluorometric detection', *Microchimica Acta*, 185(1), pp. 71–81. doi: 10.1007/s00604-017-2591-7.
Liu, S. *et al.* (2020) 'Recent advances on protein separation and purification methods', *Advances in Colloid and Interface Science*, 284, p. 102254. doi: 10.1016/j.cis.2020.102254.
Liu, H. *et al.* (2013) 'A method for systematic mapping of protein lysine methylation identifies functions for HP1β in DNA damage response', *Molecular Cell*, 50(5), pp. 723–735. doi: 10.1016/j.molcel.2013.04.025.
Lönne, M. *et al.* (2015) 'Development of an aptamer-based affinity purification method for vascular endothelial growth factor', *Biotechnology Reports*, 8, pp. 16–23. doi: 10.1016/j.btre.2015.08.006.
López, F. E. *et al.* (2012) '*Salmonella* Typhimurium general virulence factors: a battle of David against Goliath?', *Food Research International*, 45(2), pp. 842–851. doi:

10.1016/j.foodres.2011.08.009.
Lothrop, A. P., Torres, M. P. and Fuchs, S. M. (2013) 'Deciphering post-translational modification codes', *FEBS Letters*, 587(8), pp. 1247–1257. doi: 10.1016/j.febslet.2013.01.047.
Lowry, R. C. *et al.* (2022) 'Heterogeneous glycosylation and methylation of the *Aeromonas caviae* flagellin', *MicrobiologyOpen*, 11(4), pp. 1–14. doi: 10.1002/mbo3.1306.
Lozupone, C. *et al.* (2003) 'Selection of the simplest RNA that binds isoleucine', *RNA*, 9(11), pp. 1315–1322. doi: 10.1261/rna.5114503.ample.
Luo, M. (2018) 'Chemical and biochemical perspectives of protein lysine methylation', *Chemical Reviews*, 118(14), pp. 6656–6705. doi: 10.1021/acs.chemrev.8b00008.
Luo, Y. *et al.* (2015) 'A hierarchical cascade of second messengers regulates *Pseudomonas aeruginosa* surface behaviors', *mBio*, 6(1), pp. 1–11. doi: 10.1128/mBio.02456-14.
Lupas, A. and Stock, J. (1989) 'Phosphorylation of an N-terminal regulatory domain activates the CheB methylesterase in bacterial chemotaxis', *Journal of Biological Chemistry*, 264(29), pp. 17337–17342. doi: 10.1016/s0021-9258(18)71497-x.
Luu, R. A. *et al.* (2019) 'Hybrid two-component sensors for identification of bacterial chemoreceptor function', *Applied and Environmental Microbiology*, 85(22), pp. 1–21. doi: 10.1128/AEM.01626-19.
Ly, K. T. and Casanova, J. E. (2007) 'Mechanisms of *Salmonella* entry into host cells', *Cellular Microbiology*, 9(9), pp. 2103–2111. doi: 10.1111/j.1462-5822.2007.00992.x.
Lyczak, J. B. and Pier, G. B. (2002) '*Salmonella enterica* serovar Typhi modulates cell surface expression of its receptor, the cystic fibrosis transmembrane conductance regulator, on the intestinal epithelium', *Infection and Immunity*, 70(11), pp. 6416–6423. doi: 10.1128/IAI.70.11.6416-6423.2002.
Lyu, C., Khan, I. M. and Wang, Z. (2021) 'Capture-SELEX for aptamer selection: a short review', *Talanta*, 229, p. 122274. doi: 10.1016/j.talanta.2021.122274.
De Maayer, P. and Cowan, D. A. (2016) 'Flashy flagella: flagellin modification is relatively common and highly versatile among the *Enterobacteriaceae*', *BMC Genomics*, 17(1), pp. 1–13. doi: 10.1186/s12864-016-2735-x.
Macek, B. *et al.* (2019) 'Protein post-translational modifications in bacteria', *Nature Reviews Microbiology*, 17(11), pp. 651–664. doi: 10.1038/s41579-019-0243-0.
Maki-Yonekura, S., Yonekura, K. and Namba, K. (2010) 'Conformational change of flagellin for polymorphic supercoiling of the flagellar filament', *Nature Structural and Molecular Biology*. Nature Publishing Group, 17(4), pp. 417–422. doi: 10.1038/nsmb.1774.
Małecki, J. *et al.* (2016) 'The METTL20 homologue from agrobacterium tumefaciens is a dual specificity protein-lysine methyltransferase that targets ribosomal protein L7/L12 and the β subunit of electron transfer flavoprotein (ETFβ)', *Journal of Biological Chemistry*, 291(18), pp. 9581–9595. doi: 10.1074/jbc.M115.709261.
Mairal Lerga, T. *et al.* (2019) 'High affinity aptamer for the detection of the biogenic amine histamine', *Analytical Chemistry*, 91(11), pp. 7104–7111. doi: 10.1021/acs.analchem.9b00075.
Mairal, T. *et al.* (2008) 'Aptamers: molecular tools for analytical applications', *Analytical and Bioanalytical Chemistry*, 390(4), pp. 989–1007. doi: 10.1007/s00216-007-1346-4.
Malhotra, S. *et al.* (2021) 'Aptamer selection: choosing the appropriate SELEX aptamer', *Indian Journal of Pure & Applied Biosciences*, 9(2), pp. 240–253. doi: 10.18782/2582-2845.8214.
Mandal, M. *et al.* (2003) 'Riboswitches control fundamental biochemical pathways in *Bacillus*

*subtilis* and other bacteria', *Cell*, 113(5), pp. 577–586. doi: 10.1016/S0092-8674(03)00391-X.

Mann, D. *et al.* (2005) '*In vitro* selection of DNA aptamers binding ethanolamine', *Biochemical and Biophysical Research Communications*, 338(4), pp. 1928–1934. doi: 10.1016/j.bbrc.2005.10.172.

Mannironi, C. *et al.* (2000) 'Molecular recognition of amino acids by RNA aptamers: The evolution into an L-tyrosine binder of a dopamine-binding RNA motif', *RNA*, 6(4), pp. 520–527. doi: 10.1017/s1355838200991763.

Majerfeld, I., Puthenvedu, D. and Yarus, M. (2005) 'RNA affinity for molecular L-histidine; genetic code origins', *Genetic Code Origins*, 61(2), pp. 226–235. doi: 10.1007/s00239-004-0360-9.

Marimuthu, C. *et al.* (2012) 'Single-stranded DNA (ssDNA) production in DNA aptamer generation', *Analyst*, 137(6), pp. 1307–1315. doi: 10.1039/c2an15905h.

Mascini, M., Palchetti, I. and Tombelli, S. (2012) 'Nucleic acid and peptide aptamers: fundamentals and bioanalytical aspects', *Angewandte Chemie - International Edition*, 51(6), pp. 1316–1332. doi: 10.1002/anie.201006630.

Mastronardi, E. *et al.* (2021) 'Selection of DNA aptamers for root exudate L-serine using multiple selection strategies', *Journal of Agricultural and Food Chemistry*, 69(14), pp. 4294–4306. doi: 10.1021/acs.jafc.0c06796.

Matilla, M. A. and Krell, T. (2018) 'The effect of bacterial chemotaxis on host infection and pathogenicity', *FEMS Microbiology Reviews*, 42(1), pp. 40–67. doi: 10.1093/femsre/fux052.

Mattingly, A. E. *et al.* (2018) 'Assessing travel conditions: environmental and host influences on bacterial surface motility', *Journal of Bacteriology*, 200(11), pp. 1–39. doi: 10.1128/JB.00014-18.

Maux, S. Le, Nongonierma, A. B. and Fitzgerald, R. J. (2015) 'Improved short peptide identification using HILIC – MS / MS: retention time prediction model based on the impact of amino acid position in the peptide sequence', *Food Chemistry*, 173, pp. 847–854. doi: 10.1016/j.foodchem.2014.10.104.

Mayer, G. (2009) 'The chemical biology of aptamers', *Angewandte Chemie - International Edition*, 48(15), pp. 2672–2689. doi: 10.1002/anie.200804643.

Mcdermott, P. F., Zhao, S. and Tate, H. (2018) 'Antimicrobial resistance in nontyphoidal *Salmonella*', *Microbiology spectrum*, 6(4), pp. 1–26. doi: 10.1128/microbiolspec.ARBA-0014-2017.

McGhie, E. J. *et al.* (2009) '*Salmonella* takes control: effector-driven manipulation of the host', *Current Opinion in Microbiology*, 12(1), pp. 117–124. doi: 10.1016/j.mib.2008.12.001.

Mckeague, M. *et al.* (2015) 'Analysis of *in vitro* aptamer selection parameters', *Journal of Molecular Evolution*, 81(5), pp. 150–161. doi: 10.1007/s00239-015-9708-6.

McKeague, M. and Derosa, M. C. (2012) 'Challenges and opportunities for small molecule aptamer development', *Journal of Nucleic Acids*, 2012, pp. 1–20. doi: 10.1155/2012/748913.

Miller, J. R. *et al*. (2010) 'Assembly algorithms for next-generation sequencing data', *Genomics*, 95(6), pp. 315–327. doi: 10.1016/j.ygeno.2010.03.001.

Minamino, T. and Imada, K. (2015) 'The bacterial flagellar motor and its structural diversity', *Trends in Microbiology*, 23(5), pp. 267–274. doi: 10.1016/j.tim.2014.12.011.

Minamino, T., Imada, K. and Namba, K. (2008) 'Molecular motors of the bacterial flagella', *Current Opinion in Structural Biology*, 18(8), pp. 693–701. doi:

10.1016/j.sbi.2008.09.006.
Minamino, T. *et al*. (2021) 'Multiple roles of flagellar export chaperones for efficient and robust flagellar filament formation in *Salmonella*', *Frontiers in Microbiology*, 12, pp. 1–14. doi: 10.3389/fmicb.2021.756044.
Minamino, T., Yamaguchi, S. and Macnab, R. M. (2000) 'Interaction between fliE and flgB, a proximal rod component of the flagellar basal body of *Salmonella*', *Journal of Bacteriology*, 182(11), pp. 3029–3036. doi: 10.1128/JB.182.11.3029-3036.2000.
Mishra, M., Tiwari, S. and Gomes, A. V (2017) 'Protein purification and analysis: next generation Western blotting techniques', *Expert Review of Proteomics*, 14(11), pp. 1037–1053. doi: 10.1080/14789450.2017.1388167.
Moest, T. P. and Méresse, S. (2013) '*Salmonella* T3SSs: successful mission of the secret(ion) agents', *Current Opinion in Microbiology*, 16(1), pp. 38–44. doi: 10.1016/j.mib.2012.11.006.
Mohammed, S. and Heck, A. J. R. (2010) 'Strong cation exchange (SCX) based analytical methods for the targeted analysis of protein post-translational modifications', *Current Opinion in Biotechnology*, 22(1), pp. 9–16. doi: 10.1016/j.copbio.2010.09.005.
Monack, D. M., Mueller, A. and Falkow, S. (2004) 'Persistent bacterial infections: the interface of the pathogen and the host immune system', *Microbiology open*, 2(9), pp. 747–765. doi: 10.1038/nrmicro955.
Moore, K. E. *et al.* (2013) 'A general molecular affinity strategy for global detection and proteomic analysis of lysine methylation', *Molecular Cell*, 50(3), pp. 444–456. doi: 10.1016/j.molcel.2013.03.005.
Morimoto, Y. V and Minamino, T. (2014) 'Structure and function of the bi-directional bacterial flagellar motor', *Biomolecules*, 4(1), pp. 217–234. doi: 10.3390/biom4010217.
Mosing, R. K. and Bowser, M. T. (2009) 'Isolating aptamers using Capillary Electrophoresis–SELEX (CE–SELEX)', *Nucleic Acid and Peptide Aptamers*, 535, pp. 33–43. doi: 10.1007/978-1-59745-557-2.
Müller, J. B. *et al.* (2020) 'The proteome landscape of the kingdoms of life', *Nature*, 582(7813), pp. 592–596. doi: 10.1038/s41586-020-2402-x.
Murn, J. and Shi, Y. (2017) 'The winding path of protein methylation research: milestones and new frontiers', *Nature Reviews Molecular Cell Biology*, 18(8), pp. 517–527. doi: 10.1038/nrm.2017.35.
Myeni, S. K. and Zhou, D. (2010) 'The C terminus of SipC binds and bundles F-actin to promote *Salmonella* invasion', *Journal of Biological Chemistry*, 285(18), pp. 13357–13363. doi: 10.1074/jbc.M109.094045.
Nagatoishi, S. *et al.* (2011) 'Loop residues of thrombin-binding DNA aptamer impact G-quadruplex stability and thrombin binding', *Biochimie*, 93(8), pp. 1231–1238. doi: 10.1016/j.biochi.2011.03.013.
Nedeljković, M., Sastre, D. E. and Sundberg, E. J. (2021) 'Bacterial flagellar filament: a supramolecular multifunctional nanostructure', *International Journal of Molecular Sciences*, 22(14), p. 7521. doi: 10.3390/ijms22147521.
Neves, M. A. D. *et al.* (2015) 'Ultra-high frequency piezoelectric aptasensor for the label-free detection of cocaine', *Biosensors and Bioelectronics*, 72, pp. 383–392. doi: 10.1016/j.bios.2015.05.038.
Neuhauser, N. *et al.* (2011) 'Andromeda: a peptide search engine integrated into the MaxQuant environment', *Journal of proteome research*, 10(4), pp. 1794–1805. doi: 10.1021/pr101065j.

Nguyen, V. *et al.* (2014) 'Multiple GO-SELEX for efficient screening of flexible aptamers', *Chemical Communications*, 50(72), pp. 10513–10516. doi: 10.1039/C4CC03953J.

Ni, S. *et al*. (2021) 'Recent progress in aptamer discoveries and modifications for therapeutic applications', *ACS Applied Materials and Interfaces*, 13(8), pp. 9500–9519. doi: 10.1021/acsami.0c05750.

Niazi, J. H. *et al.* (2008) 'ssDNA aptamers that selectively bind oxytetracycline', *Bioorganic and Medicinal Chemistry*, 16(3), pp. 1254–1261. doi: 10.1016/j.bmc.2007.10.073.

Nickerson, J. L. *et al.* (2023) 'Recent advances in top-down proteome sample processing ahead of MS analysis', *Mass Spectrometry Reviews*, 42(2), pp. 457–495. doi: 10.1002/mas.21706.

Ning, Z. *et al.* (2016) 'A charge-suppressing strategy for probing protein methylation', *Chemical Communications*, 52(31), pp. 5474–5477. doi: 10.1039/c6cc00814c.

Nuccio, S. and Ba, A. J. (2007) 'Evolution of the chaperone / usher assembly pathway: fimbrial classification goes Greek', *Microbiology and Molecular Biology Reviews*, 71(4), pp. 551–575. doi: 10.1128/MMBR.00014-07.

Nutiu, R. and Li, Y. (2003) 'Structure-switching signaling aptamers', *Journal of the American Chemical Society*, 125(16), pp. 4771–4778. doi: 10.1021/ja028962o.

O'Toole, G. A. and Wong, G. C. L. (2016) 'Sensational biofilms: surface sensing in bacteria', *Current Opinion in Microbiology*, 30(1999), pp. 139–146. doi: 10.1016/j.mib.2016.02.004.

Ohl, M. E. and Miller, S. I. (2001) '*Salmonella*: a model for bacterial pathogenesis', *Annual Review of Medicine*, 52(1), pp. 259–274. doi: 10.1146/annurev.med.52.1.259.

Ohnishi, K. *et al*. (1990) 'Gene fliA encodes an alternative sigma factor specific for flagellar operons in *Salmonella typhimurium*', *Molecular & General Genetics*, 221(2), pp. 139–147. doi: 10.1007/BF00261713.

Ohsawa, K. *et al.* (2008) 'Arginine-modified DNA aptamers that show enantioselective recognition of the dicarboxylic acid moiety of glutamic acid', *Analytical Sciences*, 24(1), pp. 167–172. doi: doi:10.2116/analsci.24.167.

Olsen, J. E. *et al.* (2013) 'The role of flagella and chemotaxis genes in host pathogen interaction of the host adapted *Salmonella enterica* serovar Dublin compared to the broad host range serovar *S*. Typhimurium', *BMC Microbiology*, 67(13), pp. 1–11. doi: 10.1186/1471-2180-13-67.

Olsen, J. V. and Mann, M. (2013) 'Status of large-scale analysis of posttranslational modifications by mass spectrometry', *Molecular and Cellular Proteomics*, 12(12), pp. 3444–3452. doi: 10.1074/mcp.O113.034181.

Olsen, J. V, Ong, S. and Mann, M. (2004) 'Trypsin cleaves exclusively C-terminal to arginine and lysine residues', *Molecular and Cellular Proteomics*, 3(6), pp. 608–614. doi: 10.1074/mcp.T400003-MCP200.

Ong, S. E., Mittler, G. and Mann, M. (2004) 'Identifying and quantifying *in vivo* methylation sites by heavy methyl SILAC', *Nature Methods*, 1(2), pp. 119–126. doi: 10.1038/nmeth715.

Orabi, A. *et al.* (2015) 'An aptamer against the matrix binding domain on the hepatitis B virus capsid impairs virion formation', *Journal of Virology*, 89(8), pp. 9281–9287. doi: 10.1128/JVI.00466-15.

Ortega, D. R. and Zhulin, I. B. (2016) 'Evolutionary genomics suggests that CheV is an additional adaptor for accommodating specific chemoreceptors within the chemotaxis signaling complex', *PLoS Computational Biology*, 12(2), pp. 1–19. doi:

10.1371/journal.pcbi.1004723.
Otto, K. and Silhavy, T. J. (2002) 'Surface sensing and adhesion of *Escherichia coli* controlled by the Cpx-signaling pathway', *Proceedings of the National Academy of Sciences of the United States of America*, 99(4), pp. 2287–2292. doi: 10.1073/pnas.042521699.
Pan, W. and Clawson, G. A. (2009) 'The shorter the better: reducing fixed primer regions of oligonucleotide libraries for aptamer selection', *Molecules*, 14(4), pp. 1353–1369. doi: 10.3390/molecules14041353.
Parry, C. M. and Threlfall, E. J. (2008) 'Antimicrobial resistance in typhoidal and nontyphoidal salmonellae', *Current Opinion in Infectious Diseases*, 21(5), pp. 531–538. doi: 10.1097/QCO.0b013e32830f453a.
Paul, K. *et al.* (2010) 'The c-di-GMP binding protein YcgR controls flagellar motor direction and speed to affect chemotaxis by a "backstop brak" mechanism', *Molecular Cell*, 38(1), pp. 128–139. doi: 10.1016/j.molcel.2010.03.001.
Paul Zolg, D. *et al.* (2018) 'Proteometools: systematic characterization of 21 post-translational protein modifications by liquid chromatography tandem mass spectrometry (lc-ms/ms) using synthetic peptides', *Molecular and Cellular Proteomics*, 17(9), pp. 1850–1863. doi: 10.1074/mcp.TIR118.000783.
Perez-Burgos, L. *et al.* (2003) 'Generation and characterization of methyl-lysine histone antibodies', *Methods in Enzymology*, 376, pp. 234–254. doi: 10.1016/S0076-6879(03)76016-9.
Pestourie, C., Tavitian, B. and Duconge, F. (2005) 'Aptamers against extracellular targets for *in vivo* applications', *Biochimie*, 87(9–10), pp. 921–930. doi: 10.1016/j.biochi.2005.04.013.
Pethe, K. *et al.* (2002) 'Mycobacterial heparin-binding hemagglutinin and laminin-binding protein share antigenic methyllysines that confer resistance to proteolysis', *Proceedings of the National Academy of Sciences of the United States of America*, 99(16), pp. 10759–10764. doi: 10.1073/pnas.162246899.
Petrossian, T. C. and Clarke, S. G. (2011) 'Uncovering the human methyltransferasome', *Molecular and Cellular Proteomics*, 10(1), pp. 1–12. doi: 10.1074/mcp.M110.000976.
Phillips, J. A. *et al.* (2008) 'Applications of aptamers in cancer cell biology', *ScienceDirect*, 621(1), pp. 101–108. doi: 10.1016/j.aca.2008.05.031.
Phizicky, E. *et al.* (2003) 'Protein analysis on a proteomic scale', *Nature*, 422(6928), pp. 208–215. doi: 10.1038/nature01512.
Pilehvar, S. *et al*. (2015) 'Intercalation of proflavine in ssDNA aptamers: effect on binding of the specific target chloramphenicol', *Electroanalysis*, 27(8), pp. 1836–1841. doi:10.1002/elan.201500192.
Pisithkul, T., Patel, N. M. and Amador-Noguez, D. (2015) 'Post-translational modifications as key regulators of bacterial metabolic fluxes', *Current Opinion in Microbiology*, 24, pp. 29–37. doi: 10.1016/j.mib.2014.12.006.
Pobran, T. D. *et al.* (2021) 'Aptamer-based enrichment of TDP-43 from human cells and tissues with quantification by HPLC-MS / MS', *Journal of Neuroscience Methods*, 363, p. 109344. doi: 10.1016/j.jneumeth.2021.109344.
Polevoda, B. and Sherman, F. (2007) 'Methylation of proteins involved in translation', *Molecular Microbiology*, 65(3), pp. 590–606. doi: 10.1111/j.1365-2958.2007.05831.x.
Pontius, W., Sneddon, M. W. and Emonet, T. (2013) 'Adaptation dynamics in densely clustered chemoreceptors', *PLoS Computational Biology*, 9(9), pp. 1–13. doi: 10.1371/journal.pcbi.1003230.

Popoff, M. Y., Bockemühl, J. and Gheesling, L. L. (2004) 'Supplement 2002 (no. 46) to the Kauffmann-White scheme', *Research in Microbiology*, 155(7), pp. 568–570. doi: 10.1016/j.resmic.2004.04.005.

Prus, G. *et al.* (2019) 'Analysis and interpretation of protein post-translational modification site stoichiometry', *Trends in Biochemical Sciences*, 44(11), pp. 943–960. doi: 10.1016/j.tibs.2019.06.003.

Punnia-Moorthy, G. *et al.* (2021) 'Lysine demethylases: promising drug targets in melanoma and other cancers', *Frontiers in Genetics*, 12, p. 680633. doi: 10.3389/fgene.2021.680633.

Qian, S. *et al.* (2022) 'Aptamers from random sequence space: accomplishments, gaps and future considerations', *Analytica Chimica Acta*, 1196, p. 339511. doi: 10.1016/j.aca.2022.339511.

Qiu, J. *et al.* (2022) 'Integration of solid phase extraction with HILIC-MS / MS for analysis of free amino acids in source water', *Journal of Environmental Sciences*, 117, pp. 190–196. doi: 10.1016/j.jes.2022.04.025.

Quang, N. N., Perret, G. and Ducongé, F. (2016) 'Applications of high-throughput sequencing for *in vitro* selection and characterization of aptamers', *Pharmaceuticals*, 9(4), pp. 1–15. doi: 10.3390/ph9040076.

Rabal, O. *et al.* (2016) 'In silico aptamer docking studies: from a retrospective validation to a prospective case study'tim3 aptamers binding', *Molecular Therapy - Nucleic Acids*,5, p. e376. doi: 10.1038/mtna.2016.84.

Raddatz, M. S. L. *et al.* (2008) 'Enrichment of cell-targeting and population-specific aptamers by fluorescence-activated cell sorting', *Angewandte Chemie - International Edition*, 47(28), pp. 5190–5193. doi: 10.1002/anie.200800216.

Raffatellu, M. *et al.* (2005) 'SipA, SopA, SopB, SopD, and SopE2 contribute to *Salmonella enterica* serotype typhimurium invasion of epithelial cells', *Infection and Immunity*, 73(1), pp. 146–154. doi: 10.1128/IAI.73.1.146-154.2005.

Raina, J. B. *et al.* (2019) 'The role of microbial motility and chemotaxis in symbiosis', *Nature Reviews Microbiology*, 17(5), pp. 284–294. doi: 10.1038/s41579-019-0182-9.

Rangel, A. E. *et al.* (2018) 'In vitro selection of an XNA aptamer capable of small-molecule recognition', *Nucleic Acids Research*, 46(16), pp. 8057–8068. doi: 10.1093/nar/gky667.

Rappold, B. A. and Grant, R. P. (2011) 'HILIC-MS / MS method development for targeted quantitation of metabolites: practical considerations from a clinical diagnostic perspective', *Journal of separation science*, 34(24), pp. 3527–3537. doi: 10.1002/jssc.201100550.

Rappsilber, J., Mann, M. and Ishihama, Y. (2007) 'Protocol for micro-purification, enrichment, pre-fractionation and storage of peptides for proteomics using StageTips', *Nature Protocols*, 2(8), pp. 1896–1906. doi: 10.1038/nprot.2007.261.

Ravipaty, S. and Reilly, J. P. (2010) 'Comprehensive characterization of methicillin-resistant *Staphylococcus aureus* subsp. *aureus* COL secretome by two-dimensional liquid chromatography and mass spectrometry', *Molecular and Cellular Proteomics*, 9(9), pp. 1898–1919. doi: 10.1074/mcp.M900494-MCP200.

Reese, H. *et al.* (2020) 'Purification of animal immunoglobulin G (IgG) using peptoid affinity ligands', *Biotechnology progress*, 36(4), pp. 1–13. doi: 10.1002/btpr.2994.

Reeves, M. W. *et al.* (1989) 'Clonal nature of *Salmonella* typhi and its genetic relatedness to other salmonellae as shown by multilocus enzyme electrophoresis and proposal of *Salmonella bongori* comb. nov.', *Journal of Clinical Microbiology*, 27(2), pp. 313–320.

doi: 10.1128/jcm.27.2.313-320.1989.
Rehman, T. *et al.* (2019) 'Adhesive mechanism of different *Salmonella* fimbrial adhesins', *Microbial Pathogenesis*, 137(4), pp. 103748–103777. doi: 10.1016/j.micpath.2019.103748.
Reinholt, S. J. *et al.* (2016) 'Highly multiplexed RNA aptamer selection using a microplate-based microcolumn device', *Scientific Reports*, 6(1), p. 29771. doi: 10.1038/srep29771.
Reinstein, O. *et al.* (2011) 'Engineering a structure switching mechanism into a steroid-binding aptamer and hydrodynamic analysis of the ligand binding mechanism', *Biochemistry*, 50(43), pp. 9368–9376. doi: 10.1021/bi201361v.
Rodesney, C. A. *et al.* (2017) 'Mechanosensing of shear by *Pseudomonas aeruginosa* leads to increased levels of the cyclic-di-GMP signal initiating biofilm development', *Biological Sciences*, 114(23), pp. 5906–5911. doi: 10.1073/pnas.1703255114.
Romig, T. S., Bell, C. and Drolet, D. W. (1999) 'Aptamer affinity chromatography: combinatorial chemistry applied to protein purification', *Journal of Chromatography B*, 731(2), pp. 275–284. doi: 10.1016/S0378-4347(99)00243-1.
Rossez, Y. *et al.* (2015) 'Bacterial flagella: twist and stick, or dodge across the kingdoms', *PLoS Pathogens*, 11(1), pp. 1–15. doi: 10.1371/journal.ppat.1004483.
Rothbart, S. B. *et al.* (2015) 'An interactive database for the assessment of histone antibody specificity', *Molecular Cell*, 59(3), pp. 502–511. doi: 10.1016/j.molcel.2015.06.022.
Röthlisberger, P. and Hollenstein, M. (2018) 'Aptamer chemistry', *Advanced Drug Delivery Reviews*, 134, pp. 3–21. doi: 10.1016/j.addr.2018.04.007.
Rourke, M. B. O. *et al.* (2019) 'What is Normalization? The strategies employed in top-down and bottom-up proteome analysis workflows', *Proteomes*, 7(3), pp. 1–19. doi: 10.3390/proteomes7030029.
Rubio, M. A. T. *et al.* (2017) 'Editing and methylation at a single site by functionally interdependent activities', *Nature*, 542(7642), pp. 494–497. doi: 10.1038/nature21396.
Running, W. E. *et al.* (2007) 'A top-down/bottom-up study of the ribosomal proteins of *Caulobacter crescentus*', *Journal of Proteome Research*, 6(1), pp. 337–347. doi: 10.1021/pr060306q.
Ruscito, A. and DeRosa, M. C. (2016) 'Small-molecule binding aptamers: selection strategies, characterization, and applications', *Frontiers in Chemistry*, 4, p. 14. doi: 10.3389/fchem.2016.00014.
Russo, K. I. *et al.* (2013) 'Duplex–quadruplex motifs in a peculiar structural organization cooperatively contribute to thrombin binding of a DNA aptamer', *Acta Crystallographica Section D: Biological Crystallography*, 69(12), pp. 2403–2411. doi: 10.1107/S0907444913022269.
Sabbir, M. G. (2019) 'Progesterone induced Warburg effect in HEK293 cells is associated with post-translational modifications and proteasomal degradation of progesterone receptor membrane component 1', *Journal of Steroid Biochemistry and Molecular Biology*, 191(2), p. 105376. doi: 10.1016/j.jsbmb.2019.105376.
Safarik, I. and Safarikova, M. (2004) 'Magnetic techniques for the isolation and purification of proteins and peptides', *BioMagnetic Research and Technology*, 2(1), pp. 7–25. doi: 10.1186/1477-044X-2-7.
Saini, S., Pearl, J. A. and Rao, C. V. (2009) 'Role of FimW, FimY, and FimZ in regulating the expression of type I fimbriae in *salmonella enterica* serovar typhimurium', *Journal of Bacteriology*, 191(9), pp. 3003–3010. doi: 10.1128/JB.01694-08.

Sakamoto, T., Ennifar, E. and Nakamura, Y. (2018) 'Thermodynamic study of aptamers binding to their target proteins', *Biochimie*, 145, pp. 91–97. doi: 10.1016/j.biochi.2017.10.010.

Samatey, F. A. *et al.* (2001) 'Structure of the bacterial flagellar protofilament and implications for a switch for supercoiling', *Nature*, 410(6826), pp. 331–337. doi: 10.1038/35066504.

Samatey, F. A. *et al.* (2004) 'Structure of the bacterial flagellar hook and implication for the molecular universal joint mechanism', *Nature*, 431(7012), pp. 1062–1068. doi: 10.1038/nature02997.

SantaLucia, J. (1998) 'A unified view of polymer, dumbbell, and oligonucleotide DNA nearest-neighbor thermodynamics', *Proceedings of the National Academy of Sciences of the United States of America*, 95(4), pp. 1460–1465. doi: 10.1073/pnas.95.4.1460.

Santos, A. M. P. dos, Ferrari, R. G. and Conte-Junior, C. (2019) 'Virulence factors in *Salmonella Typhimurium*: the sagacity of a bacterium', *Current Microbiology*, 76(5234), pp. 762–773. doi: doi:10.1093/femsle/fny142.

Schaefer, W. H. *et al.* (1987) 'A mutant Paramecium with a defective calcium-dependent potassium conductance has an altered calmodulin: A nonlethal selective alteration in calmodulin regulation', *Proceedings of the National Academy of Sciences of the United States of America*, 84(11), pp. 3931–3935. doi: 10.1073/pnas.84.11.3931.

Schägger, H. and von Jagow, G. (1987) 'Tricine-sodium dodecyl sulfate-polyacrylamide gel electrophoresis for the separation of proteins in the range from 1 to 100 kDa', *Analytical Biochemistry*, 166(2), pp. 368–379. doi: 10.1016/0003-2697(87)90587-2.

Schmidt, A. *et al.* (2016) 'The quantitative and condition-dependent *Escherichia coli* proteome', *Nature Biotechnology*, 34(1), pp. 104–110. doi: 10.1038/nbt.3418.

Sefah, K. *et al.* (2009) 'Nucleic acid aptamers for biosensors and bio-analytical applications', *Analyst*, 134(9), pp. 1765–1775. doi: 10.1039/b905609m.

Serganov, A., Huang, L. and Patel, D. J. (2008) 'Structural insights into amino acid binding and gene control by a lysine riboswitch', *Nature*, 455(7217), pp. 1263–1268. doi: 10.1038/nature07326.

Serre, N. B. C. *et al.* (2018) 'An outlook on lysine methylation of non-histone proteins in plants', *Journal of Experimental Botany*, 69(19), pp. 4569–4581. doi: 10.1093/jxb/ery231.

Shastri, A. *et al.* (2015) 'An aptamer-functionalized chemomechanically modulated biomolecule catch-and-release system', *Nature Chemistry*, 7(5), pp. 447–454. doi: 10.1038/nchem.2203.

Shi, H. *et al.* (2020) 'Selection and application of DNA aptamers against sulfaquinoxaline sssisted by Graphene Oxide–based SELEX', *Food Analytical Methods*, 14(2), pp. 250–259. doi: 10.1007/s12161-020-01869-2.

Shimizu, T., Ichimura, K. and Noda, M. (2015) 'The surface sensor NlpE of enterohemorrhagic *Escherichia coli* contributes to regulation of the type III secretion system and flagella by the Cpx response to adhesion', *American Societ for Microbiology*, 7, pp. 1–8. doi: 10.1128/IAI.00881-15.

Silverman, M. and Simon, M. (1977) 'Bacterial flagella', *Annual Review of Microbiology*, 31(4), pp. 397–419. doi: 10.1146/annurev.mi.31.100177.002145.

Smith, L. M. and Kelleher, N. L. (2018) 'Proteoforms as the next proteomics currency', *Science*, 359(6380), pp. 1106–1108. doi: 10.1126/science.aat1884.

Slavkovic, S. and Johnson, P. E. (2018) 'Isothermal titration calorimetry studies of aptamer-small molecule interactions: practicalities and pitfalls', *Aptamers*, 2, pp. 45–51.

Sohtome, Y. *et al.* (2021) 'Propargylic *Se*-adenosyl-L-selenomethionine: a chemical tool for methylome analysis', *Accounts of Chemical Research*, 54(20), pp. 3818–3827. doi:

10.1021/acs.accounts.1c00395.
Song, F. *et al.* (2017) 'How bacteria respond to material stiffness during attachment: a role of *Escherichia coli* flagellar motility', *ACS Applied Materials and Interfaces*, 9, pp. 22176–22184. doi: 10.1021/acsami.7b04757.
Song, F. and Ren, D. (2014) 'Stiffness of cross-cinked poly (dimethylsiloxane) affects bacterial adhesion and antibiotic susceptibility of attached cells', *Langmuir*, 30(34), pp. 10354–10362. doi: 10.1021/la502029f.
Song, M. *et al*. (2020) '*De novo* post-SELEX optimization of a G-quadruplex DNA aptamer binding to marine toxin gonyautoxin 1/4', *Computational and Structural Biotechnology Journal*, 18, pp. 3425–3433. doi: 10.1016/j.csbj.2020.10.041.
Song, W. S. *et al.* (2017) 'Self-oligomerizing structure of the flagellar cap protein FliD and its implication in filament assembly', *Journal of Molecular Biology*, 429(6), pp. 847–857. doi: 10.1016/j.jmb.2017.02.001.
Sosnick, T. R., Fang, X. and Shelton, V. M. (2000) 'Application of circular dichroism to study RNA folding transitions', *Methods in Enzymology*, 317(1995), pp. 393–409. doi: 10.1016/s0076-6879(00)17026-0.
Soto, G. E. and Hultgren, S. J. (1999) 'Bacterial adhesins: common themes and variations in architecture and assembly', *Journal of Bacteriology*, 181(4), pp. 1059–1071. doi: 10.1128/jb.181.4.1059-1071.1999.
Soufi, B. *et al.* (2012) 'Proteomics reveals evidence of cross-talk between protein modifications in bacteria: focus on acetylation and phosphorylation', *Current Opinion in Microbiology*, pp. 357–363. doi: 10.1016/j.mib.2012.05.003.
Sourjik, V. and Wingreen, N. S. (2012) 'Responding to chemical gradients: Bacterial chemotaxis', *Current Opinion in Cell Biology*, 24(2), pp. 262–268. doi: 10.1016/j.ceb.2011.11.008.
Spickler, C., Brunelle, M. N. and Brakier-Gingras, L. (1997) 'Streptomycin binds to the decoding center of 16S ribosomal RNA', *Journal of Molecular Biology*, 273(3), pp. 586–599. doi: 10.1006/jmbi.1997.1323.
Springer, M. S., Goy, M. F. and Adler, J. (1979) 'Protein methylation in behavioural control mechanisms and in signal transduction', *Nature*, 280(5720), pp. 279–284. doi: 10.1038/280279a0.
Srikanth, C. V. *et al.* (2010) '*Salmonella* pathogenesis and processing of secreted effectors by Caspase-3', *Science*, 330(6002), pp. 390–393. doi: 10.1126/science.1194598.
Srikanth, C. V. *et al.* (2011) '*Salmonella* effector proteins and host-cell responses', *Cellular and Molecular Life Sciences*, 68(22), pp. 3687–3697. doi: 10.1007/s00018-011-0841-0.
Steele-mortimer, O. (2008) 'The *Salmonella*-containing vacuole—moving with the times', *Current Opinion in Microbiology*, 11(1), pp. 38–45. doi: 10.1016/j.mib.2008.01.002.
Stevens, M. P. *et al.* (2002) 'An Inv/Mxi-Spa-like type III protein secretion system in *Burkholderia pseudomallei* modulates intracellular behaviour of the pathogen', *Molecular Microbiology*, 46(3), pp. 649–659. doi: 10.1046/j.1365-2958.2002.03190.x.
Stock, A., Koshland, D. E. and Stock, J. (1985) 'Homologies between the *Salmonella typhimurium* CheY protein and proteins involved in the regulation of chemotaxis, membrane protein synthesis, and sporulation', *Proceedings of the National Academy of Sciences of the United States of America*, 82(23), pp. 7989–7993. doi: 10.1073/pnas.82.23.7989.
Stock, J. B. and Koshland, D. E. (1978) 'A protein methylesterase involved in bacterial sensing', *Proceedings of the National Academy of Sciences of the United States of America*, 75(8),

pp. 3659–3663. doi: 10.1073/pnas.75.8.3659.
Stoltenburg, R., Reinemann, C. and Strehlitz, B. (2007) 'SELEX-A (r)evolutionary method to generate high-affinity nucleic acid ligands', *Biomolecular Engineering*, 24(4), pp. 381–403. doi: 10.1016/j.bioeng.2007.06.001.
Stoltenburg, R., Schubert, T. and Strehlitz, B. (2015) 'In vitro selection and interaction studies of a DNA aptamer targeting Protein A', *PLoS ONE*, 10(7), pp. 1–23. doi: 10.1371/journal.pone.0134403.
Stoltenburg, R., Nikolaus, N. and Strehlitz, B. (2012) 'Capture-SELEX: Selection of DNA aptamers for aminoglycoside antibiotics', *Journal of Analytical Methods in Chemistry*, 1(1), pp. 1–15. doi: 10.1155/2012/415697.
Stoltenburg, R., Reinemann, C. and Strehlitz, B. (2005) 'FluMag-SELEX as an advantageous method for DNA aptamer selection', *Analytical and Bioanalytical Chemistry*, 383(1), pp. 83–91. doi: 10.1007/s00216-005-3388-9.
Strader, M. B. *et al.* (2004) 'Characterization of the 70S ribosome from *Rhodopseudomonas palustris* using an integrated "top-down" and "bottom-up" mass spectrometric approach', *Journal of Proteome Research*, 3(5), pp. 965–978. doi: 10.1021/pr049940z.
Su, Y. *et al.* (2021) 'Methylation of PhoP by CheR regulates *Salmonella* virulence', *mBio*, 12(5), pp. 1–21. doi: 10.1128/mBio.02099-21.
Sullivan, R. *et al.* (2019) 'Analyzing secondary structure patterns in DNA aptamers identified *via* compels', *Molecules*, 24(8), pp. 1–18. doi: 10.3390/molecules24081572.
Sun, L. *et al.* (2013) 'Posttranslational modification of flagellin FlaB in *Shewanella oneidensis*', *Journal of Bacteriology*, 195(11), pp. 2550–2561. doi: 10.1128/JB.00015-13.
Sun, S. W. *et al.* (2006) 'Efficiency improvements on ninhydrin method for amino acid quantification', *Journal of Food Composition and Analysis*, 19(2–3), pp. 112–117. doi: 10.1016/j.jfca.2005.04.006.
Srivastava, V. K. and Yadav, R. (2019) 'Isothermal titration calorimetry', *Data Processing Handbook for Complex Biological Data Sources*, PP. 125-137. doi: 10.1016/B978-0-12-816548-5.00009-5.
Szapacs, M. and Budamgunta, H. (2013) 'Trypsin / Lys-C protease mix for enhanced protein mass spectrometry analysis', *Nature Methods*, 10(11), pp. i–ii. doi: 10.1038/nmeth.f.371.
Szeitner, Z. *et al.* (2014) 'Is less more? Lessons from aptamer selection strategies', *Journal of Pharmaceutical and Biomedical Analysis*, 101, pp. 58–65. doi: 10.1016/j.jpba.2014.04.018.
Takahashi, M. *et al*. (2016) 'High throughput sequencing analysis of RNA libraries reveals the influences of initial library and PCR methods on SELEX efficiency', *Scientific Reports*, 6, pp. 1–14. doi: 10.1038/srep33697.
Tan, S. Y. *et al.* (2016) 'SELEX modifications and bioanalytical techniques for aptamer–target binding characterization', *Critical Reviews in Analytical Chemistry*, 46(6), pp. 521–537. doi: 10.1080/10408347.2016.1157014.
Tang, J. *et al.* (2006) 'The DNA aptamers that specifically recognize ricin toxin are selected by two *in vitro* selection methods', *Electrophoresis*, 27(7), pp. 1303–1311. doi: 10.1002/elps.200500489.
Tauxe, R. V. (1991) '*Salmonella*: a postmodern pathogen', *Journal of Food Protection*, 54(7), pp. 563–568. doi: 10.4315/0362-028X-54.7.563.
Thevendran, R. and Citartan, M. (2022) 'Assays to estimate the binding affinity of aptamers', *Talanta*, 238(1), p. 122971. doi: 10.1016/j.talanta.2021.122971.

Thormann, K. M. and Paulick, A. (2010) 'Tuning the flagellar motor', *Microbiology society*, 156(5), pp. 1275–1283. doi: 10.1099/mic.0.029595-0.

Thomas, P. and Smart, T. G. (2005) 'HEK293 cell line: a vehicle for the expression of recombinant proteins', *Journal of Pharmacological and Toxicological Methods*, 51(3), pp. 187–200. doi: 10.1016/j.vascn.2004.08.014.

Tijerina, P., Mohr, S. and Russell, R. (2007) 'Dms footprinting of structured rnas and rna-protein complexes', *Nature Protocols*, 2(10), pp. 2608–2623. doi: 10.1038/nprot.2007.380.

Tillotson, G. S. and Tillotson, J. (2009) 'Bacterial secreted proteins: secretory mechanisms and role in pathogenesis', *Expert Review of Anti-infective Therapy*, 7(6), pp. 691–693. doi: 10.1586/eri.09.47.

Tillotson, B. J., Cho, Y. K. and Shusta, E. V. (2013) 'Cells and cell lysates: a direct approach for engineering antibodies against membrane proteins using yeast surface display', *Methods*, 60(1), pp. 27–37. doi: 10.1016/j.ymeth.2012.03.010.

Toby, T. K., Fornelli, L. and Kelleher, N. L. (2016) 'Progress in Top-Down Proteomics and the analysis of proteoforms', *Annual review of analytical chemistry*, 9(1), pp. 499–521. doi: 10.1146/annurev-anchem-071015-041550.

Toews, M. L. *et al.* (1979) 'Attractants and repellents control demethylation of methylated chemotaxis proteins in *Escherichia coli*', *Proceedings of the National Academy of Sciences of the United States of America*, 76(11), pp. 5544–5548. doi: 10.1073/pnas.76.11.5544.

Toh, S. Y. *et al.* (2015) 'Aptamers as a replacement for antibodies in enzyme-linked immunosorbent assay', *Biosensors and Bioelectronics*, 64(80), pp. 392–403. doi: 10.1016/j.bios.2014.09.026.

Tolle, F. and Mayer, G. (2013) 'Dressed for success-applying chemistry to modulate aptamer functionality', *Chemical Science*, 4(1), pp. 60–67. doi: 10.1039/c2sc21510a.

Troisi, R. and Sica, F. (2022) 'Aptamers: functional-structural studies and biomedical applications', *International Journal of Molecular Sciences*, 23(9), pp. 12–13. doi: 10.3390/ijms23094796.

Truong, D. *et al.* (2018) '*Salmonella* exploits host Rho GTPase signalling pathways through the phosphatase activity of SopB', *Cellular Microbiology*, 20(10), pp. 1–12. doi: 10.1111/cmi.12938.

Tseng, T. T., Tyler, B. M. and Setubal, J. C. (2009) 'Protein secretion systems in bacterial-host associations, and their description in the Gene Ontology', *BMC Microbiology*, 9(SUPPL. 1), pp. 1–9. doi: 10.1186/1471-2180-9-S1-S2.

Tsusaka, T. *et al.* (2018) 'Tri-methylation of ATF7IP by G9a/GLP recruits the chromodomain protein', *Epigenetics and Chromatin*, 11(1), pp. 1–16. doi: 10.1186/s13072-018-0231-z.

Tuerk, C. and Gold, L. (1990) 'Systematic Evolution of Ligands by Exponential Enrichment: RNA ligands to bacteriophage El-T', *Science*, 249(4968), pp. 505–510. doi: 10.1126/science.2200121.

Uhlmann, T. *et al.* (2012) 'A method for large-scale identification of protein arginine methylation', *Molecular and Cellular Proteomics*, 11(11), pp. 1489–1499. doi: 10.1074/mcp.M112.020743.

Ulrich, H. *et al.* (2006) 'DNA and RNA aptamers: from tools for basic research towards therapeutic applications', *Combinatorial Chemistry & High Throughput Screening*, 9(8), pp. 619–632. doi: 10.2174/138620706778249695.

Urmann, K. and Walter, J.-G. (2020) 'Aptamer-based affinity chromatography for protein extraction and purification', *Aptamers in Biotechnology*, doi: doi:10.1007/978-3-030-54061-6.

Van Noort, J. M. et al. (1986) 'Methylation in vivo of elongation factor EF-Tu at lysine-56 decreases the rate of tRNA-dependent GTP hydrolysis', *European Journal of Biochemistry*, 160, pp. 557–561. doi: 10.1111/j.1432-1033.1986.tb10074.x.

Vanschoenbeek, K. *et al.* (2015) 'Aptamers targeting different functional groups of 17β-estradiol', *Journal of Steroid Biochemistry and Molecular Biology*, 147, pp. 10–16. doi: 10.1016/j.jsbmb.2014.10.013.

Vaught, J. D. *et al.* (2010) 'Expanding the chemistry of DNA for *in vitro* selection', *Journal of the American Chemical Society*, 132(12), pp. 4141–4151. doi: 10.1021/ja908035g.

Velez, T. E. *et al.* (2012) 'Systematic evaluation of the dependence of deoxyribozyme catalysis on random region length', *ACS Combinatorial Science*, 14(12), pp. 680–687. doi: 10.1021/co300111f.

Velge, P. *et al.* (2012) 'Multiplicity of *Salmonella* entry mechanisms, a new paradigm for *Salmonella* pathogenesis', *Microbiology open*, 1(3), pp. 243–258. doi: 10.1002/mbo3.28.

Vianini, E., Palumbo, M. and Gatto, B. (2001) '*In vitro* selection of DNA aptamers that bind L-tyrosinamide', *Bioorganic and Medicinal Chemistry*, 9(10), pp. 2543–2548. doi: 10.1016/S0968-0896(01)00054-2.

Vijayan, A. *et al.* (2018) 'Compartmentalized antimicrobial defenses in response to flagellin', *Trends in Microbiology*, 26(5), pp. 423–435. doi: 10.1016/j.tim.2017.10.008.

Vorobyeva, M. A. *et al*. (2018) 'Key aspects of nucleic acid library design for *in vitro* selection', *International Journal of Molecular Sciences*, 19(2), pp. 470–491. doi: 10.3390/ijms19020470.

Vorontsov, E. A. *et al.* (2016) 'Abundant lysine methylation and N-terminal acetylation in sulfolobus islandicus revealed by bottom-up and top-down proteomics', *Molecular and Cellular Proteomics*, 15(11), pp. 3388–3404. doi: 10.1074/mcp.M116.058073.

Wadhams, G. H. and Armitage, J. P. (2004) 'Making sense of it all: bacterial chemotaxis', *Nature Reviews Molecular Cell Biology*, 5(12), pp. 1024–1037. doi: 10.1038/nrm1524.

Wagner, C. and Hensel, M. (2011) 'Adhesive mechanisms of *salmonella enterica*', *Advances in Experimental Medicine and Biology*, 715, pp. 17–34. doi: 10.1007/978-94-007-0940-9_2.

Walsh, C. T., Garneau-Tsodikova, S. and Gatto, G. J. (2005) 'Protein posttranslational modifications: The chemistry of proteome diversifications', *Angewandte Chemie - International Edition*, 44(45), pp. 7342–7372. doi: 10.1002/anie.200501023.

Walsh, G. (2010) 'Post-translational modifications of protein biopharmaceuticals', *Drug Discovery Today*, 15(17–18), pp. 773–780. doi: 10.1016/j.drudis.2010.06.009.

Walter, J. G., Stahl, F. and Scheper, T. (2012) 'Aptamers as affinity ligands for downstream processing', *Engineering in Life Sciences*, 12(5), pp. 496–506. doi: 10.1002/elsc.201100197.

Wang, J. *et al.* (2014) 'Particle display: a quantitative screening method for generating high-affinity aptamers', *Angwandte Communications*, 53(19), pp. 4796–4801. doi: 10.1002/anie.201309334.

Wang, C. *et al.* (2021) 'Flagellin lysine methyltransferase FliB catalyzes a [4Fe-4S] mediated methyl transfer reaction', *PLoS Pathogens*, 17(11), pp. 1–21. doi: 10.1371/journal.ppat.1010052.

Wang, J. and Zhou, H. S. (2008) 'Aptamer-based Au nanoparticles-enhanced surface plasmon resonance detection of small molecules', *Analytical Chemistry*, 80(18), pp. 7174–7178. doi: 10.1021/ac801281c.

Wang, Q., Wang, K. and Ye, M. (2017) 'Strategies for large-scale analysis of non-histone protein methylation by LC-MS/MS', *Analyst*, 142(19), pp. 3536–3548. doi: 10.1039/c7an00954b.

Wang, R. *et al.* (2018) 'The second messenger c-di-GMP adjusts motility and promotes surface aggregation of bacteria', *Biophysical Journal*, 115(11), pp. 2242–2249. doi: 10.1016/j.bpj.2018.10.020.

Wang, K. *et al.* (2016) 'Antibody-free approach for the global analysis of protein methylation', *Analytical Chemistry*, 88(23), pp. 11319–11327. doi: 10.1021/acs.analchem.6b02872.

Wang, K. and Ye, M. (2018) 'Enrichment of methylated meptides using an antibody-free approach for global methylproteomics analysis', *Current Protocols in Protein Science*, 91(1), pp. 14.18.1-14.18.14. doi: 10.1002/cpps.49.

Ward, W. W. and Swiatek, G. (2009) 'Protein purification', *Current Analytical Chemistry*, 5(2), pp. 85–105. doi: 10.2174/157341109787846171.

Warfield, B. M. and Anderson, P. C. (2017) 'Molecular simulations and Markov state modeling reveal the structural diversity and dynamics of a theophylline-binding RNA aptamer in its unbound state', *PLoS ONE*, 12 (4), pp. 1-34. doi: 10.1371/journal.pone.0176229.

Waugh, D. S. (2005) 'Making the most of affinity tags', *Trends in Biotechnology*, 23(6), pp. 316–320. doi: 10.1016/j.tibtech.2005.03.012.

Waugh, D. S. (2011) 'An overview of enzymatic reagents for the removal of affinity tags', *Protein Expression and Purification*, 80(2), pp. 283–293. doi: 10.1016/j.pep.2011.08.005.

Webb, K. J. *et al.* (2010) 'Identification of protein N-terminal methyltransferases in yeast and humans', *Biochemistry*, 49(25), pp. 5225–5235. doi: 10.1021/bi100428x.

Wee, D. H. and Hughes, K. T. (2015) 'Molecular ruler determines needle length for the *Salmonella* Spi-1 injectisome', *Proceedings of the National Academy of Sciences of the United States of America*, 112(13), pp. 4098–4103. doi: 10.1073/pnas.1423492112.

Wei, L. *et al.* (2020) 'CheY1 and CheY2 of Azorhizobium caulinodans ORS571 regulate chemotaxis and competitive colonization with the host plant', *Applied and Environmental Microbiology*, 86(15), pp. e00599-20. doi: 10.1128/AEM.00599-20.

White, A. P. *et al.* (2006) 'Thin aggregative fimbriae and cellulose enhance long-term survival and persistence of *Salmonella*', *Journal of Bacteriology*, 188(9), pp. 3219–3227. doi: 10.1128/JB.188.9.3219-3227.2006.

Wiedman, G. R. *et al.* (2017) 'An Aptamer-based biosensor for the azole class of antifungal drugs', *mSphere*, 2(4), pp. 1–10. doi: 10.1128/msphere.00274-17.

Williams, B. A. R. *et al*. (2009) 'Evolution of a histone H4-K16 acetyl-specific DNA aptamer', *Journal of the American Chemical*, 131(18), pp. 6330–6331. doi: 10.1021/ja900916p.

Williams, K. P. and Bartel, D. P. (1995) 'PCR product with strands of unequal length', *Nucleic Acids Research*, 23(20), pp. 4220–4221. doi: 10.1093/nar/23.20.4220.

Win, M. N., Klein, J. S. and Smolke, C. D. (2006) 'Codeine-binding RNA aptamers and rapid determination of their binding constants using a direct coupling surface plasmon resonance assay', *Nucleic Acids Research*, 34(19), pp. 5670–5682. doi: 10.1093/nar/gkl718.

Wiseman, T. *et al.* (1989) 'Rapid measurement of binding constants and heats of binding using a new titration calorimeter', *Analytical Biochemistry*, 179(1), pp. 131–137. doi:

10.1016/0003-2697(89)90213-3.
Wolfe, A. J. and Visick, K. L. (2008) 'Get the message out: Cyclic-Di-GMP regulates multiple levels of flagellum-based motility', *Journal of Bacteriology*, 190(2), pp. 463–475. doi: 10.1128/JB.01418-07.
Wolfgang, M. *et al.* (2000) 'Components and dynamics of fiber formation define a ubiquitous biogenesis pathway for bacterial pili', *EMBO Journal*, 19(23), pp. 6408–6418. doi: 10.1093/emboj/19.23.6408.
Wood, D. W. (2014) 'New trends and affinity tag designs for recombinant protein purification', *Current Opinion in Structural Biology*, 26(1), pp. 54–61. doi: 10.1016/j.sbi.2014.04.006.
Wu, B. *et al.* (2016) 'Detection of C-reactive protein using nanoparticle-enhanced surface plasmon resonance using an aptamer-antibody sandwich assay', *Chemical Communications*, 52(17), pp. 3568–3571. doi: 10.1039/c5cc10486f.
Wu, Y. *et al*. (2014) 'Selection of a DNA aptamer for cadmium detection based on cationic polymer mediated aggregation of gold nanoparticles', *Analyst*, 139(6), pp. 1550–1561. doi: 10.1039/c3an02117c.
Wu, Z. *et al.* (2015) 'A chemical proteomics approach for global analysis of lysine monomethylome profiling', *Molecular and Cellular Proteomics*, 14(2), pp. 329–339. doi: 10.1074/mcp.M114.044255.
Wu, Z., Connolly, J. and Biggar, K. K. (2017) 'Beyond histones – the expanding roles of protein lysine methylation', *FEBS Journal*, 284(17), pp. 2732–2744. doi: 10.1111/febs.14056.
Wu, Z. *et al.* (2018) 'Lys-C / Arg-C, a more specific and efficient digestion approach for proteomics studies', *Analytical Chemistry*, 90(16), pp. 9700–9707. doi: 10.1021/acs.analchem.8b02448.
Xu, H., Lee, H. Y. and Ahn, J. (2010) 'Growth and virulence properties of biofilm-forming *Salmonella enterica* serovar Typhimurium under different acidic conditions', *Applied and Environmental Microbiology*, 76(24), pp. 7910–7917. doi: 10.1128/AEM.01508-10.
Yamaguchi, T. *et al.* (2020) 'Structural and functional comparison of *Salmonella* flagellar filaments composed of FljB and FliC', *Biomolecules*, 10(2), p. 246. doi: 10.3390/biom10020246.
Yan, A. C. and Levy, M. (2009) 'Aptamers and aptamer targeted delivery', *RNA Biology*, 6(3), pp. 316–320. doi: 10.4161/rna.6.3.8808.
Yang, K. A. *et al.* (2014) 'Recognition and sensing of low-epitope targets *via* ternary complexes with oligonucleotides and synthetic receptors', *Nature Chemistry*, 6(11), pp. 1003–1008. doi: 10.1038/NCHEM.2058.
Yang, D. C. H. *et al.* (2017) 'Outer membrane protein OmpB methylation may mediate bacterial virulence', *Trends in Biochemical Sciences*, 42(12), pp. 936–945. doi: 10.1016/j.tibs.2017.09.005.
Yang, G. *et al.* (2021) 'Pressure controllable aptamers picking strategy by targets competition', *Chinese Chemical Letters*, 32(1), pp. 218–220. doi: 10.1016/j.cclet.2020.10.018.
Yang, J. and Bowser, M. T. (2013) 'Capillary electrophoresis−SELEX selection of catalytic DNA aptamers for a small-molecule porphyrin target', *Analytical Biochemistry*, 85(3), pp. 1525–1530. doi: 10.1021/ac302721j.
Yang, X. *et al.* (2011) 'Characterization and application of a DNA aptamer binding to L -tryptophan', *Analyst*, 136(3), pp. 577–585. doi: 10.1039/c0an00550a.
Yeh, K. S., Hancox, L. S. and Clegg, S. (1995) 'Construction and characterization of a fimZ mutant of *Salmonella typhimurium*', *Journal of Bacteriology*, 177(23), pp. 6861–6865. doi: 10.1128/jb.177.23.6861-6865.1995.

Yin, L. *et al.* (2022) 'Cinnamaldehyde resist *Salmonella* Typhimurium adhesion by inhibiting Type I Fimbriae', *Molecules*, 27(22), p. 7753. doi: 10.3390/molecules27227753.

Yonekura, K. *et al.* (2000) 'The bacterial flagellar cap as the rotary promoter of flagellin self-assembly', *Science*, 290(5499), pp. 2148–2152. doi: 10.1126/science.290.5499.2148.

Young, C. L., Britton, Z. T. and Robinson, A. S. (2012) 'Recombinant protein expression and purification: A comprehensive review of affinity tags and microbial applications', *Biotechnology Journal*, 7(5), pp. 620–634. doi: 10.1002/biot.201100155.

Yu, Y. *et al.* (2016) 'Molecular selection, modification and development of therapeutic oligonucleotide aptamers', *International Journal of Molecular Sciences*, 17(3), pp. 358–377. doi: 10.3390/ijms17030358.

Yu, H. *et al.* (2021) 'Advances and challenges in small-molecule DNA aptamer isolation, characterization, and sensor development', *Angewandte Chemie International Edition*, 60(31), pp. 16800–16823. doi: 10.1002/ange.202008663.

Yue, M. *et al.* (2012) 'Diversification of the *Salmonella* fimbriae: a model of macro- and microevolution', *PLoS ONE*, 7(6), pp. 38596–38611. doi: 10.1371/journal.pone.0038596.

Zacharias, A. O. *et al.* (2021) 'Affinity and chemical enrichment strategies for mapping low-abundance protein modifications and protein-interaction networks', *Journal of Separation Science*, 44(1), pp. 310–322. doi: 10.1002/jssc.202000930.

Zhang, X. *et al.* (2010) 'Multi-dimensional liquid chromatography in proteomics-A review', *Analytica Chimica Acta*, 664(2), pp. 101–113. doi: 10.1016/j.aca.2010.02.001.

Zhang, Y. *et al.* (2013) 'Protein analysis by shotgun / bottom-up proteomics', *Chemical Reviews*, 113(4), pp. 2343–2394. doi: 10.1021/cr3003533.

Zhang, X., Wen, H. and Shi, X. (2012) 'Lysine methylation: Beyond histones', *Acta Biochimica et Biophysica Sinica*, 44(1), pp. 14–27. doi: 10.1093/abbs/gmr100.

Zhang, M. *et al.* (2018) 'Systematic proteomic analysis of protein methylation in prokaryotes and eukaryotes revealed distinct substrate specificity', *Proteomics*, 18(1), pp. 1–35. doi: 10.1002/pmic.201700300.

Zhao, Y. and Jensen, O. N. (2009) 'Modification-specific proteomics: Strategies for characterization of post-translational modifications using enrichment techniques', *Proteomics*, 9(20), pp. 4632–4641. doi: 10.1002/pmic.200900398.

Zhou, J., Lloyd, S. A. and Blair, D. F. (1998) 'Electrostatic interactions between rotor and stator in the bacterial flagellar motor', *Proceedings of the National Academy of Sciences of the United States of America*, 95(11), pp. 6436–6441. doi: 10.1073/pnas.95.11.6436.

Zhu, C. *et al.* (2019) 'Evolution of multi-functional capillary electrophoresis for high-efficiency selection of aptamers', *Biotechnology Advances*, 37(8), p. 107432. doi: 10.1016/j.biotechadv.2019.107432.

Zuker, M. (2003) 'Mfold web server for nucleic acid folding and hybridization prediction', *Nucleic Acids Research*, 31(13), pp. 3406–3415. doi: 10.1093/nar/gkg595.